



If you have discovered material in AURA which is unlawful e.g. breaches copyright, (either yours or that of a third party) or any other law, including but not limited to those relating to patent, trademark, confidentiality, data protection, obscenity, defamation, libel, then please read our [Takedown Policy](#) and [contact the service](#) immediately

ALGINATES AS THERAPEUTIC AND

DRUG DELIVERY SYSTEMS

KEITH GRAEME HUTCHISON

SUBMITTED FOR THE DEGREE OF DOCTOR
OF PHILOSOPHY AT THE UNIVERSITY OF
ASTON IN BIRMINGHAM

SEPTEMBER 1982

SUMMARY

'Alginates as Therapeutic and Drug Delivery Systems'

Alginate is widely used as a viscosity enhancer in many different pharmaceutical formulations. The aim of this thesis is to quantitatively describe the functions of this polyelectrolyte in pharmaceutical systems. To do this the techniques used were Viscometry, Light Scattering, Continuous and Oscillatory Shear Rheometry, Numerical Analysis and Diffusion.

Molecular characterization of the Alginate was carried out using Viscometry and Light Scattering to determine the molecular weight, the radius of gyration, the second virial coefficient and the Kuhn statistical segment length. The results showed good agreement with similar parameters obtained in previous studies.

By blending Alginate with other polyelectrolytes, Xanthan Gum and 'Carbopol', in various proportions and with various methods of low and high shear preparation, a very wide range of dynamic rheological properties was found. Using oscillatory testing, the parameters often varied over several decades of magnitude. It was shown that the determination of the viscous and elastic components is particularly useful in describing the rheological 'profiles' of suspending agent blends and provides a step towards the non-empirical formulation of pharmaceutical disperse systems.

Using numerical analysis of equations describing planar diffusion, it was shown that the analysis of drug release profiles alone does not provide unambiguous information about the mechanism of rate control. These principles were applied to the diffusion of Ibuprofen in Calcium Alginate gels. For diffusion in such non-Newtonian systems, emphasis was placed on the use of the elastic as well as the viscous component of viscoelasticity. It was found that the diffusion coefficients were relatively unaffected by increases in polymer concentration up to 5 per cent, yet the elasticities measured by oscillatory shear rheometry were increased. This was interpreted in the light of several theories of diffusion in gels.

Keith Graeme Hutchison

Submitted for the Degree of Doctor of Philosophy, 1982.

Keywords: Alginate, Diffusion, Rheogoniometer, Suspending Agents, Viscoelasticity.

ACKNOWLEDGEMENTS

I am greatly indebted to the following parties for their contributions to the work of this thesis.

1. Professor M.R.W. Brown for making available the facilities of the Pharmacy Department at the University of Aston in Birmingham.
2. The Science and Engineering Research Council for granting a C.A.S.E. Award.
3. Dr. A. Li Wan Po, my academic supervisor for his patient support throughout the project.
4. Mr. R. Allison and Dr. R. Todd of Reckitt and Colman Pharmaceutical Division, my industrial supervisors, for their generous support and advice.
5. The many staff and students of the Pharmacy Department for their valuable assistance.
6. Mrs. J. Knapp and Mrs. L. Burnett for their immense patience in the typing of this thesis, and the Wellcome Foundation Ltd. for making many facilities available during writing-up.
7. Lastly, heartfelt thanks go to my wife Elizabeth without whom none of this would have been possible.

LIST OF CONTENTS

	<u>Page</u>
1. <u>Introduction</u>	
1.1 Background	1
1.2 Ion-Binding Properties of Alginate	4
1.3 Therapeutic Aspects	6
1.4 Rheology and Diffusion	7
2. <u>Molecular and Rheological Characteristics of Alginate Solutions</u>	
2.1 Introduction	10
2.2 Theory	13
2.2.1 Viscometry	13
2.2.2 Light Scattering	17
2.2.3 Rheology	20
2.3 Materials and Methods	29
2.3.1 Viscometry	29
2.3.2 Light Scattering	30
2.3.3 Determination of Alginate Content	32
2.3.4 Determination of Refractive Index Increment	33
2.3.5 Rheology	33
2.3.5.1 Continuous Shear Experiments	35
2.3.5.2 Oscillatory Shear Experiments	35
2.4 Results	37
2.4.1 Viscometry	37
2.4.2 Light Scattering	42
2.4.3 Continuous Shear Rheometry	49
2.4.4 Oscillatory Shear Rheometry	57
2.5 Discussion	66
3. <u>Rheological Properties of Suspending Agents</u>	
3.1 Introduction	70
3.2 Theory	72
3.2.1 Xanthan Gum and Carbopol	72
3.2.2 Rheological Properties and Suspending Ability	74
3.2.3 Shearing of Polymer Solutions	75
3.2.4 Quantifying non-Newtonian Flow	75

3.3	Materials and Methods	78
3.3.1	Rheological Testing	78
3.3.2	Preparation of Samples	82
3.3.3	Sedimentation Tests	83
3.4	Results	83
3.4.1	Xanthan Gum Systems	83
3.4.1.1	Effect of Concentration	83
3.4.1.2	Effect of Preparation Method	87
3.4.1.3	Effect of Shearing	99
3.4.2	Carbopol Systems	105
3.4.2.1	Effect of Concentration	105
3.4.2.2	Effect of Shearing	118
3.4.3	Proprietary Preparations	120
3.5	Discussion	139
4.	<u>Numerical Analysis of Approximations to Diffusion Rate Equations</u>	
4.1	Introduction	142
4.2	Derivation of a Diffusion Rate Equation	148
4.3	Method of Numerical Analysis	152
4.4	Results and Discussion	157
	Appendix: Glossary of Terms not Directly Explained in the Text	163
5.	<u>Diffusional and Rheological Properties of Alginate Gels</u>	240
5.1	Introduction	165
5.2	Theory	170
5.2.1	Diffusion Coefficient	170
5.2.2	Partition Coefficient	173
5.3	Materials and Methods	176
5.3.1	Diffusion Experiments	176
5.3.1.1	Apparatus and Protocol	176
5.3.1.2	Dialysis Method of Gel Formation	179
5.3.1.3	Effect of Stirrer Speed	182
5.3.1.4	Concentration Gradient within the Gel	182
5.3.2	Rheological Experiments	183
5.3.2.1	The Use of Oscillatory Rheometry	183
5.3.2.2	Chemical Method of Gel Formation	184
5.3.3	Partition Coefficient of Ibuprofen	186
5.3.4	HPLC Assay of Ibuprofen	187

5.4	Results	191
5.4.1	Partition Coefficient of Ibuprofen	191
5.4.2	Diffusion Experiments	194
5.4.2.1	Effect of Stirrer Speed	194
5.4.2.2	Concentration Gradient within the Gel	195
5.4.2.3	Drug Release Profiles	197
5.4.3	Rheological Experiments	208
5.4.3.1	Effect of Glucono- δ -lactone and Alginate Concentration on Calcium Alginate Gels	208
5.4.3.2	Effect of Calcium Ion Concentration on Storage Modulus and Dynamic Viscosity	214
5.4.3.3	Effect of Alginate Concentration on Storage Modulus	220
5.5	Discussion	224
6.	<u>Conclusion</u>	234
7.	<u>Apendices</u>	237
7.1	Appendix I. Paper : Numerical Analysis of Approximations to the Planar Diffusion Equation.	237
7.2	Appendix II. Glossary of Traditional and SI Units.	239
8.	<u>References</u>	240

LIST OF TABLES AND FIGURES

	<u>Page</u>
Figure 1.1. The Structures of α ,L-Guluronate and β ,D-Mannuronate.	3
Figure 1.2. The "Egg-Box" Model for Inter-Chain Binding of Calcium Ions, by Polyguluronate.	5
Table 2.1. Molecular Properties of Sodium Alginate.	23
Table 2.2. Principles and Parameters of Rheological Testing.	22
Figure 2.1. The Form of Experimental Data from Rheological Testing.	14
Table 2.3. Quantitative Descriptions of Non-Newtonian Behaviour.	25
Table 2.4. Clarification of Alginate Solutions.	31
Scheme 2.1. The Reaction of Phenol and Concentrated Sulphuric Acid with Uronic Acid.	32
Figure 2.2. The Weissenberg Rheogoniometer, Model R16.	34
Table 2.5. Intrinsic Viscosity Determination Before and After Ultracentrifugation at 100,000 x g for 2 hr.	38
Figure 2.3. Determination of the Intrinsic Viscosity of Alginate from a plot of Reduced Viscosity against Concentration.	39
Table 2.6. Dissymmetric Ratios of Alginate Solutions.	42
Figure 2.4. The Effect of Alginate Concentration and Centrifugation on the Intensity of Light Scattered at 90°.	44
Table 2.7. Light Scattered at 90° for Solutions Centrifuged at 3,000 x g for 2 hr.	45

	<u>Page</u>
Table 2.8. Light Scattered at 90° for Solutions Centrifuged at 25,000 x g for 2 hr.	46
Figure 2.5. Determination of the Refractive Index Increment from a plot of Refractive Index Difference against Alginate Concentration.	47
Figure 2.6. Zimm Plot for Alginate Solutions Ultracentrifuged at 100,000 x g for 2 hr.	50
Table 2.9. Light Scattering Data for Alginate Solutions Centrifuged at 100,000 x g for 2 hr.	51
Figures 2.7.-2.9. Continuous Shear $\tau(\dot{\gamma})$ Flow-Curves for Various Concentrations of Sodium Alginate Solutions.	52
Figure 2.10. The Effect of the Concentration of Alginate on Newtonian Viscosity.	56
Table 2.10. Newtonian Viscosities of Sodium Alginate Solutions at 20°C.	57
Figure 2.11. The Effect of the Frequency of Oscillation on (a) Amplitude Ratio and (b) Phase Lag for Silicone Fluid 100 cs.	58
Figure 2.12. The Effect of the Frequency of Oscillation on (a) Amplitude Ratio and (b) Phase Lag for Liquid Paraffin B.P.	60
Figure 2.13. The Effect of the Concentration of Sodium Alginate Solution on the Storage Modulus, plotted as a function of the Frequency of Oscillation.	62
Figure 2.14. The Effect of the Concentration of Sodium Alginate Solution on the Dynamic Viscosity, plotted as a function of the Frequency of Oscillation.	64

	<u>Page</u>
Table 2.11. Viscoelastic Data for Carbopol 941 1.0% w/w Measured at 28.1×10^{-4} rad. Amplitude.	65
Figure 3.1. The Structural Formula of Xanthan Gum.	73
Figure 3.2. The Structural Formula of 'Carbopol'.	73
Figure 3.3. Precision of Storage Modulus and Dynamic Viscosity Values at High Amplitude Ratio and Low Phase Angle Respectively.	79
Figure 3.4. Basic Principles of the 'Rheomat 30' Viscometer.	81
Figure 3.5. The Effect of the Frequency of Oscillation on the Storage Modulus of Various Concentrations of Xanthan Gum Solutions.	84
Figure 3.6. The Effect of the Frequency of Oscillation on the Dynamic Viscosity of Various Concentrations of Xanthan Gum Solutions.	85
Figure 3.7. The Effect of the Concentration of Xanthan Gum in Solution on the Viscoelastic Parameters at Oscillation Frequency $\omega = 2.5 \text{ rad s}^{-1}$.	86
Figure 3.8. The Effect of the Frequency of the Oscillation on the Loss Tangent of Various Concentrations of Xanthan Gum Solution.	88
Figure 3.9. The Effect of the Concentration of Xanthan Gum in Sodium Alginate 5% w/w Solution on the Storage Modulus, plotted as a function of the Frequency of Oscillation.	89
Figure 3.10. The Effect of Concentration of Xanthan Gum in Sodium Alginate 5% w/w Solution on the Storage Modulus, plotted as a function of the Frequency of Oscillation.	90

	<u>Page</u>
Figure 3.11. The Effect of Concentration of Xanthan Gum in Sodium Alginate 5% w/w Solution on the Dynamic Viscosity, plotted as a function of the Frequency of Oscillation.	91
Figure 3.12. The Effect of Concentration of Xanthan Gum in Sodium Alginate 5% w/w Solution on the Dynamic Viscosity, plotted as a function of the Frequency of Oscillation.	92
Figure 3.13. The Effect of Concentration of Xanthan Gum in Sodium Alginate 5% w/w Solution on Dynamic Viscosity and Storage Modulus at Oscillation Frequency $\omega = 2.5 \text{ rad s}^{-1}$; Industrial Laboratory Scale Preparation.	93
Figure 3.14. The Effect of the Concentration of Sodium Alginate in Xanthan Gum 2% w/w Solution on the Storage Modulus, plotted as a function of the Frequency of Oscillation.	94
Figure 3.15. The Effect of the Concentration of Sodium Alginate in Xanthan Gum 2% w/w Solution on the Dynamic Viscosity, plotted as a function of the Frequency of Oscillation.	96
Figure 3.16. The Effect of Concentration of Sodium Alginate in Xanthan Gum 2% w/w Solution on Dynamic Viscosity and Storage Modulus at Oscillation Frequency $\omega = 2.5 \text{ rad s}^{-1}$, and the Effect of High Shear.	97
Figure 3.17. The Effect of the Concentration of Xanthan Gum in Alginate 5% w/w Solution on the First Order Rate Constant for the Decreasing Sedimentation Ratio.	98
Table 3.1. The Effect of Storage Time at 20°C on the Sedimentation Ratios of Xanthan Gum Solution in Sodium Alginate 5% w/w Solution Before and After Shearing.	101

	<u>Page</u>
Figure 3.18. The Effect of the Shearing Time on the Storage Modulus, of a Solution containing Xanthan Gum 2% w/w and Sodium Alginate 5% w/w, plotted as a function of the Frequency of Oscillation.	103
Figure 3.19. The Effect of the Shearing Time on the Dynamic Viscosity, of a Solution containing Sodium Alginate 5% w/w, plotted as a function of the Frequency of Oscillation.	104
Figure 3.20. Percentage Increases in Storage Modulus, and Dynamic Viscosity, at $\omega = \text{rad s}^{-1}$ as a function of the Shearing Time of a Xanthan 2%, Alginate 5% w/w mix.	106
Figure 3.21. The Effect of the Frequency of Oscillation on the Dynamic Viscosity, and Storage Modulus, of Various Concentrations of Carbopol 934P Gels.	107
Figure 3.22. The Effect of the Concentration of Carbopol 934P on the Storage Modulus, at Oscillation Frequency, $\omega = 2.5 \text{ rad s}^{-1}$.	108
Figure 3.23. The Effect of the Concentration of Carbopol 934P on the Continuous Shear Rheological Parameters: f and b_v .	110
Figure 3.24. The Effect of the Concentration of Carbopol 934P in Sodium Alginate 3% w/w Solution on the Storage Modulus, plotted as a function of the Frequency of Oscillation.	111
Figure 3.25. The Effect of the Concentration of Carbopol in Sodium Alginate 3% w/w Solution on the Dynamic Viscosity, plotted as a function of the Frequency of Oscillation.	112
Figure 3.26. The Effect of the Concentration of Carbopol in Sodium Alginate 3% w/w Solution on Storage Modulus and Dynamic Viscosity at Oscillation Frequency $\omega = 2.5 \text{ rad s}^{-1}$.	113

	<u>Page</u>
Figure 3.27. The Effect of the Concentration of Alginate in Carbopol 0.8% w/w Solution on the Storage Modulus, plotted as a function of the Frequency of Oscillation.	114
Figure 3.28. The Effect of the Concentration of Alginate in Carbopol 0.8% w/w Solution on the Dynamic Viscosity, plotted as a function of the Frequency of Oscillation.	115
Figure 3.29. The Effect of the Concentration of Alginate in Carbopol 0.8% w/w Solution on Storage Modulus and Dynamic Viscosity at Oscillation Frequency, $\omega = 2.5 \text{ rad s}^{-1}$.	116
Figure 3.30. The Effect of the Concentration of Alginate in Carbopol 0.6% w/w Solution on the Continuous Shear Rheological Parameters η_{∞} and f .	117
Figure 3.31. The Effect of the Shearing Time of Carbopol 0.6% w/w Gel on the Continuous Shear Rheological Parameters η_{∞} and b_v .	121
Table 3.2. Effect of Shearing Time on the Continuous Shear Rheological Parameters of Carbopol 0.6% w/w and the Effect of Alginate.	119
Figure 3.32. The Effect of the Frequency of Oscillation, on the Storage Modulus, of Proprietary Oral Liquid Preparations, I to VII.	122
Figure 3.33. The Effect of the Frequency of Oscillation, on the Storage Modulus, of Proprietary Oral Liquid Preparations, VIII to XV.	123
Figure 3.34. The Effect of the Frequency of Oscillation, on the Dynamic Viscosity, of Proprietary Oral Liquid Preparations, I to VII.	125
Figure 3.35. The Effect of the Frequency of Oscillation, on the Dynamic Viscosity, of Proprietary Oral Liquid Preparations, VIII to XV.	127

	<u>Page</u>
Figure 3.36. The Effect of the Frequency of Oscillation, on the Loss Tangent, of Proprietary Oral Liquid Preparations, I to VII.	129
Figure 3.37. The Effect of the Frequency of Oscillation, on the Loss Tangent, of Proprietary Oral Liquid Preparations, VIII to XV.	130
Table 3.3. Key to Figures 3.30. through 3.35. for Storage Modulus, Dynamic Viscosity and Loss Tangent curves of Proprietary Oral Liquid Preparations.	131
Figure 3.38. The Effect of Aging time at 50°C on the Storage Modulus, of Formulation XI plotted as a function of the Frequency of Oscillation.	135
Figure 3.39. The Effect of Aging time at 50°C on the Dynamic Viscosity, Formulation XI plotted as a function of the Frequency of Oscillation.	136
Figure 3.40. The Effect of Aging time at 50°C on the Storage Modulus, of Formulation IV plotted as function of the Frequency of Oscillation.	137
Figure 3.41. The Effect of Aging time at 50°C on the Dynamic Viscosity, of Formulation IV plotted as a function of the Frequency of Oscillation.	138
Table 3.4. Reproducibility of Amplitude Ratio and Phase Angle measurements of Three Batches of 'Calpol' Suspension in Oscillatory Shear.	134
Figure 3.42. Comparison of Dynamic and Steady Shear Viscosities; Absolute Value of Complex Viscosity against Frequency, and Apparent Viscosity against Shear Rate.	140
Figure 4.1. Scheme for the Planar Diffusion of a Drug from a Donor Phase Matrix to a Sink.	145

	<u>Page</u>
Figure 4.2. Algorithm for the Determination of the Fractions Released according to the Three Diffusion Equations.	155
Table 4.1. Listing of the Double Precision Fortran IV Programme for Calculating the Fractions Released, according to the Three Diffusion Equations.	156
Figure 4.3. The Fraction of Drug Released by Planar Diffusion to a Perfect Sink; the Short-time Approximation, the Rigorous Solution and the Long-time Approximation.	159
Table 4.2. Results of Numerical Analysis using the Programme Listed in Table 4.1.	158
Table 4.3. Diffusional Data used for the First Order Plot of Figure 4.4.	162
Figure 4.4. First Order Plot of the Actual Fraction of Drug Released by Planar Diffusion into a Perfect Sink.	161
Figure 5.1. Partitioning of a Weak Acid.	174
Figure 5.2. Apparatus for the Determination of Diffusion Coefficients of Ibuprofen Through Alginate Gel.	177
Figure 5.3. The Hydrolysis of Glucono- δ -Lactone in Water.	184
Figure 5.4. A Typical HPLC Trace for Ibuprofen Assay in n-Octanol: Methanol, 1:1.	190
Table 5.1. Results for the Determination of the Ionised and Unionised Partition Coefficients of Ibuprofen.	192
Figure 5.5. Determination of the Ionised and Unionised Partition Coefficients of Ibuprofen in water/ n-Octanol at 25°C.	193

	<u>Page</u>
Table 5.2. The Concentration of Ibuprofen in the Gel Phase as a function of the Distance from the Interface.	196
Table 5.3. Experimental Data for the Diffusion of Ibuprofen in 0.25 g dl ⁻¹ Alginate Gels.	198
Table 5.4. Experimental Data for the Diffusion of Ibuprofen in 0.5 g dl ⁻¹ Alginate Gels.	199
Table 5.5. Experimental Data for the Diffusion of Ibuprofen in 1.0 g dl ⁻¹ Alginate Gels.	200
Table 5.6. Experimental Data for the Diffusion of Ibuprofen in 3.0 g dl ⁻¹ Alginate Gels.	201
Table 5.7. Experimental Data for the Diffusion of Ibuprofen in 5.0 g dl ⁻¹ Alginate Gels.	202
Figure 5.6. The Amount Released per Unit Area plotted against (Time) ^{1/2} for the Diffusion of Ibuprofen in a 5.0 g dl ⁻¹ Alginate Gel.	203
Figure 5.7. Drug Release Profile for the Diffusion of Ibuprofen from a 5.0 g dl ⁻¹ Alginate Gel to a n-Octanol Sink.	205
Table 5.8. Results of Least Mean Square Linear Regression Analysis of Data for the Amount of Ibuprofen Released per Unit Area against (Time) ^{1/2} .	206
Table 5.9. Summary of Results for the Diffusion of Ibuprofen in Calcium Alginate Gels.	207
Table 5.10. The Effect of the Concentration of Glucono-δ-Lactone on the pH and Gelation of Calcium Alginate Gels.	209

	<u>Page</u>
Table 5.11. The Effect of the Concentration of Alginate on the pH and Gelation of Calcium Alginate Gels.	209
Figure 5.8. The Effect of the Concentrations of Glucono- δ -Lactone and Alginate on the pH of Calcium Alginate Gels.	210
Table 5.12. Results for the Potentiometric Titration of Alginic Acid according to the Method of Section 5.3.2.2.	211
Figure 5.9. Determination of the Dissociation Constant for Alginic Acid using the Modified Henderson-Hasselbach Equation.	213
Figure 5.10. The Effect of the Frequency of Oscillation on the Storage Modulus and the Dynamic Viscosity of a Calcium Alginate Gel.	215
Table 5.13. The Storage Modulus, $G'(\omega)$ of 3.0 g dl^{-1} Alginate Gels as a function of the Calcium Ion Concentration.	216
Figure 5.11. The Effect of the Frequency of Oscillation on the Storage Modulus of a Calcium Alginate Gel showing the Effect of the Natural Frequency.	217
Table 5.14. Summary of the Results for Gel Rigidity as a function of Calcium Ion Concentration.	218
Figure 5.12. The Effect of Calcium Ion Concentration on the Storage Modulus of 3.0 g dl^{-1} Alginate Gels.	219
Table 5.15. The Effect of Alginate Concentration on the Storage Modulus of Calcium Alginate Gels containing 50 mMol Ca^{2+} .	221
Table 5.16. Summary of Results for the Effect of Alginate Concentration on the Storage Modulus for Gels Containing 50 mMol Ca^{2+} .	222

	<u>Page</u>
Figure 5.13. The Effect of Alginate Concentration on the Storage Modulus of Gels Containing 50 mMol Ca^{2+} .	213
Table 5.17. Sample Set of Experimental Data for the Diffusion of Ibuprofen through a Calcium Alginate Gel.	225
Figure 5.14. Experimental Data for Drug Release by Diffusion: The Fraction Released Plotted as Square Root of Time and First Order Relationships.	226
Figure 5.15. Partial Molal Volume of Ibuprofen from Substituent Values.	227

1.

INTRODUCTION

1.1 Background

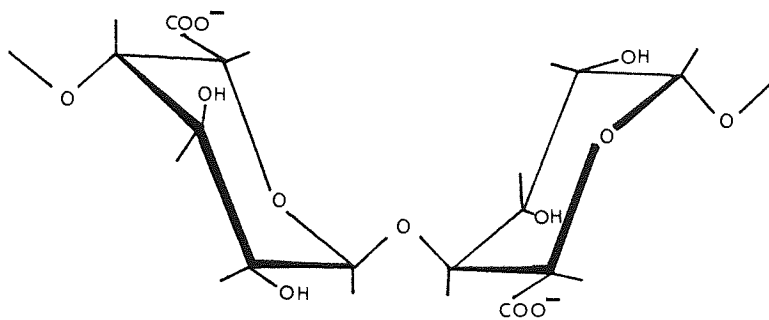
Alginate systems are capable of displaying a very wide range of physicochemical properties. The polyuronate copolymer molecules of Alginate are used mainly because of their ability to form viscous solutions, to bind divalent metal ions and to form gels. These characteristics have found wide application in many commercial areas, particularly in the food industry, eg. for enhancing viscosity, stabilising emulsions and gelling (1). The range of uses in pharmaceuticals and cosmetics is second only to the uses in foods. Alginates have been used as binders in compressed tablets (2), thickeners for suspensions (3) and in fibre form as haemostatic and absorbable dressings (4).

Alginate is a polyuronate derived from brown algae seaweed of the genus Phaeophyceae; Alginate is the principal carbohydrate component. Agar and Carrageenan possess similar gelling characteristics but are extracted from red seaweed. The acid form of Alginate, ie, Alginic acid is a block copolymer of mannuronic and guluronic acids, M and G respectively. Many of the physicochemical properties change with the relative proportion of M and G residues present in Alginate extracted from different species of Phaeophyceae (5). In the coastal waters around the British Isles, the most common species are Laminaria and Ascophyllum.

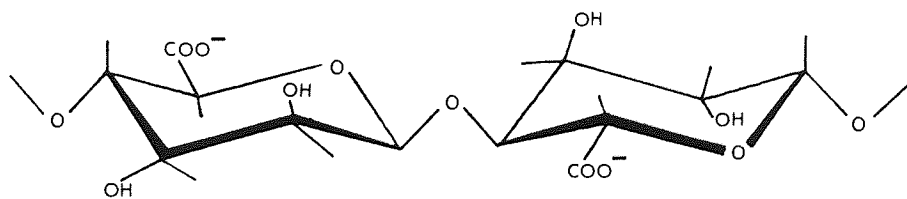
In the 1880's, Stanford first isolated and investigated Alginic acid and its salts with several metals (6). He thought that Alginate contained nitrogen but this was probably due to the presence of amino acids following inadequate purification. This was confirmed by Hoagland and Lieb in 1915 (7) who proposed $H_2 (C_{21} H_{25} O_{20})$ as the formula for Alginic acid. After the discovery in 1926 that uronic acid, $C_6 H_{10} O_7$, was present (8, 9), investigations soon demonstrated the present of D-mannuronic acid (10, 11). Hirst et al in 1939 (12) first showed the molecule to be built up of 1,4 - glycosidic linkages but it was not until the chromatographic studies of Fischer and Dörfel in 1955 (13) that the presence of L-guluronic acid was established. Hirst and coworkers (14) then proved that M and G units were present in the same molecule.

Following this, comprehensive studies by Haug and others (5) at the Norwegian Institute of Seaweed Research examined the block copolymer nature of Alginate mainly from a chemical view-point. This work firmly established Alginate as being composed of 1,4 - linked α ,L-guluronate and β ,D-mannuronate as shown in Figure 1.1..

Figure 1.1. The Structures of α ,L-Guluronate and β ,D-Mannuronate.



α ,L-Guluronate



β ,D-Mannuronate

1.2 Ion-Binding Properties of Alginate

The detailed chemical data for Alginate provided by Haug paved the way for other studies to apply the information to ion-binding, gelling and molecular conformation. Much of this work was carried out by Smidsrød at the same Institute (15).

All monovalent metal ion salts of Alginate are soluble except Silver, and Sodium Alginate is the most common form. All divalent metal ions except Magnesium form either insoluble salts or gels and of these, Calcium Alginate is the most commonly used. Many of the commercial applications of Alginate depend on its ability to bind Ca^{2+} ions to form gels and work in this field is of considerable interest (16, 17). One important finding of ion-exchange experiments is that the affinity of Alginates for divalent metal ions increases with increasing content of α , L-gulonate residues (18, 19). Smidsrød (15) defined a selectivity coefficient $K_A^B = \frac{X_A^B}{X_A^A} \cdot \frac{C_B^A}{C_B^B}$ where X_A^B represents the ratio of the bound fraction of incoming ion B to the bound fraction of outgoing ion A, and C_B^A represents the ratio of the concentrations of the ions A and B. Thus a high K_A^B indicates a high affinity of Alginate for ion B. He studied the exchange of Ca^{2+} for Mg^{2+} ions which resulted in a reduction of Alginate in the soluble fraction. It was found that $K_{\text{Mg}}^{\text{Ca}}$ increased with the fraction of bound Ca^{2+} ions and Smidsrød suggested an auto-cooperative inter-chain binding mechanism whereby an initial $\text{G} - \text{Ca}^{2+} - \text{G}$ linkage

promotes the formation of further linkages by steric advantage. The strength of the inter-chain binding is proportional to the rigidity of the resulting gel; this was shown by binding studies using various divalent metal ions and comparing values of K_A^B with the mechanical strength, (15, 20).

The specificity of Ca^{2+} ions for α , L-gulonate residues was studied by Atkins et al (21) who used experimental X-ray fibre diffraction and theoretical conformational calculations to show that polyguluronate residues required water between the chains for stability. The space so formed meant that it was energetically favourable for guluronate residues to be cross-linked by Ca^{2+} . This finding led to the well known "Egg-box" model of inter-chain binding as visualized by Rees (22). which is illustrated in Figure 1.2..

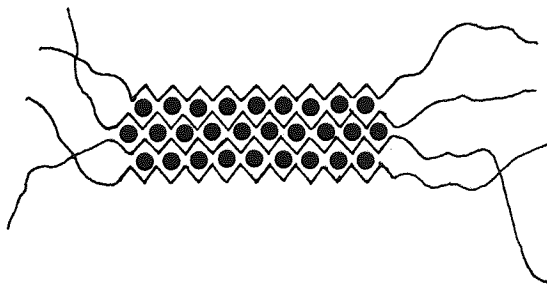



Figure 1.2. The "Egg-box" model for inter-chain binding of Ca^{2+} ions, ●, by polyguluronate,  .

A recent review of polyuronate conformation and ion-binding by Kohn (23) showed that the "Egg-box" model provides a useful representation of inter-chain binding. These binding sites are probably heterogeneous since the chains are unable

to pack into perfectly alligned dimers (20), but regular packing as suggested by the "Egg-box" model, is thought to be the main reason for high chain inflexibility, (24).

Intra-chain binding, although probably less significant in terms of gel rigidity, is more closely defined. It has been shown (25, 26) that single chain segments utilize a binding site composed of COO^- , O(5), O(4) in one guluronate residue and O(2), O(3) of the preceding unit.

1.3 Therapeutic Aspects

In addition to their role in pharmaceutical formulation, the properties of Alginate can be of therapeutic advantage in certain circumstances. The use of Alginate in haemostatic and absorbable dressings has already been acknowledged. A particular example of the application of Alginate to therapeutic systems is a formulation of Sodium Alginate or Alginic acid in combination with Calcium Carbonate and Sodium Bicarbonate antacids, which is indicated for the treatment of reflux oesophagitis (27).

The rationale is based on the precipitation of Alginic acid from a Sodium Alginate solution in the low gastric pH. Alginic acid is capable of absorbing several hundred times its own weight of water (28) and thereby a swollen gel-like precipitate is formed. The presence of Ca^{2+} ions may lead to strengthening of the gel by the formation of Calcium Alginate but this has not been demonstrated conclusively. On

precipitation, it is claimed that the Alginate layer forms a physical barrier to reflux (29) and in the event of reflux, the mucosa of the oesophagus is protected by a viscous layer.

Many published studies have shown that marketed formulations of Alginate with antacids are significantly more effective against reflux oesophagitis than either Alginate alone or a placebo (30-35). The formulations contain levels of antacids below the therapeutic dosage and there is little effect on bulk gastric pH. This was demonstrated by pH measurements and was attributed to the viscous nature of the Alginate precipitate (36). The same authors also used an X-ray contrast medium to show that the gel-like precipitate covered the stomach contents for the duration of gastric residence. These findings have been supported by the work of other authors (33, 37).

Any optimization of such a therapeutic system requires the collation of clinical data and a knowledge of the ion-binding and rheological properties of, and mass transfer in, Alginate systems.

1.4 Rheology and Diffusion

In any pharmaceutical formulation containing Alginate, the mechanical characteristics of the gel or viscous solution are of prime importance. In this respect, the rheological and diffusional properties are of particular interest. The two properties are related in the simplest way by the expression

known as the Stokes-Einstein Equation (38):

$$D = \frac{RT}{6 \pi \eta N_{AV} r} \quad 1.1$$

where D = diffusion coefficient.

R = universal gas constant.

T = absolute temperature.

η = viscosity of medium

N_{AV} = Avogadro's number.

r = radius of spherical diffusant.

The derivation and assumptions of Equation 1.1. will be discussed fully in Section 5.2.1.. Clearly, the Stokes-Einstein Equation proposes that the diffusion coefficient is inversely proportional to the viscosity of the medium in which the solute diffuses. However, even for the free diffusion coefficients of solutes in pure solvents, significant deviations from Equation 1.1. have been shown to occur according to the work of Wilke and Chang (39). These authors used a large quantity of experimental data to collate diffusion and viscosity, thereby obtaining an empirical relationship.

The situation can become further complicated by the presence of Alginate and other polymers which are viscoelastic in solution. Here, it appears that there are two problems involved in the correlation of diffusion and viscosity. Firstly, we should change the rheological approach from a

straightforward measurement of apparent viscosity to a method that will quantify both the viscous and the elastic components which comprise viscoelasticity. Secondly, we may need to reappraise the relationship with diffusional properties to take account of the elastic as well as the viscous component of rheological behaviour.

In this thesis, emphasis is placed on the wide range of rheological properties available by using one particular low molecular weight Alginate in combination with other polymeric agents. Clearly, since polyelectrolytes are widely used adjuncts in pharmaceutical formulation, the principle is not restricted to Alginate systems.

By combining various polymers in solution, formulations can be 'tailored' to obtain a certain rheological profile, ie, a viscoelastic balance of viscous and elastic properties. For disperse systems, only recently have relationships been proposed which correlate the settling rate of solid in liquid suspensions with the zero shear viscosity (40) and the modulus of elasticity (41). It is likely that such relationships, which are based on fundamental rheological data (in contrast to semi-empirical measurements of earlier work) will gain widespread use in the search for a non-empirical approach to formulation.

2.

MOLECULAR AND RHEOLOGICAL CHARACTERISTICS
OF ALGINATE SOLUTIONS

2.1. Introduction

Alginates, in common with other hydrophilic polymers such as methylcellulose, polyvinylpyrrolidone and pectin (2) are frequently used in pharmaceutical formulations as thickeners for stabilizing drug suspensions. This study is concerned with the comparison of molecular and rheological properties of Sodium Alginate in order to characterize the polymeric system.

Long polymer chains possess elastic properties when deformed. In solution, this is manifested as viscoelasticity (42) as will be explained in Section 2.2.3.. The flow behaviour of polyelectrolyte solutions is mainly a function of the coiling, or tertiary structure, of the molecule. In the case of Alginate, the chemical composition is highly variable, therefore primary and secondary structures are also important (5). Ionic strength affects the flow behaviour of Alginate (49); salt in solution causes extension of the polyelectrolyte molecule which gives rise to an increase in viscosity (50,51).

As detailed in Section 1, Alginate is a block copolymer comprised of mannuronic, M, and guluronic, G, acids; the relative proportion, or M/G ratio, depends primarily on the species of brown algae used in the extraction (47,48). In addition, the geographical region and season of harvesting can affect the M/G ratio, (46).

Because of the above properties many experimental investigations have been carried out on Alginates in dilute solutions. Smidsrød and Haug performed a considerable amount of work in this field (5,15,20,52), particularly using viscometry. Since viscometry is only an indirect method of molecular weight determination, Smidsrød and co-workers validated many of their results with light scattering data (49,53,54). They showed that Alginate is a highly extended linear flexible coil whereby the guluronic acid imparts the greater contribution to chain rigidity. Several other studies (16,55,56) supplement the work of Smidsrød et al, and the contrast in results is interesting. Table 2.1. gives the collated results from these studies, showing that as the molecular weight of the Alginate increases, the derived parameters do not always follow the expected trend. All determinations were made in 0.1 M NaCl solution.

Table 2.1 Molecular Properties of Sodium Alginate

Weight-average Molecular weight ^a (g mol ⁻¹)	M/G ratio ^b	$(\overline{R}_G^2)^{\frac{1}{2}}$ ^c (nm)	$[\eta]$ ^d (dl g ⁻¹)	Reference
178,000	0.82	-	10.0	55
180,000	1.60	100	8.3	54
180,000	1.60	65	-	49
180,000	9.00	73	-	49
190,000	-	40	9.4	16
257,000	2.72	-	8.8	55
407,500	1.68	-	11.0	55
500,000	0.43	133	-	49
500,000	1.60	105	-	49
525,000	1.60	122	10.1	53
690,000	5.67	200	17.0	56
880,000	0.33	260	25.0	56
1,670,000	19.0	370	28.5	56

- a. Determined from light scattering measurements
- b. Ratio of the mannuronic to guluronic acid content in alginate.
- c. Root-mean-square radius of gyration from light scattering measurements.
- d. Intrinsic viscosity.

Light scattering and viscometry are both methods for which extrapolation to zero concentration is necessary and therefore, very dilute solutions are used to minimize polymer - polymer interactions.

At the other extreme of the concentration range, polymer entanglement is observed (57). The concentration at which entanglement is seen, is entirely dependent on the molecular weight and other such properties of the polymer. Certain details of molecular conformation in entanglements can then be obtained from rheological measurements, (58,59).

However, in the concentration range intermediate between dilute and entangled polymer solutions, viscoelastic phenomena are observed for which interpretation in terms of molecular conformation is possible only for the simplest models (45,60).

In this study, a low molecular weight Alginate was used to contrast the molecular characteristics obtained by viscometry and light scattering, with the rheological properties obtained from continuous shear and oscillatory rheometry.

2.2 Theory

2.2.1 Viscometry

In contrast to the absolute methods of molecular weight determination such as the colligative methods and light scattering, viscometry is a relative method. This is because

the mechanical behaviour measured is only a reflection of the actual molecular dimensions. For this reason, viscometry results should always be calibrated against an absolute method.

Staudinger (61) first showed an empirical relationship between the molecular weight and the specific viscosity, η_{sp} , for polystyrene solutions, given in Equation 2.1.

$$\eta_{sp}/c = K_m M \quad 2.1.$$

where $\eta_{sp} = \eta_r - 1 = (\eta/\eta_0) - 1$

η_r = relative viscosity

η = solution viscosity

η_0 = solvent viscosity

K_m = constant

M = molecular weight

c = concentration of polymer in solvent

By extrapolation to zero concentration, the intrinsic viscosity is obtained, ie $[\eta] = (\eta_{sp}/c)_{c \rightarrow 0}$, representing the capacity of a polymer to enhance the viscosity. The so-called modified Staudinger Equation is then obtained from Equation 2.1.

$$[\eta] = K_m M_\eta^\alpha \quad 2.2$$

where M_η = viscosity average molecular weight

α = exponent

It should be noted that $M_\eta = M_w$, the weight-average molecular weight, only when the exponent, $\alpha = 1.0$ (62). Although this

equation was developed empirically, theoretical justification was later shown for random coil structure by Kuhn (65), Huggins (66) and Kramer (67), notably for theta conditions where the exponent $\alpha = 0.5$ (68). This gives Equation 2.3.

$$[\eta]_{\theta} = K_{\theta} M_{\eta}^{0.5} \quad 2.3.$$

In practice, theta, θ , conditions are achieved at a particular critical temperature and in a particular solvent system such that there are negligible polymer-solvent interactions. Hence, the polymer exists in an unperturbed state. If theta conditions have not been determined, as is the case for Alginate, the best approximation is achieved by measuring $[\eta]$ at increasing ionic strength, μ , and then extrapolating to $\mu = \infty$

The unperturbed dimensions have been frequently determined in this manner (52,69,70). It is thought that the polyelectrolyte is in an effectively uncharged state at $\mu = \infty$ because the salt swamps the fixed charges on the polymer so that the mutual repulsion between polymer and solvent is effectively removed. Smidsrød found that for Alginate, $[\eta]$ at $\mu = \infty$ was quite high and corresponded to an exponent α value of 0.84, (20,71).

The deviation of the exponent α from 0.5 gives a measure of the extension of the polymer. As a guide, if $\alpha = 0.5 - 0.8$, the molecules are randomly coiled; $0.8 - 1.8$ indicates a stiffly coiled molecule and 1.8 a rigid rod, (72).

Flory and Fox pointed out that $[\eta]$ should be proportional to the ratio of the volume occupied by the molecule and the

molecular weight, (75,76). This is encompassed in Equation 2.4. (32):

$$[\eta] = \frac{\Phi (\bar{r}^2)^{3/2}}{M \eta} \quad 2.4.$$

where Φ = Flory constant

$$\Phi = 0.01588 (\pi/6)^{3/2} \cdot N_{av} = 3.62 \times 10^{21}$$

N_{av} = Avogadro's number

$(\bar{r}^2)^{1/2}$ = Root-mean-square end-to-end distance of chain (cm).

It was originally claimed that Φ is independent of the characteristics of the molecule provided it is a random coil. However, other values of $\Phi = 2.0 \times 10^{21}$ (77) and $\Phi = 2.86 \times 10^{21}$ (78) have been determined. Bloomfield and Zimm (79) introduced the expansion factor ϵ to express the deviation of a polymer chain from the dimensions defined by a Gaussian distribution. They considered deviations due to excluded volume (free draining) effects, polyelectrolyte (non-draining) effects, or mechanical chain stiffness. From a knowledge of ϵ , values of the Flory constant $\Phi(\epsilon)$ can be calculated using Equation 2.5.

$$\Phi(\epsilon) = 2^{-\epsilon/2} N_{av} (2\pi^3)^{1/2} (6 + 5\epsilon + \epsilon^2)^{1/2} \frac{1}{24} \left(\sum \lambda'_k{}^{-1} \right) \quad 2.5.$$

where $\epsilon = \frac{(2\alpha - 1)}{3}$ from Elias (67)

$\sum \lambda'_k{}^{-1}$ = summed reciprocal eigenvalues

Values of $\Phi(\epsilon)$ were tabulated by Bloomfield and Zimm (79) and range from 2.81×10^{21} for $\epsilon = 0$ to 0.686×10^{21} for $\epsilon = 0.5$, in straight chain polymers.

2.2.2 Light Scattering

The use of light scattering as a technique for studying the molecular properties of polymer solutions is well established (73,80,81). In 1871, Lord Rayleigh (82) first showed that the intensity of light scattered by small particles in gases is inversely proportional to the fourth power of the wavelength of incident light. The theoretical application of this principle to molecules in solution is due to Mie in 1908 (83) and Einstein in 1910 (84); the practical development of this theory was carried out by Debye from 1944 (85,86). It was found that the intensity of light scattered by a polymer solution is related to its molecular mass, M_w , by Equation 2.7.

$$\frac{Kc}{R_\theta} = \frac{1}{M_w} + 2Bc + 3Cc^2 + \dots \quad 2.7.$$

where c = concentration

$$K = \frac{2\pi^2 n_0^2}{N_{av} \lambda_0^4} \left(\frac{dn}{dc} \right)^2 \quad 2.8.$$

dn/dc = refractive index increment of polymer solution.

n_0 = refractive index of solvent.

λ_0 = wavelength of incident beam.

$$R_\theta = \text{Rayleigh ratio} = \frac{r^2 i_\theta}{I_0 (1 + \cos^2 \theta)} \quad 2.9.$$

i_θ = intensity of light scattered at angle θ at a distance r between sample and observation port.

I_0 = intensity of incident radiation

B = Second virial coefficient

C = Third virial coefficient

The expression is greatly simplified on extrapolation to zero concentration and angle.

$$\left[\frac{Kc}{R_\theta} \right]_{\substack{\theta \rightarrow 0 \\ c \rightarrow 0}} = \frac{1}{M_w} \quad 2.10.$$

In the case of the 'SOFICA' light scattering instrument used in this study, benzene was employed as a standard for converting the instrument meter reading to absolute scattering intensity by Equation 2.11. (87):

$$R_\theta = R_b \left(\frac{\alpha I_\theta}{I_b} \right) \left(\frac{n}{n_b} \right)^2 \quad 2.11.$$

$$\text{where } \alpha = \frac{\sin \theta}{1 + \cos^2 \theta} \quad 2.12.$$

$$R_b = \text{Rayleigh ratio of benzene at } 25^\circ \text{ C} \\ = 16.3 \times 10^{-6} .$$

$$I_b = \text{Galvanometer deflection for benzene}$$

$$I_\theta = \text{Galvanometer deflection for solution in excess of the solvent contribution} = \\ i_\theta - I_0 .$$

$$n = \text{refractive index of solution}$$

$$n_b = \text{refractive index of benzene.}$$

$$\sin \theta = \text{correction factor for converting scattering volume viewed at angle } \theta \text{ into that at } 90^\circ .$$

$$1 + \cos^2 \theta = \text{correction for use of unpolarised light.}$$

By substituting R_θ in Equation 2.11. into Equation 2.10 we obtain

$$\frac{2\pi^2 n_b^2}{N_{av} \lambda_0^4 R_b} \left(\frac{dn}{dc} \right)^2 (I_b) \left[\frac{c}{\alpha I_\theta} \right]_{\substack{\theta \rightarrow 0 \\ c \rightarrow 0}} = \frac{1}{M_w} \quad 2.13$$

The terms N_{av} , R_b , n_b and λ_0 are all independent of the polymer-

solvent system and can be substituted to obtain

$$0.506 \left(\frac{dn}{dc} \right)^2 (I_b) \left[\frac{c}{\alpha I_\theta} \right]_{\substack{\theta \rightarrow 0 \\ c \rightarrow 0}} = \frac{1}{M_w} \quad 2.14.$$

where

$$\begin{aligned} n_b &= 1.496 \\ \lambda_0 &= 54.61 \times 10^{-6} \text{ cm} \\ N_{av} &= 6.023 \times 10^{23} \end{aligned}$$

By plotting the experimental data as a Zimm plot of $c/\alpha I_\theta$ against $\sin^2 \theta/2 + kc$ where k is an arbitrary constant, then extrapolations to zero concentration and zero angle are possible. Hence, M_w is obtained from Equation 2.14. Other parameters which can be determined are the root-mean-square radius of gyration $(R_G^2)^{1/2}$ from Equation 2.15. and second virial coefficient, B , from Equation 2.16.

$$(R_G^2)^{1/2} = \frac{3\lambda}{2\pi\sqrt{2}} \left[\frac{\text{Slope of line } c = 0}{\text{intercept}} \right]^{1/2} \quad 2.15.$$

where

$$\lambda = \frac{\lambda_0}{n_0}$$

$(R_G^2)^{1/2}$ is defined as the root-mean-square distance of any element of a molecule from the centre of gravity of that molecule.

$$B = 0.506 \left(\frac{dn}{dc} \right)^2 (I_b) \frac{(\text{Slope of line } \theta = 0)}{2} \quad 2.16.$$

The second virial coefficient is frequently neglected in molecular studies because it relates not to molecular dimensions, but to the thermodynamics of the solvent with respect to the polymer it contains (86). In an ideal solution, there is no change in the properties of polymer or solvent on

mixing and B is negligible. Therefore B provides a measure of the closeness to ideality and of the accuracy of the extrapolation used to obtain Equation 2.10. from Equation 2.7.. B decreases with M_w (87) and with ionic strength (74).

Another molecular parameter frequently used by Smidsrød (15,20,52,53) is the Kuhn statistical segment, A_m , introduced by Kuhn in 1951 (88) to model a molecule in terms of N_m straight chain segments, each of length A_m .

If the mean-square end-to-end distance of the molecule is \bar{r}^2 , then A_m is given by Equation 2.17.

$$A_m = \frac{\bar{r}^2}{b_0 P} \quad 2.17.$$

where P = degree of polymerisation

and b_0 = monomer length

$b_0 = 5.15 \times 10^{-8}$ cm for each uronic acid residue (89).

\bar{r}^2 can be related to the radius of gyration obtained from light scattering experiments by:

$$R_G^2 = \frac{\bar{r}^2}{6} \quad 2.18.$$

It is now clear that a considerable amount of information about the molecular characteristics of Alginate can be obtained from viscometric and light scattering studies.

2.2.3 Rheology

In rheological studies of materials, there are three basic experimental methods available, namely continuous shear, creep

compliance and oscillatory testing (43,90). The principles, derived parameters and illustrations of the data obtained for each method are summarised in Table 2.2. and Figure 2.1.. The continuous shear technique is distinguished from the other two methods by its inability to fully characterise materials of a viscoelastic nature. Firstly, it is necessary to understand the term viscoelasticity.

Hooke's law of elasticity and Newton's law of viscosity explain the two extremes of flow behaviour. However, there are numerous materials, many of pharmaceutical interest such as ointments, gels and suspensions, (91), whose flow behaviour follows neither classical hypothesis, except perhaps at infinitesimal rates of strain for predominantly viscous materials or at infinitesimal strains for predominantly elastic materials. Such materials are termed viscoelastic since they possess both viscous and elastic properties. If the material does not continually deform when stress is applied, then it is a viscoelastic solid; otherwise it is known as a viscoelastic liquid.

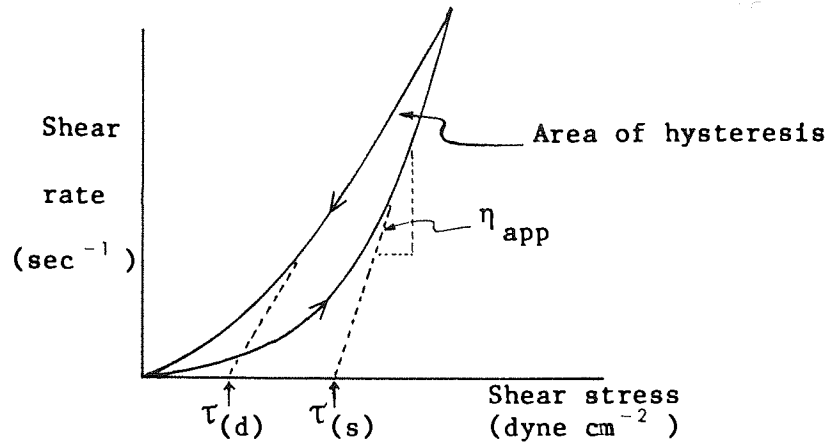
The shortcomings of the continuous shear testing method therefore arise from the inability to measure elastic components. For pharmaceutical materials especially, these inadequacies have been listed elsewhere by Barry (91) and Davis (92,93). The readings obtained from a continuous shear 'rheogram' do not provide fundamental rheological parameters; they measure the stresses that occur as the structure is

Table 2.2. Principles and Parameters of Rheological Testing

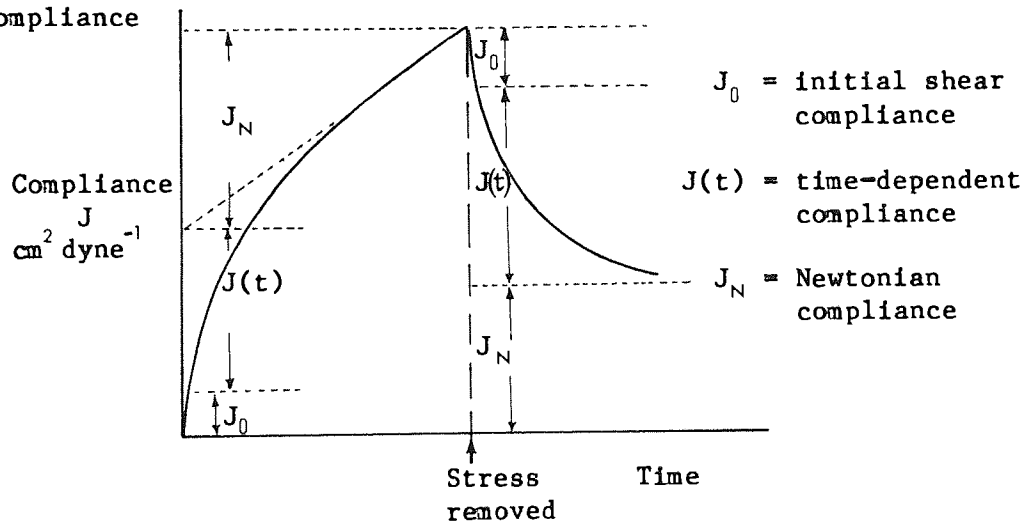
Method	Input Function	Output Function	Protocol	Parameters obtained	Traditional Units	Equivalent S.I. Units
Continuous Shear	Rate of Strain	Stress	Sample is sheared between two surfaces	Apparent Viscosity Apparent Yield Values i. dynamic $\tau(\dot{\gamma})$ ii. static $\tau(s)$ Area of hysteresis loop.	Poise Dyne cm^{-2}	10^{-1} Pa s 10^{-1} Nm ⁻²
Creep Compliance	Stress	Strain	Stress is applied to one of the surfaces in contact with the sample.	Compliance $J(t)$ (reciprocal elasticity) Retardation times	$\text{cm}^2 \text{ dyne}^{-1}$ S	$10^1 \text{ m}^2 \text{ N}^{-1}$ S
Oscillatory Testing	Strain	Stress	Sinusoidally oscillating signal of low amplitude is applied to one surface	Real and Imaginary Moduli G' and G'' Real and Imaginary Viscosities η' and η''	Dyne cm^{-2} Poise	10^{-1} Nm ⁻² 10^{-1} Pa s

Figure 2.1 The Form of Experimental Data from Rheological Testing

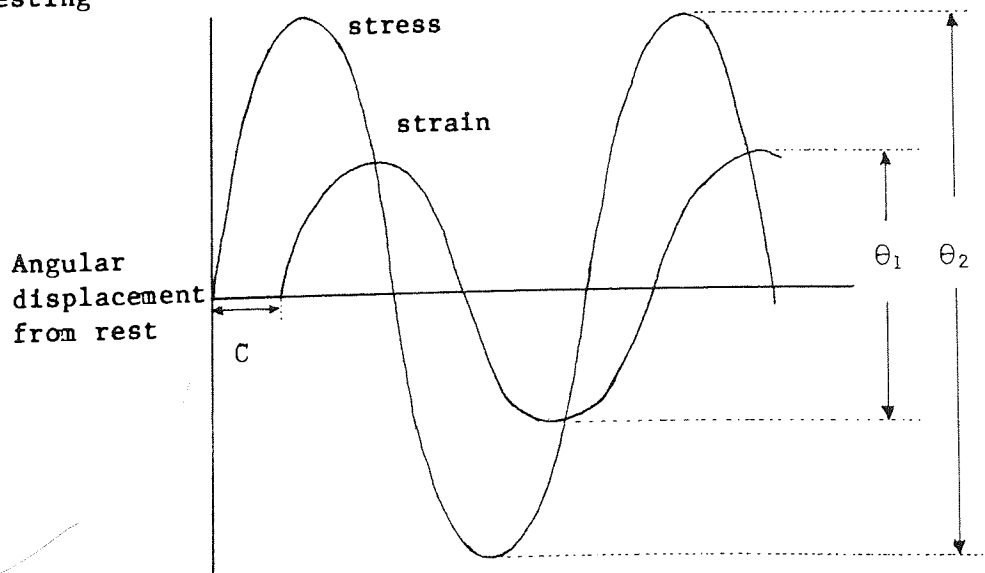
a. Continuous Shear



b. Creep Compliance



c. Oscillatory testing



C = Phase difference between stress and strain waves.

ν = Amplitude ratio = θ_1/θ_2

broken down. The parameters derived are often only of use in comparative studies. Many theories have been proposed in attempts to overcome this problem, by fitting of the non-Newtonian flow-curve to various equations and often ascribing physical significance to certain coefficients. Notable examples are summarised in Table 2.3.. Cheng (100) has suggested that such semi-empirical equations should be used freely to allow the best possible expression of continuous shear data for comparative purposes.

Table 2.3 Quantitative Descriptions of Non-Newtonian Behaviour

Equation	Parameters	Reference
$\tau = k\dot{\gamma}^N$	k and N are empirical constants	Metzner (94)
$\tau = \tau_y + \eta_p \dot{\gamma}$	Yield value = τ_y Plastic viscosity = η_p	Bingham (95)
$\tau^{\frac{1}{2}} = \tau_y^{\frac{1}{2}} + k\dot{\gamma}^{\frac{1}{2}}$	Yield value = τ_y Empirical constant = a	Casson (96)
$\tau = f + \eta_{\infty} \dot{\gamma} - b_v e^{-a\dot{\gamma}}$	Yield value = $f - b_v$ Infinite shear viscosity = η_{∞} Empirical constant = a	Shangraw <u>et al</u> (97)
$\tau = \eta_{\infty} \dot{\gamma} + f(1 - e^{-a\dot{\gamma}})$	As above but yield value = 0	Yakatan <u>et al</u> (98)
$\eta_{app} = \eta_{\infty} + \left(\frac{\eta_0 - \eta_{\infty}}{1 + \alpha \dot{\gamma}^{2/3}} \right)$	Zero Shear viscosity = η_0 Empirical constant = α	Cross (99)

Creep compliance testing has not been used in this study of Alginate solutions and gels and will not be discussed in detail. Suffice it to say that $J(t)$ can be analysed in terms of Maxwell and Voigt mechanical models thereby giving various retardation times. A retardation time gives a measure of the relaxation of strain on removal of stress. The technique has been widely applied to pharmaceuticals in general (91,101-103) and has also been used for Alginate gel systems by Mitchell and Blanchard, (104,105).

In oscillatory testing, the experimental data is obtained in terms of the amplitude ratio, ν and the phase difference, C as shown in Figure 2.1.c. The instrument used in this study was the Weissenberg Rheogoniometer described in Section 2.3.4.2.. The theory for forced oscillatory testing developed by Walters and Kemp (106) is most readily illustrated for the parallel plate geometry (107,108). During testing, when the sample behaves as a perfectly elastic solid, then the phase difference between the two surfaces is zero and the energy is stored; a perfectly viscous liquid would give a phase difference of $\pi/2$ rad between input and output, and the energy involved is dissipated as heat. Because of the difficulty in expressing viscous and elastic components in one term, convention dictates that complex variables be used. Hence, we obtain the complex modulus of elasticity G^* and the complex viscosity η^* , (43,90), given by Equations 2.19 and 2.20 respectively.

$$G^* = G' + iG'' \quad 2.19$$

$$\eta^* = \eta' - i\eta'' \quad 2.20$$

where G' = storage modulus
 G'' = imaginary or loss modulus = $\eta' \omega$
 η' = dynamic viscosity
 η'' = imaginary viscosity = G' / ω
 ω = radian frequency = $2\pi n_f$
 n_f = frequency of oscillation in Hz.

The theory for parallel plate geometry (106) gives the result:

$$\frac{\exp^{iC}}{\nu} = \cos \alpha h + S \alpha h \sin \alpha h \quad 2.21.$$

$$\text{where } S = \frac{2}{\pi \rho a^4 h} \left(\frac{K}{4\pi^2 n_f^2} = I \right) \quad 2.22.$$

$$\begin{aligned}
 I &= \text{moment of inertia of instrument members} \\
 &= \frac{K_t}{4\pi^2 n_a^2}
 \end{aligned}$$

ρ = density of sample

a = radius of platen

h = gap between parallel plates

K_t = torsion bar constant for the instrumental
in dyne cm μm^{-1}

n_a = free oscillation frequency of torsion bar,
ie, in air.

$$\alpha = \frac{-i\omega\rho}{\eta^*} \quad 2.23.$$

α = "fundamental inertia parameter"

$$i = \sqrt{-1}$$

Expression of Equation 2.21 in terms of α and substitution of η' for η^* in Equation 2.23 should allow the derivation of η' from experimental ν and C values. In practice this is

a difficult mathematical manoeuvre (106) but fortunately, approximate equations for η' and G' are available provided that $\alpha h \ll 1$ (107).

$$\eta' = \frac{-2\pi n_f \rho S h^2 \nu \sin C}{(-2 \cos C + 1)} \quad 2.24.$$

$$G' = \frac{4\pi^2 n_f^2 \rho S h^2 \nu (\cos C - \nu)}{(\nu^2 - 2\nu \cos C + 1)} \quad 2.25.$$

α is a fundamental parameter which is dependent on the inertia present in a sample during a test. High frequencies used for thin fluids result in high values of α ; low α values occur at lower frequencies (thick fluids). Walters and Kemp (106) showed that for a Newtonian liquid of viscosity 0.1 poise, the neglect of fluid inertia in the αh term leads to significant errors only at frequencies above n_a , the natural frequency of the rheogoniometer torsion bar. It therefore seems reasonable that measurement of samples showing viscosities greater than 0.1 poise at frequencies below n_a should not lead to significant errors caused by neglect of fluid inertia.

Oscillatory testing leads to the expression of η' and G' as functions of the frequencies ω , ie, $\eta(\omega)$ and $G'(\omega)$. These are the relationships which describe the viscoelasticity.

In conclusion it should be noted that the three methods of rheological testing may be inter-related. Values of $J(t)$ can be determined from a knowledge of $G'(\omega)$ and vice-versa (44).

Cox and Merz proposed an empirical rule to relate the apparent viscosities at known shear rates to the absolute values of the complex viscosity at corresponding frequencies (109). Similar theories have followed (110,111) and recently, Williams (112) has suggested a method of obtaining viscometric data from a 'Brookfield' continuous shear viscometer.

2.3 Materials and Methods

The Sodium Alginate used was Protanal LFR5/60¹ which is a low molecular weight grade produced by degradation of Alginate from Laminaria hyperborea stipes.

2.3.1 Viscometry

Viscometry measurements were carried out using a U-tube viscometer² immersed in a water bath at $25 \pm 0.1^{\circ}$ C. In order to determine η_{sp} values to an accuracy of $\pm 1\%$, alginate concentrations were chosen such that $1.2 < \eta_r < 2.0$ relative to the calibration standard of water (28). Solutions were prepared from a 1% w/v solution in 0.1 M NaCl by stirring for 16 hours followed by dialysis against 0.1 M NaCl for 4 days. The dialysis tubing was boiled in double distilled water for 30 min. and rinsed prior to use.

Values of η_r were obtained using Equation 2.26

$$\eta_r = \frac{\eta}{\eta_0} = \frac{\rho t}{\rho_0 t_0} \quad 2.26.$$

where η_r = relative viscosity

ρ = density of solution

ρ_0 = density of solvent = $0.99707 \text{ g cm}^{-3}$ at 25° C. (113).

¹ Protan A/F, Norway.

² Ostwald viscometer, Size A

³ Grant Instruments, Cambridge, England

η = solution viscosity

η_0 = solvent viscosity = 0.008904 poise at 25⁰ C
(114)

t = time taken by the solution

t₀ = time taken by the solvent

The y-intercept of the linear plot of η_{sp}/c against c gave values of $[\eta]$ in the conventional units of dl g⁻¹.

Density determinations were made using a 25 ml glass specific gravity bottle calibrated with water at 25⁰ C.

2.3.2 Light Scattering

Light scattering measurements were made using a Photo Gonio Diffusometer¹. The instrument has been used previously for studying alginate (55,117) and is described in detail by Chiang (87). In principle, an unpolarised beam of monochromatic light (mercury source $\lambda_0 = 546.1$ nm) passes through the cell containing the sample; the scattered light is detected, and amplified by a photomultiplier to be displayed as a galvanometer reading, I. A constant temperature of 25⁰ C was maintained using an external source of water circulation².

Marked dissymmetry of the Zimm plot can occur if solutions are contaminated with dust particles, therefore cleanliness and clarification are important. All glassware was soaked overnight in chromic acid cleaner, thoroughly rinsed with water and finally rinsed under laminar flow conditions with double distilled³ and filtered (1.0 μ m) water.

¹ S.O.F.I.C.A., Model 42000, Le Mesnil-Saint-Denis, France.

² Churchill Thermocirculator, Churchill Inst.Co.Ltd., Perivale, Middlesex, U.K.

³ 'Fi-stream' all glass still, Fisons.

The light scattered by 2 x 0.2 μm filtered benzene was compared to that of the glass standard provided. The manufacturer's calibration was found to be valid, i.e.,

$$0.92 = \frac{R_{90^0}(\text{glass})}{R_{90^0}(\text{benzene})} = \frac{\text{Scale Reading at } 90^0(\text{glass})}{\text{Scale Reading at } 90^0(\text{benzene})}$$

The light scattered by the glass standard and the benzene were symmetrical in the range 30⁰ - 150⁰ indicating that the benzene in the vat was free of dust.

Clarification of the Alginate solutions was carried out by three regimens of centrifugation and filtration as shown in Table 2.4.

Table 2.4 Clarification of Alginate Solutions

Centrifugation		Temperature (⁰ C)	Filtration
g-force	Time (hr.)		
3000 ¹	2	20	1 x 0.45 μm
25,000 ²	2	4	4 x 0.45 μm
100,000 ³	2	4	4 x 0.45 μm

The intensities of light scattered by the samples were measured in order of increasing angle and increasing concentration, with the use of a Y - T chart recorder⁴. Readings were adjusted to correspond to the sensitivity used for the benzene standard and the intensity due to the solvent alone was then subtracted to

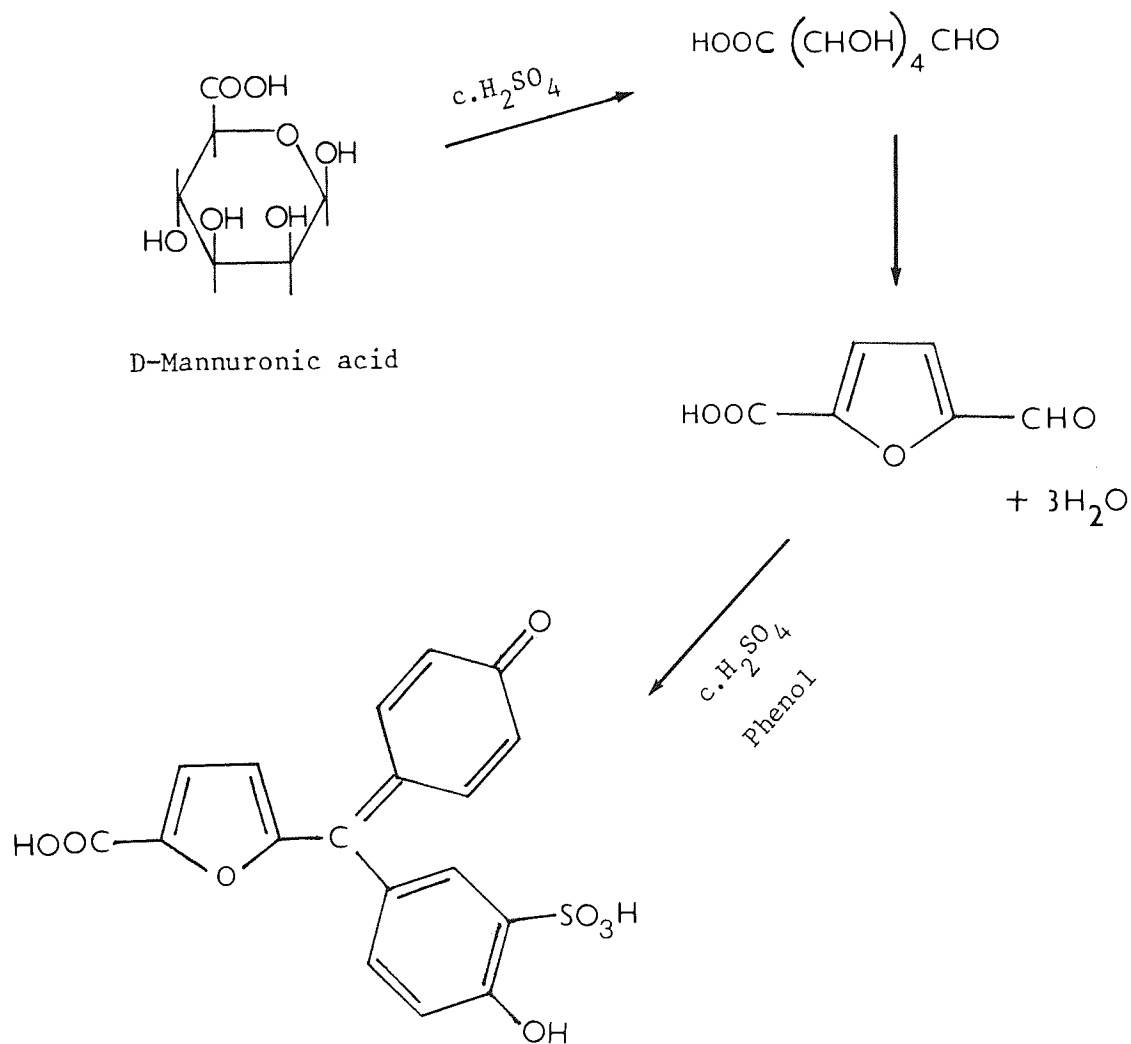
¹ Hereaus Christ 03400, V.A. Howe & Co Ltd, Peterborough Rd, London SW6, UK.
² MSE High Speed 18 } MSE Scientific Instruments, Crawley, Sussex, UK.
³ MSE Superspeed 50 }
⁴ Bryans Model 28000, Bryans Limited, Mitchan, Surrey, U.K.

obtain values of I_{θ} , see Section 2.2.2. A Zimm plot may then be constructed by plotting $c/\alpha I_{\theta}$ against $\sin^2\theta/2 + kc$.

2.3.3 Determination of Alginate Content

Alginate solutions were assayed for uronic acid content based on the Phenol-Sulphuric Acid method of Dubois (116). The mechanism of this reaction (145) is summarised in Scheme 2.1. below.

Scheme 2.1. The Reaction of a Uronic Acid with Concentrated Sulphuric Acid and Phenol.



Phenol sulphonic acid furan derivative, $\lambda_{max} = 285 \text{ nm}$.

Standard solutions for calibration were prepared using Alginate which had been dried to constant weight immediately prior to use. The procedure was as follows:

1. Add 0.5 cm^3 of 5% w/w Phenol solution to 2 cm^3 solution containing 10-200 μg of Alginate.
2. Add 5 cm^3 of conc. $\text{H}_2\text{SO}_4^{\text{a}}$ rapidly.
3. Stir carefully with a glass rod.
4. Shake in a water bath at 25°C for at least 20 minutes.
5. Read the UV-absorbance at 285 nm.

2.3.4 Determination of Refractive Index Instrument.

Values of dn/dc were determined using a differential refractometer^b calibrated with ten NaCl solutions.

A 1% w/v solution of Sodium Alginate in 0.1 M NaCl was diluted to give a range of concentrations from 0.1 to 1.0% w/v. The mean of six readings of refraction distance were taken in each case.

2.3.5 Rheology

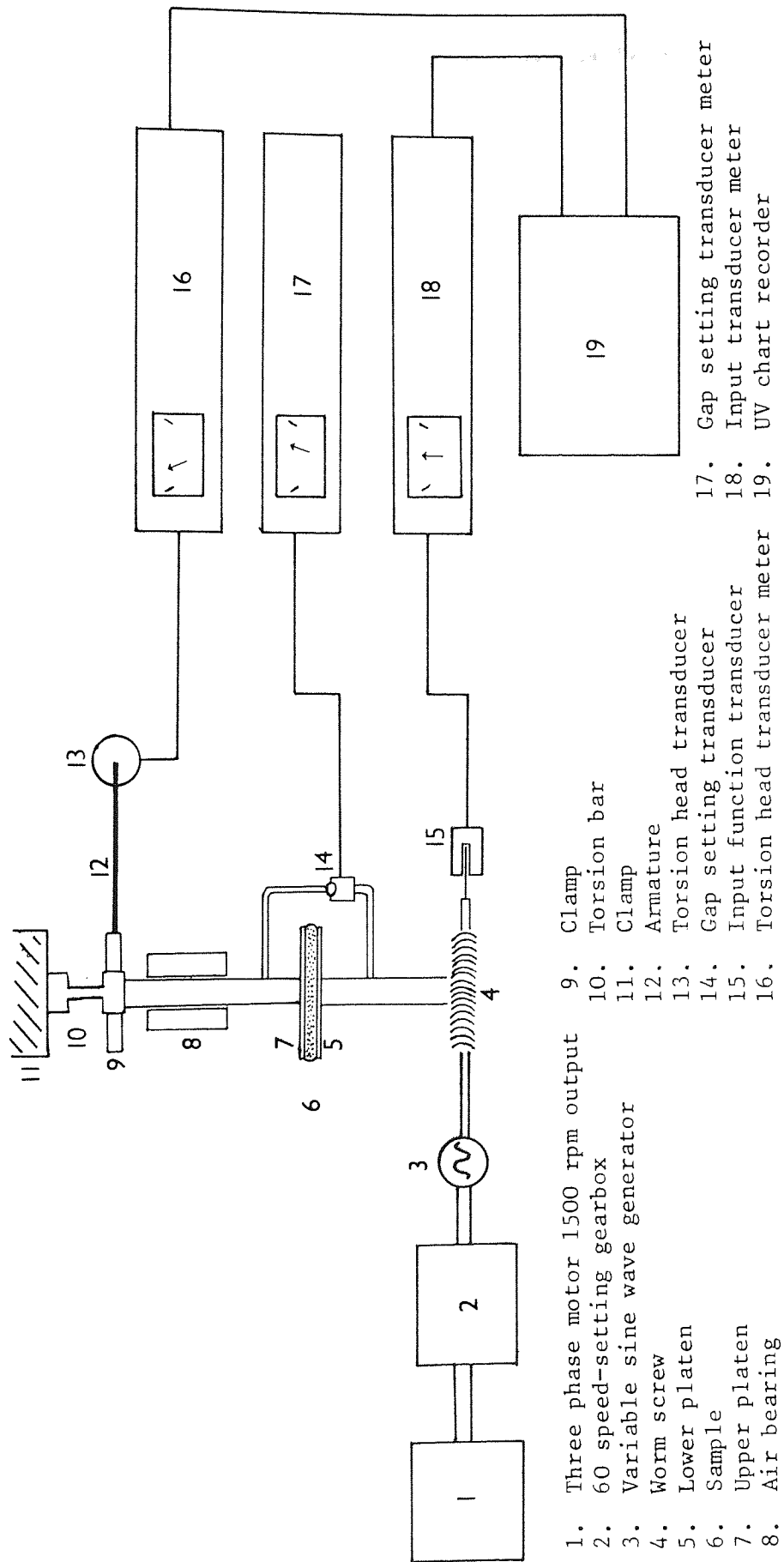
A Weissenberg Rheogoniometer model R16^c was used in a constant 20°C temperature laboratory, for both continuous shear and oscillatory shear experiments. Figure 2.2 shows the main

^aAR grade; e.g. = 1.84 g cm^{-3}

^bPhoenix Precision Instruments

^cSangamo Controls Ltd., Bognor Regis, Sussex. U.K.

Figure 2.2. The Weissenberg Rheogoniometer model RL6



components of this instrument; its functioning has been described elsewhere (91). Basically, the lower member is rotated or oscillated and the response of the sample in the gap is measured by angular displacement of the upper member via a torsion bar and distance transducer assembly. Different speeds of rotation or frequencies of oscillation are achieved by a manual change gearbox.

2.3.5.1 Continuous Shear Experiments

The continuous shear behaviour of Alginate solutions in 0.1 M NaCl was carried out for the concentration range 0.25 - 10.0 g dl⁻¹. Cone and plate geometry was used; the diameter was 7.5 cm and the non-truncated cone angle was 1°32'. The gap between the cone and plate was set to 0.061 mm using the gap-setting transducer. The torsion bar used was of Size No. 7 with $K_t = 104 \text{ dyne cm } \mu\text{m}^{-1}$. The shear rate range used was 0.5855 to 1467 sec⁻¹ and the shear stress was obtained from transducer meter readings. The calibration was checked using water and Silicone Fluid 100 cs. The viscosity of the latter was determined using a calibrated U-tube Ostwald Viscometer. Values of η obtained using the Rheogoniometer and the Ostwald viscometer differed by no more than 4%.

2.3.5.2 Oscillatory Shear Experiments

The oscillatory shear behaviour of Alginate solutions in double distilled water was carried out for the concentration range 5.0 to 20.0 g dl⁻¹. Parallel plate geometry was used with 7.5 cm plates and the gap between the plates was set to 0.508 mm

throughout. The input and output waveforms were recorded on UV-chart paper¹ from which the amplitude ratio, ν , and phase lag, C , were determined graphically. Values of ν and C were substituted into Equations 2.24 and 2.25 to obtain η' and G' . The natural frequency of the torsion bar (Size No.7) was found to be 4.00 Hz and therefore the range of frequencies used for measurements was 7.91×10^{-3} to 3.97 Hz. Anomalies in readings taken near the natural frequency are known to occur, therefore it is wise to avoid these measurements, (108,117,118).

The calibration of the gap-setting, torsion head and oscillation transducers was carried out using a micrometer; the latter two transducers were also calibrated with respect to the UV chart paper and appropriate adjustments were made.

In order to check the oscillatory function of the rheogoniometer, tests were carried out using the Newtonian liquids Silicone Fluid 100 cs, and Liquid Paraffin B.P. to obtain (ν, ω) and (C, ω) curves. Theory dictates that when $\omega = \omega_0$, $\nu = 1$ and $C = 0$. In addition, a viscoelastic sample of Carbopol 941² 1% w/w was tested in order to compare the values of η' and G' with those obtained by Barry (119).

¹ S.E. Laboratories, Farnborough, Hants., UK.
² Honeywell & Stein, Wallington, Surrey, UK.

2.4 Results

2.4.1 Viscometry

Calibration of the Ostwald viscometer with double distilled water at 25°C yielded $t_0 = 277.50 \pm 2.23$ sec, which was a sufficiently long time to negate the need for kinetic energy correction (120). The density of a 1.0 g dl⁻¹ solution of Sodium Alginate was found to be 1.00505 g cm⁻³. Although small, the density correction of 0.8% was ten times greater than the standard deviation of the viscometer times and was therefore used in Equation 2.26..

The results given in Tables 2.5(a) and (b) are for Alginate solutions before and after ultracentrifugation. Each value represents the mean of three t-determinations for each of two sample solutions used in the viscometer. The linear plots of η_{sp}/c against c given in Figure 2.3 gave least mean square correlation coefficients in excess of 0.99; $[\eta] = 1.056 \pm 0.05$ dl g⁻¹ before and $[\eta] = 1.046 \pm 0.12$ dl g⁻¹ after ultracentrifugation.

Due to the variable nature of Alginate several values of K and exponent α for the modified Staudinger Equation 2.2 are to be found in the literature. The values of $K = 2.0 \times 10^{-5}$ and $\alpha = 1.0$ (ionic strength $\mu = 0.1$) have been determined by Snidsrød (52) for Alginate from L. digitata with $M/G = 1.60$. This would provide the viscosity-average molecular weight, $M_\eta = 52,000$ g mol⁻¹. The K and α values of Mackie et al. (56) do not

Table 2.5 Viscometric Data

(a) Intrinsic viscosity determination before ultracentrifugation.

Concentration (g dl ⁻¹)	Mean Viscometer time (secs)	η_{sp}/c (dl g ⁻¹)
0.12	315.61	1.154
0.2	342.39	1.179
0.4	427.47	1.363
0.6	524.23	1.497
1.0	765.83	1.782

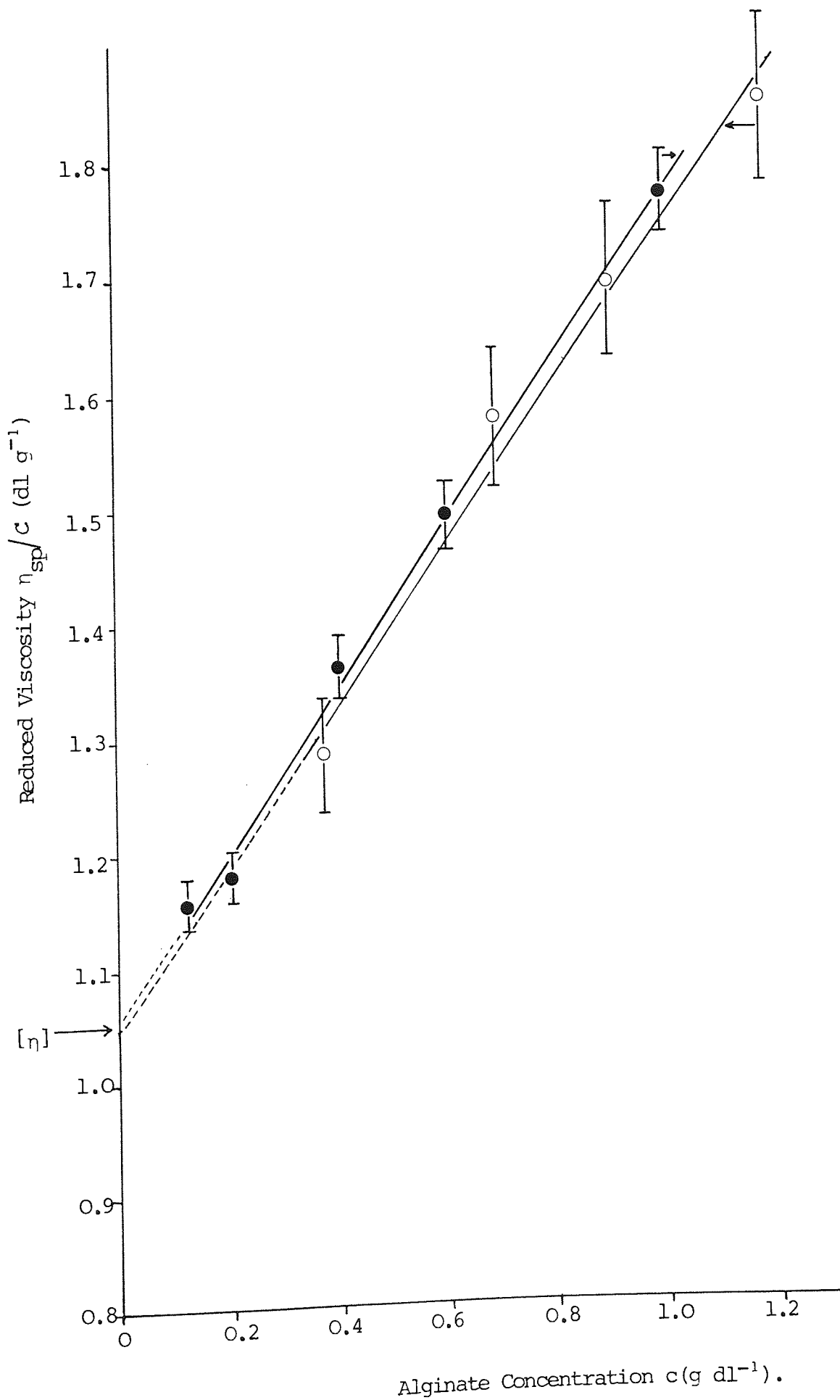
(b) Intrinsic viscosity determination after ultracentrifugation at 100,000 x g for 2 hr.

Nominal Concentration (g dl ⁻¹)	Assay Concentration (g dl ⁻¹)	Mean Viscometer time (secs)	η_{sp}/c (dl g ⁻¹)
0.4	0.376	414.40	1.286
0.8	0.696	579.75	1.582
1.0	0.906	700.16	1.701
1.4	1.182	880.94	1.865

Figure 2.3. Determination of the Intrinsic Viscosity, $[\eta]$, of Alginate from a plot of Reduced Viscosity against Concentration.

Before Centrifugation ● and After Centrifugation ○ .

Figure 2.3 (see facing page).



appear to follow any simple relationship with respect to the M/G ratio and consequently, the calibration of $[\eta]$ from the weight average molecular weight, M_w , is necessary for each Alginate sample used. To do this, Smidsrød and Mackie utilised fractionation by acid hydrolysis of a high molecular weight Alginate. In contrast, Protanal LFR5/60 Sodium Alginate is already a low molecular weight polymer as reflected by the $[\eta]$ values, therefore calibration by hydrolysis would be difficult. By substituting for $[\eta]$ using K and α values due to Mackie et al, values of M_η ranging from 35,400 to 59,300 g mol⁻¹ are obtained. Clearly, the use of viscometry alone is insufficient to characterise the Alginate.

The higher standard error limits of $[\eta]$ for the ultracentrifuged solutions are due to errors involved in the phenol-sulphuric acid assay. The mean calibration line follows Equation 2.27.

$$\text{Absorbance} = (63.1 \pm 1.3) c + (0.046 \pm 0.014) \quad 2.27$$

where c = concentration in g dl⁻¹

The assay method is sensitive to approximately $\pm 10 \mu\text{g}$ and inevitably, some errors are introduced during the dilution of stock solutions to achieve such low concentrations. The assay of a 1.0 g dl⁻¹ dialysed stock solution after centrifugation at 3000 g for 2 hr. gave a response line with a slope not significantly different from that of Equation 2.27. However, the turbidity at 420 nm had decreased from 38.0 to 76.8% indicating that the main cause of opacity in solutions was not Alginate material.

2.4.2 Light Scattering

The method of clarification of the polymer solutions proved to be critical with respect to the results obtained. Solutions that were not sufficiently clarified gave rise to anomalous results and dissymmetry, quantified by the dissymmetric ratio

$Z_{45^{\circ}, 135^{\circ}}$:

$$Z_{45^{\circ}, 135^{\circ}} = \frac{I_{45^{\circ}} - I_{0, 45^{\circ}}}{I_{135^{\circ}} - I_{0, 135^{\circ}}} \quad 2.28$$

where $I_{45^{\circ}}$ and $I_{135^{\circ}}$ = Intensities of light scattered by the sample solution at 45° and 135° respectively.

$I_{0, 45^{\circ}}$ and $I_{0, 135^{\circ}}$ = Intensities of light scattered by solvent at 45° and 135° respectively.

Table 2.6 shows the reduction in values of $Z_{45^{\circ}, 135^{\circ}}$ towards unity as centrifugation is increased from 3,000 to 100,000 x g.

Table 2.6 Dissymmetric Ratios, $Z_{45^{\circ}, 135^{\circ}}$ of Alginate Solutions

Centrifugation					
3,000 x g 2 hr.		25,000 x g 2 hr.		100,000 x g 2 hr.	
c(g dl ⁻¹)	$Z_{45,135^{\circ}}$	c(g dl ⁻¹)	$Z_{45,135^{\circ}}$	c(g dl ⁻¹)	$Z_{45,135^{\circ}}$
0.10	2.36	0.04	1.52	0.376	0.97
0.15	4.99	0.10	1.22	0.696	1.05
0.23	3.54	0.16	1.23	0.906	1.03
0.32	3.52	0.20	1.15	1.182	1.16
0.46	3.49			1.674	1.17

Although the method of Zimm (121) provides the most accurate graphical analysis of light scattering data, significant dissymmetry disrupts such a plot. This is the case for solutions centrifuged at 3000 and 25,000 x g. It may, however, be possible to use the data for light scattered at 90° only by applying Equation 3.29 (122).

$$\frac{Kc}{R_{90^{\circ}}} = \frac{1}{M_w} + 2Bc \quad 2.29$$

In this way, M_w and the second virial coefficient, B , may be obtained, but the radius of gyration cannot. Figure 2.4. shows plots of $c/\alpha I_{90^{\circ}}$ against c for solutions centrifuged at 3000 and 25,000 x g respectively. $c/\alpha I_{90^{\circ}}$ is related to Kc/R_{θ} by Equations 2.17 and 2.13.

The values for solutions centrifuged at 3000 x g, see Table 2.7., do not give a linear relationship and extrapolation to zero concentration is not feasible. In contrast, 25,000 x g was sufficient to provide a linear plot with at least mean square correlation coefficient of 0.9986; $M_w = 20,600 \pm 1,000 \text{ g mol}^{-1}$ and $B = 9.03 \pm 1.17 \times 10^{-3} \text{ mol cm}^3 \text{ g}^{-2}$. The data is shown in Table 2.8.

Figure 2.4. The Effect of Alginate Concentration and Centrifugation on the Intensity of Light Scattered at 90° .

Centrifugation of Solutions : $3000 \times g$ for 2 hr. \circ ,
 $25000 \times g$ for 2 hr. \bullet .

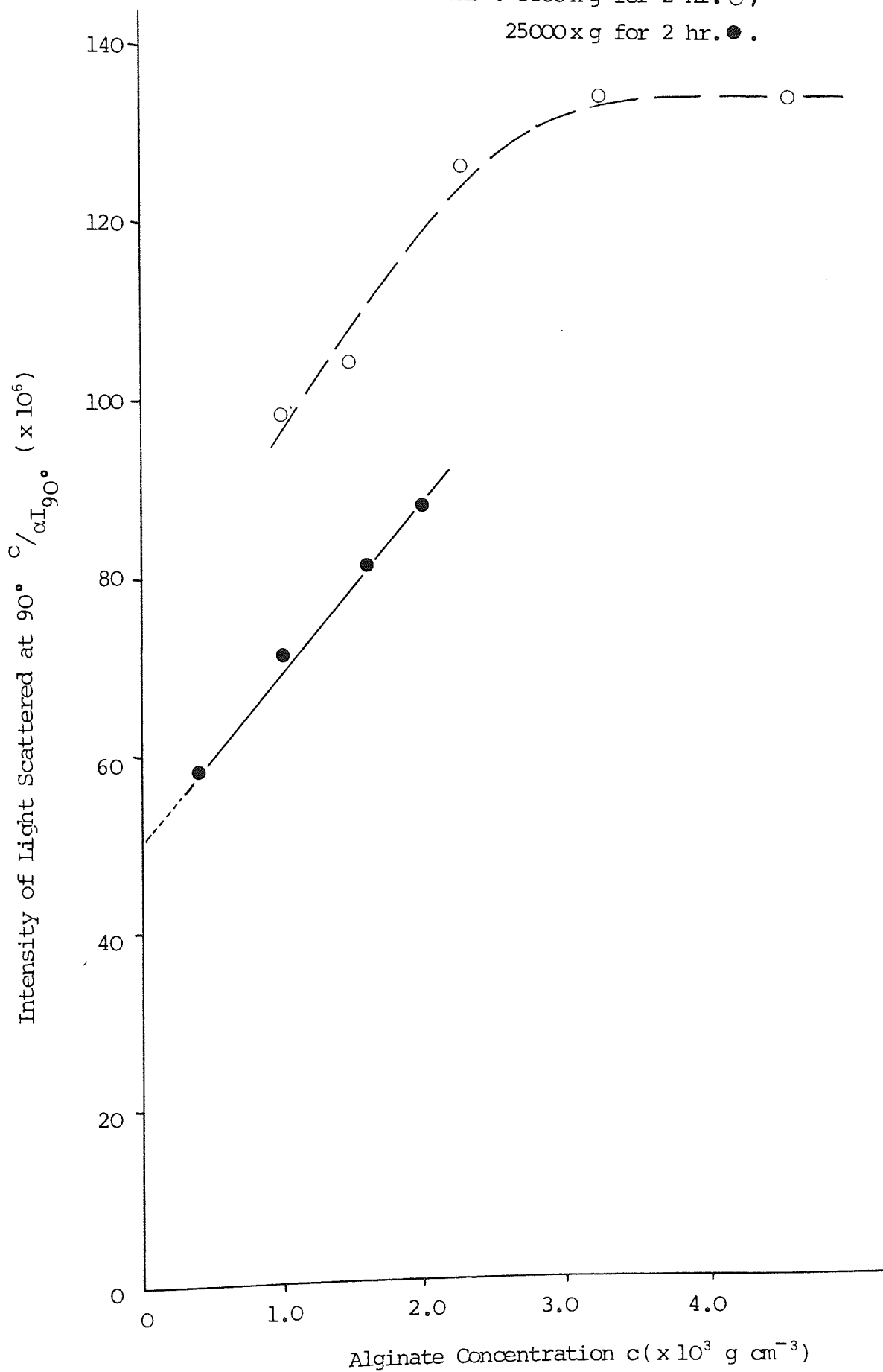


Table 2.7 Light scattered at 90° for solutions centrifuged at $3000 \times g$ for 2 hr.

I_{θ} (divs)	$c / \alpha I_{\theta} \times 10^6$	c (g dl $^{-1}$)
10.14	98.60	0.100
13.98	104.4	0.146
17.88	127.5	0.228
23.98	135.1	0.324
33.78	134.7	0.455

Table 2.8 Light scattered at 90° for solutions centrifuged at $25,000 \times g$ for 2 hr.

I_{θ} (divs)	$c / \alpha I_{\theta} \times 10^6$	c (g dl $^{-1}$)
6.85	58.39	0.04
14.00	71.43	0.10
19.60	81.63	0.16
22.40	89.29	0.20

Values of the refractive index increment dn/dc were obtained after calibration of the differential refractometer with sodium chloride solutions. The instrumental constant k' was equal to $0.9434 \times 10^{-3} \text{ div}^{-1}$.

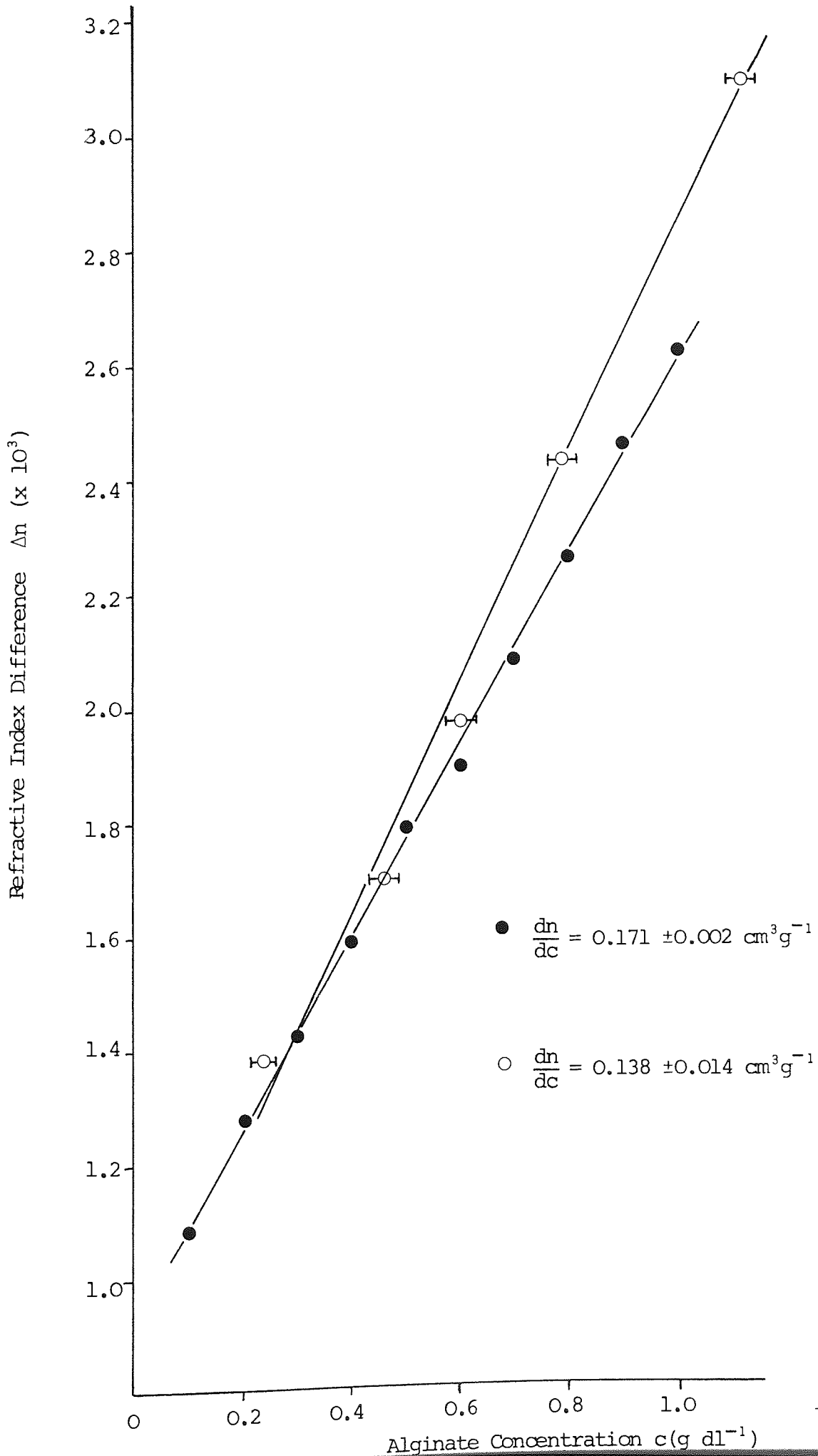
Alginate solutions tested before and after ultracentrifugation gave dn/dc values of 0.171 ± 0.002 and $0.138 \pm 0.014 \text{ cm}^3 \text{ g}^{-1}$ respectively. The plots of the refraction distance, d , against c are given in Figure 2.5.. These values compare favourably with dn/dc of Alginate in 0.1 N NaCl due to previous workers. Buchner et al (16) obtained $0.165 \text{ cm}^3 \text{ g}^{-1}$; Haug and Smidsrød (53) $0.157 \text{ cm}^3 \text{ g}^{-1}$, Brucker et al (55) 0,180, 0.153 and $0.168 \text{ cm}^3 \text{ g}^{-1}$ for unfractionated, G-rich and M-rich Alginates respectively; Mackie et al (56) $0.154 \text{ cm}^3 \text{ g}^{-1}$ irrespective of M/G ratio.

There appears to be a significant difference between dn/dc before and after ultracentrifugation, which may have been due to the presence of contaminant plant material. In fact, Haug and Smidsrød (53) examined the light scattering properties of non-clarified Alginate solutions and concluded that spherical and ellipsoid particles were present, and assumed them to be of plant origin.

Scott et al (115) studied the light scattering of Sodium Alginate using a Photo-Gonio Diffusometer instrument and they failed to obtain Zimm plots capable of providing $(R_G^2)^{\frac{1}{2}}$ and B values after centrifugation at $35,000 \times g$ for 1 hr.

Figure 2.5. Determination of the Refractive Index Increment, dn/dc from a plot of Refractive Index Difference against Alginate Concentration.
Before Centrifugation ● and After Centrifugation ○

Figure 2.5 (see facing page).



Using pectin solutions, Cohen and Eisenberg (123) found considerable dissymmetry in their Zimm plot following centrifugation at 32,000 x g for 15 hr. This was blamed on the presence of aggregates. Further, Holt et al (124) described the aggregates as microgel and showed the usefulness of ultracentrifugation in reducing the downward curvature of the Zimm plot which occurs at low angles. The fact that the molecular weight may be reduced by ultracentrifugation itself is inevitable but under specified conditions, the technique is still valid.

For the Alginate solutions centrifuged at 100,000 x g for 2 hr., a Zimm plot was constructed with $k = 20$, as shown in Figure 2.6. The corresponding data is detailed in Table 2.9.. The values of the derived parameters were

$M_w = 22,500 \pm 2000 \text{ g mol}^{-1}$; $(R_G^2)^{\frac{1}{2}} = 66.8 \pm 6.7 \text{ nm}$;
 $B = 2.11 \pm 0.21 \times 10^{-3} \text{ mol cm}^3 \text{ g}^{-1}$. These values compare favourably with those of previous studies (17,20).

2.4.3 Continuous Shear Rheometry

By subjecting the Alginate solutions to a wide range of shear rates and measuring the resultant shear stress, it is possible to observe the onset of non-Newtonian behaviour. The shear thinning which occurs due to some ordering and rotation of the molecules is important in relating the dilute solution behaviour to the bulk properties of the polymer (78,125). The flow-curves given in Figures 2.7 to 2.9 show that derivations from Newtonian behaviour are seen at concentrations in excess

Figure 2.6. Zimm Plot for Alginate Solutions Ultracentrifuged at 100,000 x g for 2 hr.

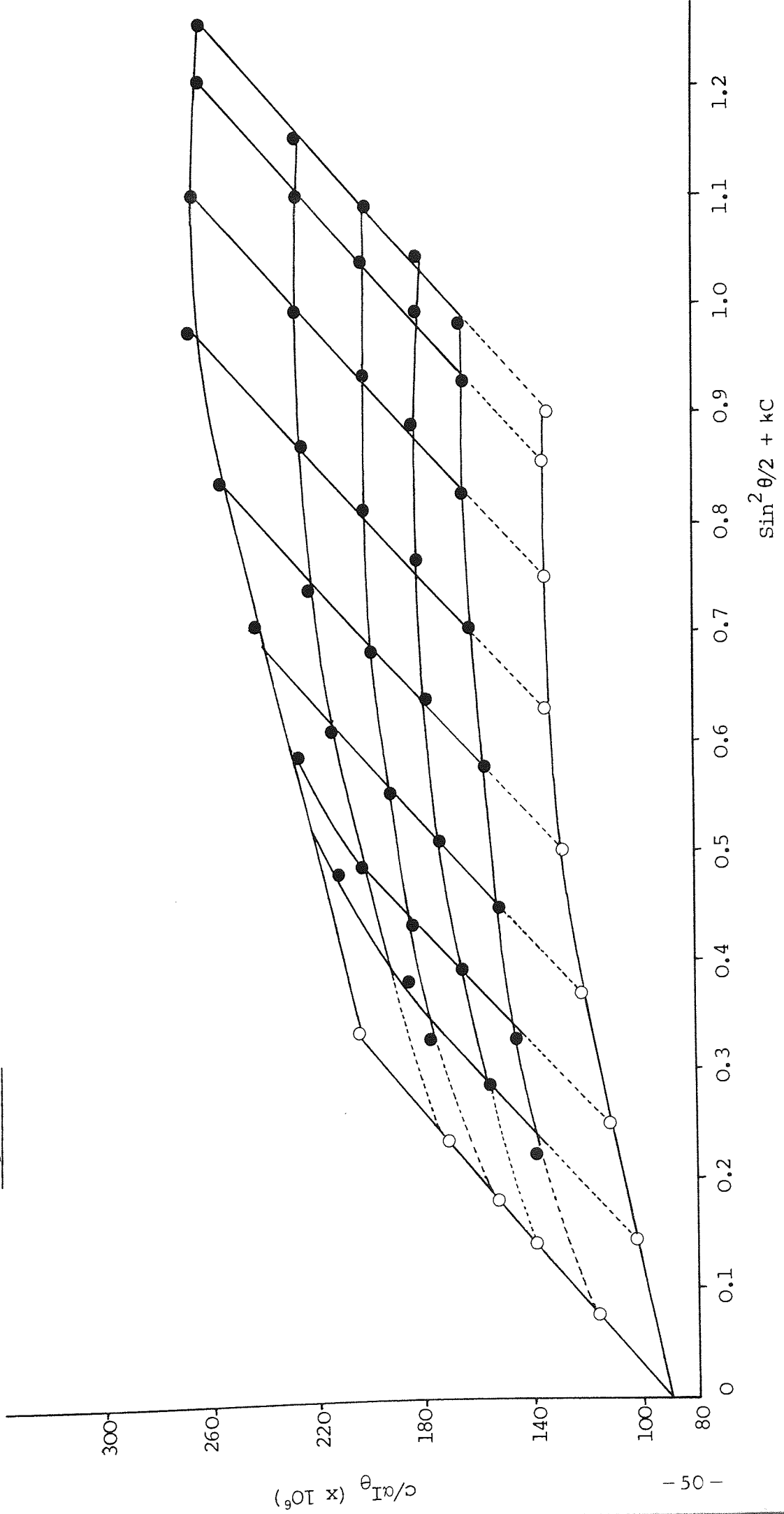


Table 2.9 Light Scattering Data for Solutions Ultracentrifuged at 100,000 x g for 2 hr.

Angle (deg)	Concentration (x10 g cm ⁻³)											
	0.0		3.76		6.96		9.06		11.82		16.74	
	y*	x†	y	x	y	x	y	x	y	x	y	x
0	90.0	0.0	116.0	0.075	139.0	0.139	152.0	0.181	171.0	0.236	205.0	0.335
45	102.0	0.146	138.4	0.221	156.1	0.285	178.6	0.327	184.9	0.382	212.5	0.481
60	111.0	0.250	145.5	0.325	165.5	0.389	184.4	0.431	204.6	0.486	227.9	0.585
75	121.0	0.371	151.8	0.446	174.7	0.510	193.6	0.552	215.8	0.607	244.9	0.706
90	128.0	0.500	157.0	0.675	178.9	0.639	201.3	0.681	224.7	0.736	257.9	0.835
105	134.0	0.629	162.0	0.704	182.6	0.768	202.2	0.810	227.1	0.865	269.6	0.964
120	135.0	0.750	164.9	0.825	183.7	0.889	203.1	0.931	229.6	0.986	267.0	1.085
135	135.0	0.854	165.1	0.929	182.3	0.993	203.2	1.035	228.4	1.090	263.0	1.190
142.5	133.0	0.902	166.6	0.977	182.1	1.041	201.6	1.093	228.8	1.140	264.0	1.240

* y = c/αI_θ x 10⁶

† x = sin²θ/2 + kc where k = 20

Figure 2.7. Continuous Shear $\tau(\dot{\gamma})$ Flow-Curves for various Concentrations of Sodium Alginate Solutions. Concentrations (g dl^{-1}) : 0.25 Δ , 0.5 \blacktriangle , 0.75 \circ , 1.0 \bullet , 1.5 \circ , 2.0 \bullet .

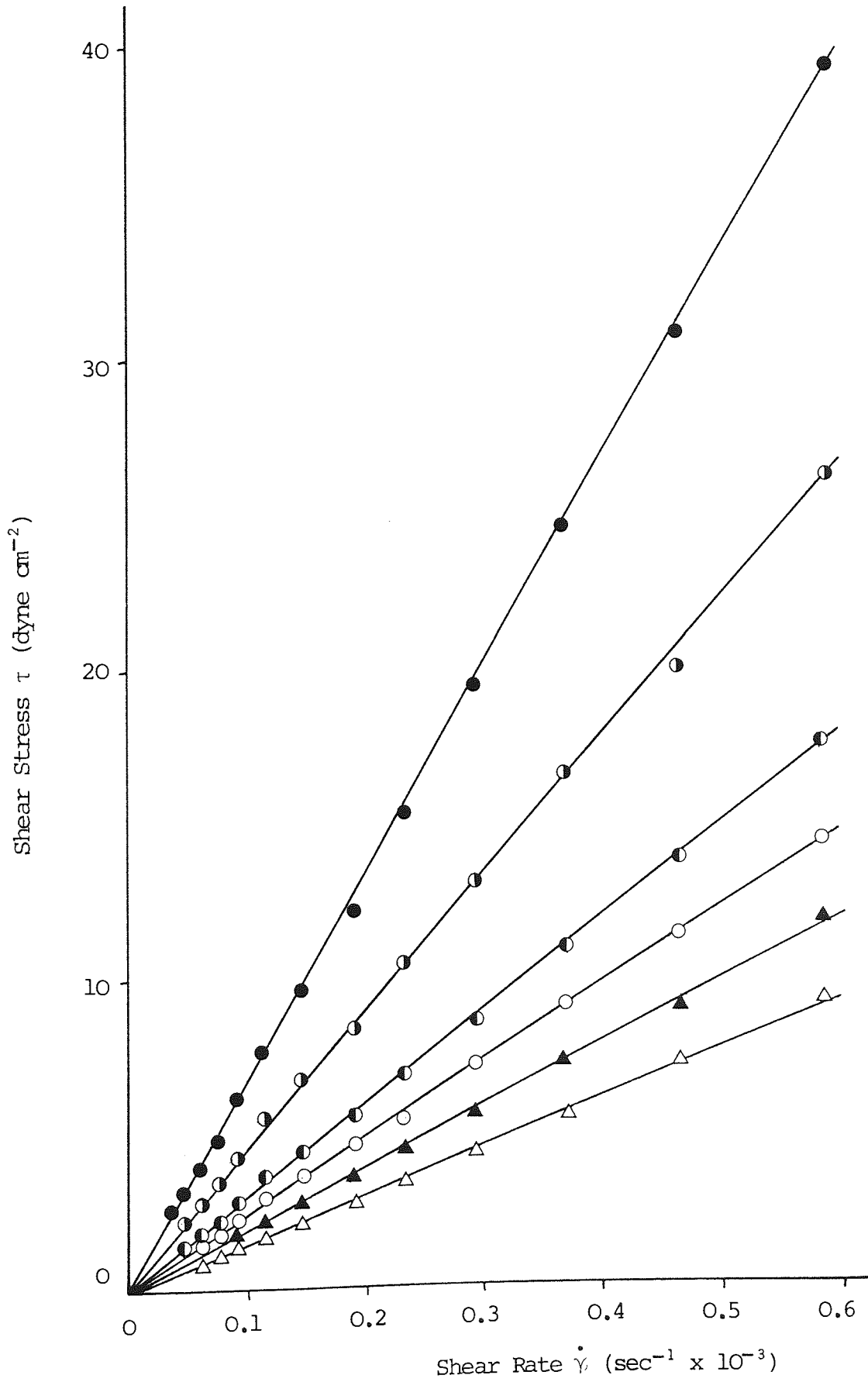


Figure 2.8. Continuous Shear $\tau(\dot{\gamma})$ Flow-Curves for Various Concentrations of Sodium Alginate Solutions. Concentrations (g dl^{-1}): 3.0 \circ , 4.0 \bullet , 5.0 \circ , 6.0 \bullet .

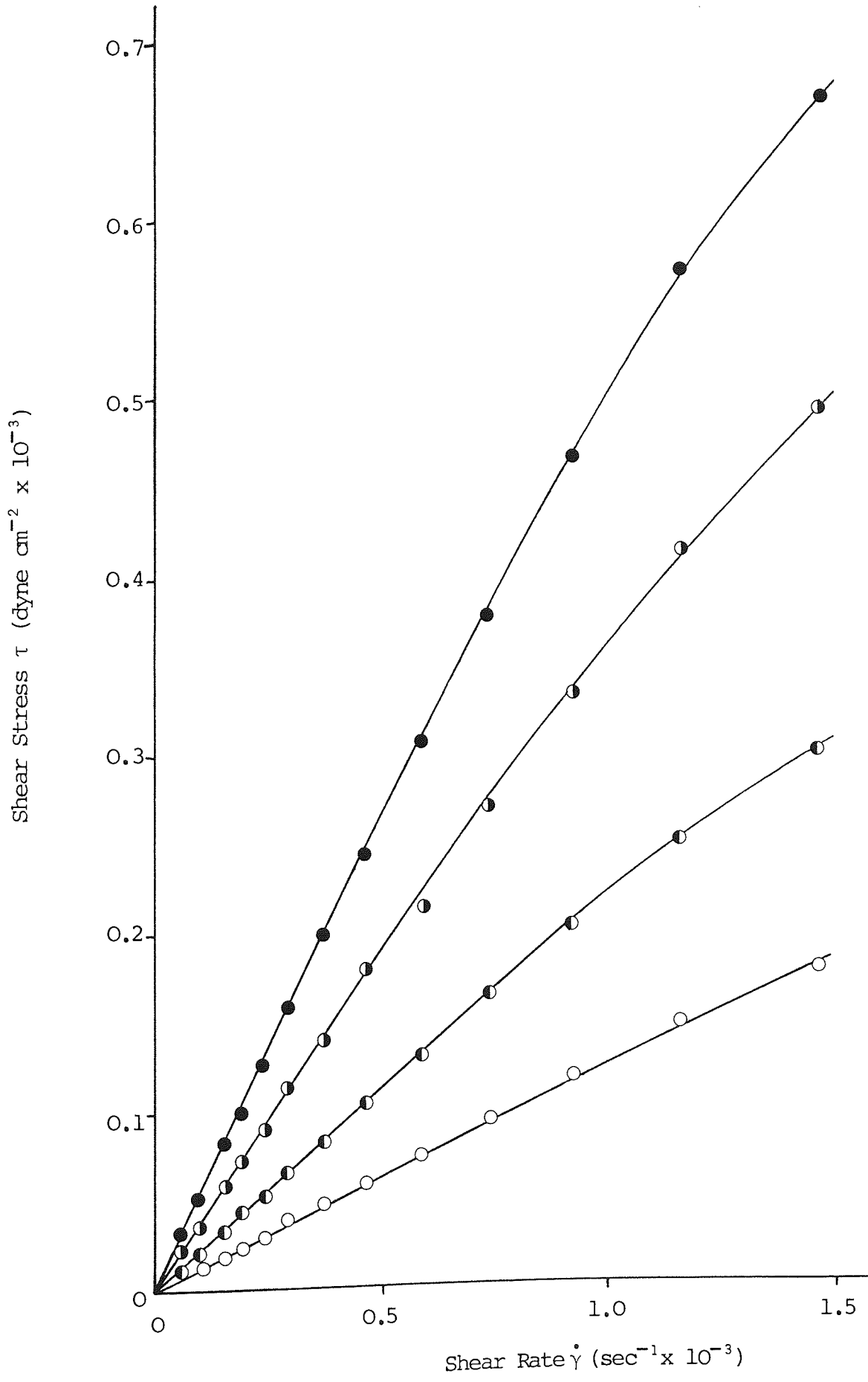
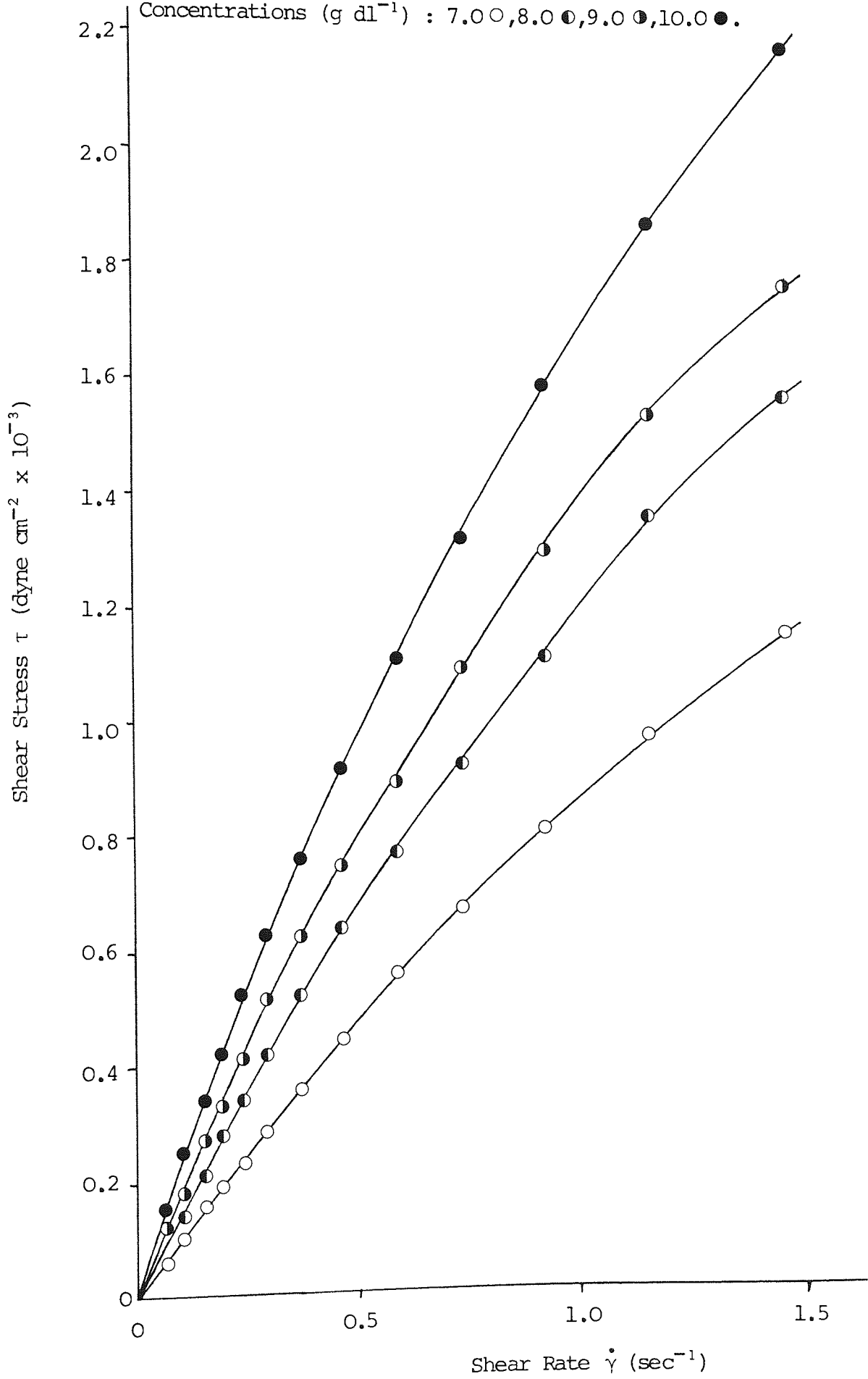


Figure 2.9. Continuous Shear τ ($\dot{\gamma}$) Flow-Curves for Various Concentrations of Sodium Alginate Solutions. Concentrations (g dl^{-1}) : 7.0 \circ , 8.0 \bullet , 9.0 \circ , 10.0 \bullet .



of about 6 g dl^{-1} . This was not due to any spurious effects such as expulsion of the sample from the gap since apparent shear thinning was absent in lower concentrations.

The reproducibility of the cone and plate system for measuring viscosity was demonstrated using (a) Silicone Fluid 100 cs. and (b) Sodium Alginate 5 g dl^{-1} solution. The results were (a) $\eta = 1.091 \pm 0.014$ poise ($n = 8$) and (b) $\eta = 0.353 \pm 0.017$ poise ($n = 10$), showing that more reproducible results were obtained using a pure Newtonian liquid, probably due to its homogeneity.

The Newtonian viscosities, ie, apparent viscosities calculated at low shear rates and approximating to zero shear viscosities, are given in Table 2.10. The relationship with concentration can be described by Equation 2.30. Equations of this type were suggested by McDowell (1).

$$\log_{10} \eta = 0.858 c^{\frac{1}{2}} - 2.43 \quad 2.30$$

The line is illustrated in Figure 2.10 where the least mean square correlation coefficient $r = 0.9983$.

Figure 2.10. The Effect of the Concentration of Alginate on Newtonian Viscosity.

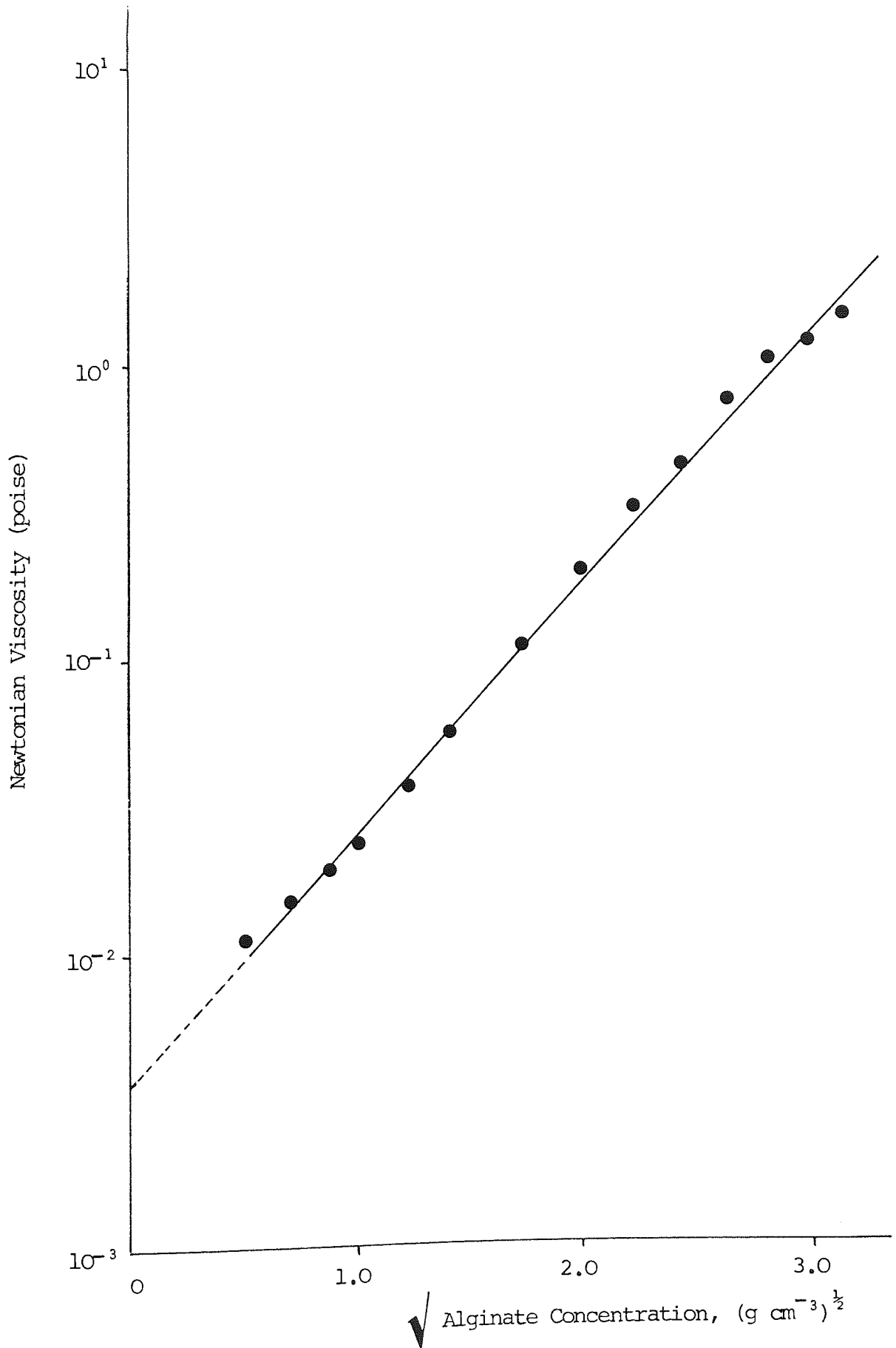


Table 2.10 Newtonian Viscosities of Sodium Alginate Solutions at 20°C.

Concentration (g dl ⁻¹)	Viscosity (poise)
0.0	0.0090
0.25	0.0115
0.5	0.0152
0.75	0.0193
1.0	0.0242
1.5	0.0377
2.0	0.0578
3.0	0.115
4.0	0.205
5.0	0.343
6.0	0.478
7.0	0.814
8.0	1.13
9.0	1.29
10.0	1.59

2.4.4 Oscillatory Shear Rheometry

The (ν, ω) and (C, ω) curves for two Newtonian liquids shown in Figures 2.11 and 2.12. give the expected results, namely that $\nu = 1$ and $C = 0$ when $\omega = \omega_0$. The value of ω_0 for the size 7 torsion bar was 25.1 rad s⁻¹. The viscoelastic determinations for Carbopol 941 1.0 g 100g⁻¹ detailed in Table 2.11 are in good agreement with the results of Barry and Meyer (82) showing that viscoelastic measurements were comparable. The amplitude used for these measurements was 28.1 x 10⁻⁴ rad. which compares with 31 x 10⁻⁴ rad. used by Barry and Meyer (119), therefore the collation is unaffected by any non-linear viscoelastic effects.

Figures 2.13. and 2.14. illustrate the oscillatory data for

Figure 2.11. The Effect of the Frequency
on (a) the Amplitude Ratio and (b) the Phase
Silicone Fluid 100 cs.

Figure 2.11 (see facing page).

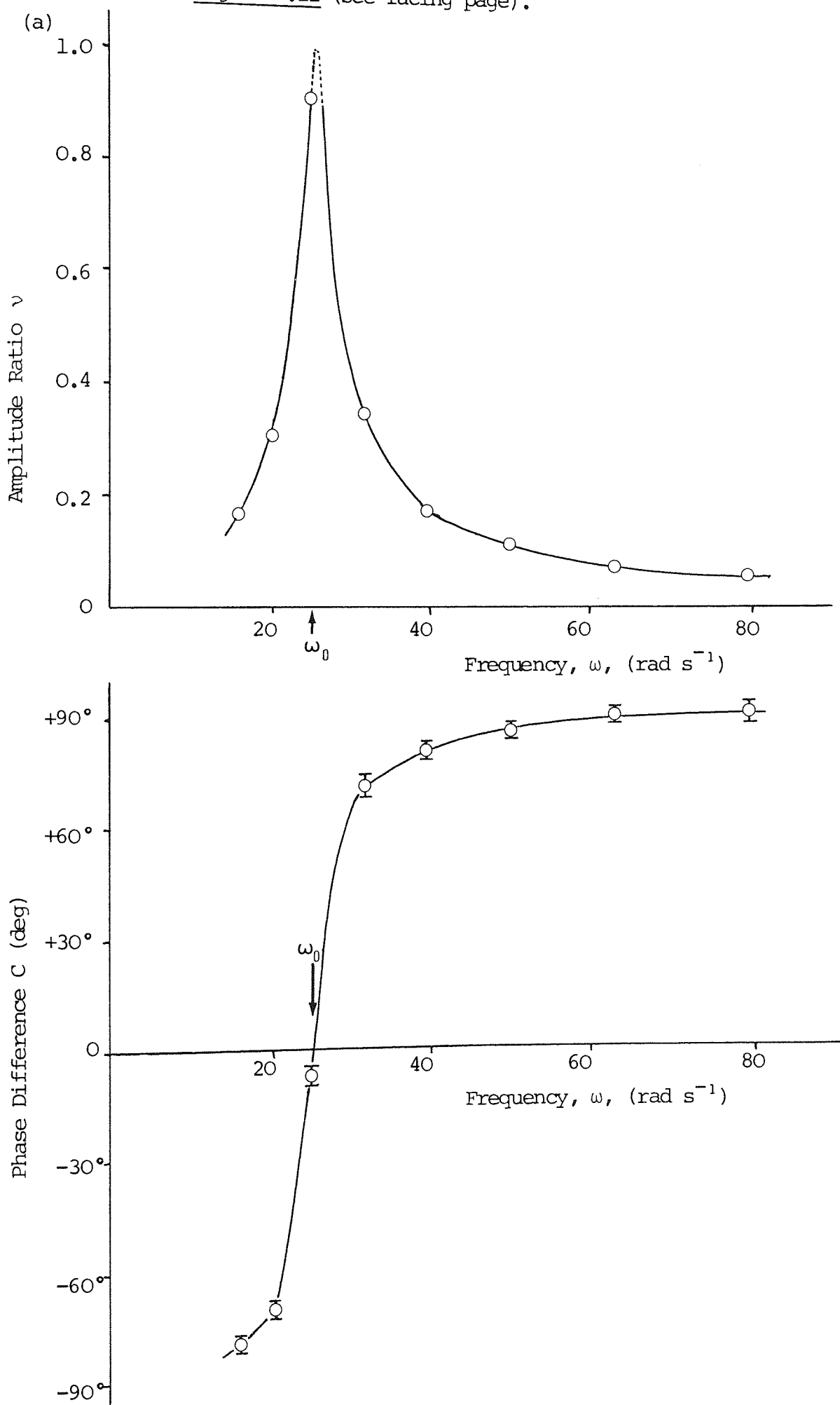


Figure 2.12. The Effect of the Frequency of C on (a) the Amplitude Ratio and (b) the Phase L Liquid Paraffin B.P.

Figure 2.12 (see facing page)

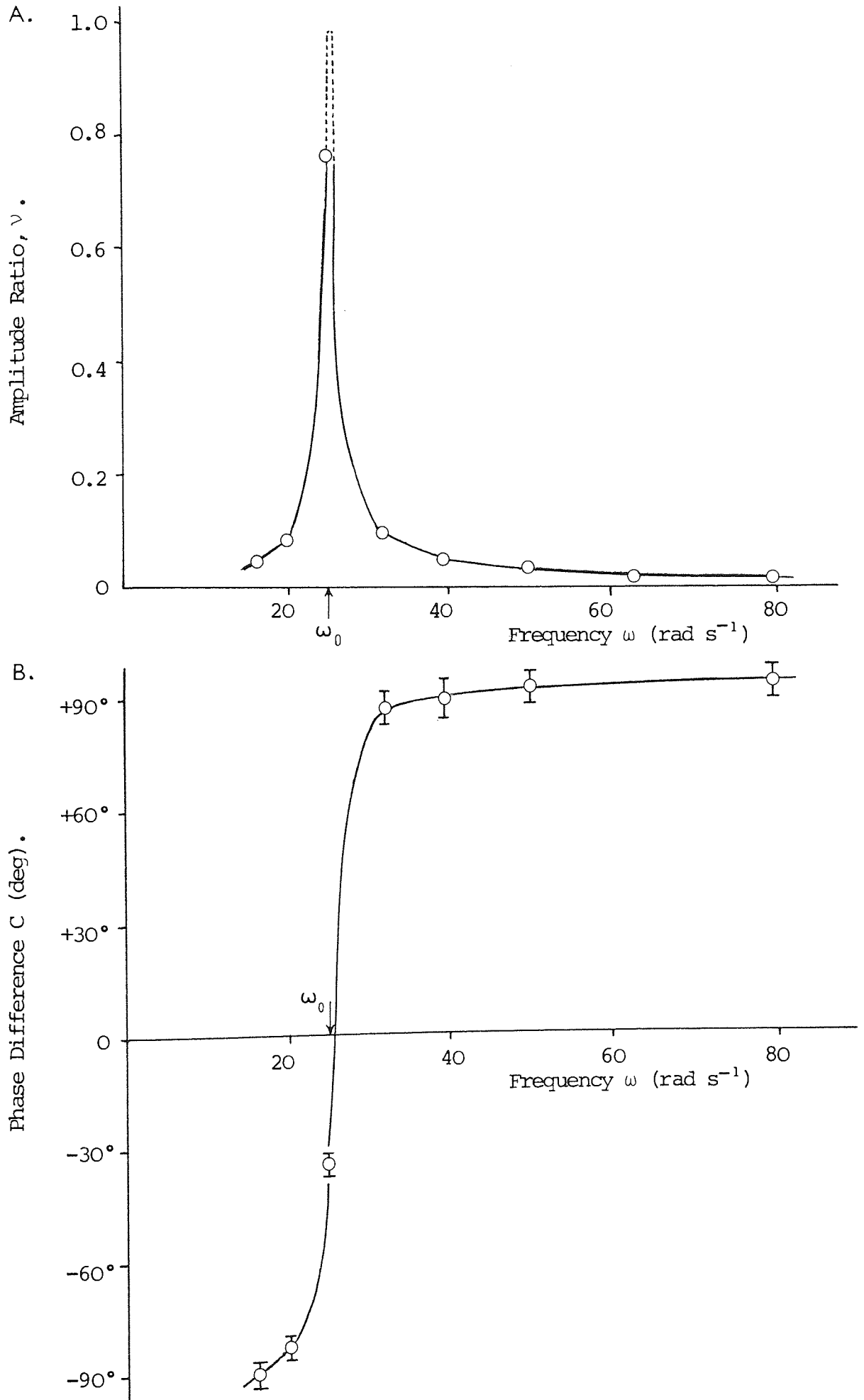


Figure 2.13. The Effect of the Concentration of Sodium Alginate Solution on the Storage Modulus, G' , plotted as a function of the Frequency of Oscillation.

Concentrations (% w/w) : 5.1 ○, 10.0 ●, 12.7 ●, 15.0 ●,
17.8 △, 19.8 ▲.

Figure 2.13 (see facing page)

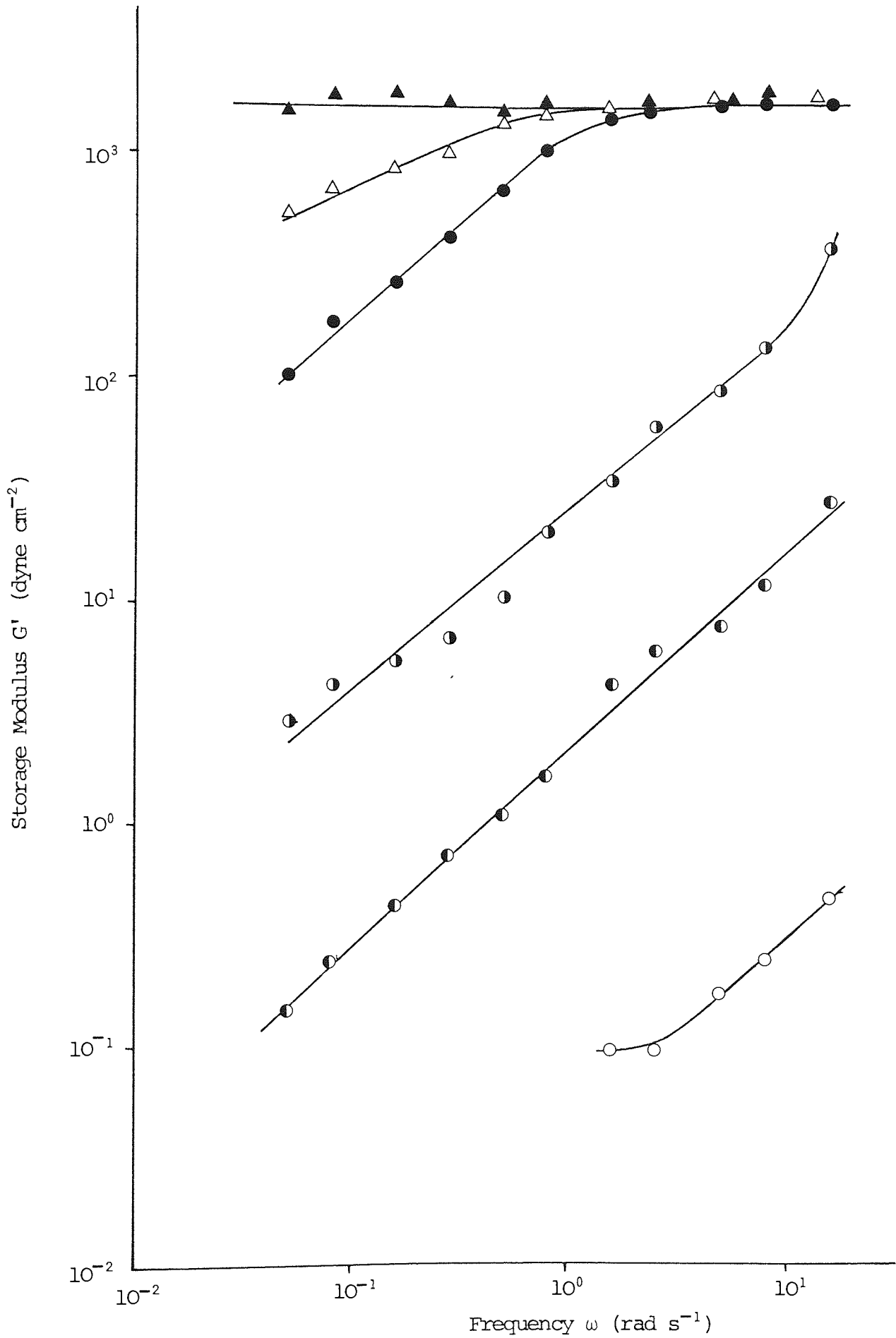
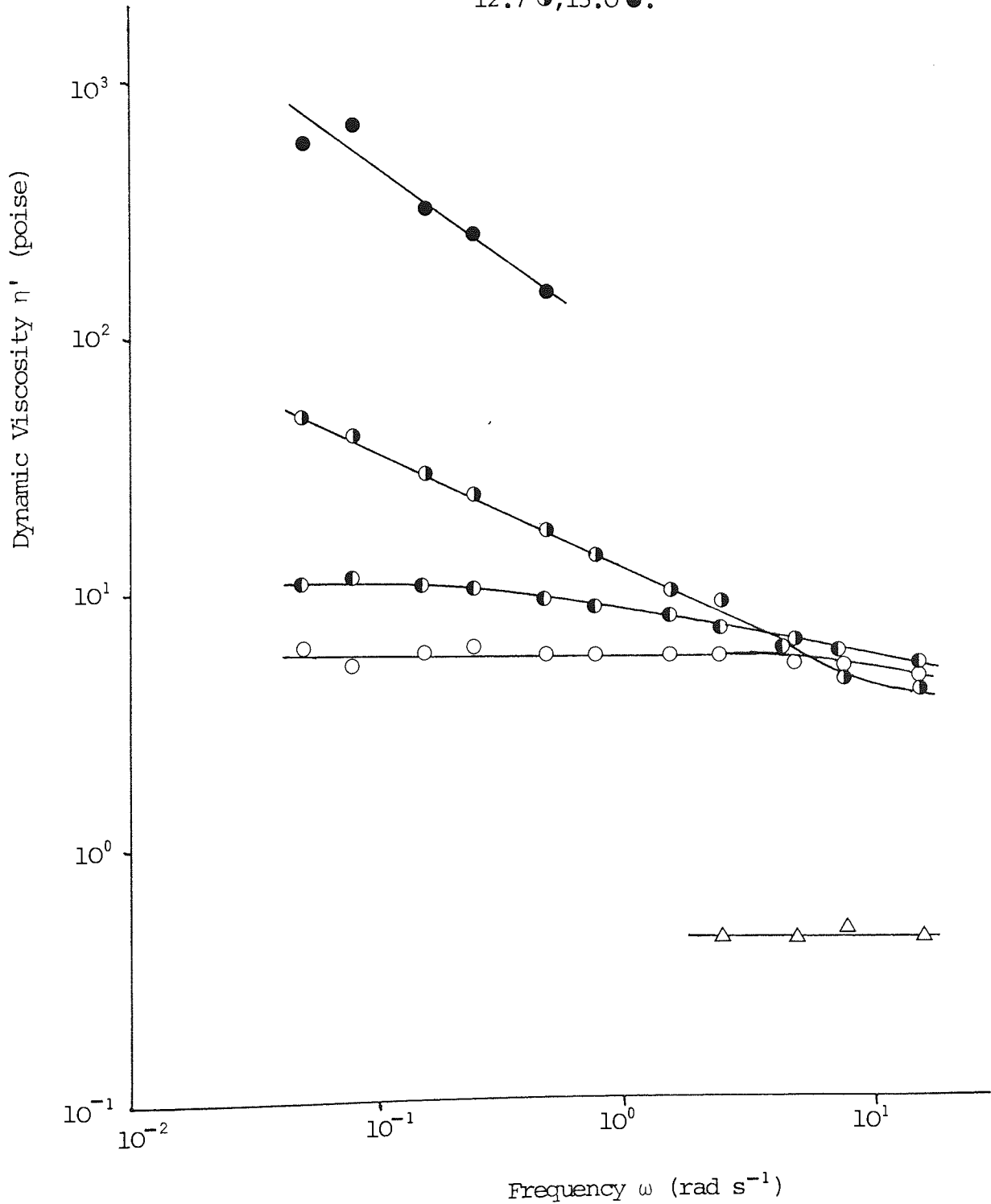


Figure 2.14. The Effect of the Concentration of Sodium Alginate Solution on the Dynamic Viscosity, η , plotted as a function of the Frequency of Oscillation.

Concentration (% w/w) : 5.1 Δ , 8.2 \circ , 10.0 \bullet ,
12.7 \circ , 15.0 \bullet .



Sodium Alginate solutions in terms of $G'(\omega)$ and $\eta'(\omega)$ respectively. The incomplete curves for 5.1 g dl^{-1} Alginate occurred because the measuring system was not sufficiently sensitive to distinguish the output amplitude from background movements caused by air convection currents. On the other hand, properties and therefore $\eta'(\omega)$ values depend on the accurate measurement of small phase angles. As would be expected, the phase angle becomes smaller as the frequency is increased until eventually, accurate $\eta'(\omega)$ values are no longer obtained.

Table 2.11 Viscoelastic Data for Carbopol 941 $1.0 \text{ g } 100 \text{ g}^{-1}$ measured at 28.1×10^{-4} rad. amplitude.

Frequency, ω (rad s^{-1})	Storage Modulus, G' (dyne cm^{-2})	Dynamic Viscosity, η' (poise)
0.0497	210	-
0.0792	218	-
0.157	227	-
0.249	235	-
0.497	247	78.4
0.792	253	58.0
1.57	262	40.1
2.49	272	24.9
4.97	295	12.6

The $\eta'(\omega)$ curves suggest that viscoelastic behaviour commences at approximately 10 g dl^{-1} concentration whereas the $G'(\omega)$ curves show a small elastic contribution in a 5 g dl^{-1}

solution. At 20 g dl^{-1} Alginate, the solution was completely elastic within the frequency range measured. However, the fact that the solution would still flow under gravity suggested that the frequencies used were much higher than the retardation time of the material and therefore the viscosity may only be measured at lower frequencies.

2.5 Discussion

Several studies have been published on the properties of Alginate either at the molecular level (5,15,16,20,46-50,52-56) or in bulk solutions (1,126,127) but rarely have the two aspects been investigated simultaneously. Such information would be potentially useful for choosing bulk properties of a system from a knowledge of the molecule. Rees (22,128,129) and Morris (130,131) have studied polysaccharides in solution using techniques such as circular dichroism, optical rotation, and nuclear magnetic resonance from which it was possible to make qualitative conclusions on conformation and solute-solute interactions. However, any attempt to unite the two fields of molecular and bulk properties falls short of its goal because of the lack of theoretical knowledge. For example, Franks (132) succeeded in showing only tentative links between optical rotation measurements, second virial coefficients, and 'Monte Carlo' ab initio calculations of molecular conformation for carbohydrates.

Nevertheless, even without such an exhaustive knowledge of the polysaccharide under study, it is useful to characterise

the material in terms of both molecular and bulk parameters for dilute and concentrated solutions (133).

It can be seen from the molecular data for $(R_G^2)^{\frac{1}{2}}$, M_w and $[\eta]$, that the Flory Equation (see Equation 2.4) can be used to calculate Φ . ie., $\Phi = 0.544 \times 10^{21}$.

Equation 2.18 was used to convert the radius of gyration, $(R_G^2)^{\frac{1}{2}}$, to the root-mean-square end-to-end distance, $(\bar{r}^2)^{\frac{1}{2}}$. By consulting the tabulated values of $\Phi(\epsilon)$ according to Bloomfield and Zimm, (79) the lowest $\Phi(\epsilon)$ values given are 0.686 and 0.422×10^{21} for straight- and ring-chain polymers respectively. In this case, $\epsilon = 0.5$ and therefore the exponent α in the modified Staudinger Equation (see Equation 2.2) is equal to 1.25. This high value of α is indicative of a very stiffly coiled molecule and is in contrast to the value of 1.0 derived by Smidsrød (52). Because of the nature of the exponential term, small differences in α lead to large differences in M_η . If $\alpha = 1.25$ is arbitrarily substituted for $\alpha = 1.0$ in Smidsrød's equation, we obtain $M_\eta = 6000 \text{ g mol}^{-1}$. Therefore, the most appropriate equation for Protanal LFR5/60 Sodium Alginate is $[\eta] = 3.8 \times 10^{-6} M_w^{1.25}$. However, it should be noted that M_η is equivalent to M_w only when $\alpha = 1.0$ (62).

The relationship between two variables can always be written as an exponential rule if the range of applicability is limited. Hence, the range of Smidsrød's Equation has been exceeded by substituting $[\eta] = 1.056 \text{ dl g}^{-1}$ and a separate



calibration would be required for the low molecular weight Protonal LFR5/60.

The value of A_m , the Kuhn statistical segment from light scattering data using Equation 2.17., was 452 nm. This compares favourably with $A_m = 390$ nm at $\mu = 0.1$ due to Smidsrød (20) obtained from viscosity data using the Bloomfield-Zimm theory for the Flory Equation to obtain $(\bar{r}^2)^{\frac{1}{2}}$. Comparisons such as this substantiate the absolute value of M_w obtained as well as providing an indication of the relative extension of the molecule.

The hydrodynamic characteristics are of most interest with respect to the rheological properties of Alginate solutions. A free draining molecule would provide a lower frictional resistance in flow than would a non-draining molecule of the Flory 'equivalent sphere' theory. The free draining behaviour seen in rigid chain molecules in good solvents and non-draining behaviour of very flexible chains in poor solvents, are two extremes and most molecules are probably best described in terms of partial free drainage. However, only the behaviour of the two extremes has been quantified. Both the Kirkwood-Riseman (78,125) and the Debye and Bueche (134,135) theories attempt to quantify the fractional coefficient of free-draining molecules. The theory of Rouse (136) goes further and is based on a bead-spring molecular model whereby the energy storage and dissipation in sinusoidally oscillating displacements, are calculated; from this, the complex modulus or the complex

viscosity is calculated (60).

The theory attributed to Zimm (137) deals with non-draining molecules whereby frictional resistance is considered to include the viscous drag due to hydrodynamic interactions. Under conditions of diminishing viscous drag within a molecule, the Zimm theory reduces to the Rouse theory (138).

In conclusion, it can be seen that the Sodium Alginate molecule under study is of a low molecular weight and does not show any extreme deviations from Newtonian behaviour in solution. The molecular parameters determined agree well with previously published data. At high polymer concentrations, in excess of about 15 g dl^{-1} , entanglements are sufficient to lead to dominant elastic behaviour over and above the viscous properties.

3. RHEOLOGICAL PROPERTIES OF SUSPENDING AGENTS

3.1 Introduction

The most frequently used and the simplest method of suspending drug particles in a liquid medium is by the use of thickening agents. These may be dispersed, for example, sodium montmorillonite and bentonite, or dissolved as is the case for polyelectrolytes for example. The formulation of pharmaceutical suspensions, in contrast to formulation in other industrial products is limited in its choice of suspending agent by toxicological and regulatory restraints. This demands a good working knowledge of the agents available.

The most useful methods for assessing suspending agent performance are sedimentation and rheological testing. Many studies have been published in the general rheological (eg. 100,139-142) and pharmaceutical (eg.143,144) literature on the flow behaviour of systems with particles dispersed in non-Newtonian polymer solutions. When the volume fraction of particles, $\phi < 0.05$ (139) then the rheological properties are primarily those of the suspending agent alone. For this reason, many studies have characterised the behaviour of such agents as 'Carbopol' (144,146-148) and Xanthan Gum (149-152). Few studies have appeared in the pharmaceutical or allied literature (153-155) which consider the rheological aspects of combining two different suspending agents; such a process may be deemed necessary in order to obtain a certain rheological 'profile', or for pharmacological reasons.

In this study, the polyelectrolyte suspending agents Xanthan gum and Carbopol 934P were investigated with respect to their rheological properties in the presence of Sodium Alginate. For therapeutic reasons, outlined in Section 1.3., a low molecular weight Sodium Alginate is present in the formulation under study. The viscosity of the Alginate alone is insufficient to suspend the required particles for the desired length of time and a further agent is necessary.

In general, the conformation of a polyelectrolyte chain is usually disturbed by the presence of another polyelectrolyte, resulting in an antagonistic effect. Therefore, in suspension formulation, higher concentrations of combined suspending agents would be necessary.

Interactions between polyelectrolytes are usually of an ionic nature (156) although specific binding mechanisms have been noted in certain cases (157,158). In the present study, the combinations of 'Carbopol' - Sodium Alginate and Xanthan gum - Sodium Alginate were investigated for the effects of concentration, storage, shearing and the method of measurement on the rheological parameters obtained.

Two types of rheological testing were carried out, namely continuous shear and oscillatory methods. By comparing the results obtained using the two techniques, it may be possible to pinpoint certain characteristics in the continuous shear rheograms which are normally only quantified using a more

elaborate technique, eg. oscillatory testing.

Finally, in order to illustrate the applicability of oscillatory shear measurements to formulated products, some proprietary oral liquid preparations were tested. The proposal by Davis (151) that $\tan \delta (\omega)$ curves could be used as "fingerprints" for individual preparations will be discussed.

3.2 Theory

The rheological methods used in this work involved oscillatory and continuous shear techniques. The reader is referred to Section 2.2.3 for the theoretical basis of these methods.

3.2.1 Xanthan Gum and Carbopol

Xanthan gum is an extracellular polysaccharide produced by Xanthomonas campestris. It has a cellulose backbone with trisaccharide side chains on alternate residues as shown in Figure 3.1. according to Jansson et al (159). A pyruvate moiety is attached to approximately half of the terminal mannose units of the side chain, (160). The molecular weight of 'Keltrol' ¹ has been estimated to be 1.0×10^7 (152) and $1.75 \times 10^6 \text{ g mol}^{-1}$ (161), so it is likely that polydispersity is high. The wide use of Xanthan gum stems from its excellent stability over a wide range of pH, temperature, and ionic strength, and also its remarkable viscosity reduction on shearing, (149). 'Carbopol' ² is a synthetic poly (acrylic acid) cross-linked with polyalkyl ether (162), of general formula as given in Figure 3.2. Only one grade, Carbopol 934P,

¹ 'Keltrol' is a registered trademark of Kelco Co. for Xanthan Gum.

² 'Carbopol' is a registered trademark of B.F. Goodrich Co., Cleveland, Ohio, U.S.A.

Figure 3.1. The Structural Formula of Xanthan Gum.

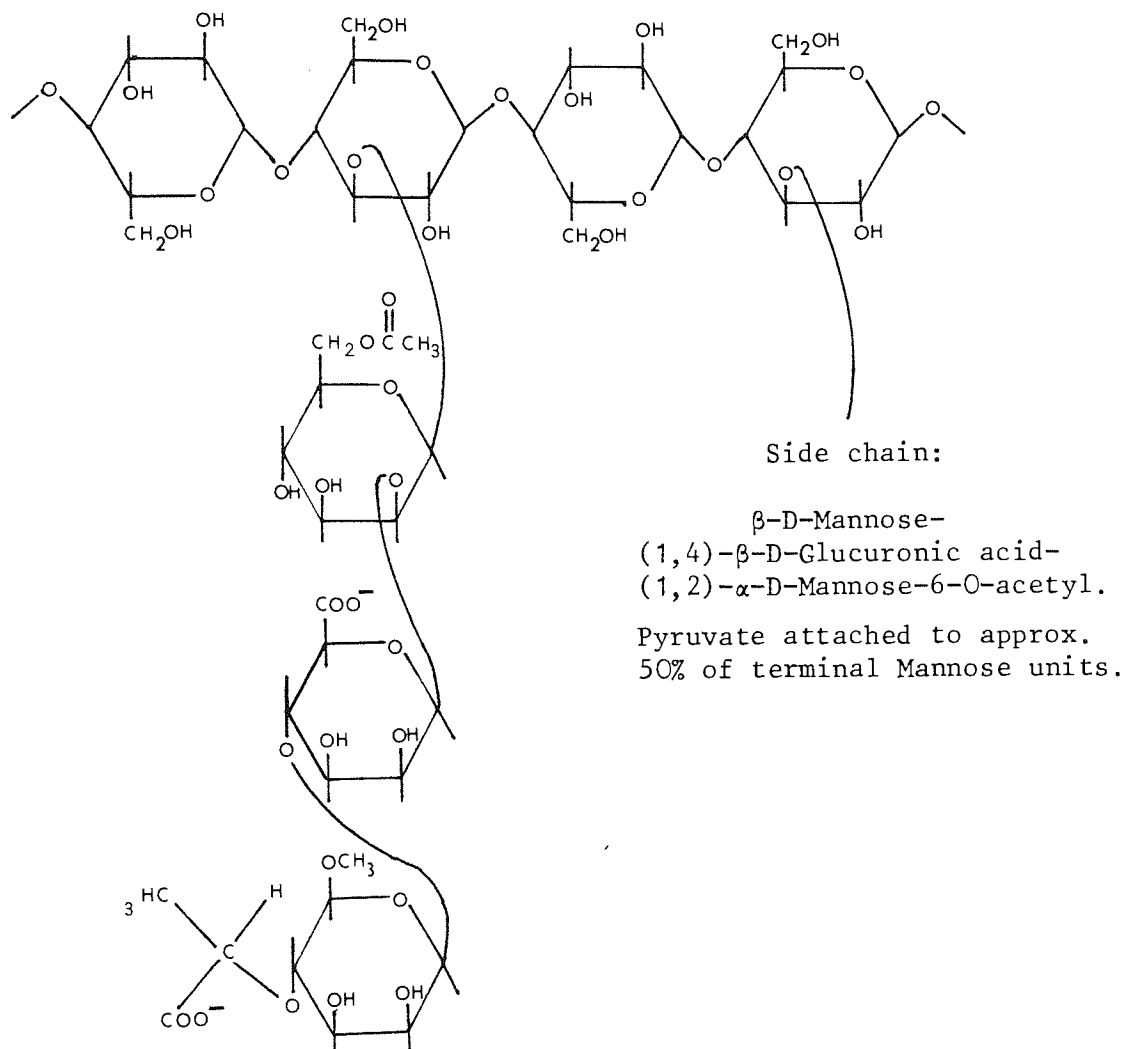
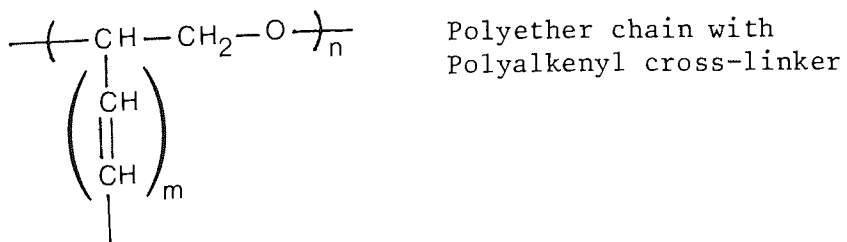


Figure 3.2. The Structural Formula of 'Carbopol'.



is suitable for use in pharmaceuticals, because of the presence of vinyl monomers in other grades (163). Since Carbopol 934P is a commercial product, it probably has high polydispersity (148), which is reflected in the molecular weight determinations of $22 \pm 3 \times 10^6$ (164) and $3.0 \times 10^6 \text{ g mol}^{-1}$ (165,166). An equivalent weight of 73.5 g was determined by Testa and Etter (164, 167) although 76 g is the more generally accepted value (162), Carbopol is used widely because of its high viscosity at low concentrations but it suffers from being sensitive to ionic strength and to small deviations from neutral pH.

3.2.2 Rheological Properties and Suspending Ability

There are three rheological parameters which have been useful as indicators of suspending ability. First, and at present highly favoured, is the zero shear viscosity, η_0 , obtainable at very low shear rates or frequencies. Buscall et al (40) showed the settling rates in non-Newtonian media to be inversely proportional to η_0 . This is a sensible result since the settling rates in Newtonian media as defined by Stokes' Law, are inversely proportional to the media viscosity. The second parameter is the instantaneous shear modulus, G_0 , the reciprocal of the instantaneous compliance, J_0 , from creep measurements. Its use has been suggested by Streng and Sonntag (41), and a theoretical justification for using the shear modulus was provided by Goodwin and Khidher (168). Thirdly, the yield value, τ_y , has frequently

been used in the past (169) but not without difficulty because of the problem of sharply defining the point at which flow commences, independently of the test method.

3.2.3 Shearing of Polymer Solutions

A decrease in apparent viscosity, η , with increasing shear rate, $\dot{\gamma}$, can occur as a result of either intra- or inter-molecular effects, (170), for dilute and concentrated solutions respectively. The terms 'dilute' and 'concentrated' are used with reference to the molecular weight. Shear thinning in dilute solutions leads to relatively small reductions in η , (171), but in concentrated solutions, η is frequently reduced by several orders of magnitude where viscosity is due to long relaxation times associated with entanglements. Rearrangement of entanglements takes place during shearing and Graessley (57) quantified this using a characteristic relaxation time, $t_{\eta} = 1/\dot{\gamma}_{\eta}$ where $\dot{\gamma}_{\eta}$ is the shear rate at which non-Newtonian behaviour becomes apparent. The use of $\dot{\gamma}_{\eta}$ required that η_0 be known and for some high polymers, it may be difficult to perform experiments at sufficiently low $\dot{\gamma}$ to determine η_0 . Values of $\dot{\gamma}_{\eta}$ of the order of 10^{-6} sec^{-1} are not unusual for suspending agent systems, (40).

3.2.4 Quantifying Non-Newtonian Flow

As mentioned in Section 2.2.3. many equations are available for quantifying the shear rate dependence of viscosity in non-Newtonian flow. Physical significance is frequently attached

to coefficients of such equations when little theoretical evidence is available. However, other relationships have been derived from first principles with certain assumptions concerning molecular motions.

Bueche (135, 172) considered both dilute solutions and bulk polymers. During shear, a spherical free draining molecule is alternately compressed and stretched whilst rotating in the direction of the applied force. A similar mathematical approach was derived by Debye (134).

Ree and Eyring (173) considered flow in terms of a number of different flow species within the fluid per unit area of the shear plane, each contributing to the stress. The shear stress was then the summation over all flow species.

The Doi-Edwards theory (174-177) uses a different approach to shear thinning in entangled systems. The model assumes that a molecule is contained within a tube of the same length. Entanglement effects become significant when the shear rate is less than the reciprocal time taken for the entire molecule to diffuse out of the tube. Hence, disentanglement takes place faster than entanglement and good qualitative agreement with experimental data was achieved.

Although some of the above mentioned theories have been available for a long time, their application to experimental data is far from universal. This is because the theories are derived for single polymers with narrow molecular weight

distributions in solutions without other substances present. In contrast, systems of pharmaceutical interest always contain several ingredients and the non-Newtonian behaviour may only be quantified using semi-empirical or wholly empirical equations. A few of these equations were listed in Table 2.3.. The ubiquity of such empirical equations is the result of rheological measurements on numerous different materials by many different methods. In this study, the 'Structure Equation' due to Shangraw et al (97) was found to adequately model all the continuous shear experimental data.

The relationship is based on the hypothesis of Williamson (178) that the shear stress, τ , measured during a continuous shear test of a pseudoplastic sample is made up of two component stresses τ_1 , and τ_2 . In common with Williamson, Shangraw used the equation for plastic flow to describe τ_1 , ie:

$$\tau_1 = f + \eta_{\infty} \dot{\gamma} \quad 3.1.$$

where f = yield stress

η_{∞} = viscosity coefficient

$\dot{\gamma}$ = shear rate

Whilst Williamson considered τ_2 to be a hyperbolic function of $\dot{\gamma}$, Shangraw chose an exponential form such that

$$\tau_2 = b_v \exp^{-a\dot{\gamma}} \quad 3.2.$$

where b_v = coefficient of viscous resistance

a = constant with the units of time

Since the exponential term represents shear thinning, the component stresses are combined as $\tau = \tau_1 - \tau_2$. Therefore

$$\tau = f + \eta_{\infty} \dot{\gamma} - b_v \exp^{-a\dot{\gamma}} \quad 3.3.$$

which is the Shangraw 'Structure' Equation. When $\dot{\gamma} = 0$,
 $\tau = f - b_v$ which is claimed to represent the yield stress.
This conflicts with Equation 3.1. where f alone is the yield
stress. Therefore little weight can be placed on the physical
significance of these coefficients, although η_{∞} agrees well
with the high shear limiting viscosity.

3.3 Materials and Methods

The Sodium Alginate used was Protonal LFR5/60 as in Section 2;
the 'Carbopol' was of pharmaceutical grade 934P¹; the Xanthan
gum was 'Keltrol F'² and Thiomersal was of laboratory reagent
grade³.

3.3.1 Rheological Testing

The experimental technique of oscillatory testing has been
detailed in Section 2.3.4.2. To test for linear
viscoelasticity in a narrow range, representative samples were
tested for input amplitudes of 1.7 and 4.3×10^{-3} rad. No
significant differences in amplitude ratio, ν , or phase lag, C ,
were found, therefore all samples were tested using the minimum
amplitude necessary.

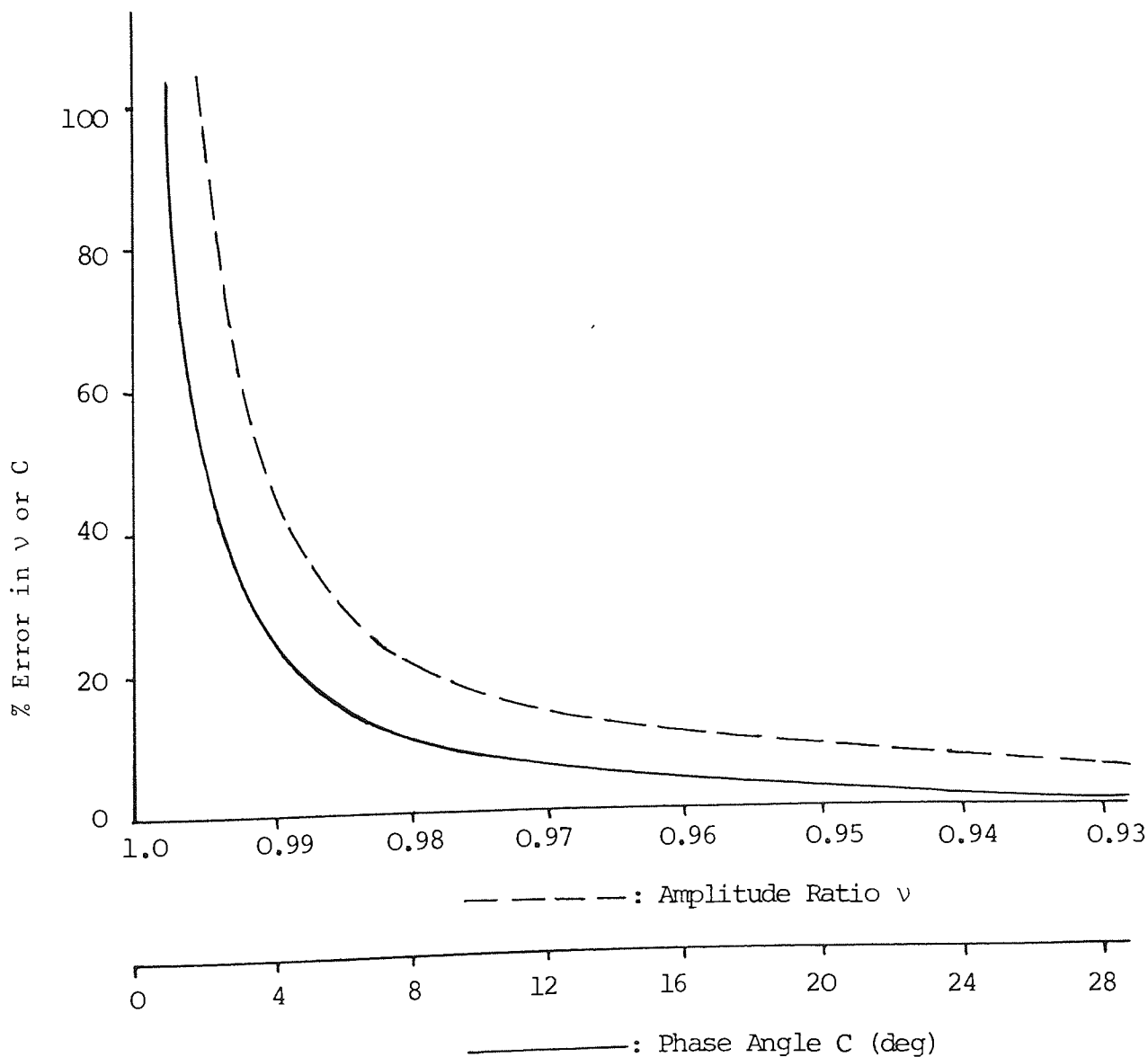
Repeated testing of several viscoelastic samples showed that
 G' and η' could be determined with a precision of $\pm 5\%$.
However, at low phase angles, small errors in C lead to large
errors in η' due to the \sin term in Equation 2.24.: at values
of ν approaching 1.0., small errors in ν lead to large errors
in G' . Both of these aspects are quantified in Figure 3.3.

¹ B.F. Goodrich, Cleveland, Ohio, USA.

² Kelco Co., San Diego, California, USA.

³ B.D.H., Poole, Dorset, UK.

Figure 3.3. Precision of Storage Modulus, G' , and Dynamic Viscosity, η' , Values at High Amplitude Ratio ν and Low Phase Angle C Respectively. Amplitude Ratio (broken line) : Error in $G'(\omega)$ determined from a precision of ± 0.002 ; $C = 0$ rad, $\omega = 0.792$ rad s^{-1} . Phase Angle (solid line) : Error in $\eta'(\omega)$ determined from a precision of ± 0.0087 rad; $\nu = 0.5$, $\omega = 0.792$ rad s^{-1}).



showing that additional significant errors are introduced at $C \neq 0$, $C \lesssim 15^0$ and $\nu < 0.96$.

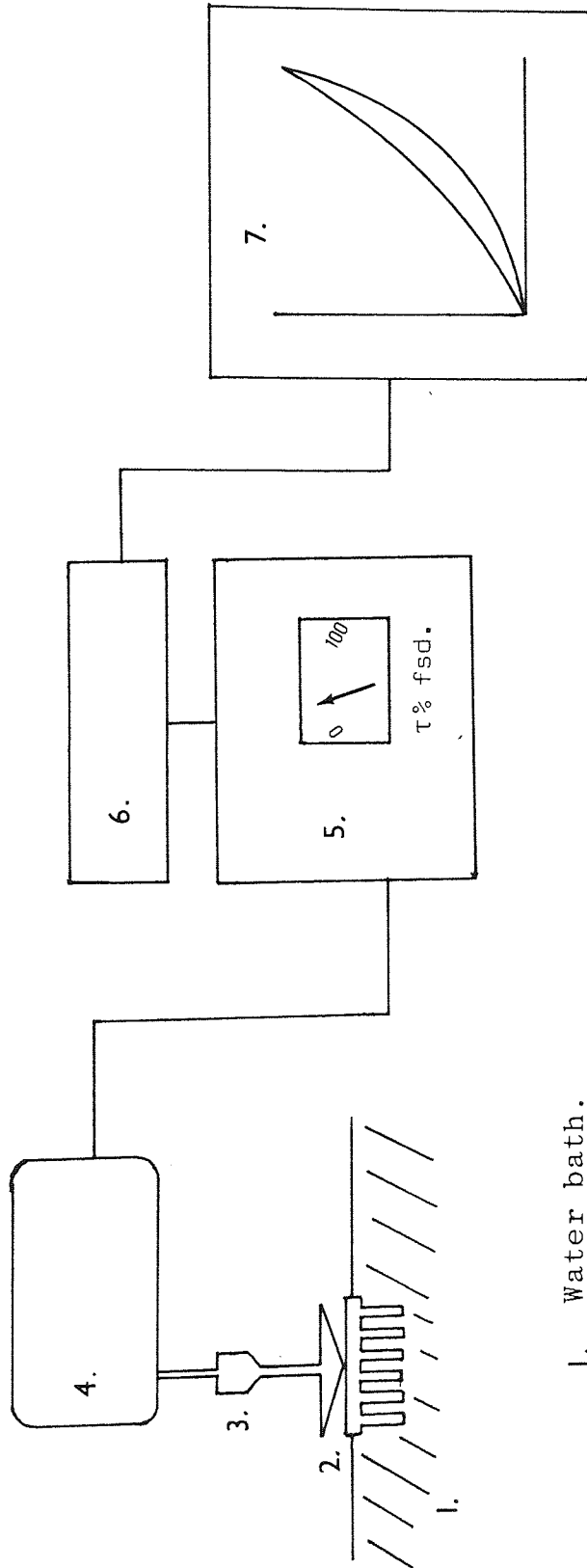
Continuous shear testing was carried out using a Rheomat 30 viscometer¹, the basic design of which is shown in Figure 3.4. A variable speed motor rotating at known angular velocity, applies a shear rate via the upper member of the system and the resultant torque on the sample is monitored. By calibration, a $\tau(\dot{\gamma})$ rheogram curve was constructed automatically with an X-Y chart recorder².

In order to maintain certain consistencies with the rheogoniometer, cone and plate geometry was used. The non-truncated cone angle was $30'54''$ and the plate diameter 5.312 cm. Tests were carried out at 21.5^0 C with applied shear rates starting at 53.6 sec^{-1} and taking 0.5 min to reach the peak of 3950 sec^{-1} . Only up-curves were analysed although down-curves were also obtained. Attempts were made to fit the data to several empirical equations using graphical analysis and non-linear regression analysis routine, 'NONLIN' (179). From these, Equation 3.3., derived by Shangraw, was used throughout. Similar regression analysis using the 'Structure' Equation 3.3. was recommended by Neibergall et al (180).

¹ Contraves AG, Schaffhauserstrasse 580, CH-8052, Zurich, Switzerland.

² Bryans Model 25000, Bryans Southern Instruments Limited, Mitcham, Surrey, UK.

Figure 3.4. BASIC PRINCIPLES OF THE 'RHEOMAT 30' VISCOMETER.



1. Water bath.
2. Cone and Plate geometry.
3. Rotating shaft.
4. Motor and torque sensor by torsion bar.
5. Amplifier for torque and tachometer signals.
6. Automatic shear rate programmer.
7. X-Y chart recorder.

3.3.2 Preparation of Samples

Samples of mixtures of suspending agents were prepared by using two separate methods.

Method A - Industrial Pilot Plant Equipment.

Dispersions or solutions of Carbopol, Xanthan gum or Sodium Alginate in deionised water were obtained using a 'Lightnin'¹ high speed mixer with a 10 cm blade paddle stirrer. Thiomersal 0.002% w/w was included as a preservative. Carbopol was neutralised to pH 7 using 20% w/w NaOH, and suspending agents combined in a 5 Kg capacity 'Hobart'² planetary mixer. When the effect of additional high shear was investigated, a 'Silverson' AXR homogeniser³ was employed. It was used at the maximum speed setting and contained the small square mesh which produced high shearing of the sample.

Method B - Laboratory Scale Equipment.

The minimum necessary shear required for dispersion was achieved using a Heidolph variable speed stirrer motor⁴ with a 3 cm stainless steel paddle blade. Admixtures were prepared manually by stirring in a glass beaker.

Samples prepared by each method were centrifuged to remove air bubbles and for comparison of methods A and B, samples were stored at 20⁰ C for at least seven days prior to rheological measurement.

¹ Lightnin Mixers Ltd., Stockport, Cheshire, U.K.

² Hobart Manuf. Co. Ltd., New Southgate, London, N11, U.K.

³ Silverson Machines Ltd., Waterside, Chesham, Bucks. U.K.

⁴ Heidolph Elektro KG, W. Germany

3.3.3 Sedimentation Tests

When Xanthan gum and Sodium Alginate solutions were mixed without shearing, sedimentation of the denser Xanthan phase occurred. The sedimentation heights were determined in 10 x 2 cm specimen tubes stored at 20°C for five months and compared with samples that had been sheared using the 'Silverson' homogeniser.

3.4 Results

The rheological data obtained from oscillatory testing is presented as $G'(\omega)$ and $\eta'(\omega)$, ie, the real components of the complex modulus and viscosity respectively. The appearance of plateaux indicates limiting elastic or viscous behaviour at high and low frequencies respectively; besides this, the manner in which either G' or η' change with ω is characteristic of the system.

Within Sections 3.4.1. and 3.4.2., all $G'(\omega)$ and $\eta'(\omega)$ curves are drawn to the same scale for comparison purposes, although the ordinate may be shifted vertically.

3.4.1 Xanthan Gum Systems

3.4.1.1 Effect of Concentration

As would be expected, G' and η' both increased with Xanthan concentration as shown in Figures 3.5., 3.6. and summarised for $\omega = 25 \text{ rad s}^{-1}$ in Figure 3.7 (a) and (b). $G'(\omega)$ shows curvature with a tendency to plateau at perhaps 10^2 to 10^3 rad s^{-1} ; for $\eta'(\omega)$, no clue is apparent as to the lower

Figure 3.5. The Effect of the Frequency of Oscillation on the Storage Modulus of Various Concentrations of Xanthan Gum Solutions.

Concentrations (% w/w) : 0.4 ∇ , 0.5 \triangle , 0.7 \blacktriangle , 0.8 \blacktriangle , 1.0 \circ , 1.5 \bullet , 1.8 \bullet , 4.0 \bullet .

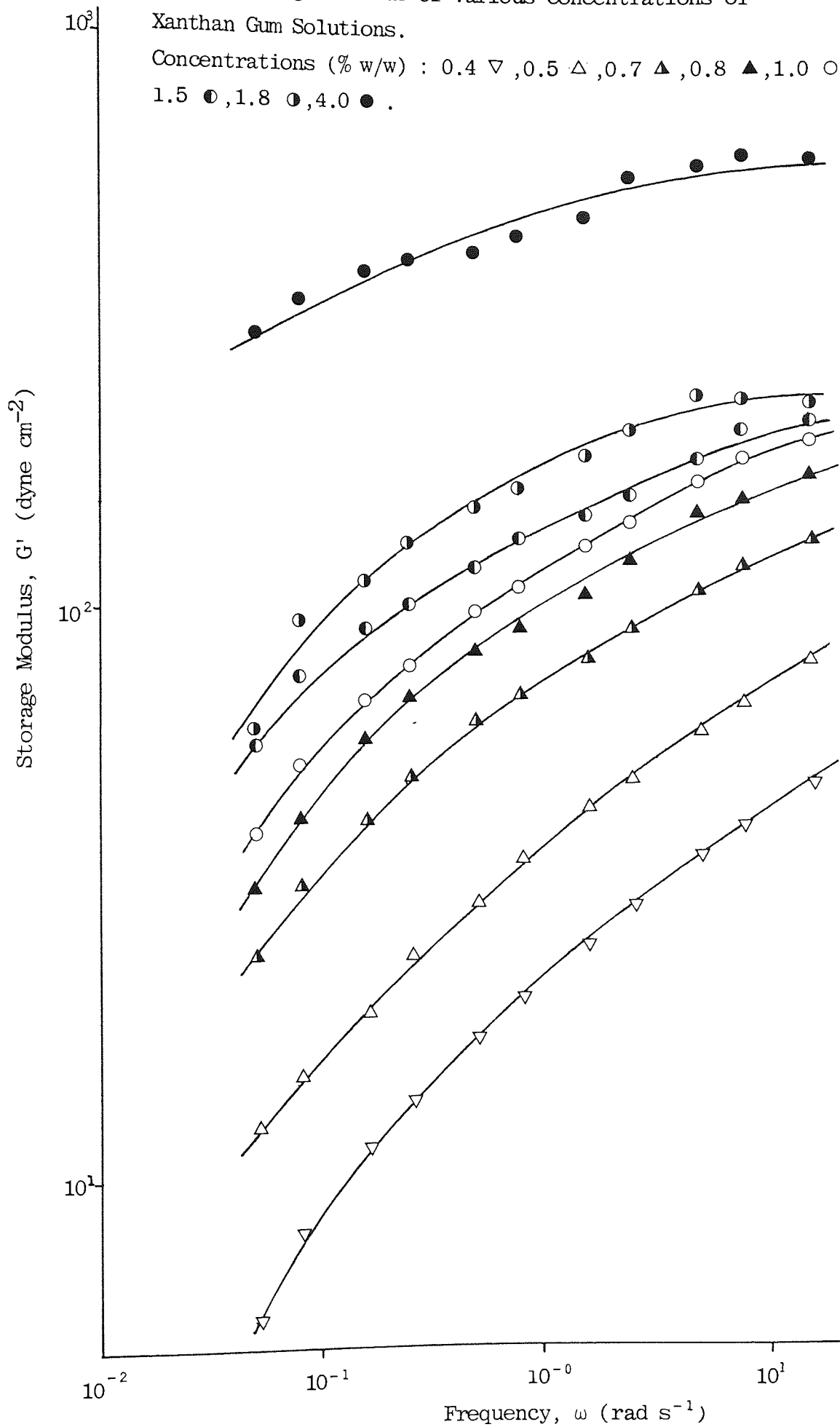


Figure 3.6. The Effect of the Frequency of Oscillation on the Dynamic Viscosity of Various Concentrations of Xanthan Gum Solution.

Concentrations (% w/w) : 0.4 ∇ , 0.5 \triangle , 0.7 \blacktriangle , 0.8 \blacktriangle , 1.8 \circ , 4.0 \bullet .

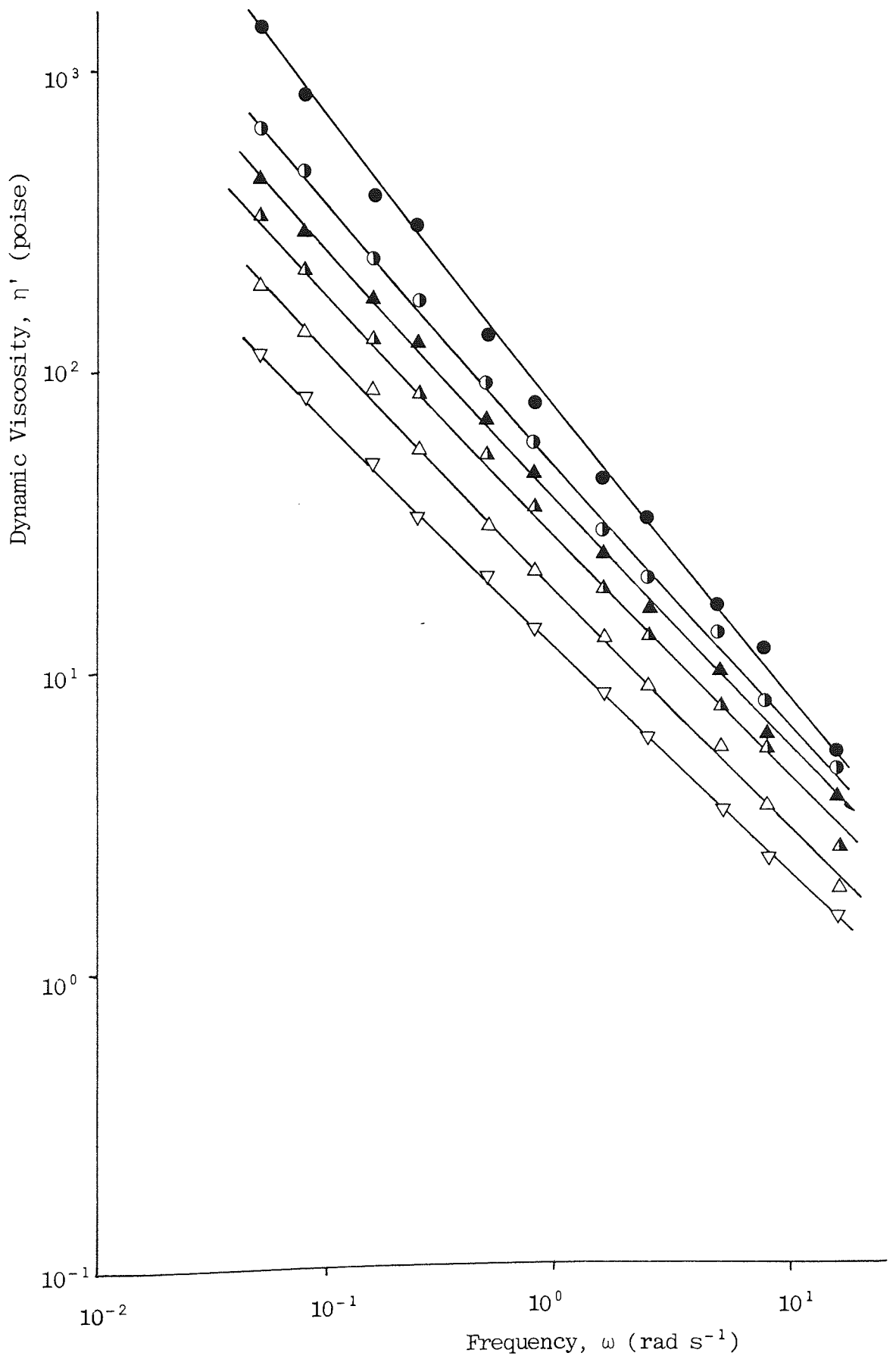
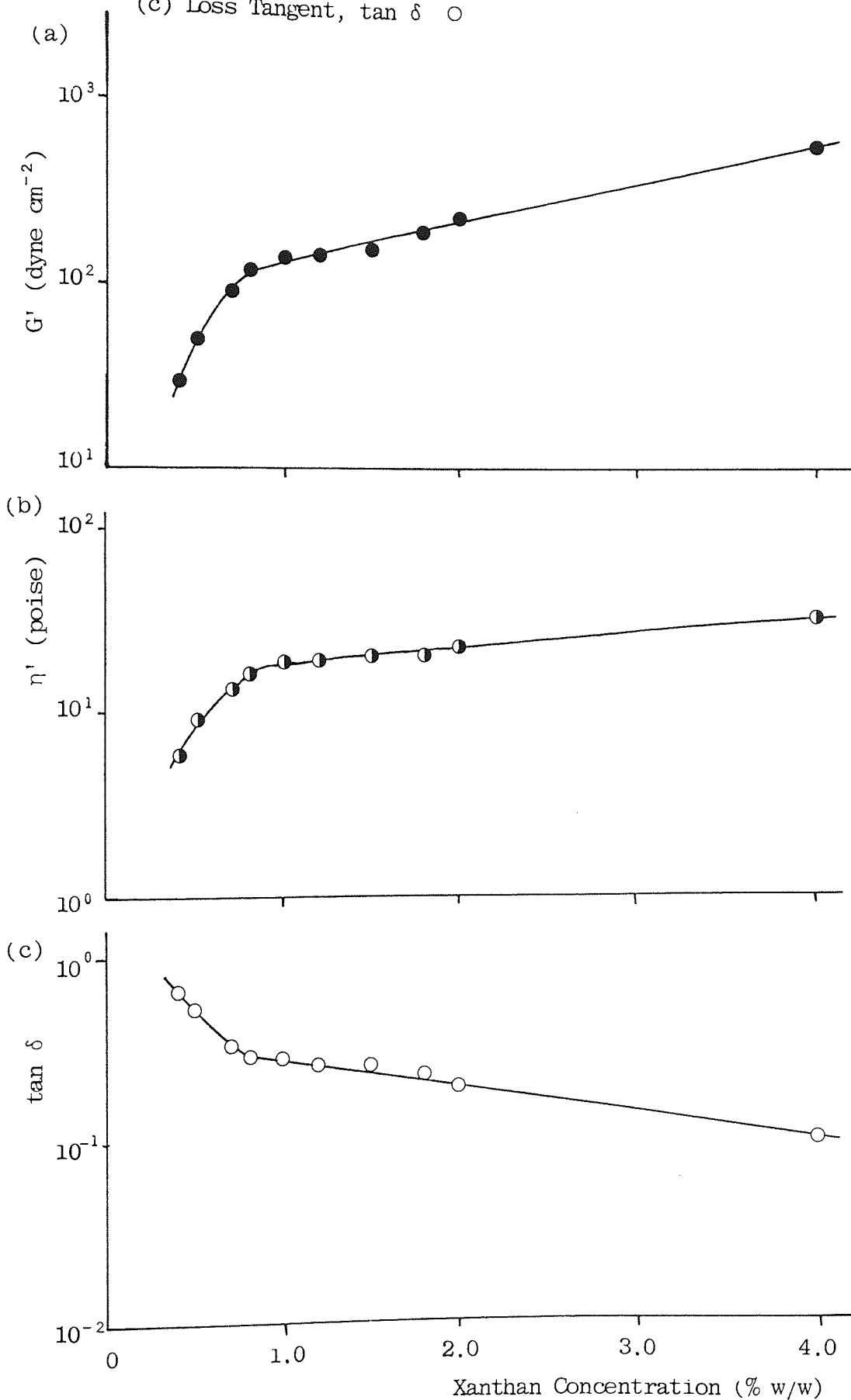


Figure 3.7. The Effect of the Concentration of Xanthan Gum in Solution on the Viscoelastic Parameters at Oscillation Frequency $\omega = 2.5 \text{ rad s}^{-1}$.

(a) Storage Modulus, G' ● (b) Dynamic Viscosity, η' ○
 (c) Loss Tangent, $\tan \delta$ ○



frequency necessary to attain a limiting viscosity η_0 .

The loss tangent, $\tan \delta (\omega)$ curves in Figure 3.8., which are summarised for $\omega = 2.5 \text{ rad s}^{-1}$ in Figure 3.7.(c), tell us that although both elastic (storage) and viscous (loss) components increased with concentration, the former increased more rapidly. Hence, one would expect the higher Xanthan concentrations to exhibit gel-like rigidity, which did in fact occur.

With regard to the mixed Xanthan and Alginate systems, there was an interesting contrast. Increasing the concentration of Xanthan in Alginate solutions showed a different effect to increasing the concentration of Alginate in Xanthan solutions. In the case of the former, see Figure 3.9. to 3.13., the viscoelastic parameters increased steadily but in the latter instance, see Figures 3.14 to 3.16., the concentration range 1.0 to 3.0 % w/w Alginate had a very marked effect. In this range, $G' (\omega)$ and $\eta' (\omega)$ were reduced by a logarithmic cycle whereas other concentrations had relatively little effect. This infers that the Alginate was being 'titrated' against the Xanthan and that the concentration range 1.0 to 3.0% w/w Alginate represents the end-point.

3.4.1.2 Effect of Preparation Method

The high speed mixer used in the industrial 'pilot scale' preparation, Method A, was found to cause irreversible shear breakdown of the Xanthan-Alginate mixes studied. With

Figure 3.8. The Effect of the Frequency of Oscillation on the Loss Tangent of Various Concentrations of Xanthan Gum Solution.

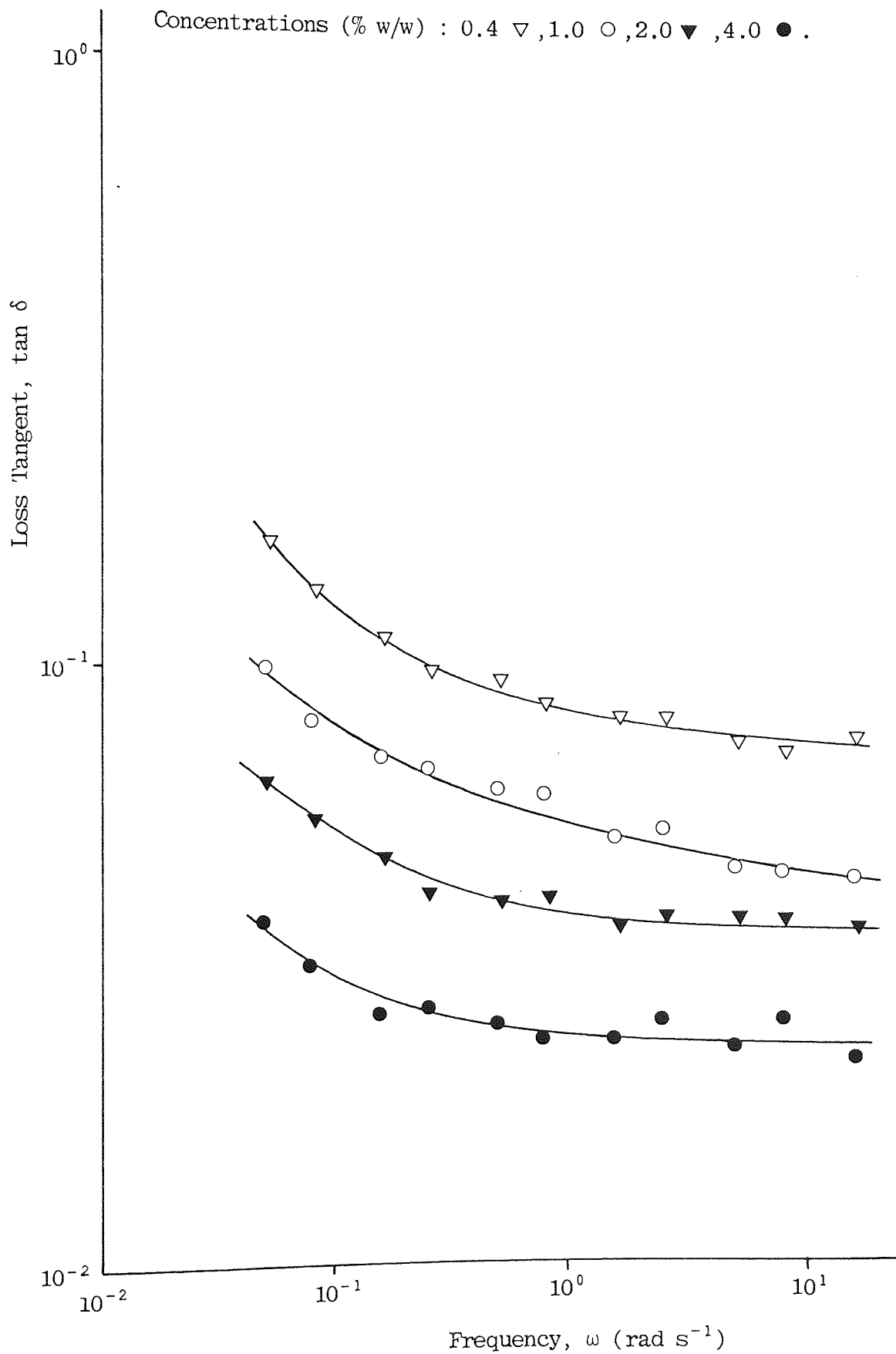


Figure 3.9. The Effect of the Concentration of Xanthan Gum in Sodium Alginate 5% w/w Solution on the Storage Modulus, G' plotted as a function of the Frequency of Oscillation.
Method A. Industrial Pilot Scale Preparation.

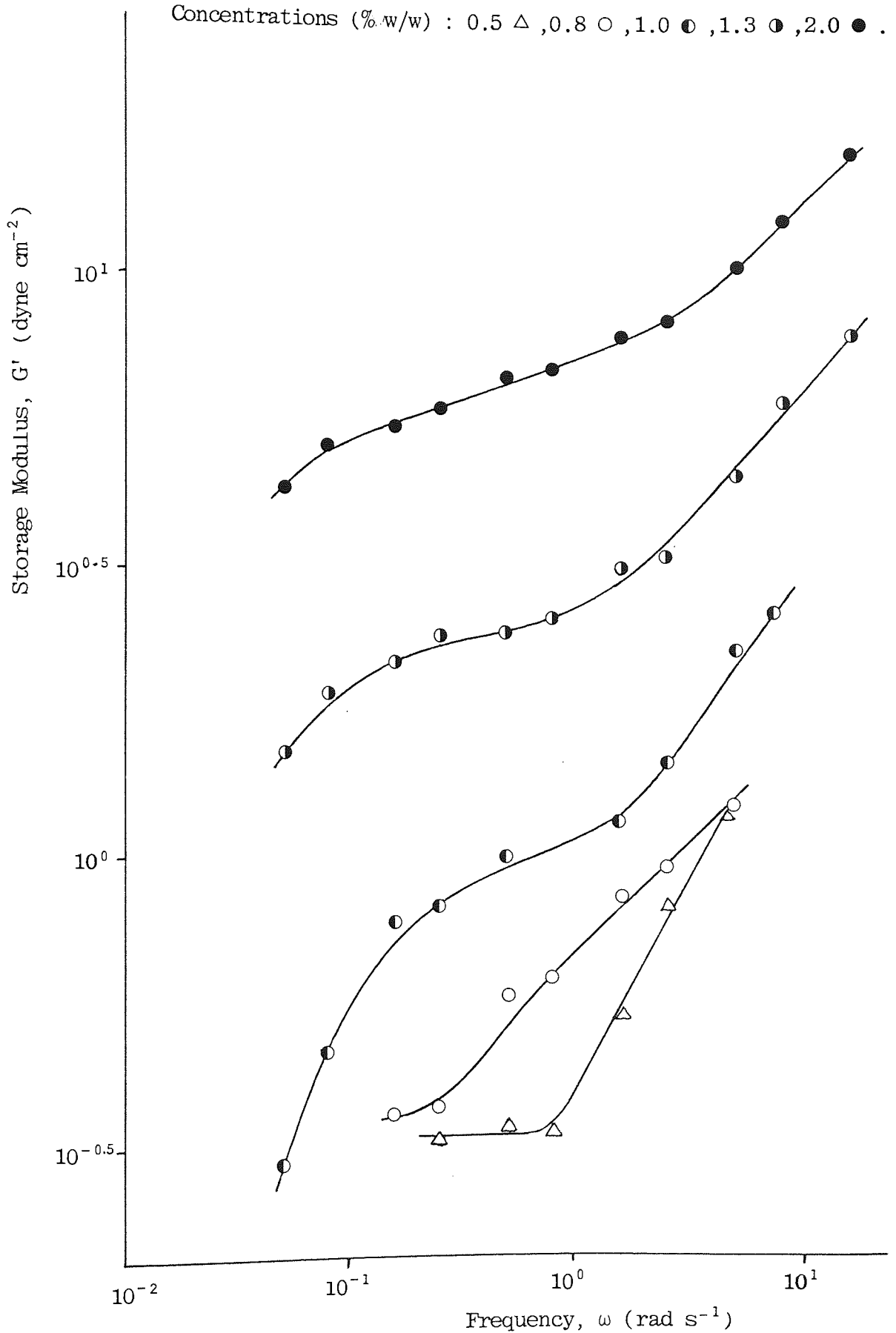


Figure 3.10. The Effect of Concentration of Xanthan Gum in Sodium Alginate 5% w/w Solution on the Storage Modulus, G' , plotted as a function of the Frequency of Oscillation, ω .

Method B : Laboratory Scale Preparation.

Xanthan Concentrations (% w/w) : 0.2 Δ , 0.4 \circ ,
0.5 \bullet , 0.8 \circ , 1.0 \bullet .

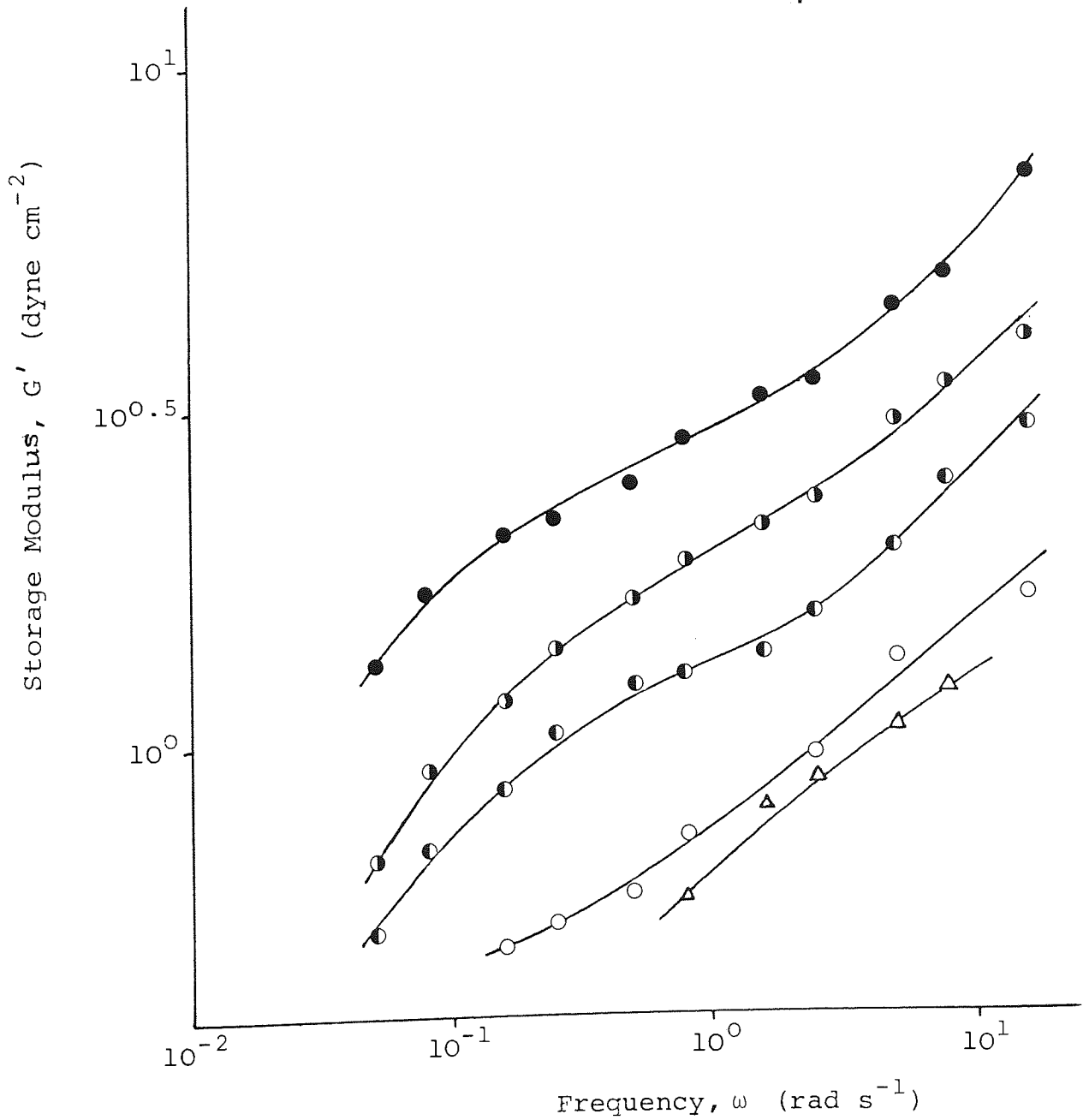


Figure 3.11. The Effect of Concentration of Xanthan Gum in Sodium Alginate 5% w/w Solution on the Dynamic Viscosity, η' , plotted as a function of the Frequency of Oscillation, ω .

Method A : Industrial Pilot Scale Preparation.

Xanthan Concentrations (% w/w) : 0.0 Δ , 0.5 \circ , 0.8 \bullet , 1.3 \circ , 2.0 \bullet .

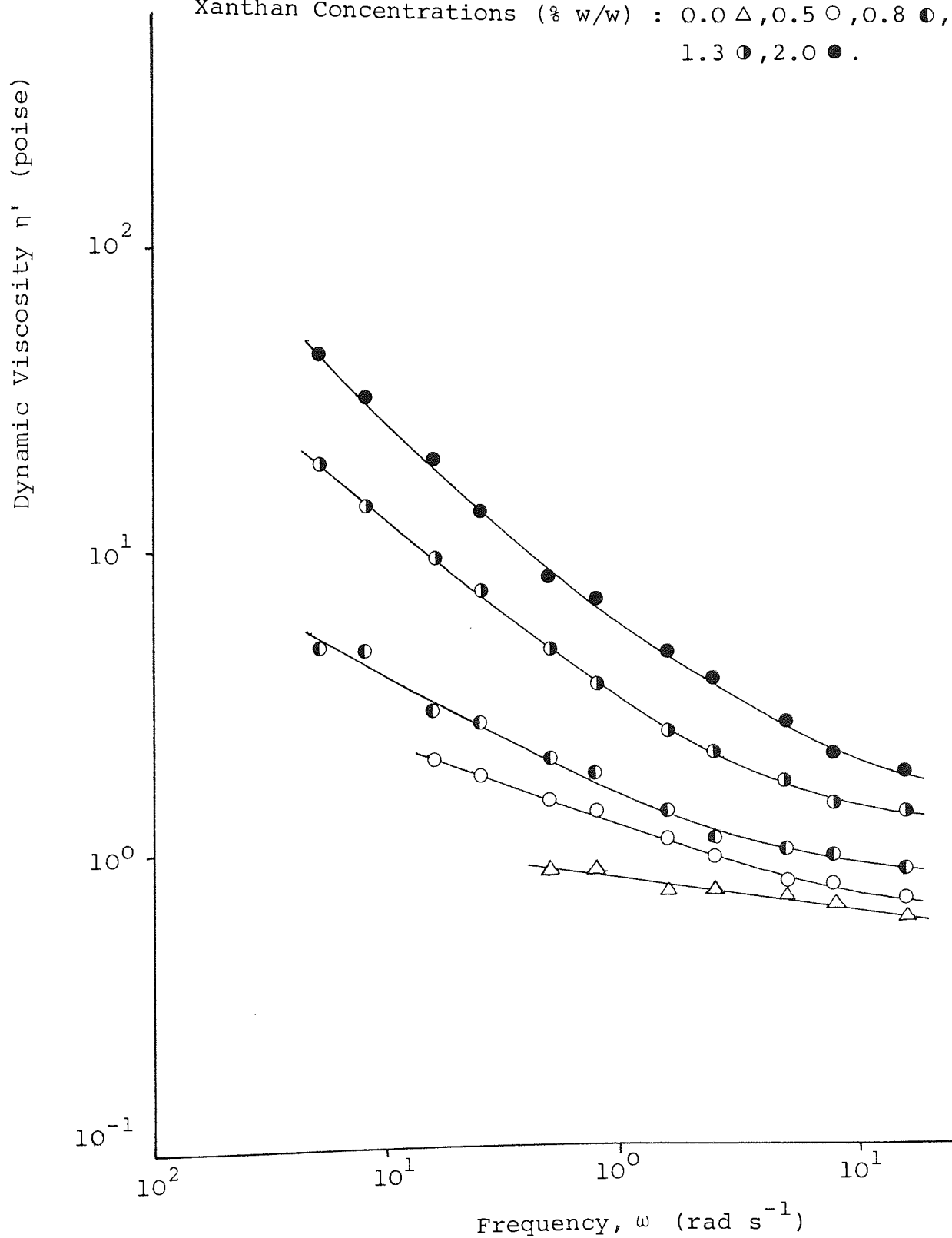


Figure 3.12. The Effect of Concentration of Xanthan Gum in Sodium Alginate 5% w/w Solution on the Dynamic Viscosity, η' , plotted as a function of the Frequency of Oscillation, ω .

Method B : Laboratory Scale Preparation.

Xanthan Concentrations (% w/w) : 0.2 Δ , 0.4 \circ , 0.5 \bullet ,
0.8 \bullet , 1.0 \bullet

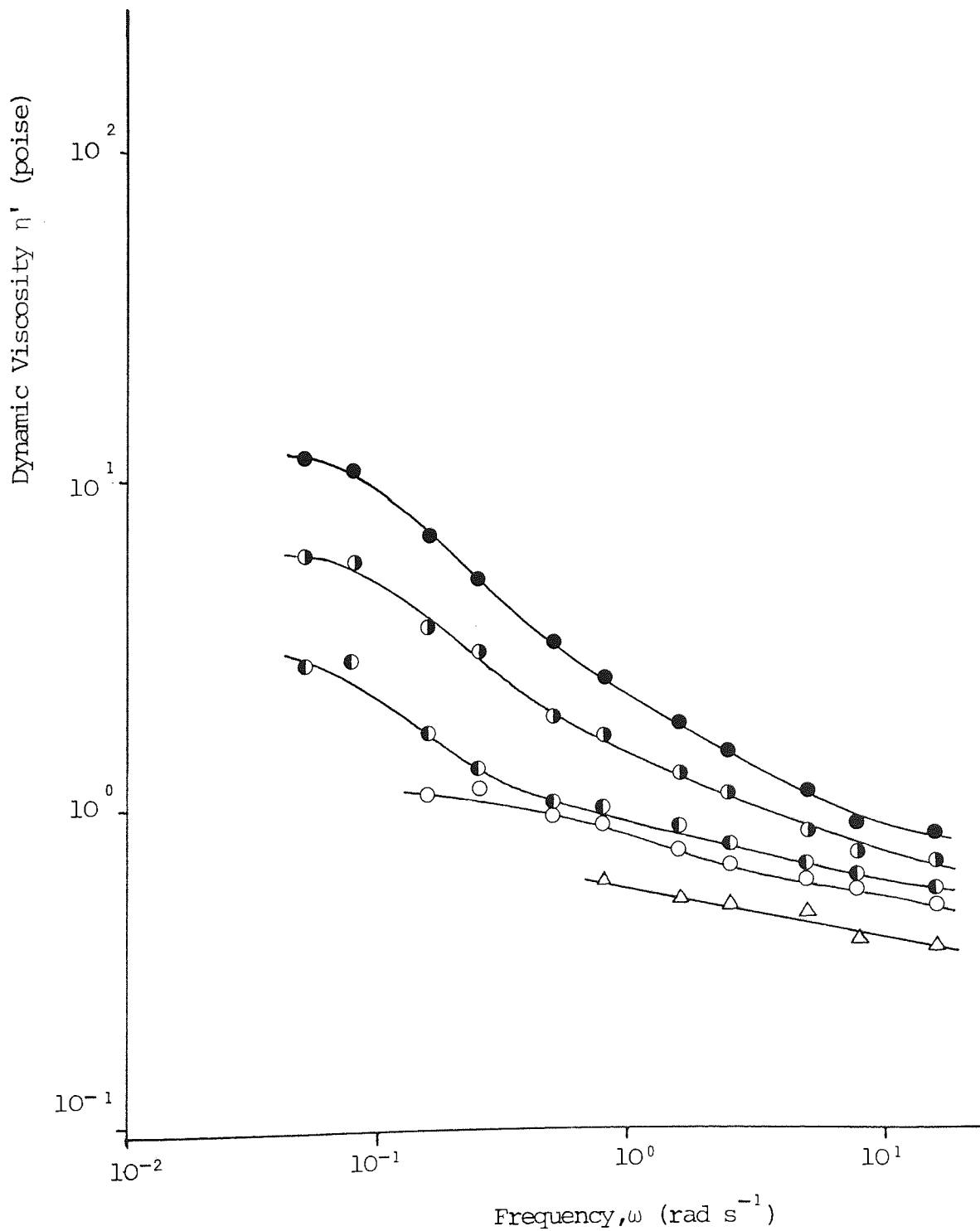


Figure 3.13. The Effect of Concentration of Xanthan Gum in Sodium Alginate 5% w/w Solution on (a) Dynamic Viscosity and (b) Storage Modulus at Oscillation Frequency, $\omega = 2.5 \text{ rad s}^{-1}$.

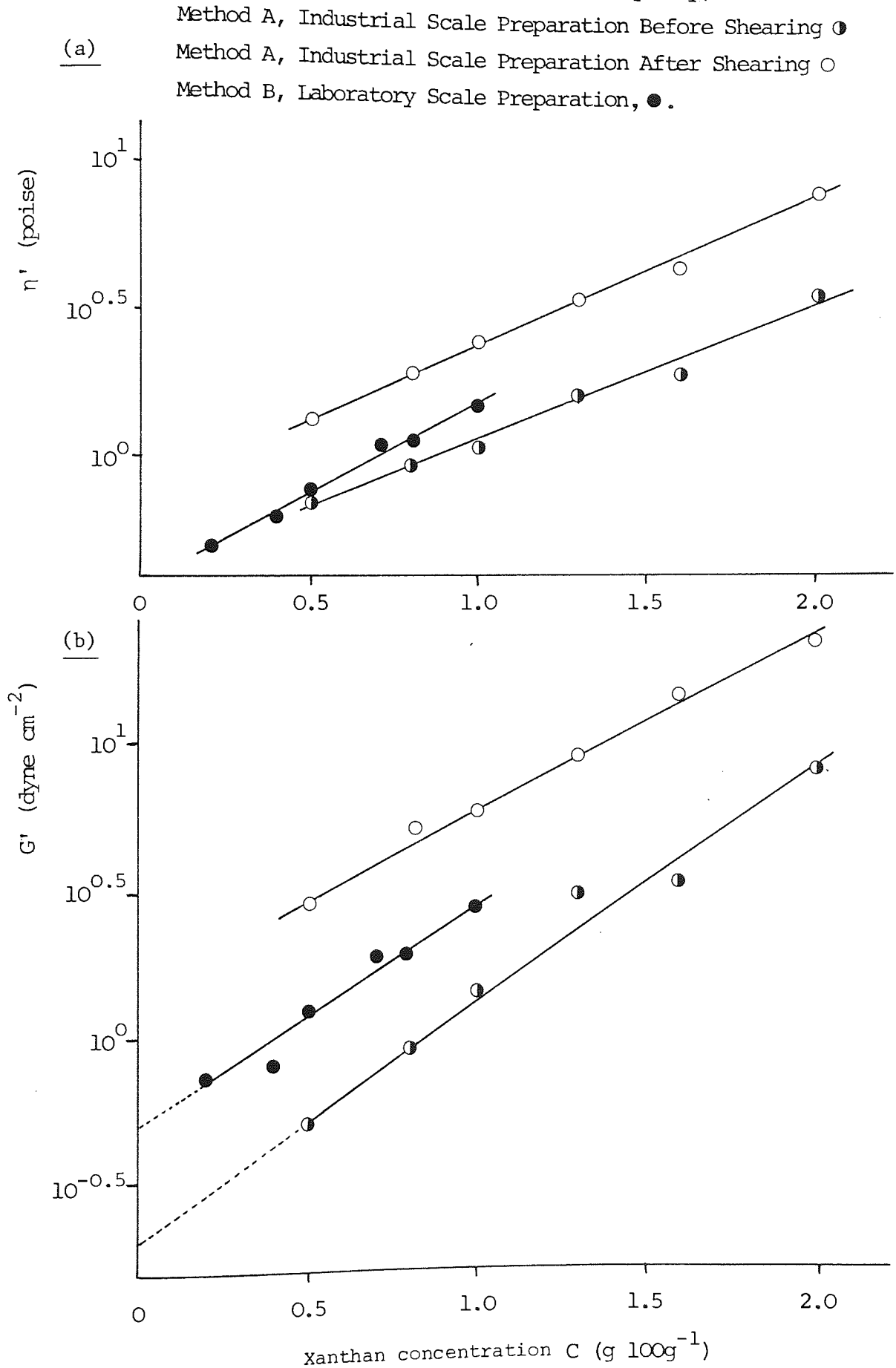


Figure 3.14. The Effect of the Concentration of Sodium Alginate in Xanthan Gum 2% w/w Solution on the Storage Modulus G' , plotted as a function of the Frequency of Oscillation, ω .

Concentrations (% w/w) : 0.0 ●, 0.5 ○, 1.0 ◐, 2.0 ◑
2.5 ▲, 3.0 △, 4.0 ▽, 5.0 ▼
8.0 Δ.

Figure 3.14 (see facing page)

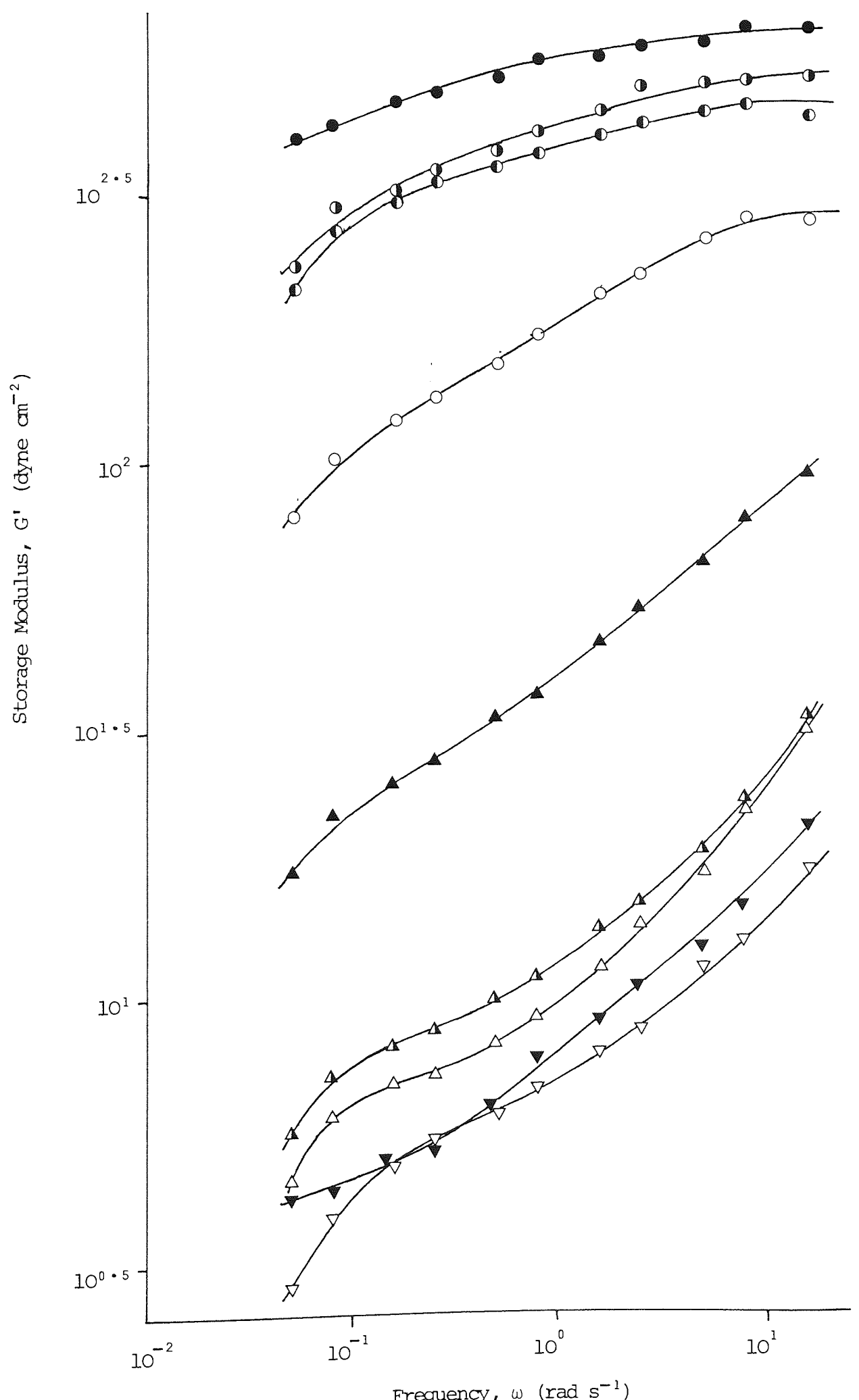


Figure 3.15. The Effect of the Concentration of Sodium Alginate in Xanthan Gum 2% w/w Solution on the Dynamic Viscosity, η' , plotted as a function of the Frequency of Oscillation, ω .

Alginate Concentrations (% w/w) : 0.0 ●, 2.5 ▲, 3.0 ▲, 8.0 ▲.

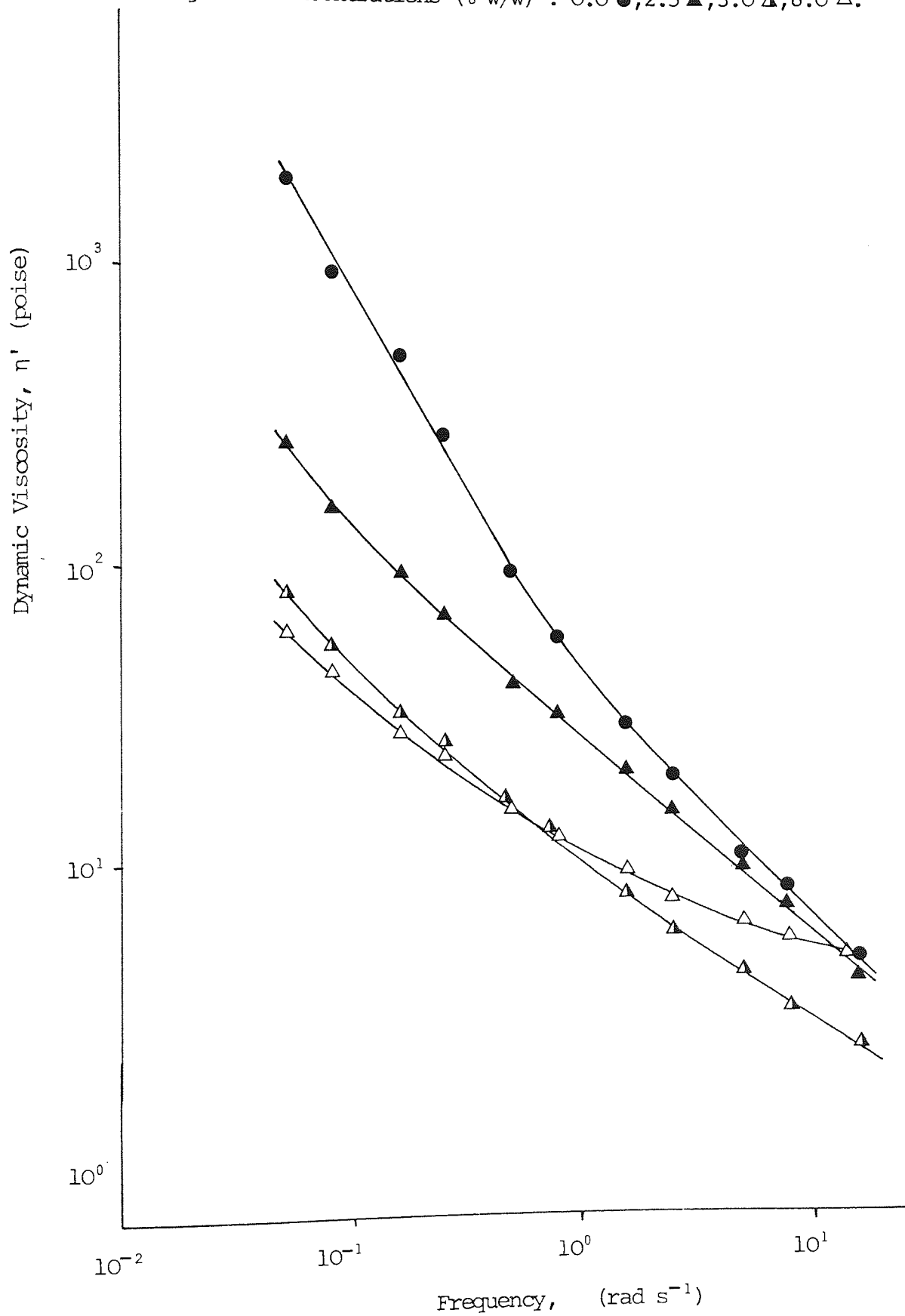
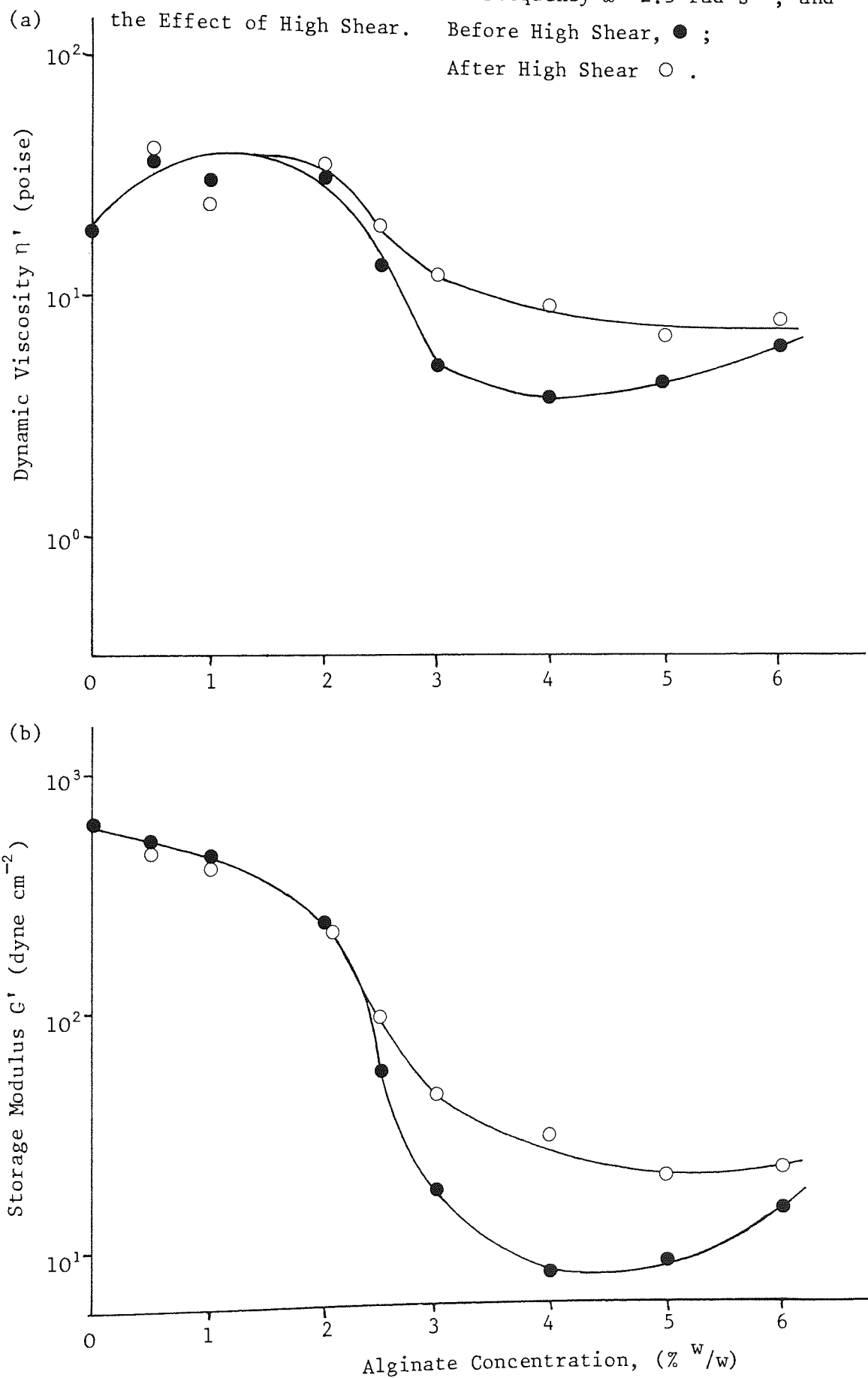


Figure 3.16. The Effect of Concentration of Sodium Alginate in Xanthan Gum 2% ^w/_w Solution on (a) Dynamic Viscosity and (b) Storage Modulus at Oscillation Frequency $\omega = 2.5 \text{ rad s}^{-1}$, and the Effect of High Shear. Before High Shear, ● ; After High Shear ○ .



reference to Figures 3.9 to 3.12., $G'(\omega)$ and $\eta'(\omega)$ were significantly higher for the relatively low shear samples prepared by Method B. Figures 3.13. (a) and (b), which summarise G' and η' at $\omega = 2.5 \text{ rad s}^{-1}$ as a function of Xanthan concentration, show that the effect was marked for elasticity. The intrinsic modulus, $[G'_{\omega}]_{C=0}$ obtained by extrapolation of Figure 3.13. (b) to zero Xanthan concentration, is $0.52 \text{ dyne cm}^{-2}$ for Method B but only $0.20 \text{ dyne cm}^{-2}$ for Method A. This suggests that the effect of the mixing time in an industrial situation can be quantitatively linked with the rheological performance of the final product. For example, if the suspending ability of the vehicle is correlated with η_0 , (137), then the mixing time may not be so critical with respect to the physical stability as if the instantaneous modulus G_0 , (138), had been correlated.

Twelve Xanthan - Alginate mixes were prepared on two separate occasions using Method A. The samples were allowed to equilibrate for similar periods of time prior to rheological testing. The viscoelastic parameters measured using the Weissenberg Rheogoniometer occasionally differed by more than 5% but the distribution of differences was non-systematic.

Comparison of the two preparation methods show the results to be consistent with a significant irreversible shear breakdown of the Xanthan gum leading to reduced gel-like properties of the Xanthan-Alginate mixes. The Sodium Alginate used was of low molecular weight and prolonged shearing of a 10% w/w

solution did not reduce the viscoelastic parameters significantly below those found in Section 2.4.4.

3.4.1.3 Effect of Shearing

It was found that low shear blending in a planetary mixer did not produce stable Xanthan-Alginate mixes; separation of the denser Xanthan phase occurred unless good blending was achieved by applying high shear for example, by the use of a 'Silverson' mixer. The effect of high shear on the separation of Xanthan was quantified by monitoring the sedimentation rate of the Xanthan component. Rate constants were obtained from first order plots of the sedimentation ratio against time.

Figure 3.17. shows that increasing the concentration of Xanthan in Alginate solution reduced the separation rates as would be expected; increasing the Alginate content in Xanthan solution did not yield a significant trend. The sedimentation rate data before and after shearing is given in Table 3.1.. More importantly, after shearing the samples for 5 min. using the 'Silverson' mixer, the separation rates were extremely low.

To study the effect of shearing time and subsequent recovery on rheological properties, Xanthan 2% - Alginate 5% w/w mix was sheared for 0,5,10,20,40, min. and oscillatory shear measurements were made 24 hours after preparation. The results given in Figures 3.18. and 3.19. for $G'(\omega)$ and $\eta'(\omega)$ respectively, show that on shearing, the elastic component was increased by a greater proportion than the viscous component.

Figure 3.17. The Effect of the Concentration of Xanthan Gum in Alginate 5% w/w Solution on the First Order Rate Constant for the Decreasing Sedimentation Ratio.

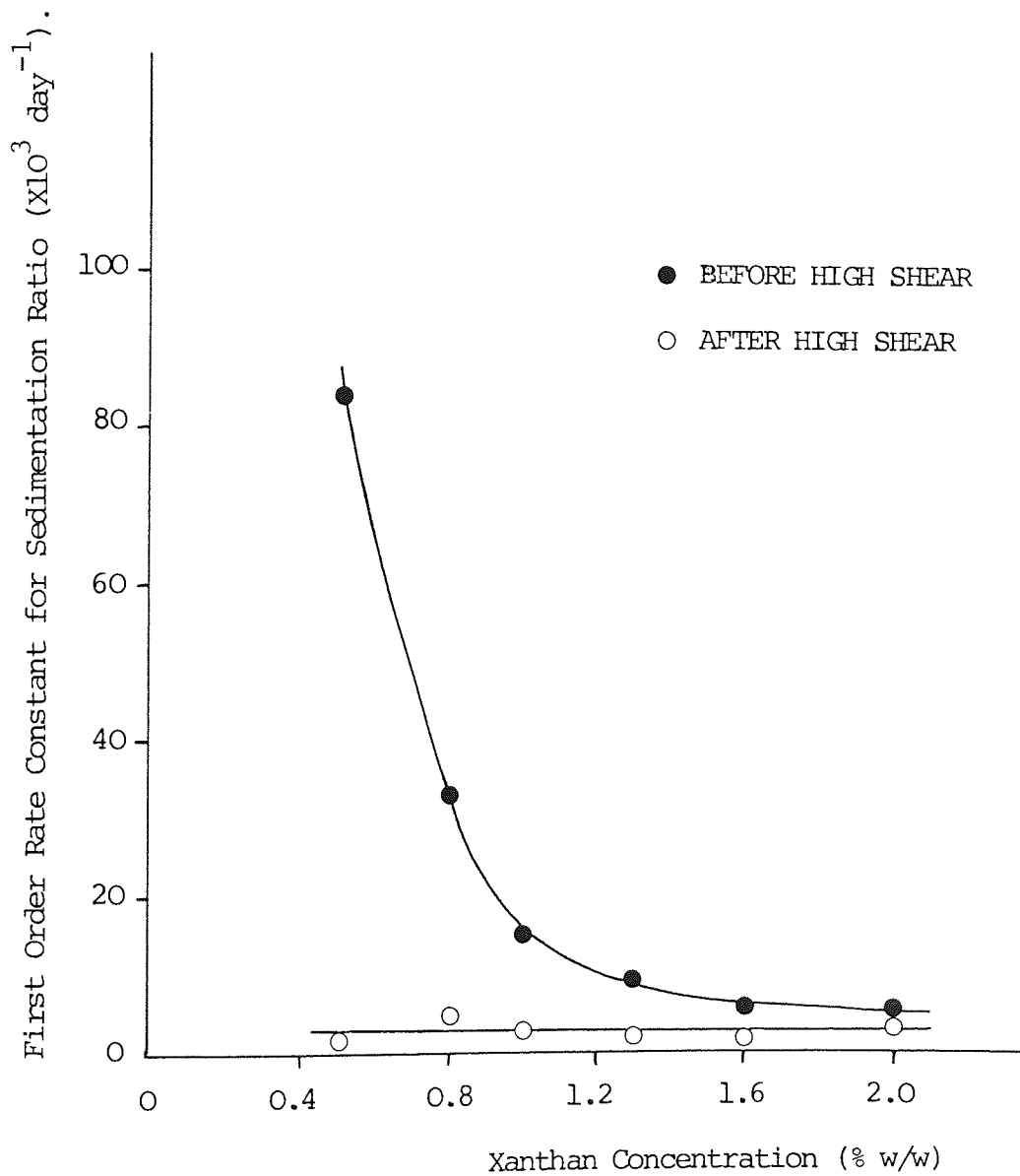


Table 3.1 The Effect of Storage Time at 20°C on the Sedimentation Ratios of Xanthan Gum Solution in Sodium Alginate 5% w/w Solution: (a) before and (b) after shearing.

(a) Before Shearing

Time (days)	Sedimentation Ratio, F					
	Xanthan Gum Concentration (% w/w)					
	0.5	0.8	1.0	1.3	1.6	2.0
3.75	0.767	0.901	0.949	0.949	0.976	0.966
4.75	0.706	0.870	0.942	0.942	0.970	0.953
6.9	0.558	0.815	0.917	0.923	0.959	0.953
7.9	0.509	0.790	0.904	0.910	0.959	0.946
12	0.344	0.679	0.846	0.878	0.935	0.913
15	0.270	0.605	0.801	0.833	0.917	0.903
19	0.221	0.506	0.750	0.801	0.888	0.859
26	0.208	0.415	0.672	0.755	0.842	0.800
34	0.190	0.302	0.596	0.708	0.805	0.767
39	0.184	0.278	0.551	0.672	0.781	0.734
50	0.184	0.196	0.474	0.604	0.722	0.624
76	0.178	0.195	0.404	0.553	0.604	0.570
88	0.172	0.195	0.378	0.521	0.550	0.570
95	0.166	0.190	0.378	0.514	0.538	0.557
144	0.160	0.190	0.340	0.582	0.542	0.523
r *	-0.9935	-0.9981	-0.9995	-0.9982	-0.9989	-0.9952
K *	-0.0847	-0.0377	-0.0154	-0.00978	-0.00657	-0.00610
i *	0.016	0.0097	0.0123	0.020	0.0055	0.012

* Correlation coefficient, r, slope K (day⁻¹), and intercept, i, of first order plots of Ln (F) against time.

Table 3.1. The Effect of Storage Time at 20°C on the Sedimentation Ratios of Xanthan Gum Solution in Sodium Alginate 5% w/w Solution: (a) before and (b) after shearing.

(b) After Shearing.

Time (days)	Sedimentation Ratio, F					
	Xanthan Gum Concentration (% w/w)					
	0.5	0.8	1.0	1.3	1.6	2.0
3.75	0.994	1.0	1.0	1.0	1.0	0.988
4.75	1.0	1.0	1.0	1.0	1.0	0.988
6.9	0.994	1.0	1.0	1.0	1.0	0.963
7.9	0.988	1.0	1.0	1.0	1.0	0.963
12	0.969	0.987	1.0	0.994	1.0	0.951
15	0.957	0.967	0.975	0.969	1.0	0.921
19	0.957	0.960	0.969	0.963	0.965	0.915
26	0.942	0.921	0.943	0.939	0.958	0.889
34	0.920	0.880	0.938	0.920	0.943	0.854
39	0.914	0.860	0.925	0.907	0.943	0.841
50	0.889	0.813	0.901	0.889	0.922	0.805
76	0.858	0.720	0.870	0.846	0.887	0.774
88	0.827	0.673	0.839	0.809	0.851	0.774
95	0.815	0.660	0.826	0.809	0.851	0.738
144	0.747	0.567	0.770	0.753	0.830	0.713
r *	-0.9941	-0.9993	-0.9965	-0.9867	-0.9908	-0.9948
K *	-0.0021	-0.0049	-0.0020	-0.0021	-0.0017	-0.0044
i *	-0.0035	0.044	0.043	0.0043	0.0428	0.0016

* Correlation coefficient, r, slope K (day^{-1}), and intercept, i, of first order plots of $\ln(F)$ against time.

Figure 3.18. The Effect of the Shearing Time on the Storage Modulus G' , of a Solution containing Xanthan Gum 2% w/w and Sodium Alginate 5% w/w, plotted as a function of the Frequency of Oscillation, ω .

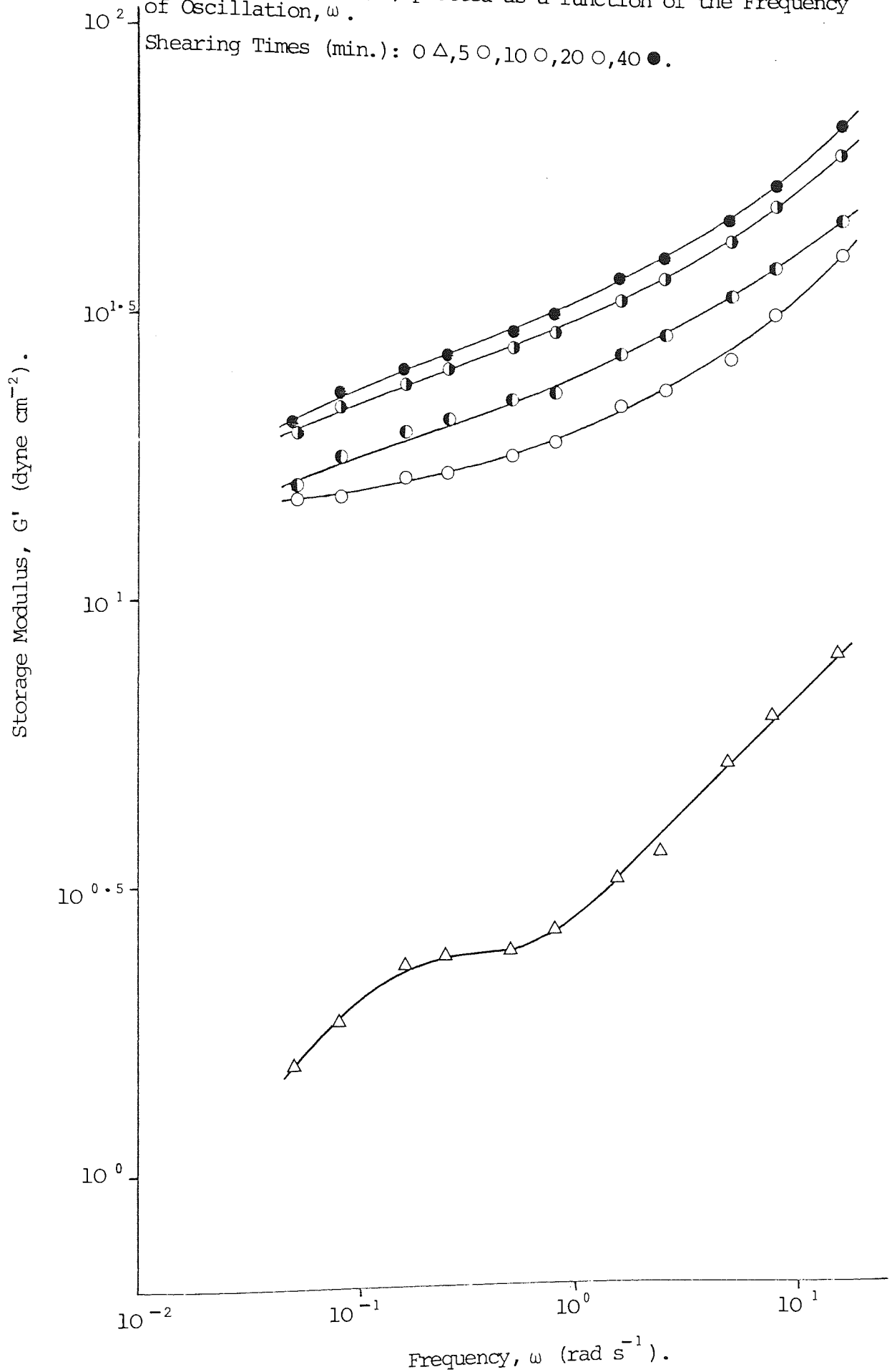
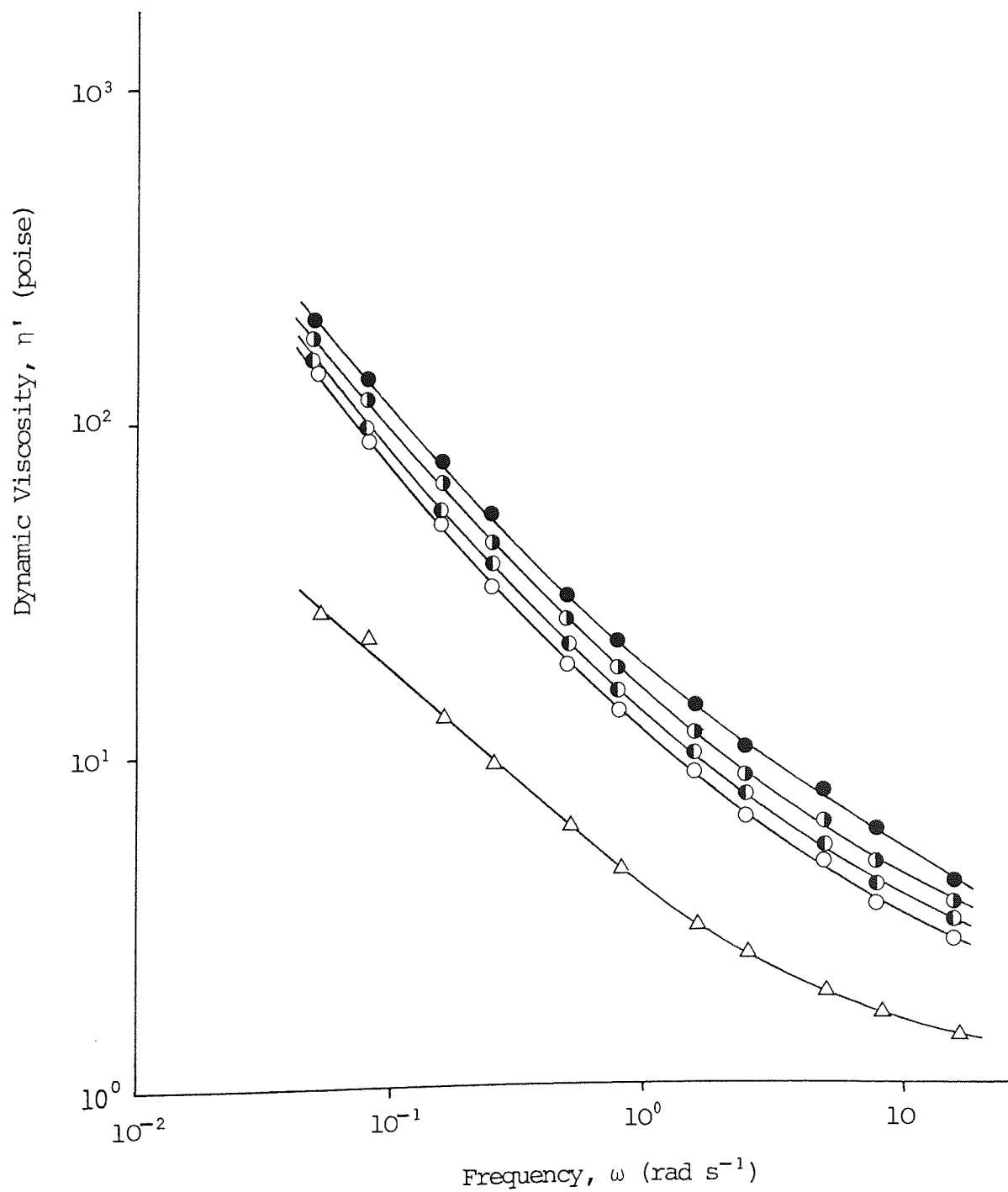


Figure 3.19. The Effect of the Shearing Time on the Dynamic Viscosity, η' , of a Solution containing Sodium Alginate 5% w/w, plotted as a function of the Frequency of Oscillation, ω .

Shearing Times (min) : 0 Δ , 5 \circ , 10 \bullet , 20 \ominus , 40 \bullet .



That the increases applied to absolute values is illustrated in Figure 3.20. where the percentage increase in G' at $\omega = 1.57 \text{ rad s}^{-1}$ is significantly greater than that for η' ($P > 0.995$). This tends to support the similar findings of Section 3.4.1.2.

Measurements made at time intervals from 24 to 264 hours after preparation showed no significant increase in the viscoelastic parameters which indicated that the structural recovery was either longer or shorter than the time period studied. Shearing of 0.6 and 2.0% w/w Xanthan solutions using the 'Silverston' mixer had no significant effect on $G'(\omega)$ or $\eta'(\omega)$ when measured up to 264 hours after preparation.

3.4.2 'Carbopol' Systems

3.4.2.1 Effect of Concentration

Carbopol alone in neutralised solution exhibits completely different rheological characteristics to Xanthan Gum, but certain similarities appear on admixture with Alginate. Figure 3.21. of $G'(\omega)$ for Carbopol above shows the result that solutions were almost purely elastic when the concentration was less than 0.5% w/w concentration. The summarised data in Figure 3.22. for G' at $\omega = 2.5 \text{ rad s}^{-1}$ suggests that increasing the concentration above 1.0% w/w does not significantly increase the storage modulus. It is probably more accurate to say that the increase in G' at high concentrations lies within the limits of error inherent when ν approaches 1.0 as shown in

Figure 3.20. Percentage Increases in Storage Modulus, ●, and Dynamic Viscosity, ○, at $\omega = 1.57 \text{ rad s}^{-1}$ as a function of the Shearing Time of a Xanthan 2%, Alginate 5% w/w mix.

Error bars show 95% confidence limits ($n = 5$).

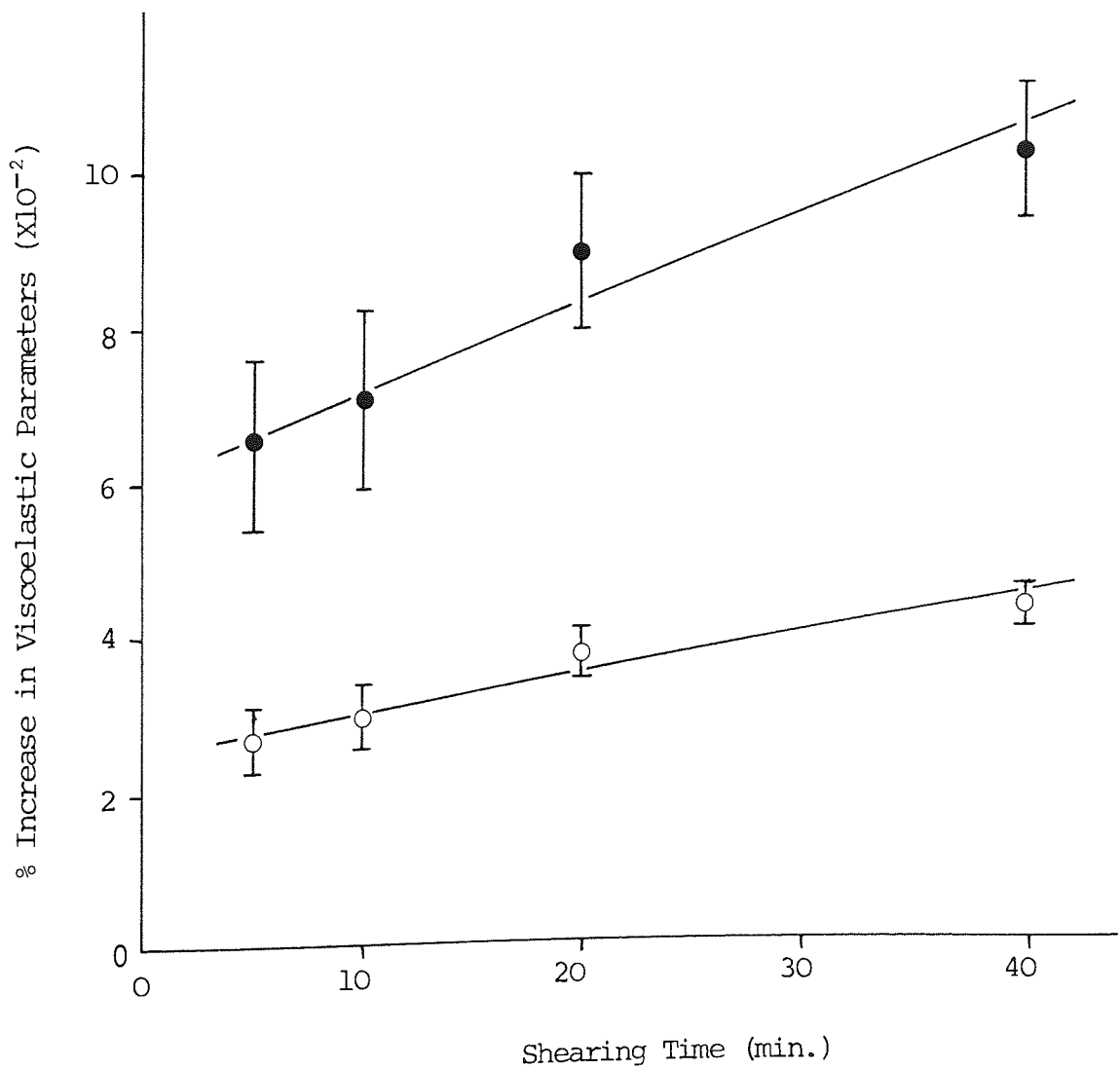


Figure 3.21. The Effect of the Frequency of Oscillation on the Dynamic Viscosity, η' , and Storage Modulus, G' , of Various Concentrations of Carbopol 934P Gels.

Carbopol Concentrations (% w/w) : 0.21 Δ , (Dynamic Viscosity) and 0.21 \circ , 0.46 \bullet , 0.64 \circ , 1.61 \bullet , (Storage Modulus).

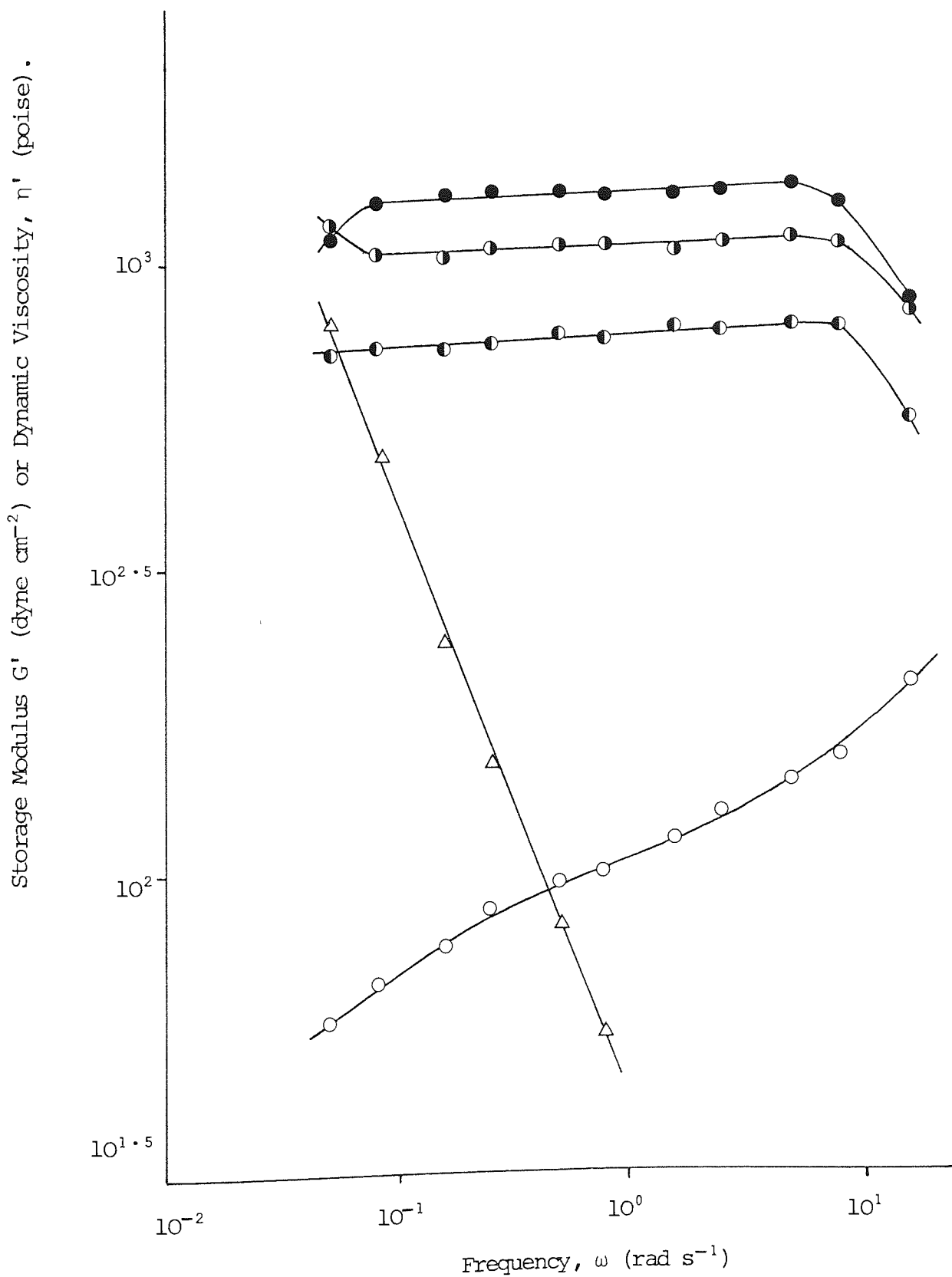


Figure 3.22. The Effect of the Concentration of Carbopol 934P on the Storage Modulus, G' , at Oscillation Frequency, $\omega = 2.5 \text{ rad s}^{-1}$.

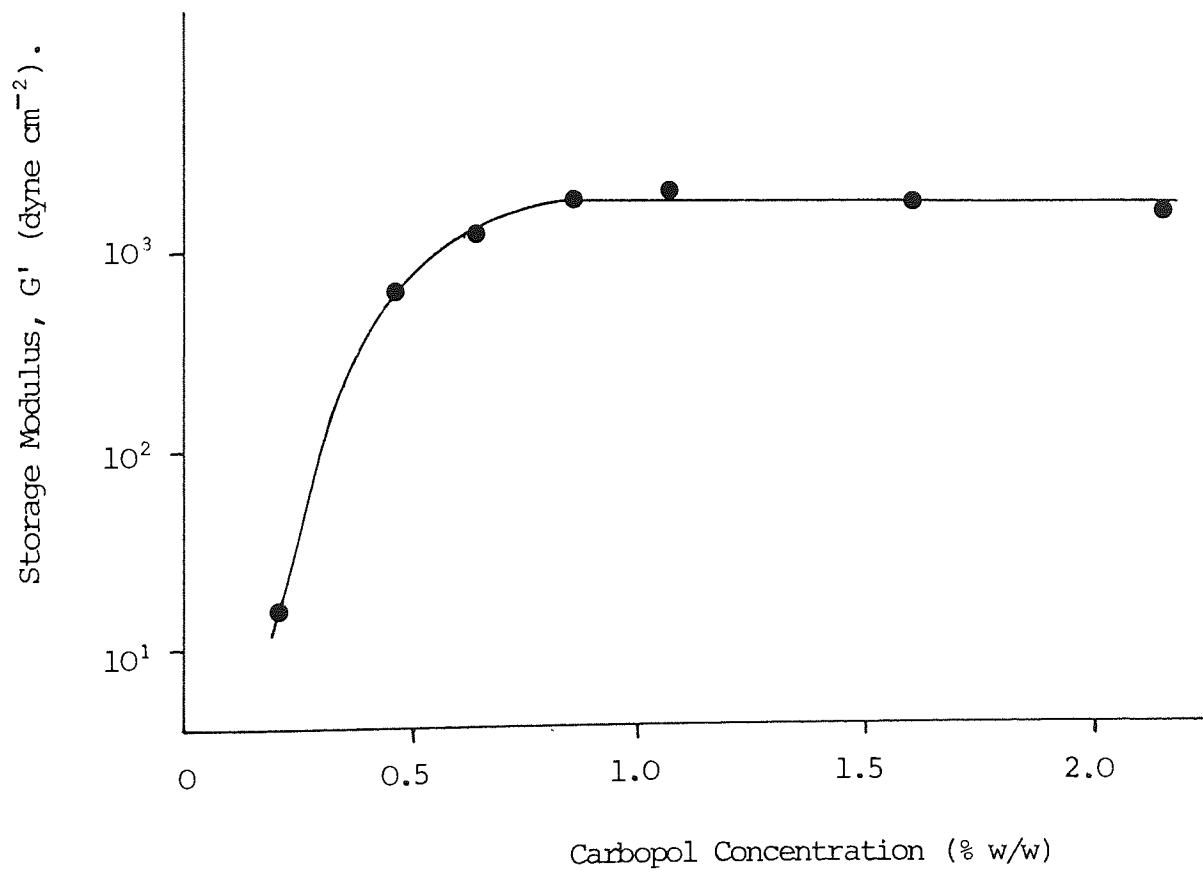


Figure 3.4.; the parameters f and b_v from the Shangraw expression, Equation 3.3., using continuous shear data gave a similar trend to G' but without such a plateau. These are plotted in Figure 3.23. The only $\eta'(\omega)$ line for Carbopol 0.2% w/w shown in Figure 3.21. has a high slope which suggests a very high η_0 value at a sufficiently low frequency. This line would move to lower frequencies with higher Carbopol concentrations making $\eta'(\omega)$ measurement difficult with the rheogoniometer. It is interesting that $G'(\omega)$ for Carbopol 0.2% and Xanthan 0.8% are roughly equivalent.

On addition of Alginate, in resemblance to Xanthan systems, $G'(\omega)$ is affected to a greater extent than $\eta'(\omega)$. This was quantified by using two approaches: (i) to increase the Carbopol concentration C_1 in the presence of Sodium Alginate 5% w/w, see Figures 3.24. to 3.26., and (ii) to increase the Alginate concentration C_2 in Carbopol 0.8% w/w, see Figures 3.27. to 3.29.. As would be expected, $G'(\omega)$ and $\eta'(\omega)$ increased in protocol (i) and decreased in (ii) but the ways in which they changed is significant. For protocol (i), increasing C_1 above 1.4% w/w had little effect upon $\eta'(\omega)$ but $G'(\omega)$ continued to rise significantly; the region of $C_1 \approx 1.0\%$ w/w appeared to be most critical with respect to $G'(\omega)$ and $\eta'(\omega)$.

The corresponding continuous shear data for protocol (ii) is given in Figure 3.30. for η_∞ and f against C_2 . This data shows only qualitative similarities with the oscillatory

Figure 3.23. The Effect of the Concentration of Carbopol 934P on the Continuous Shear Rheological Parameters: f \circ and b_v \bullet . (See Section 3.2.4. for an explanation of these terms).

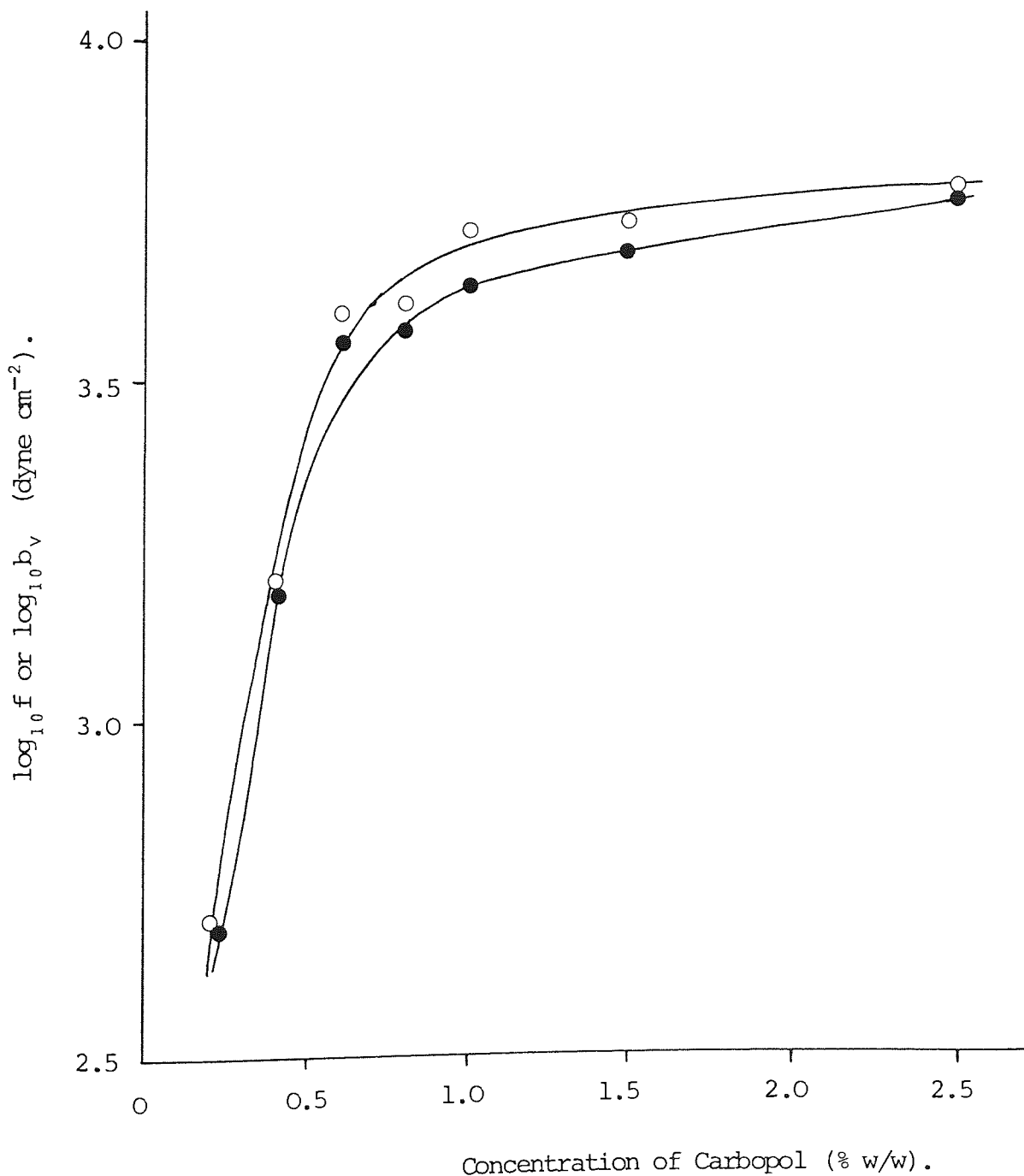


Figure 3.24. The Effect of the Concentration of Carbopol 934P in Sodium Alginate 3% w/w Solution on the Storage Modulus, G' , plotted as a function of the Frequency of Oscillation, ω .

Carbopol Concentration (% w/w) : 0.6 ∇ , 0.9 Δ , 1.1 \blacktriangle , 1.4 \blacktriangle ,
1.6 \circ , 1.8 \bullet , 2.1 \circ , 2.4 \bullet .

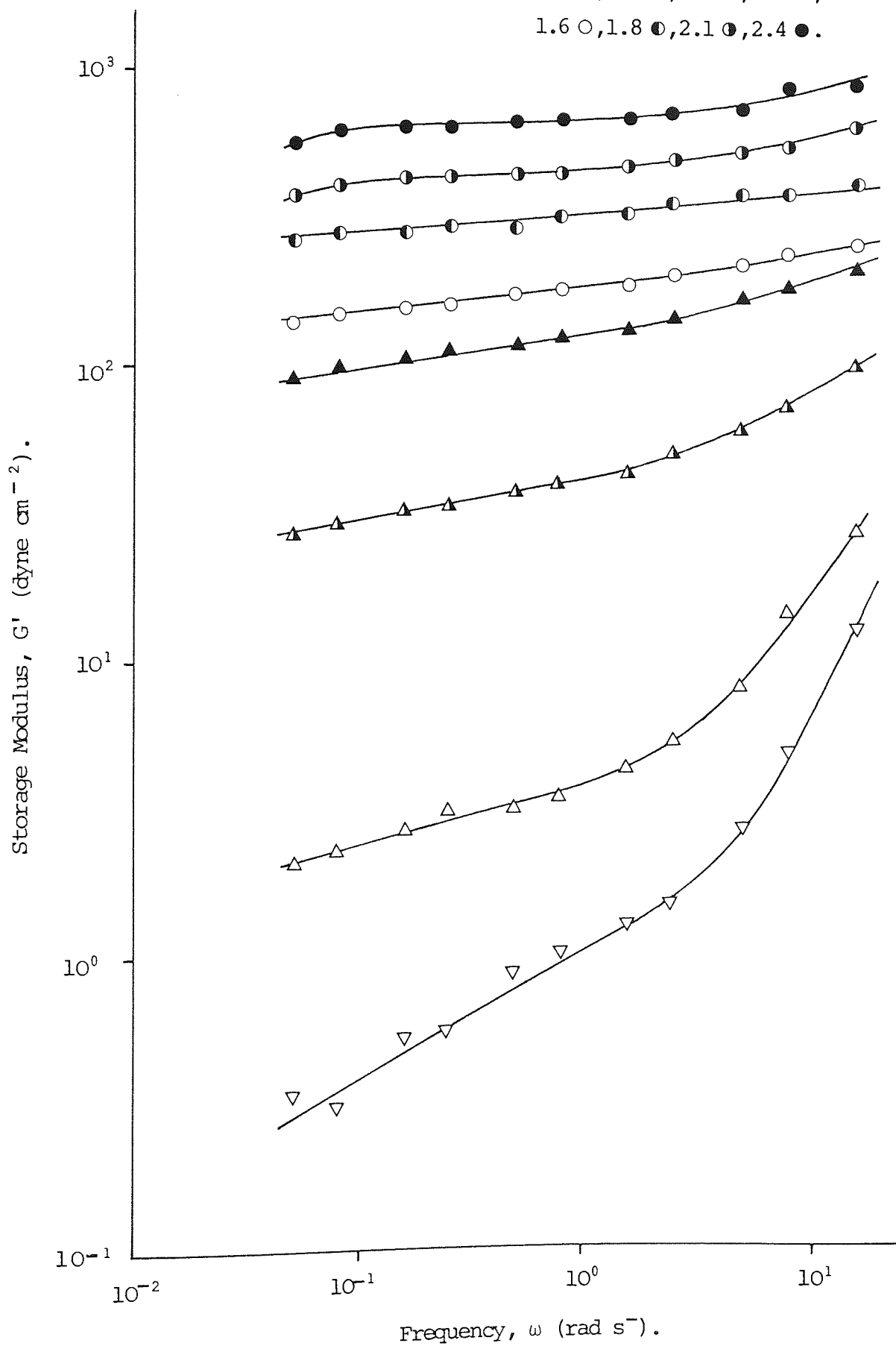


Figure 3.25. The Effect of the Concentration of Carbopol in Sodium Alginate 3% w/w Solution on the Dynamic Viscosity, η' , plotted as a function of the Frequency of Oscillation, ω .
 Concentrations (% w/w) : 0.6 ∇ , 0.9 Δ , 1.1 \blacktriangle , 1.4 \blacktriangle , 1.6 \circ , 1.8 \bullet .

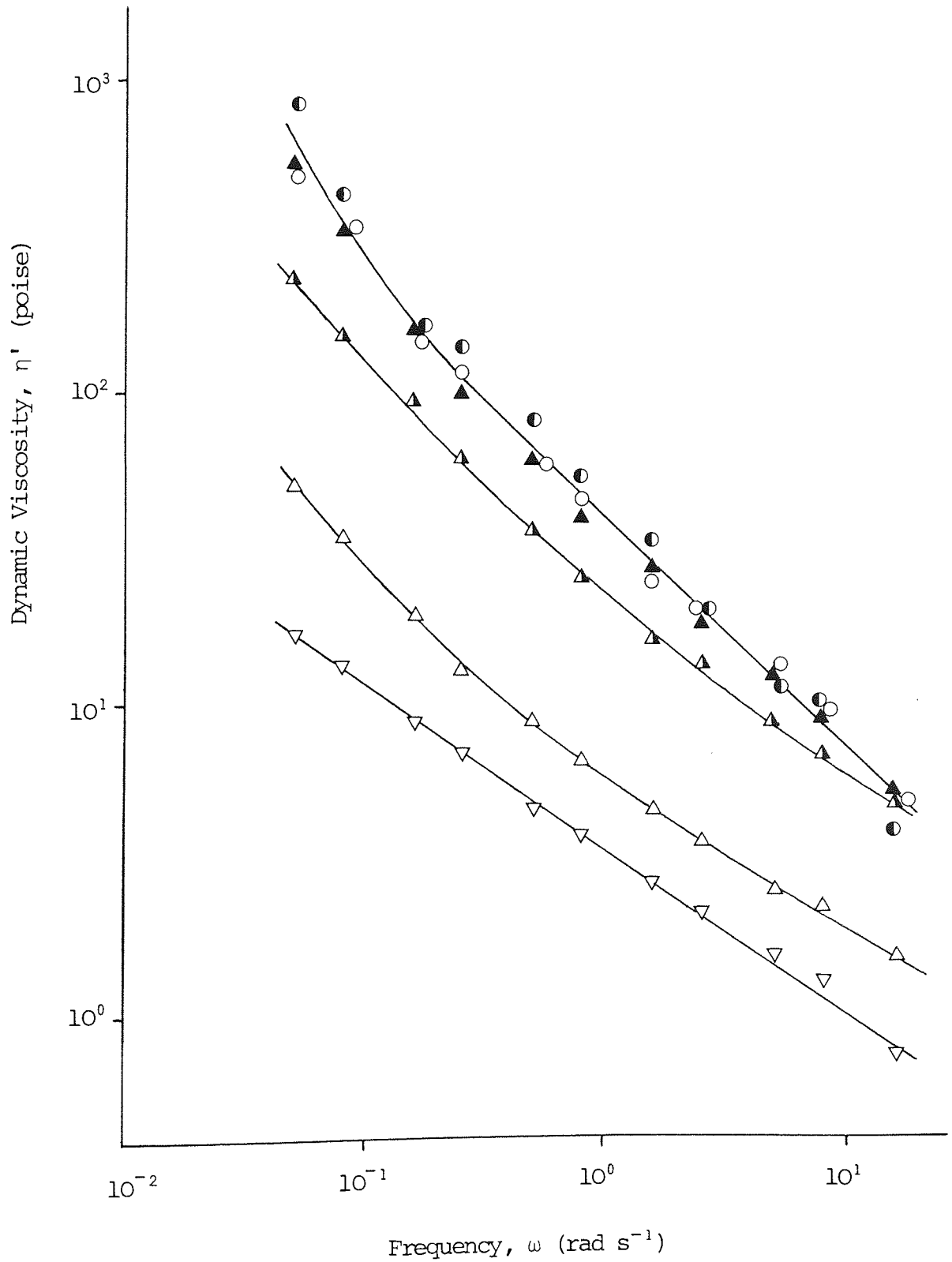


Figure 3.26. The Effect of the Concentration of Carbopol in Sodium Alginate 3% w/w Solution on (a) Storage Modulus and (b) Dynamic Viscosity at Oscillation Frequency $\omega = 2.5 \text{ rad s}^{-1}$.

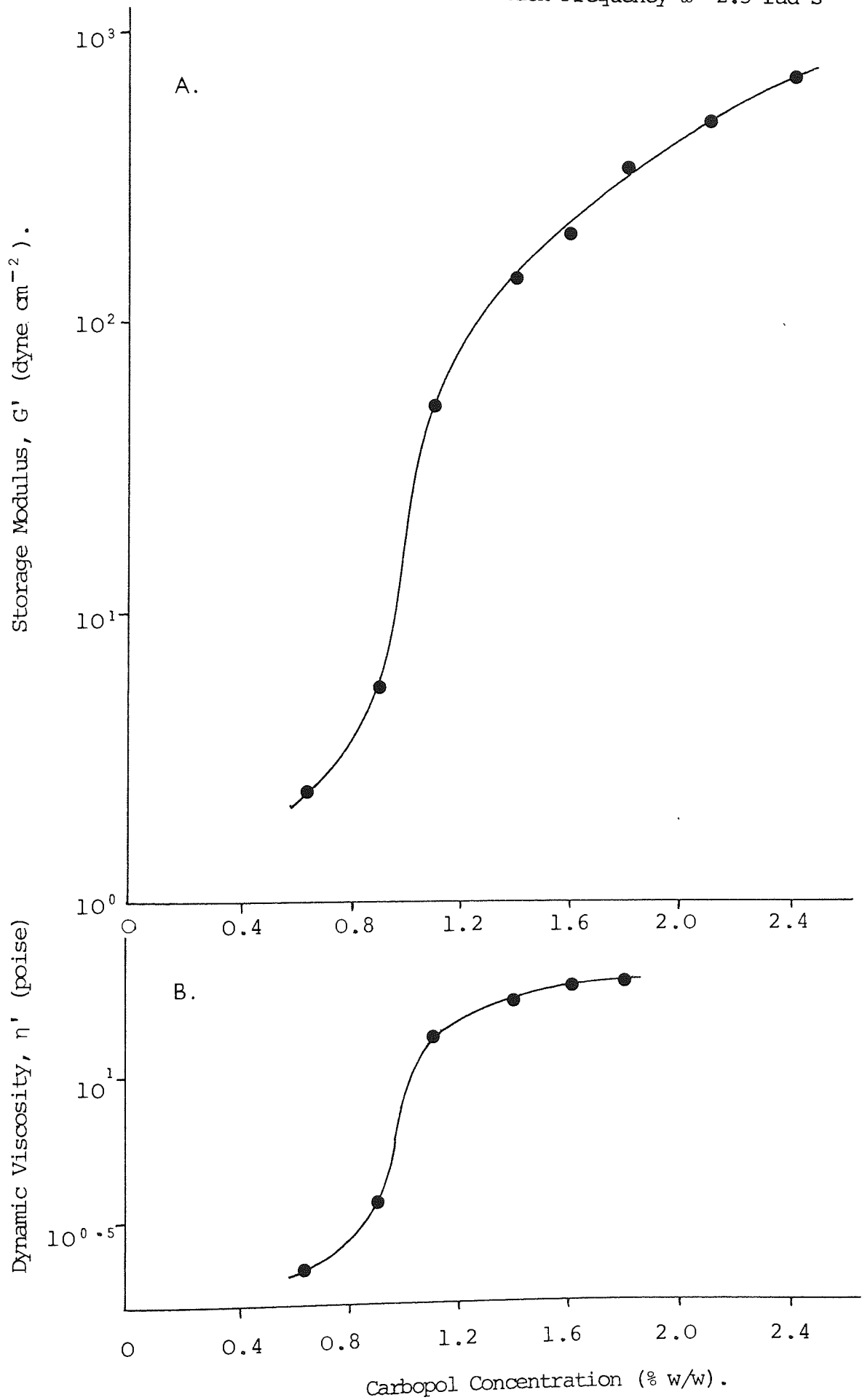


Figure 3.27. The Effect of the Concentration of Alginate in Carbopol 0.8% w/w Solution on the Storage Modulus, G' , plotted as a function of the Frequency of Oscillation, ω . Concentrations (% w/w) : 0.5 ●, 1.0 ○, 2.0 ◐, 3.0 ◑, 4.0 ▲, 5.0 △.

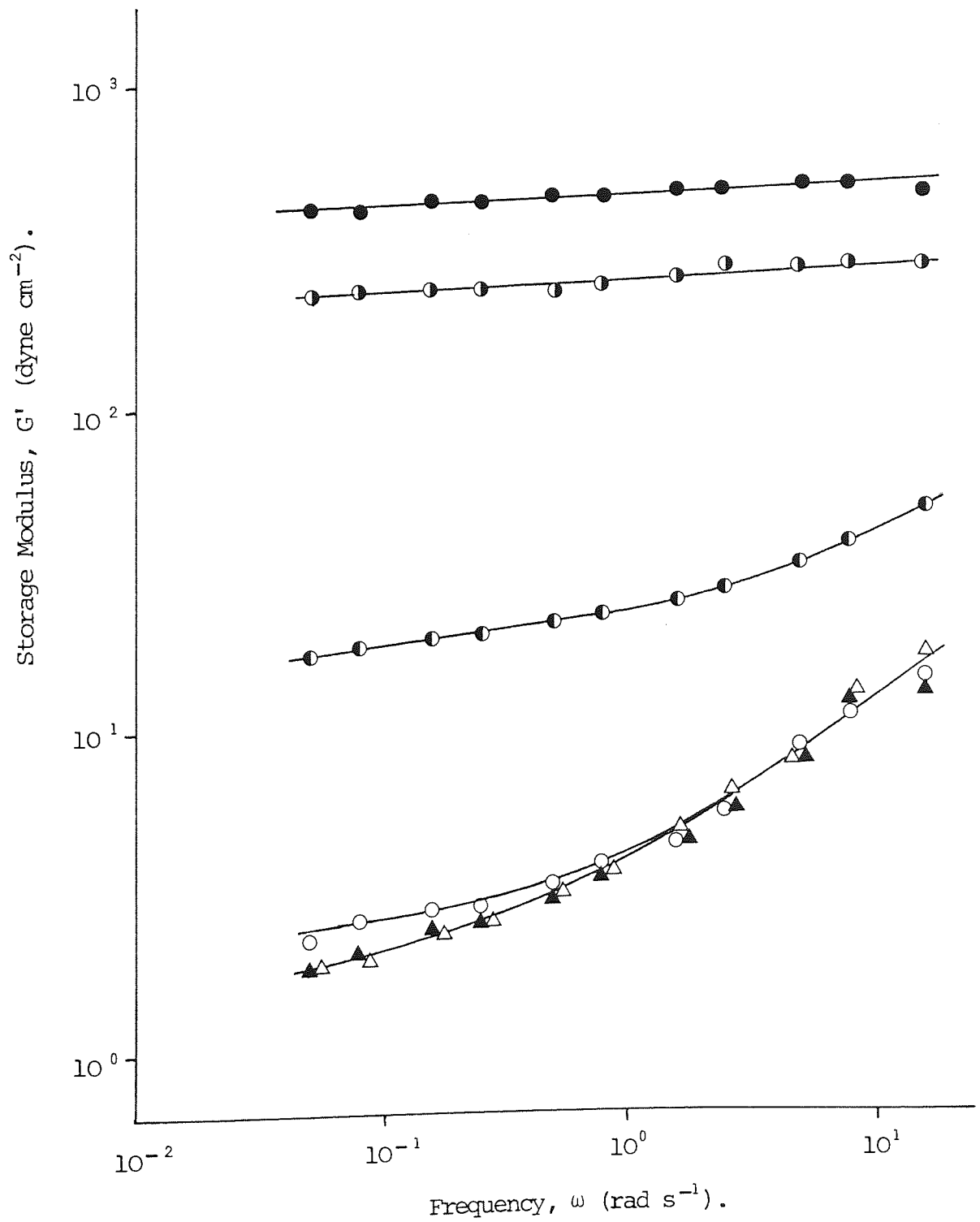


Figure 3.28. The Effect of the Concentration of Alginate in Carbopol 0.8% w/w Solution on the Dynamic Viscosity, η' , plotted as a function of the Frequency of Oscillation, ω .

Concentrations (% w/w) : 1.0 \bullet , 2.0 \circ , 3.0 \circ , 4.0 Δ .

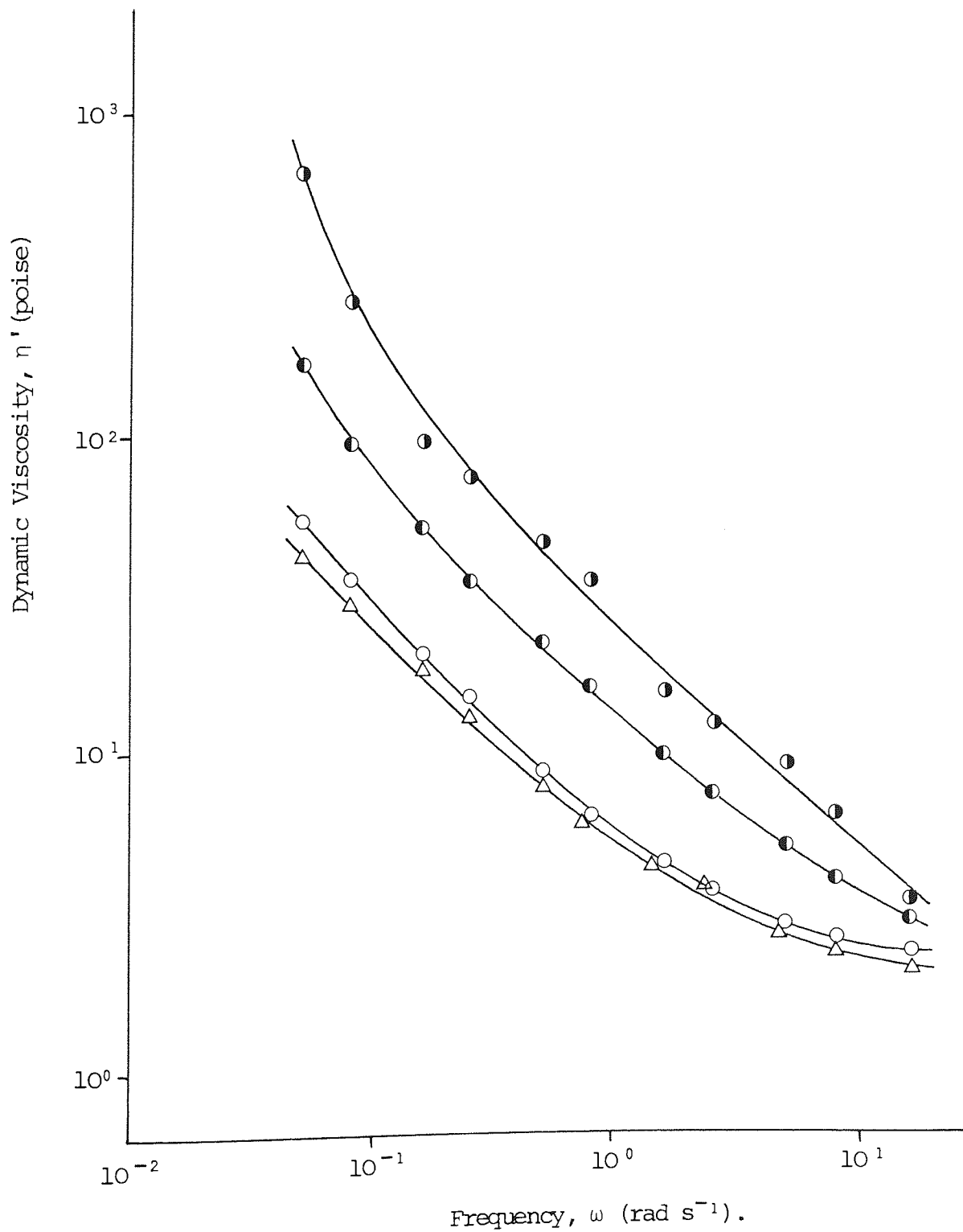


Figure 3.29. The Effect of the Concentration of Alginate in Carbopol 0.8% w/w Solution on (a) Storage Modulus and (b) Dynamic Viscosity at Oscillation Frequency $\omega = 2.5 \text{ rad s}^{-1}$.

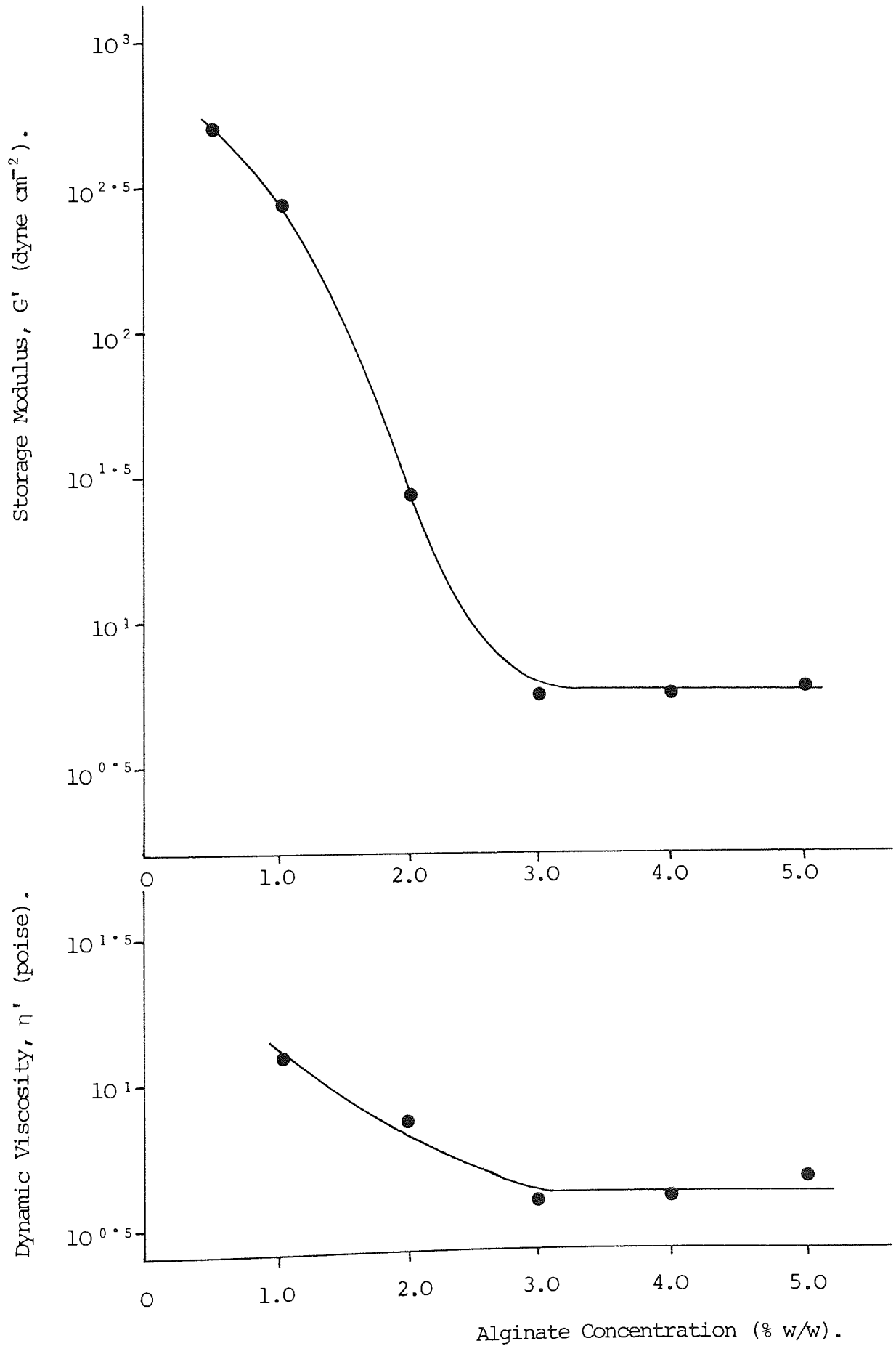
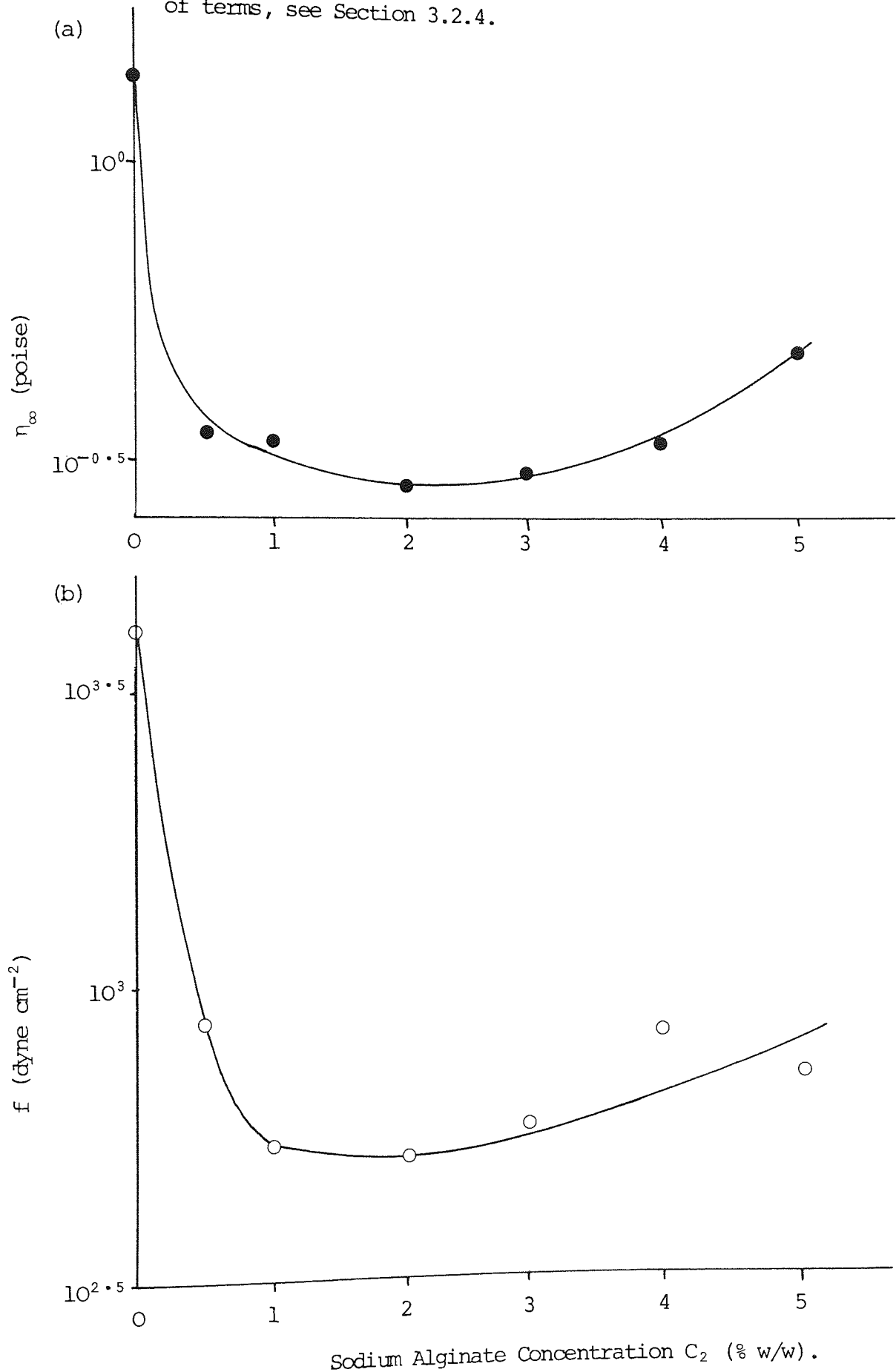


Figure 3.30. The Effect of the Concentration of Alginate in Carbopol 0.6% w/w Solution on the Continuous Shear Rheological Parameters (a) η_{∞} and (b) f . For explanation of terms, see Section 3.2.4.



data in Figure 3.29.

3.4.2.2 Effect of Shearing

In attempts to measure the effect of shearing by the 'Silverson' high shear mixer on Carbopol systems, oscillatory and continuous shear measurements were made. Samples of Carbopol 0.6%, Carbopol 2.0% and Carbopol 2.0% with Alginate 5.0% were subjected to high shear for 10 min.. All concentrations were w/w. Oscillatory measurements with the usual regimens were taken at 24,48,96,192 and 264 hr. after preparation. Due to siting of the apparatus, readings could not be obtained before 24 hours had elapsed. There was no significant difference in the viscoelastic parameters for low or high shear samples throughout the 264 hr. period studied.

In order to obtain measurements within 24 hr. of preparation, the continuous shear technique was employed. Samples of Carbopol 0.6% alone, mixed with Alginate 0.5% and also with Alginate 2.0% were sheared for up to 40 min. and $\tau - \dot{\gamma}$ curves were obtained immediately after equilibration at 21.5⁰C. The non-linear regression analysis estimates of f , η_{∞} , b_v and a are given in Table 3.2.; only Carbopol alone shows significant shear breakdown ($P > 0.999$). This is illustrated

Table 3.2. Effect of Shearing Time on the Continuous Shear Rheological Parameters of Carbopol 0.6% w/w and the Effect of Alginate.

<u>(a) Without Alginate</u>					
Shearing time (min)	f (dyne cm ⁻²)	η_{∞} (poise)	b_v (dyne cm ⁻²)	a x10 ³	f - b_v (dyne cm ⁻²)
0	4030	1.41	3670	7.35	360
10	2980	1.12	2690	6.12	290
15	2720	1.09	2570	9.06	150
20	2810	1.03	2460	4.31	350
25	2520	1.04	2340	8.57	180
30	3010	0.98	2620	3.26	390
40	2730	1.02	2430	4.33	300
<u>(b) Alginate 0.5% w/w</u>					
0	880	0.35	830	4.37	50
5	780	0.31	750	3.89	30
10	860	0.33	830	3.13	30
15	790	0.34	760	3.20	30
20	850	0.31	780	2.50	70
30	830	0.30	800	2.83	30
<u>(c) Alginate 2.0% w/w</u>					
0	507	0.28	473	1.55	34
5	524	0.25	513	1.82	11
10	439	0.22	440	2.02	0
15	441	0.24	438	1.88	3
20	461	0.25	446	2.10	15
30	458	0.30	458	1.92	0

in Figure 3.31., where the estimates of f , η_{∞} and b_V are plotted against the shearing time. The apparent shear stability in the presence of Alginate is probably due to greater ease of realignment of polymer molecules when cross-linkages are largely absent.

Carbopol systems in the presence of Alginate did not manifest the sedimentation properties of the Xanthan gum systems either with or without high shear mixing. The storage of Carbopol - Alginate mixes prepared in distilled water, at temperatures of 20 to 50°C for 6 months did not give rise to syneresis or phase separation.

3.4.3 Proprietary Preparations

Several proprietary oral liquid formulations including syrups, suspensions and an emulsion were tested in oscillatory shear with the same regimens as used in Sections 3.4.1. and 3.4.2.. The storage modulus $G'(\omega)$ and dynamic viscosity $\eta'(\omega)$ curves are given in Figures 3.32. to 3.35. where the logarithmic ordinate scale is adjusted in each Figure for clarification of the individual curves. The loss tangent $\tan \delta(\omega)$ curves, termed the 'consistency spectra' by Davis (181) since they encompass both viscous and elastic effects, are given in Figures 3.36. and 3.37.. The proprietary preparations used are listed in Table 3.3..

Most noticeable in these curves is the extremely wide range of

Figure 3.31. The Effect of the Shearing Time of Carbopol 0.6% w/w Gel on the Continuous Shear Rheological Parameters (a) η_{∞} , (b) f \circ and b_v \bullet . For explanation of terms, see Section 3.2.4.

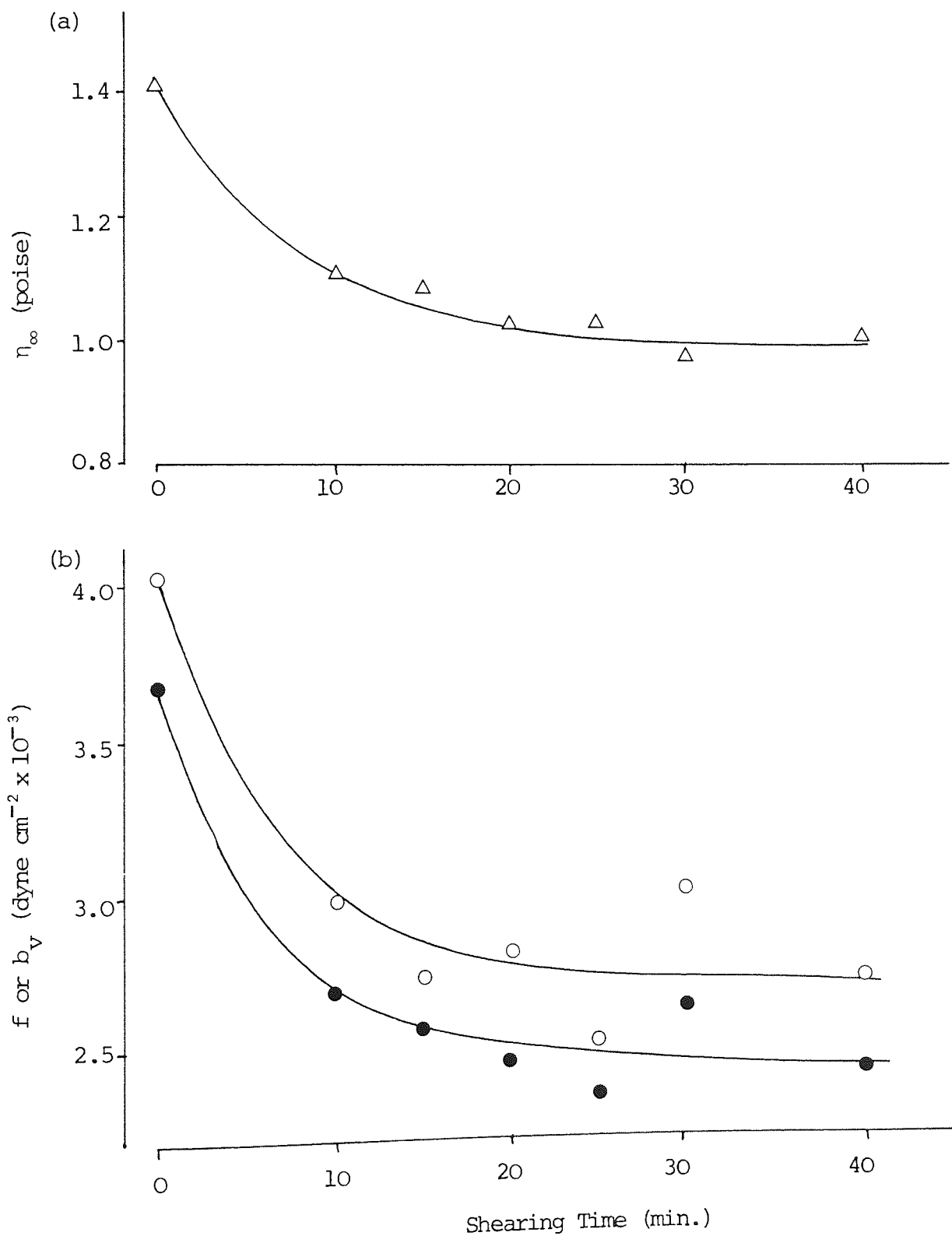


Figure 3.32. The Effect of the Frequency of Oscillation, ω , on the Storage Modulus, G' , of Proprietary Oral Liquid Preparations.

Preparations : I ●, II ○, III ◐, IV ◑, V ▲, VI △, VII ▲, for Key, see Table 3.3.

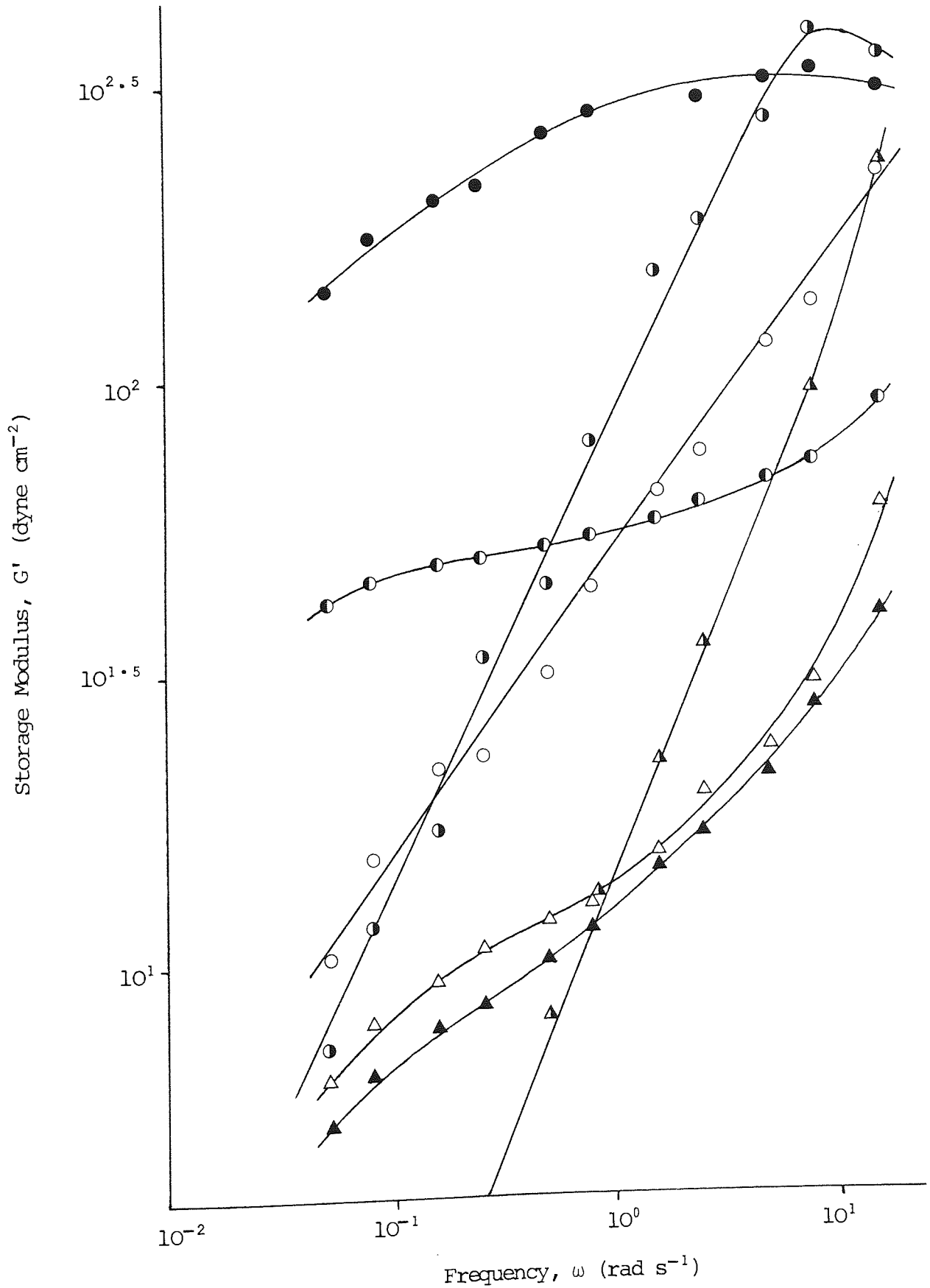


Figure 3.33. The Effect of the Frequency of Oscillation, ω , on the Storage Modulus, G' , of Proprietary Oral Liquid Preparations.

Preparations : VIII ●, IX ○, X ●, XI ○, XII ▲, XIII ▲,
XIV ▲, XV ▽, for Key, see Table 3.3.

Figure 3.33. (see facing page)

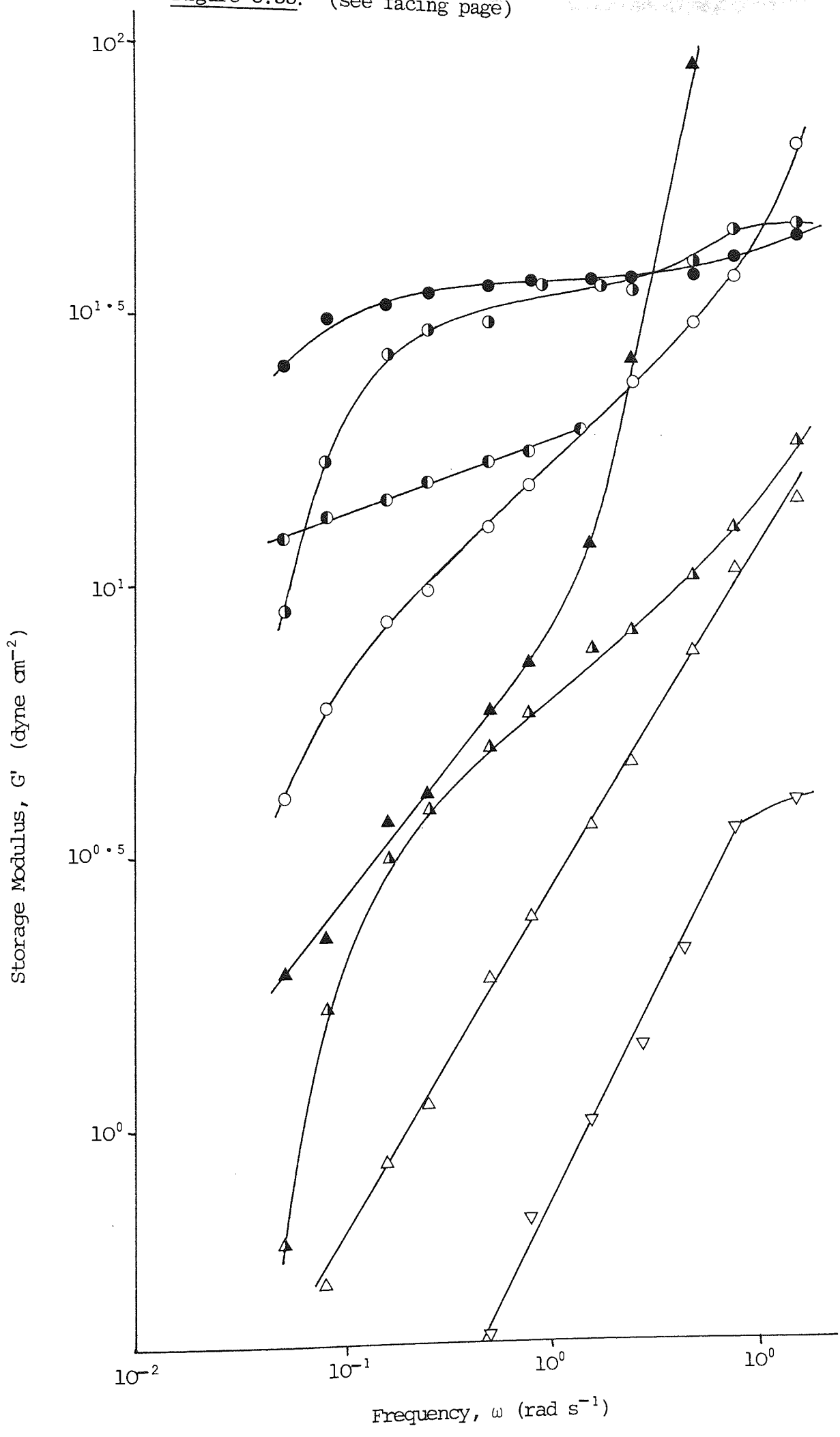


Figure 3.34. The Effect of the Frequency of Oscillation, ω , on the Dynamic Viscosity, η' , of Proprietary Oral Liquid Preparations.

Preparations : I ●, II ○, III ○, IV ○, V ▲, VI ▲, VII ▲.

Figure 3.34 (see facing page)

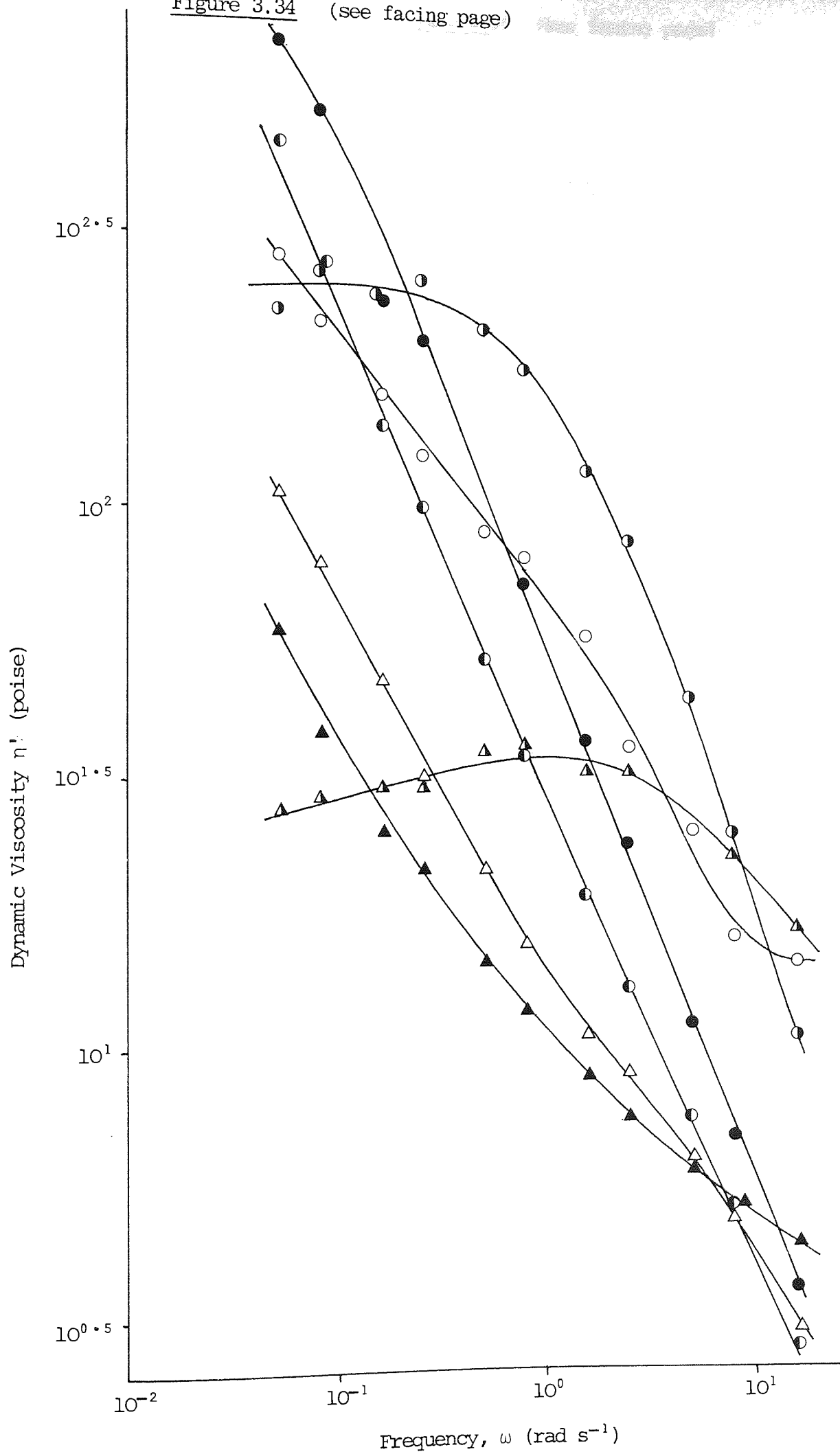


Figure 3.35. The Effect of the Frequency of Oscillation, ω , on the Dynamic Viscosity, η' , of Proprietary Oral Liquid Preparations.

Preparations : VIII ●, IX ○, X ○, XI ○, XII ▲, XIII ▲, XIV ▲, XV ▽; for key, see Table 3.3.

Figure 3.35 (see facing page)

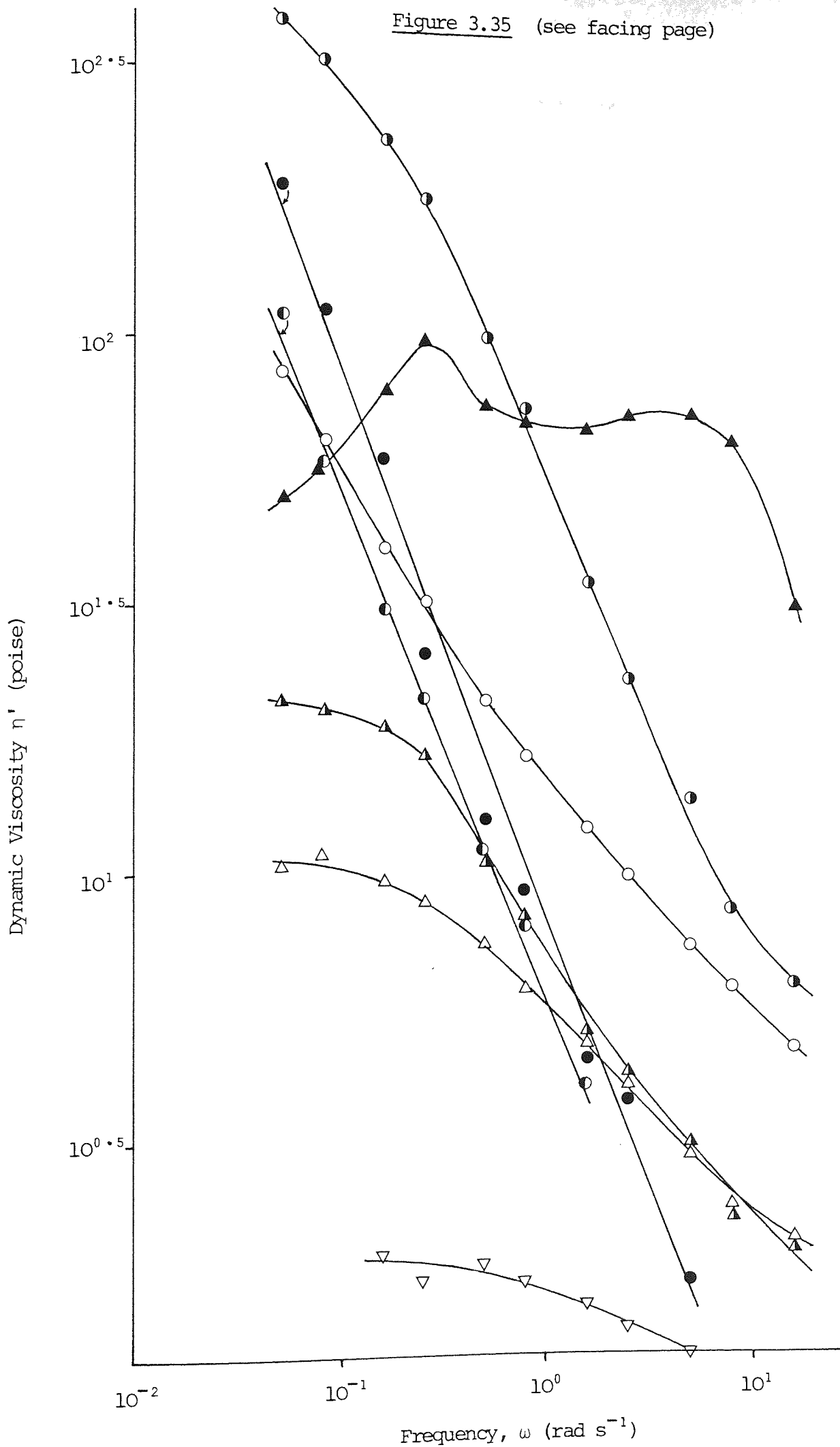


Figure 3.36. The Effect of the Frequency of Oscillation, ω , on the Loss Tangent, $\tan \delta$, of Proprietary Oral Liquid Preparations.

Preparations : I ●, II ○, III ◐, IV ◑, V ▲, VI △, VII ▲;
For Key, see Table 3.3.

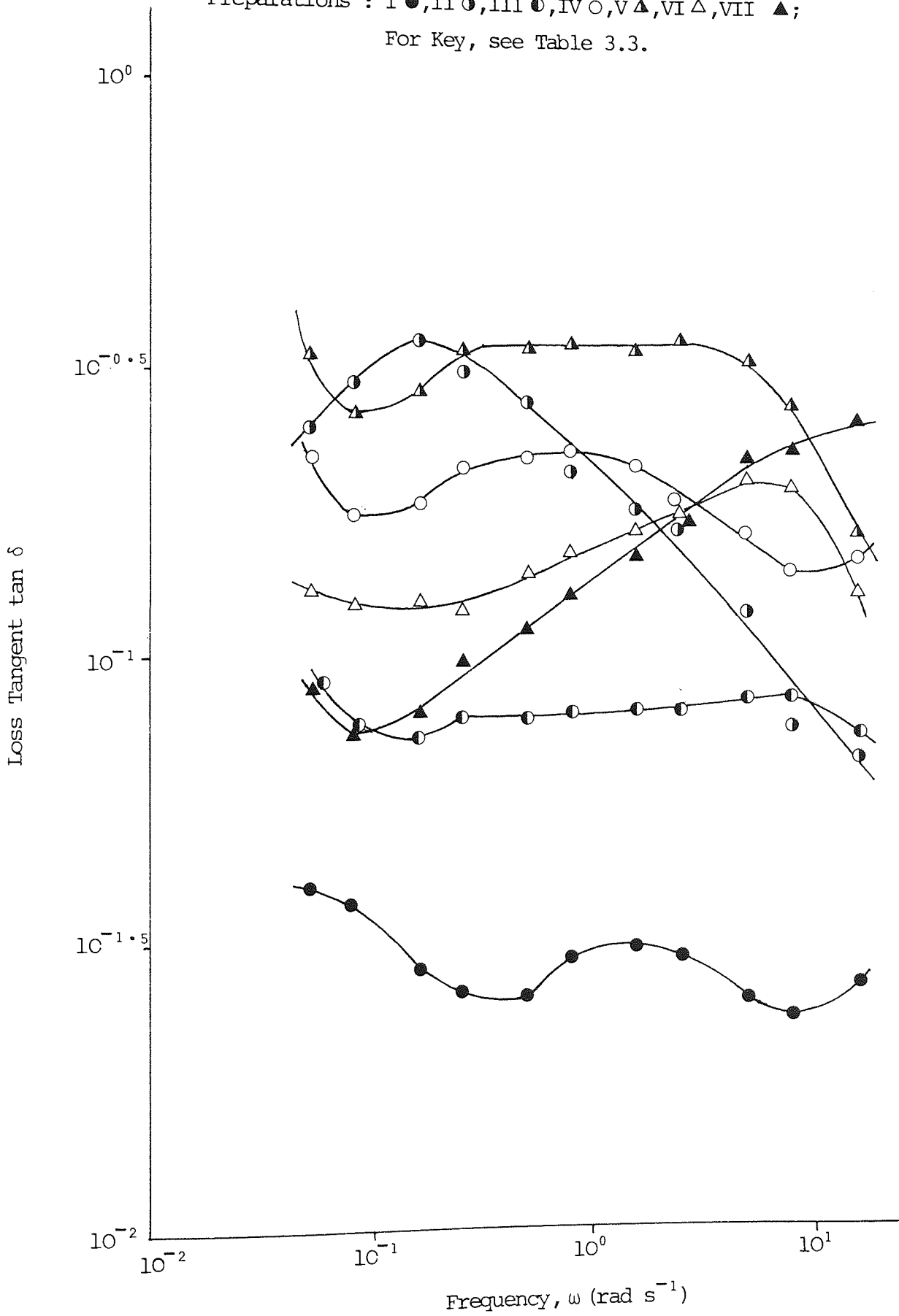


Figure 3.37. The Effect of the Frequency of Oscillation, ω , on the Loss Tangent, $\tan \delta$, of Proprietary Liquid Preparations.

Preparations : VIII ●, IX ○, X ○, XI ○, XII ▲, XIII ▲, XIV ▲, XV ▼. For Key, see Table 3.3.

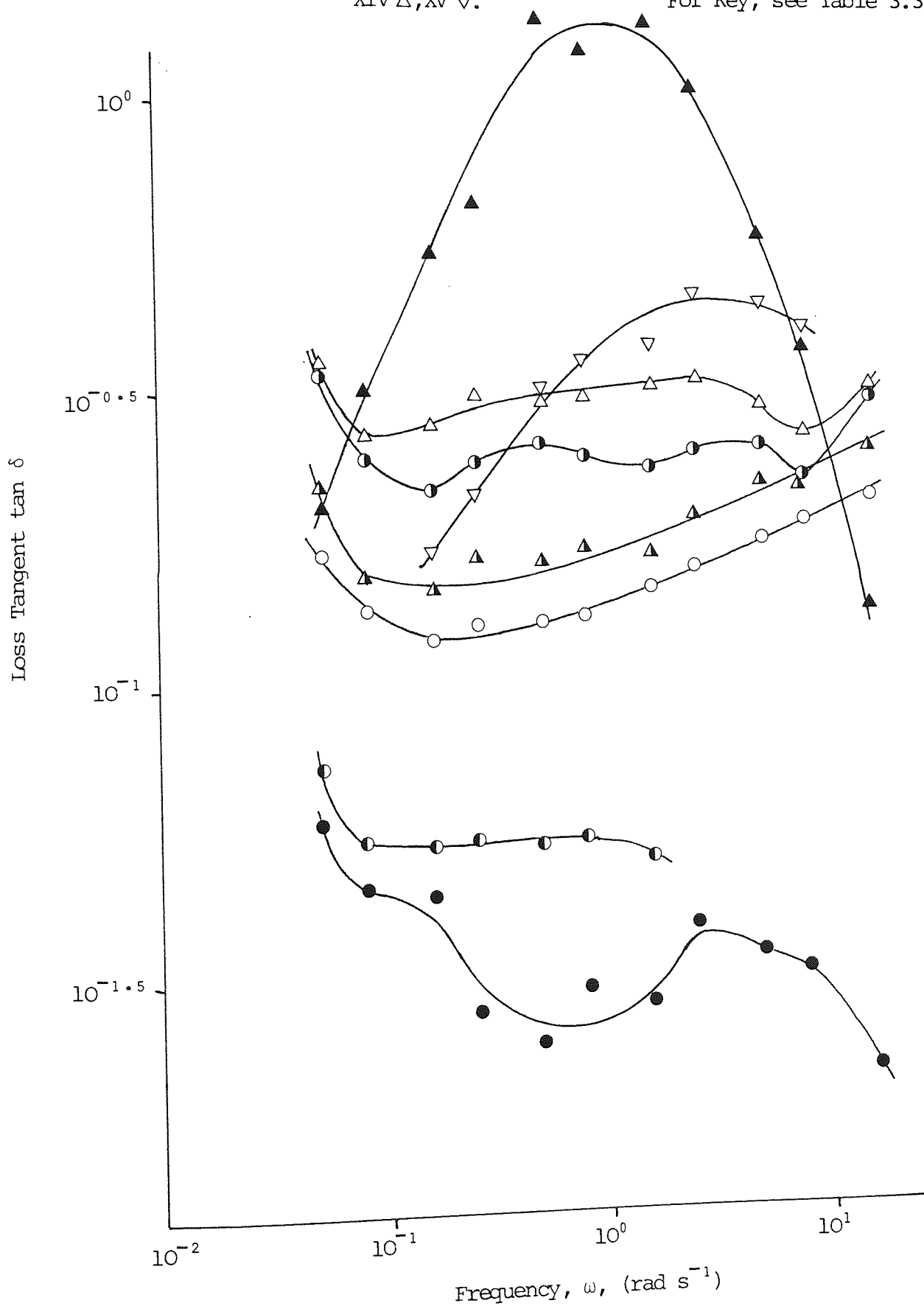


Table 3.3. Key to Figures 3.30. through 3.35. for Storage Modulus, Dynamic Viscosity and Loss Tangent curves of Proprietary Oral Liquid Preparations.

Reference Number	Commercial Name	Description	Manufacturer
I	'Pholtex'	Suspension	Riker Laboratories
II	'Andursil'	Suspension	Geigy Pharmaceuticals
III	'Furadantin'	Suspension	Eaton Laboratories
IV	'Agarol'	Emulsion	William Warner
V	'Fabahistin'	Suspension	Bayer UK.
VI	'Liquid Gaviscon'	Suspension	Reckitt and Colman
VII	'Pholcolix'	Syrup	William Warner
VIII	'Naprosyn'	Suspension	Syntex Pharmaceuticals
IX	'Mucaine'	Suspension	Wyeth Laboratories
X	'Dorbanex'	Suspension	Riker Laboratories
XI	'Calpol'	Suspension	Wellcome Foundation
XII	'Vi-Daylin'	Syrup	Abbott Laboratories
XIII	'Furoxone'	Suspension	Eaton Laboratories
XIV	'Tegretol'	Syrup	Geigy Pharmaceuticals
XV	'Juvel'	Syrup	Bencard

values of G' , η' and $\tan \delta$ exhibited, often varying by over two powers of ten at any one frequency. With regard to Figures 3.32. and 3.33., there appears to be little correlation between $G'(\omega)$ and either formulation type or subjective assessments of the preparations. Theoretically, G' will approach zero at low frequencies and many $G'(\omega)$ curves have high slopes, each indicative of a low elastic contribution to consistency. The $G'(\omega)$ curves with high slopes are found to have the highest $\tan \delta(\omega)$ values shown in Figures 3.36. and 3.37..

Several preparations, notably II, V, XIII, XIV and XV showed the tendency to plateau at low frequencies, thereby providing estimates of η_0 , the zero shear viscosity. With a knowledge of the mean particle size, R , the densities of the disperse and continuous phases, ρ and ρ_m respectively, and the close packing fraction, p , the settling rate of the suspension can be calculated from η_0 using the equation of Buscall et al (40):

$$\frac{U}{U_0} = \left(1 - \frac{\phi}{p}\right)^{kp} \quad 3.4$$

where U_0 = sedimentation velocity of a single spherical particle in a gravitational field from Stokes' Law with $U_0 = \frac{2R^2(\rho - \rho_m)g}{9\eta_0}$ 3.5

U = rate of settling of suspension in a non-Newtonian medium.

ϕ = volume fraction of disperse phase

k = constant, found to be 5.4 by Buscall et al (40) but values of 5.1 (182), 5.0 (183), 6.55 (184) and 5.8 (185) have been proposed.

Therefore, for separation to be avoided during the

manufacturer's shelf life of the product, η_0 should be chosen such that U is negligibly small.

The $\tan \delta (\omega)$ curves, or consistency spectra, may be expected to be useful since they combine elastic and viscous components. However, in practice (see Figures 3.36. and 3.37.), they appear to be of little use for the following reasons:

- (i) Any systematic errors in G' and η' are compounded in order to obtain $\tan \delta$.
- (ii) Values of $\tan \delta$ cover a narrower range than either of the components it contains, thereby reducing the resolution between curves.
- (iii) $\tan \delta$ values do not appear to show any correlation with any other suspension formulation variables.

Three different batches of formulation XI were tested on three separate occasions yielding the raw data of ν and C given in Table 3.4.. The reproducibility obtained reflects the reliability of both the measuring system and the formulation.

In order to look at the rôle of oscillatory testing as a quality control tool, samples of a suspension, XI, and an emulsion, IV, were stored at 50°C for a short period. The $G'(\omega)$ and $\eta'(\omega)$ curves of Figures 3.38. to 3.41. show considerable changes during 39 days storage; approximately one logarithmic cycle in the case of product XI. This serves to illustrate that sensitive rheological measurements yielding fundamental parameters are capable of exposing any physical instability in the early stages of storage testing.

Table 3.4. Reproducibility of Amplitude Ratio and Phase Angle measurements of Three Batches of 'Calpol' Suspension in Oscillatory Shear.

(a) Amplitude Ratio, ν .

Frequency (rad s ⁻¹)	Batch		
	1	2	3
0.0497	0.0318	0.0361	0.0364
0.0792	0.0413	0.0491	0.0462
0.157	0.0563	0.0673	0.0615
0.249	0.0681	0.0767	0.0739
0.497	0.0880	0.0979	0.0947
0.792	0.107	0.116	0.116
1.57	0.139	0.154	0.156
2.49	0.167	0.187	0.193
4.97	0.225	0.253	0.268
7.92	0.286	0.325	0.344
15.7	0.484	0.539	0.570

(b) Phase angle, C (Rad)

Frequency (rad s ⁻¹)	Batch		
	1	2	3
0.0497	0.822	0.770	0.794
0.0792	0.725	0.663	0.641
0.157	0.679	0.556	0.586
0.249	0.654	0.619	0.642
0.497	0.624	0.589	0.661
0.792	0.613	0.617	0.642
1.57	0.635	0.646	0.673
2.49	0.648	0.659	0.677
4.97	0.654	0.649	0.682
7.92	0.627	0.627	0.656
15.7	0.518	0.472	0.469

Figure 3.38. The Effect of Aging time at 50°C on the Storage Modulus, G' of Formulation XI plotted as a function of the Frequency of Oscillation, ω . Aging time (days) : 0 ●, 7 ○, 14 ◐, 24 ◑, 31 △, 39 ▲.

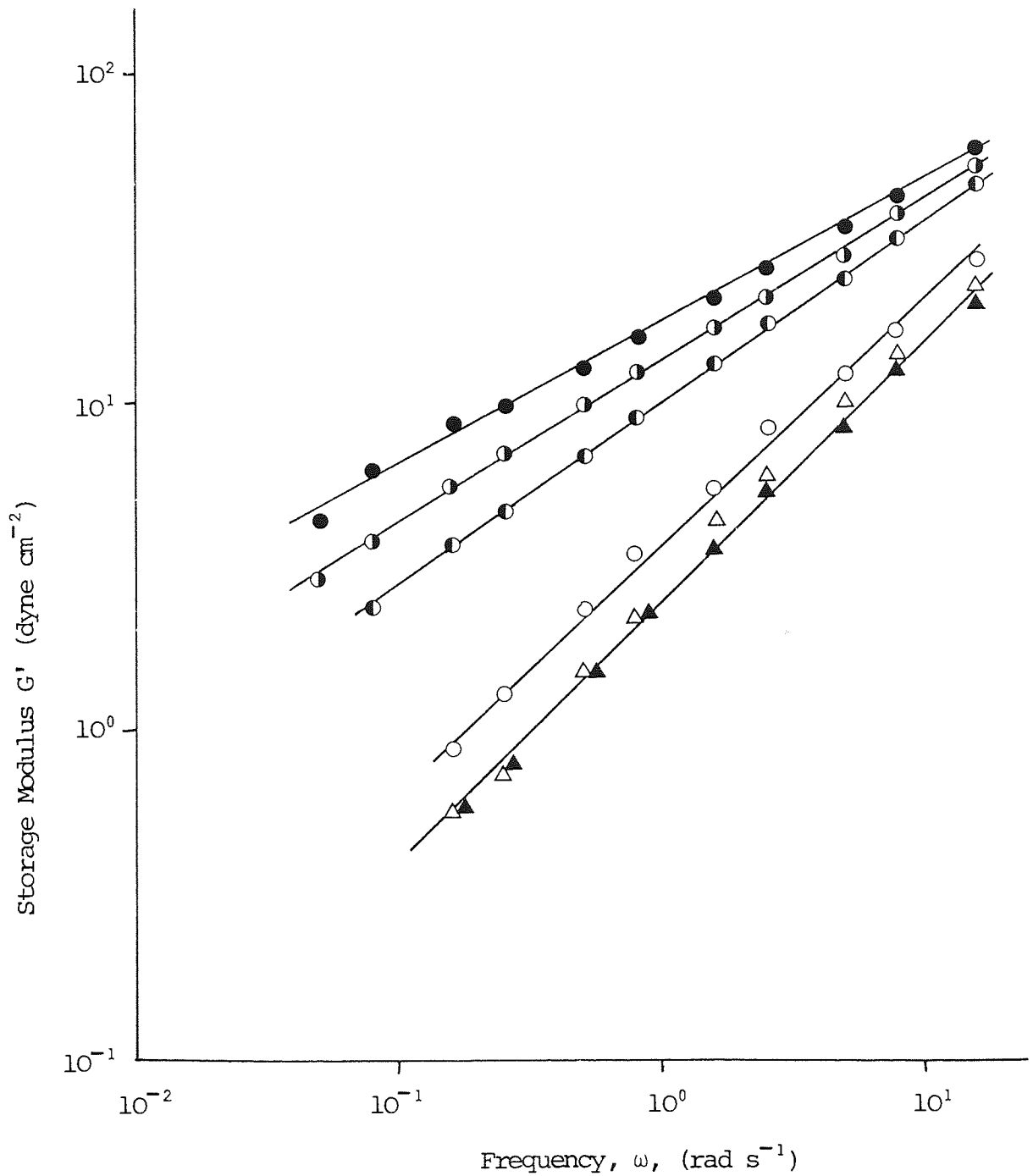


Figure 3.39. The Effect of Aging time at 50°C on the Dynamic Viscosity, η' , Formulation XI plotted as a function of the Frequency of Oscillation, ω .

Aging time (days) : 0 ●, 7 ○, 14 ◐, 24 ◑, 31 △, 39 ▲.

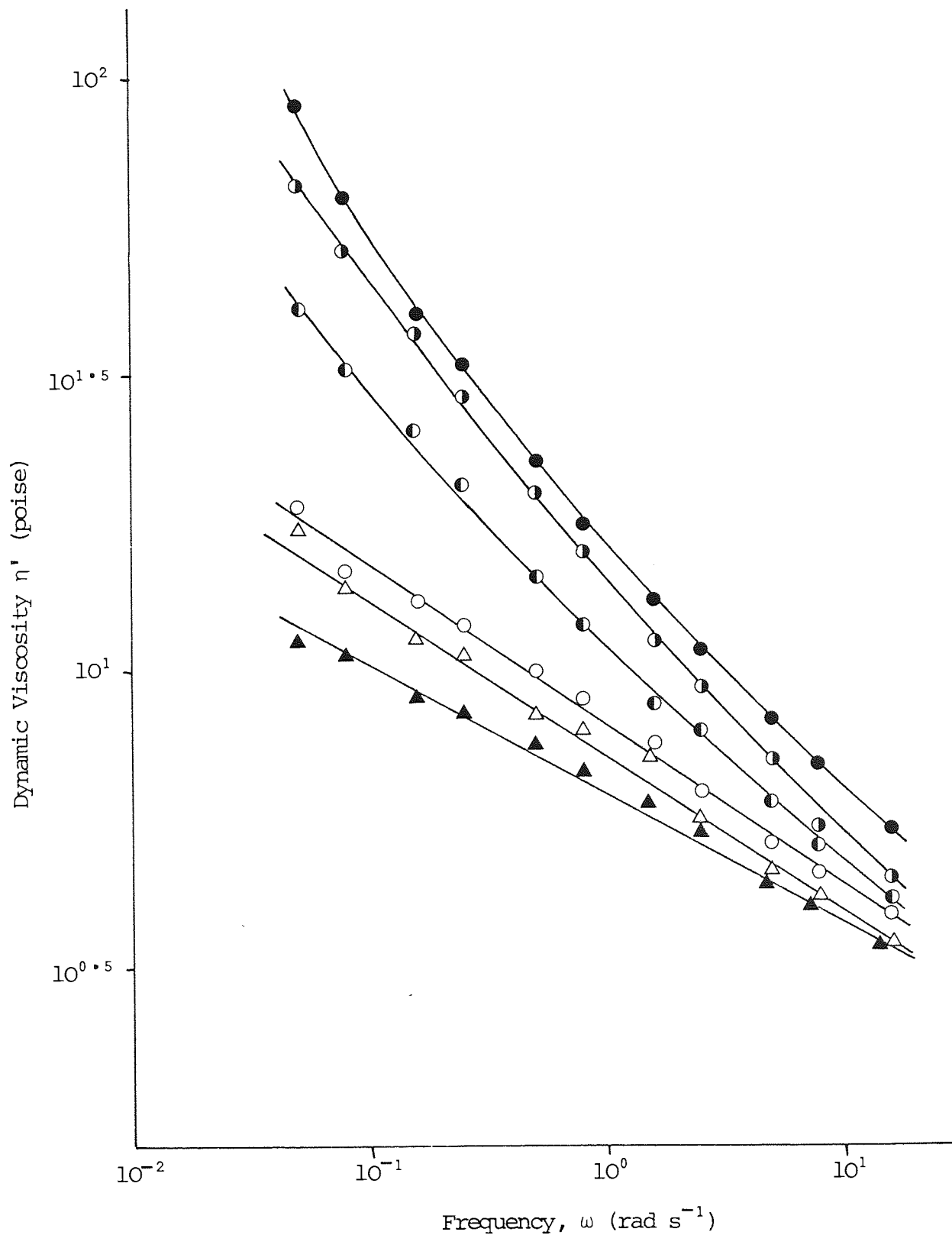


Figure 3.40. The Effect of Aging time at 50°C on the Storage Modulus, G' , of Formulation IV plotted as a function of the Frequency of Oscillation, ω .

Aging time (days) : 0 ●, 7 ○, 14 ◐, 24 ◑.

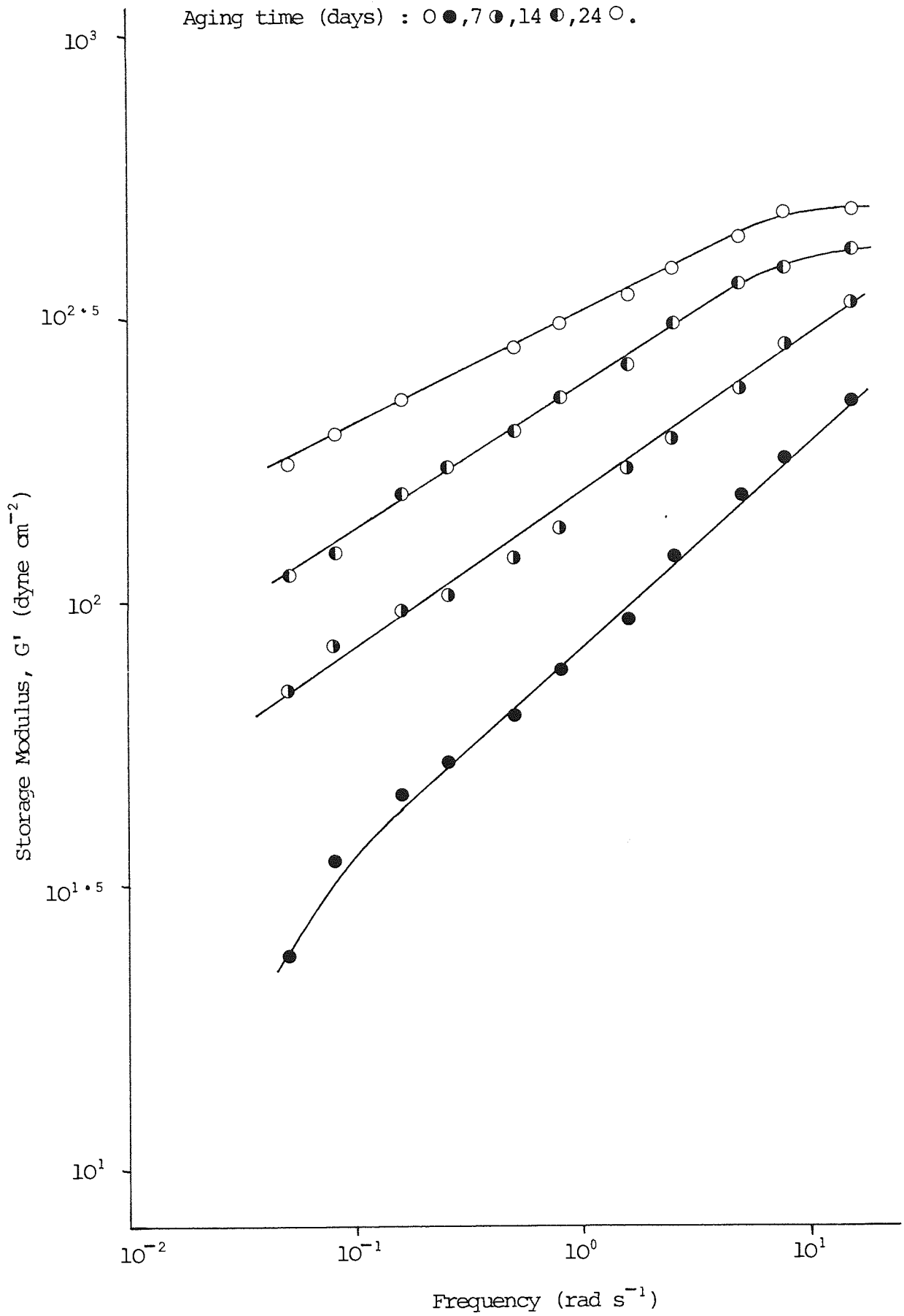
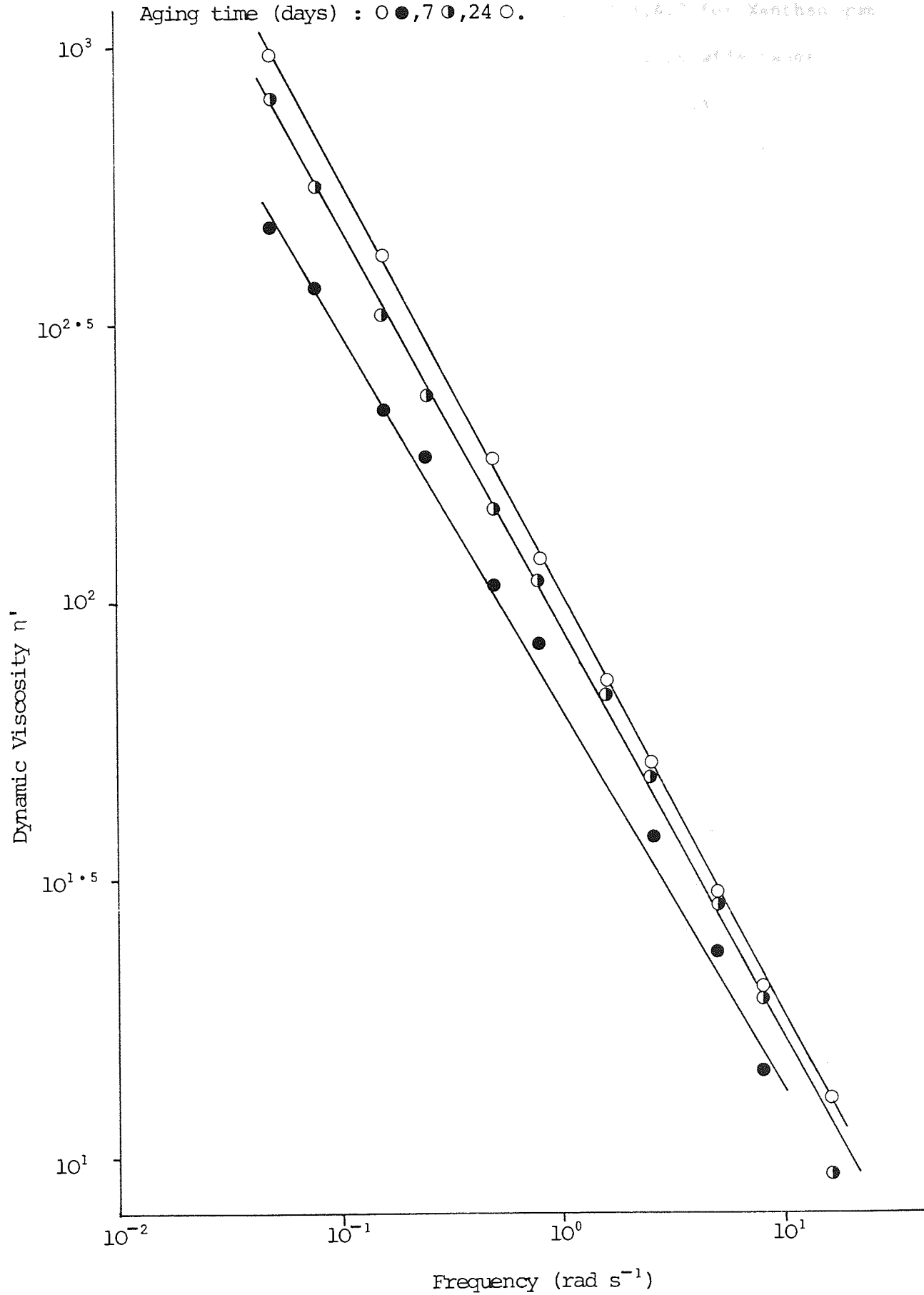


Figure 3.41. The Effect of Aging time at 50°C on the Dynamic Viscosity, η' , of Formulation IV plotted as a function of the Frequency of Oscillation, ω .

Aging time (days) : \circ ●, 7 \bullet , 24 \circ .



3.5 Discussion

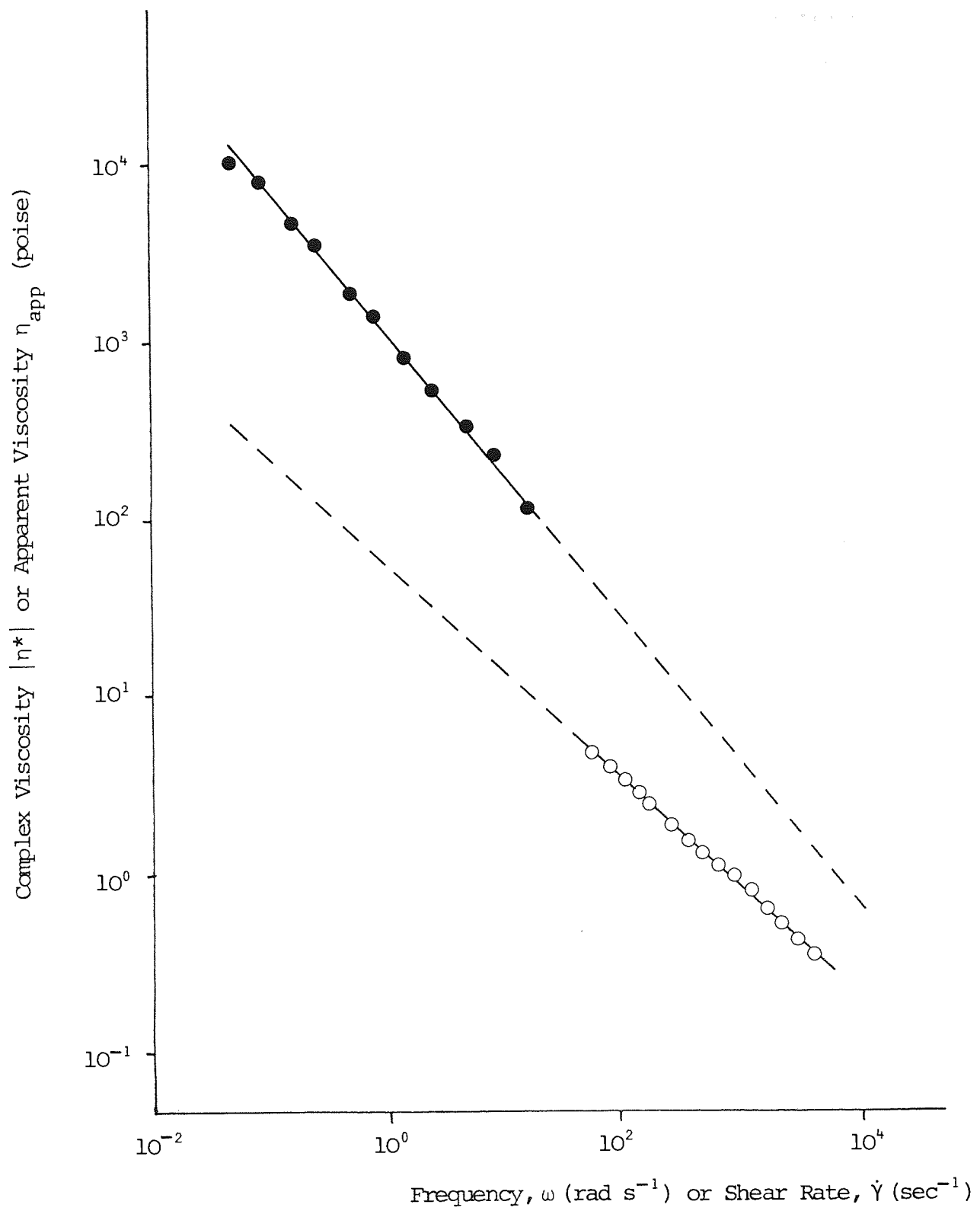
From the results of Sections 3.4.1. and 3.4.2 for Xanthan gum and Carbopol systems, it is clear that a very wide range of rheological properties is available with the use of polyelectrolyte combinations. The range can be further extended by applying high shear to the systems. The accurate rheological measurements from oscillatory testing can then be used in conjunction with correlations with settling rate, such as that of Equation 3.4., to calculate the time for which a suspension can stand without significant sedimentation.

Application of the Cox-Merz rule (109) to collate oscillatory and continuous shear data for single and mixed polyelectrolyte systems did not yield good correlations. The absolute value of the complex viscosity, $|\eta^*|$, was calculated using Equation 3.6.

$$|\eta^*| = [(\eta')^2 + (\eta'')^2]^{\frac{1}{2}} \quad 3.6$$

$|\eta^*|$ and the apparent viscosity, η_{app} , were plotted against frequency and shear rate respectively using log-log axis. An example of such a plot is shown in Figure 3.42.. The frequencies and shear rates used do not overlap, therefore direct comparisons are difficult but generally, it was found that $|\eta^*|$ decreased with ω more rapidly than η_{app} decreased with $\dot{\gamma}$ as experienced by previous workers (186,187). Hence, from the data available, it is not possible to extend the range of oscillatory results with continuous shear data.

Figure 3.42. Comparison of Dynamic and Steady Shear Viscosities; Absolute Value of Complex Viscosity, $|\eta^*|$ against Frequency, \bullet , and Apparent Viscosity, η_{app} against Shear Rate, \circ .



If meaningful results for viscoelastic systems can be obtained from $\tau(\dot{\gamma})$ curves, then there is little point in carrying out oscillatory tests which are more time consuming and more expensive. However, transformation of continuous shear parameters to obtain elasticities has not been demonstrated. It is also difficult to accurately determine the zero shear viscosity of many non-Newtonian materials using an instrument such as the 'Rheomat 30', even with the aid of the Cross Equation (see Table 2.3). Despite the curve-fitting of continuous shear rheograms to semi-empirical equations such as the Shangraw Equation, more useful rheological information is obtained from more elaborate techniques.

From the data presented here, it is clear that a very wide range of rheological 'profiles' are available when different polyelectrolytes are combined in solution. Close monitoring of the rheological parameters in terms of the viscous and elastic components is possible using oscillatory shear testing. Fundamental data such as this should be capable of correlation with some other formulation factor, for example, sedimentation rate of solid in liquid dispersions.

4. NUMERICAL ANALYSIS OF APPROXIMATIONS TO DIFFUSION RATE EQUATIONS.

4.1 Introduction

The diffusion process is applicable to many areas of pharmaceuticals research. One of the most studied applications is the release of drugs from polymer devices (188-191) whereby the polymer properties are chosen such that diffusion becomes the rate-determining step for drug release. However, whilst it is scientifically pleasing to be able to design a dosage form such that the drug is released at a predicted rate, it is frequently the case that diffusion is the rate-determining step by default, not by design.

An example of this is reflected in the work of Barzegar-Jalali and Richards (192,193) who showed a rank order correlation between kinetic parameters describing the in vitro and in vivo release of Aspirin with the viscosity of the suspension medium. The most likely link between drug release and viscosity in this case, is diffusion of the drug through the viscous medium; the drug solubility is unlikely to be drastically affected by low concentrations of suspending agents. In effect, the thickness of the boundary layer around the dissolving drug particles is greater in more viscous media.

That Barzegar-Jalali and Richards were only able to describe a rank order correlation was probably in the first place a deficiency of the experimental method. Tyrrell (194) has

explained the practical difficulties involved in studying diffusion in viscous media caused by the large time scale during which measurements need to be taken. In the second place, Barzegar-Jalali and Richards' measurements of viscosity by continuous shear methods probably contributed to the inconclusive results. It can be hypothesised that accurate measurement of diffusion coefficients and viscoelastic parameters for the drug in solutions of suspending agents would lead to a quantitative relationship.

For quantitative interpretation of experimental data from diffusion experiments, it is necessary to use the appropriate equation to describe the mass transfer. If the diffusion can be described by steady state kinetics, then solutions to Fick's First Law, Equation 4.1. are used; if unsteady state conditions prevail, then solutions to Fick's Second Law, Equation 4.2. are applied.

$$F = -D \frac{\partial C}{\partial x} \quad \text{-----} \quad 4.1$$

$$\frac{\partial C}{\partial t} = D \frac{\partial^2 C}{\partial x^2} \quad \text{-----} \quad 4.2$$

The terms in all Equations are defined in the Appendix to this chapter. These Equations were derived by Fick in 1855 (195) who developed the analogy of diffusion with heat conduction, the theories for which were developed by Fourier in 1822 (196).

Solutions to Fick's Second Law can take many different forms

depending upon the geometry and behaviour of the diffusion system under study. Many examples are dealt with by Crank (197) and Barrer (198); many of the equations are derived exhaustively in the treatise on heat conduction by Carslaw and Jaeger (199). It should be noted that systems exist which do not obey Fick's Laws (200).

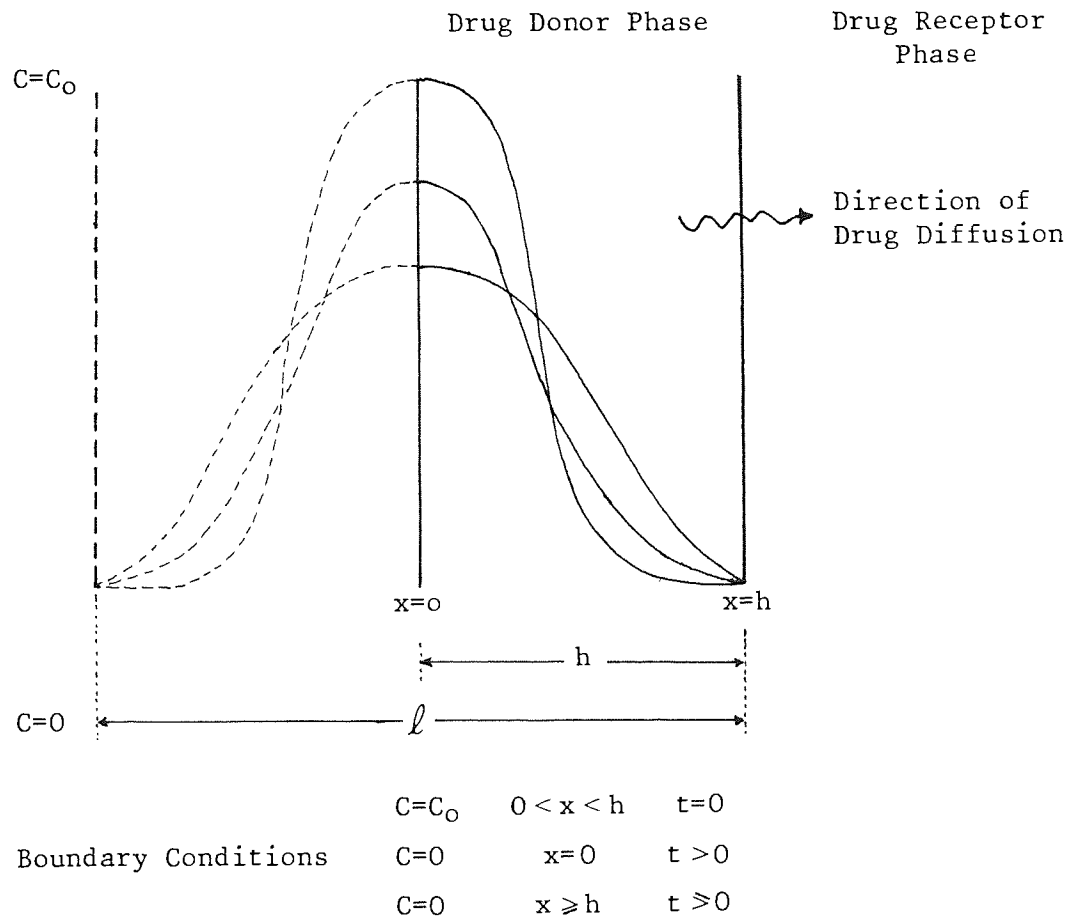
In diffusion problems of pharmaceutical interest, the systems described by Higuchi (201,202) are widely applicable. These are based on the planar diffusion solution to Fick's Second Law:

$$Q = hC_0 \left[1 - \frac{8}{\pi^2} \sum_{n=0}^{\infty} \frac{1}{(2n+1)^2} \exp\left(\frac{-D(2n+1)^2 \pi^2 t}{4h^2}\right) \right]$$

———— 4.3.

when applied to a system such as that described in Figure 4.1. With regard to Figure 4.1., we are interested in a donor phase of thickness h . The model is based on a profile of thickness $l = 2h$ reflected about $x = 0$ and superposed upon $0 < x < h$. Therefore, the effective thickness for the purpose of the solution is $2h$.

Figure 4.1. Scheme for the Planar Diffusion of a drug from a Donor Phase Matrix to a Sink.



Higuchi (201) stated: "it can be easily shown that" the Equation:

$$Q = 2C_0 \sqrt{\frac{Dt}{\pi}} \quad \text{--- 4.4.}$$

is a useful short time approximation for Equation 4.3. "for up to about 30 - 50% drug release" (202). Ostrenga et al (203) wrongly stated that Equation 4.4. is obtained by considering the first term in the sum of Equation 4.3.. Hadgraft (204) recognised that Equation 4.4. is actually derived from an alternative solution to Fick's Second Law:

$$Q = hC_0 \left[2 \sqrt{\frac{Dt}{h^2}} \left(\frac{1}{\sqrt{\pi}} + 2 \sum_{n=1}^{\infty} (-1)^n \text{ierfc} \frac{nh}{2\sqrt{Dt}} \right) \right] \quad \text{4.5.}$$

At short times, the second term of the inner brackets disappears, thus leaving Equation 4.4.. Ierfc is the integral error function, a standard function for which tabulated values are available (205,206) although it can be evaluated from the equation:

$$\text{ierfc}(x) = \frac{1}{\sqrt{\pi}} \exp^{-x^2} - x \text{erfc}(x) \quad \text{--- 4.6.}$$

$$\text{where } \text{erfc}(x) = 1 - \text{erf}(x) \quad \text{--- 4.7.}$$

$$\text{and the error function } \text{erf}(x) = \frac{2}{\sqrt{\pi}} \int_0^x \exp^{-z^2} dz \quad \text{--- 4.8.}$$

Equation 4.3. is useful for its rapid convergence at long times where only the first term in the exponential series

is significant and we obtain:

$$Q = hC_0 \left[1 - \frac{8}{\pi^2} \exp \left(- \frac{Dx^2 t}{4h^2} \right) \right] \quad \text{--- 4.9.}$$

The use of approximations to the diffusion rate equations has been studied by Hadgraft and Guy (204,207) who have shown graphically the difference between the "square-root-time approximation", Equation 4.4., and the rigorous solution. As a further development of this theme, the intention of the work presented here is to rigorously quantify the errors involved in using either the short or long time approximations. An accurate knowledge of the inherent errors of these equations should provide a basis for obtaining quantitative correlations with, for example, viscoelastic parameters of non-Newtonian diffusion media.

Certain studies on drug release from creams and ointments, for example by Ostrenga et al (203) and Chowhan and Pritchard (208) show data analysis in terms of Equation 4.4. with good agreement. However, from the numerical method used in the present study, it can be shown that analysis of drug release profiles alone does not provide unambiguous information about the mechanism of rate control. In other words, for experimental systems concerning such complex materials as creams and ointments, it is necessary to obtain further evidence for rate controlling diffusion before Equation 4.4. can be applied.

4.2 Derivation of a Diffusion Rate Equation

Equation 4.3. and 4.5. are solutions to Fick's second Law obtained by different methods. The former can be obtained by the method of Separation of Variables; the latter by Reflection and Superposition and both equations can be obtained by Laplace transformation (197,198). Equation 4.3. has been widely used in the pharmaceutical and allied literature (202,209) and its derivation from Equation 4.2. as the most straightforward.

The method of Separation of Variables is a standard solution method for partial differential equations (210). In this case, we assume that Equation 4.2. can be solved by an equation of the form:

$$C(x, t) = X(x) \cdot T(t) \quad 4.10.$$

where X is a function of x only and T a function of t only. If we consider the partial differential Equations 4.11 and 4.12.:-

$$\frac{\partial C}{\partial t} = X \frac{dT}{dt} \quad 4.11.$$

$$\frac{\partial^2 C}{\partial x^2} = T \frac{\partial^2 X}{\partial x^2} \quad 4.12.$$

then from Equation 4.2. we obtain Equation 4.13.:

$$\frac{1}{DT} \frac{dT}{dt} = \frac{1}{X} \frac{d^2 X}{dx^2} \quad 4.13.$$

Here, the left hand side is dependent on t only and the right hand side only on x . The next stage involves setting each side of Equation 4.13 equal to a constant, $-\lambda^2$, where λ is a real number and the negative sign ensures an exponentially decreasing solution in t .

Considering the left hand side of Equation 4.13. we obtain

$$\frac{dT}{T} = -\lambda^2 D dt \quad 4.14.$$

which on integration gives:

$$T = E \exp(-\lambda^2 D t) \quad 4.15.$$

where E is the integration constant.

The solution to the right hand side of Equation 4.13. is given by

$$X = A \sin \lambda x + B \cos \lambda x \quad 4.16.$$

with A and B as integration constants. Substitution into Equation 4.10. gives:

$$C(x, t) = (A' \sin \lambda x + B' \cos \lambda x) e^{-\lambda^2 D t} \quad 4.17.$$

where $A' = AE$ and $B' = BE$. Substituting the relevant boundary conditions:

$$C(0, t) = B' e^{-\lambda^2 Dt} = 0 \quad 4.18.$$

therefore $B' = 0$ for all values of t . This leads to the result:

$$C(\ell, t) = A' \sin \lambda \ell e^{-\lambda^2 Dt} = 0 \quad 4.19.$$

which gives non-trivial solutions of C for $\sin \lambda \ell = 0$,

i.e. $\lambda = n\pi/\ell$ where $n = 1, 2, 3, \dots$. For convenience, $\ell = 2h$, see Figure 4.1. Substituting $B' = 0$ and $\lambda = n\pi/\ell$ into Equation 4.17. gives:

$$C(x, t) = \sum_{n=1}^{\infty} A'_n \sin\left(\frac{n\pi x}{\ell}\right) \exp\left(\frac{-n^2 \pi^2 Dt}{\ell^2}\right) \quad 4.20.$$

where A'_n is a constant such that at $t = 0$,

$$C(x, 0) = C_0 = \sum_{n=1}^{\infty} A'_n \sin\left(\frac{n\pi x}{\ell}\right) \quad 4.21$$

The next stage, the evaluation of A'_n , involves the use of a Fourier series which is defined by an equation of the form:

(211)

$$f(x) = \frac{a_0}{2} + \sum_{r=1}^{\infty} a_r \cos rx + b_r \sin rx \quad 4.22.$$

The shape of the concentration profile within the drug donor phase is sinusoidal, similar to $-\pi/2 < x < \pi/2$. In this region, $\sin(x)$ is an odd function; an odd function occurs when $f(x) = -f(-x)$ i.e., it is not symmetrical about the

y-axis. If $f(x)$ in Equation 4.22. is odd then we obtain

$$f(x) = \sum_{r=1}^{\infty} b_r \sin rx \quad 4.23.$$

because the Cosine term becomes zero on integration and consideration of $a_0/2$ is not necessary. It is now seen that A_n' is equivalent to b_r . The infinite series can be simplified using Dirichlet's condition (212) for a periodic function that $f(x) = f(x + 2k\pi)$ where k is any integer. Thereby,

$$b_r = \frac{2}{\pi/2} \int_{\pi/2}^{\pi} f(x) \sin rx \, dx \quad 4.24.$$

from a consideration of the shape of the concentration profile compared to the Sine wave in the region of interest.

From Equations 4.21. and 4.24., A_n' can be evaluated:

$$A_n' = \frac{2}{l} \int_0^l C_0 \sin\left(\frac{n\pi x}{l}\right) dx \quad 4.25.$$

On integration, we obtain

$$A_n' = \frac{2C_0}{l} \cdot \frac{l}{n\pi} \left\{ -\cos\left(\frac{n\pi x}{l}\right) \right\}_0^l \quad 4.26$$

$$A_n' = \frac{4C_0}{n\pi} \quad \text{for } n = 1, 3, 5, \dots \quad 4.27$$

Substituting into Equation 4.20.:

$$C = C(x,t) = \sum_{n=0}^{\infty} \frac{4C_0}{(2n+1)\pi} \exp\left(-\frac{D(2n+1)^2 \pi^2 t}{l^2}\right) \sin\left(\frac{(2n+1)\pi x}{l}\right) \quad 4.28$$

Integration of Equation 4.28. between the limits 0 and ℓ will provide Q, the cumulative amount of drug released from the matrix. On integration, the Sine term becomes a Cosine term such that $\text{Cos}(y) = +1$ when $x = \ell$ and $\text{Cos}(y) = -1$ when $x = 0$, where $y = (2n + 1)\pi x / \ell$. Therefore the trigonometrical term disappears and we are left with:

$$Q = hC_0 \left\{ 1 - \frac{8}{\pi^2} \sum_{n=0}^{\infty} \frac{1}{(2n + 1)^2} \exp \left(- \frac{D(2n+1)^2 \pi^2 t}{4h^2} \right) \right\}$$

4.29.

where $Q + Q_r = hC_0$, Q_r being the quantity of drug remaining in the donor phase matrix. This is identical to Equation 4.3..

4.3 Method of Numerical Analysis

In order to assess the limits of applicability of the approximate Equations 4.4. and 4.9. compared to the rigorous expressions, it is necessary to employ a variable term that is common to all of the Equations. First of all, since Equations 4.3. and 4.5. are for all practical purposes equivalent, only Equation 4.3. will be considered in the numerical analysis; accurate comparison of these two equations using a double precision Fortran IV computer programme of the type described below revealed discrepancies only in the eighth decimal place for the fraction of drug released at time, t.

By dividing Equations 4.4., 4.3, and 4.9. by hC_0 , the left hand sides become the dimensionless ratio Q/hC_0 representing

the fraction, F , of drug released from the matrix at time, t .

Hence,

$$\frac{Q_1}{hC_0} = F_1 = 2 \left\{ \frac{Dt}{h^2 \pi} \right\}^{\frac{1}{2}} \quad 4.30.$$

$$\frac{Q_2}{hC_0} = F_2 = \left\{ 1 - \frac{8}{\pi^2} \sum_{n=0}^{\infty} \frac{1}{(2n+1)^2} \exp \left(- \frac{D(2n+1)^2 \pi^2 t}{4h^2} \right) \right\} \quad 4.31.$$

$$\frac{Q_3}{hC_0} = F_3 = \left\{ 1 - \frac{8}{\pi^2} \exp \left(- \frac{D \pi^2 t}{4h^2} \right) \right\} \quad 4.32.$$

It is noticeable that all three expressions contain the term Dt/h^2 and that this term is dimensionless with reference to Equation 4.30.. Crank (197) has made extensive use of the Dt/h^2 term. By substituting χ for $(\pi^2 Dt/4h^2)^{\frac{1}{2}}$ in Equations 4.30. to 4.32. we obtain:

$$F_1 = \frac{4 \chi}{\pi^{3/2}} \quad 4.33.$$

$$F_2 = \left\{ 1 - \frac{8}{\pi^2} \sum_{n=0}^{\infty} \frac{1}{(2n+1)^2} \exp \left(-(2n+1)^2 \chi^2 \right) \right\} \quad 4.34.$$

$$F_3 = \left\{ 1 - \frac{8}{\pi^2} \exp \left(- \chi^2 \right) \right\} \quad 4.35$$

The approximation of interest is now $F_1 \approx F_2 \approx F_3$.

By inserting suitable values for χ into Equations 4.33. to 4.35., the fractions released according to Equations 4.4.,

4.3. and 4.9. respectively, were obtained. To ensure that the calculated differences between F_1 , F_2 and F_3 were due to the respective equations and not to the method of calculation, a double precision Fortran IV Computer programme was used. The algorithm for this programme is given in Figure 4.2. and the corresponding listing is given in Table 4.1.. The exponential series in Equation 4.34. was evaluated such that the sum of the last ten terms was less than 10^{-10} . This guaranteed that the series had converged.

Figure 4.2. Algorithm for Determination of the Fractions Released,

F_1 , F_2 and F_3 according to the

Three Diffusion Equations.

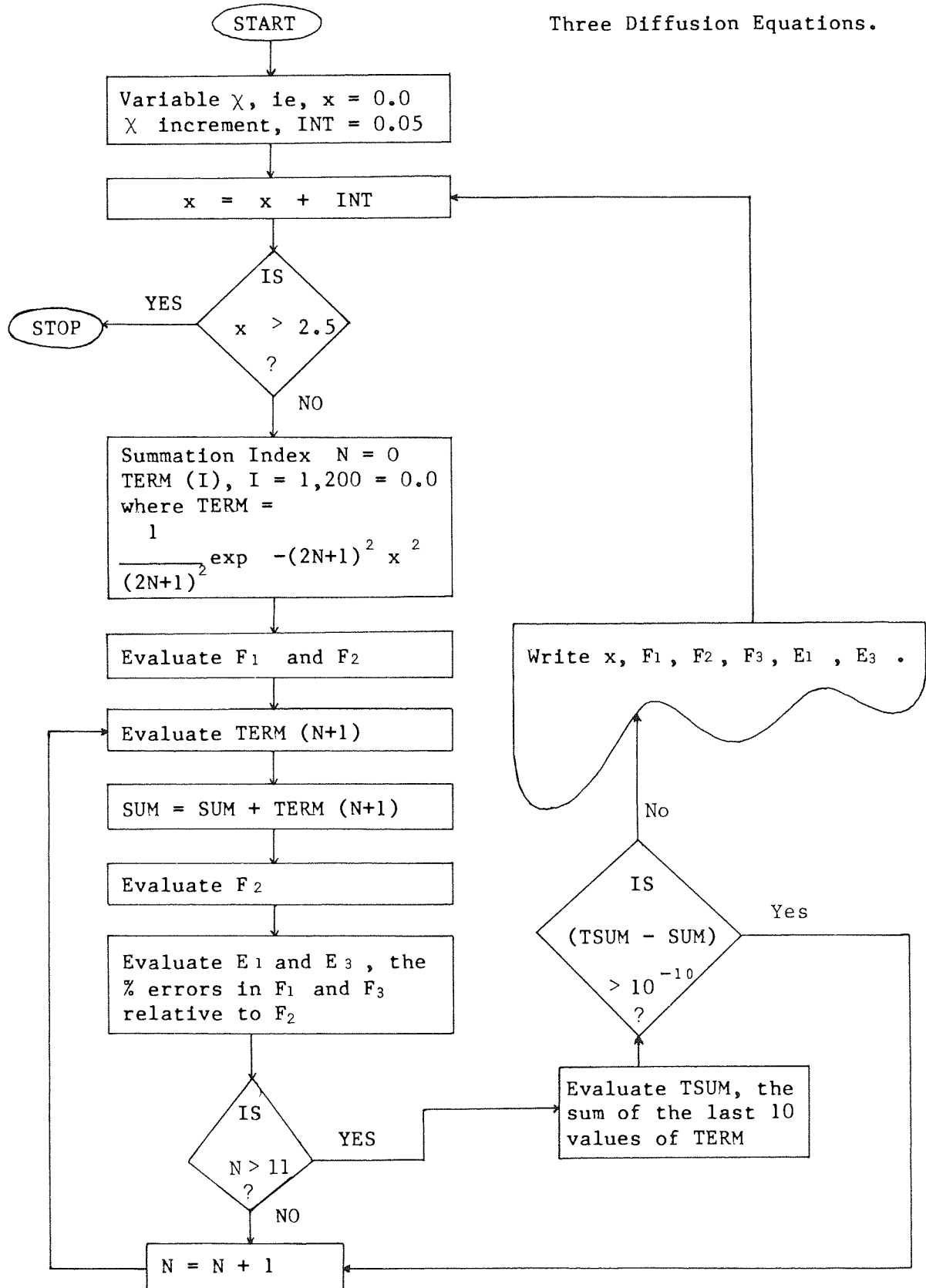


Table 4.1. Listing of the Double Precision Fortran IV Programme for Calculating the Fractions Released F_1 , F_2 , F_3 according to the Three Diffusion Equations.

```

MASTER SEGMENT
REAL INT
DOUBLE PRECISION PI, F1, F2, F3, E1, E3, D, Y
1      TERM, SUM, TSUM
DIMENSION TERM (200)
X = 0.0
INT = 0.05
1  X = X + INT
   IF (X.GT.2.5) GOTO 7
   M = 0
   DO 6  I = 1,200
   TERM (I) = 0.0
6  CONTINUE
   SUM = 0.0
   PI = 3.141592653589793238462643
C  EVALUATE F1:
   F1 = (4.0 * DBLE(X)/(PI * SQRT(PI)))
C  EVALUATE F2:
2  D = DBLE ((2.0 + FLOAT(N) + 1.0) **2)
   Y = EXP (-D * DBLE (X **2))
   TERM (N+1) = Y/D
   SUM = SUM + TERM (N+1)
   F2 = (1.0 - ((8.0/(PI**2))*SUM))
   E1 = 100.0 * ((F1-F2)/F2)
   IF (N.GT.11) GOTO 4
5  N = N + 1
   GOTO 2
4  TSUM = 0.0
   DO 20 J = N - 10,N
   TSUM = TSUM + TERM(J)
20 CONTINUE
   TSUM = TSUM + SUM
   IF (ABS(TSUM - SUM). GE.1.0.D-10) GOTO 5
C  EVALUATE F3:
   F3 = 1.0 - (8.0/(PI**2)*TERM(1))
   E3 = 100.0*((F3-F2)/F2)
WRITE(6,23)X,F1,F2,F3,E1,E3
23 FORMAT (1X,F5.2,5(1X,D25.20))
   GOTO 1
7  STOP
   END
   FINISH
* * * *

```

The percentage errors involved in using either approximate equation at any stage of an experiment were quantified by E_1 and E_3 where

$$E_1 = 100 \left(\frac{F_1 - F_2}{F_2} \right) \quad 4.36$$

$$E_3 = 100 \left(\frac{F_3 - F_2}{F_2} \right) \quad 4.37$$

4.4 Results and Discussion

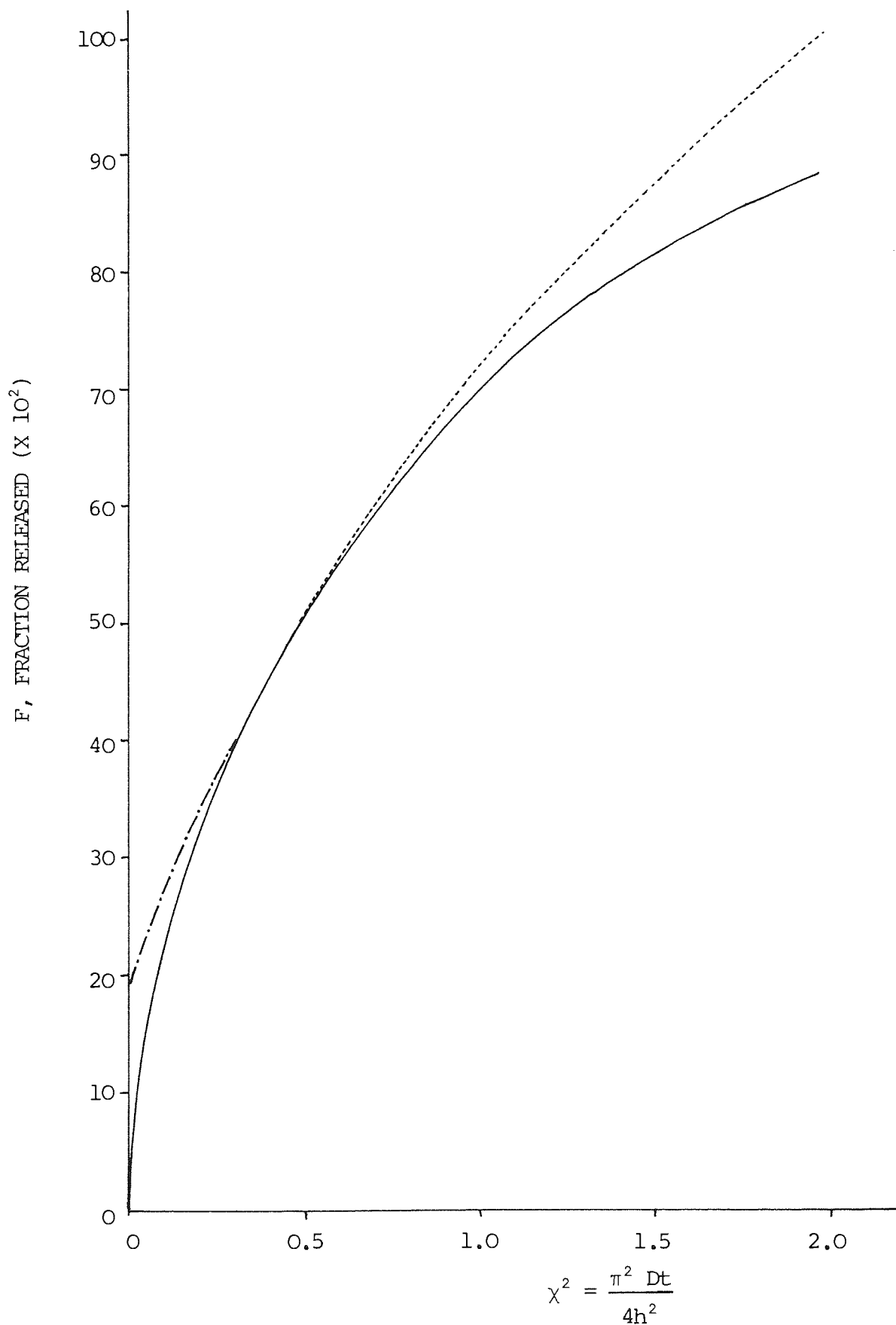
The abridged results of the computation described above are listed in Table 4.2. showing the errors involved in using either approximation Equation 4.4 or 4.9. relative to the 'exact' fraction released, F_2 . To avoid the use of Equation 4.3., it is clearly justified to apply Equation 4.4. for less than 50% release or a first order plot according to Equation 4.9. for greater than 50% release. No more than about 0.2% error is thus incurred in values of F . This is illustrated in Figure 4.3. where F_1 , F_2 , and F_3 are plotted against χ^2 , which is proportional to time.

If data for the true fraction released, F_2 , is plotted in a first order fashion against χ^2 , then linear least mean square regression analysis in the range $0.07 < F < 0.97$ gave correlation coefficients in excess of 0.999 ($N=11$).

Table 4.2. Results of Numerical Analysis using the Programme listed in Table 4.1.

χ	F_1	F_2	F_3	E_1	E_3
0.1	0.07184	0.07184	0.19750	} $< 10^{-6}$	174.95
0.2	0.14367	0.14364	0.22121		53.974
0.3	0.21550	0.21550	0.25920		20.274
0.4	0.28734	0.28734	0.30928		1.1941×10^{-6}
0.5	0.35917	0.35917	0.36873	4.5958×10^{-4}	2.6604
0.6	0.43101	0.43095	0.43448	0.012867	0.81940
0.7	0.50284	0.50233	0.50342	0.10254	0.21796
0.8	0.57468	0.57231	0.57259	0.41407	0.049500
0.9	0.64651	0.63935	0.63941	1.1204	9.6117×10^{-3}
1.0	0.71835	0.70180	0.70181	2.3584	1.5837×10^{-3}
1.1	0.79018	0.75829	0.75829	4.2061	2.2143×10^{-4}
1.2	0.86202	0.80795	0.80795	6.6916	2.6167×10^{-5}
1.3	0.93385	0.85043	0.85043	9.8090	2.6330×10^{-6}
1.4	1.00569	0.88582	0.88582	13.531	
1.5	1.07752	0.91457	0.91457	17.818	
1.6	1.14936	0.93734	0.93734	22.619	} $< 10^{-6}$
1.7	1.22119	0.95495	0.95495	27.880	
1.8	1.29303	0.96825	0.96825	33.942	
1.9	1.36486	0.97807	0.97807	39.546	
2.0	1.43669	0.98515	0.98515	48.835	
2.1	1.50853	0.99015	0.99015	52.354	
2.2	1.58037	0.99359	0.99359	59.056	
2.3	1.65220	0.99591	0.99591	65.898	
2.4	1.72404	0.99745	0.99745	72.845	

Figure 4.3. The Fraction F of Drug Released by Planar Diffusion to a Perfect Sink. F_1 ----- Short time approximation; F_2 —— Rigorous solution; F_3 ----- long time approximation.



This result is illustrated in Figure 4.4. and the data used is given in Table 4.3.. It is important when considered in the light of a set of experimental drug release data where the mechanism of rate control has not been firmly established as diffusion. Clearly, if data from a wholly diffusion controlled process, as is the case for F_2 , can provide a good fit to first order behaviour, then it must be difficult, within experimental error, to distinguish the mechanism of rate control merely from analysis of drug release profiles.

Figure 4.4. First Order Plot of the Actual Fraction, F_2 , of Drug Released by Planar Diffusion into a Perfect Sink.

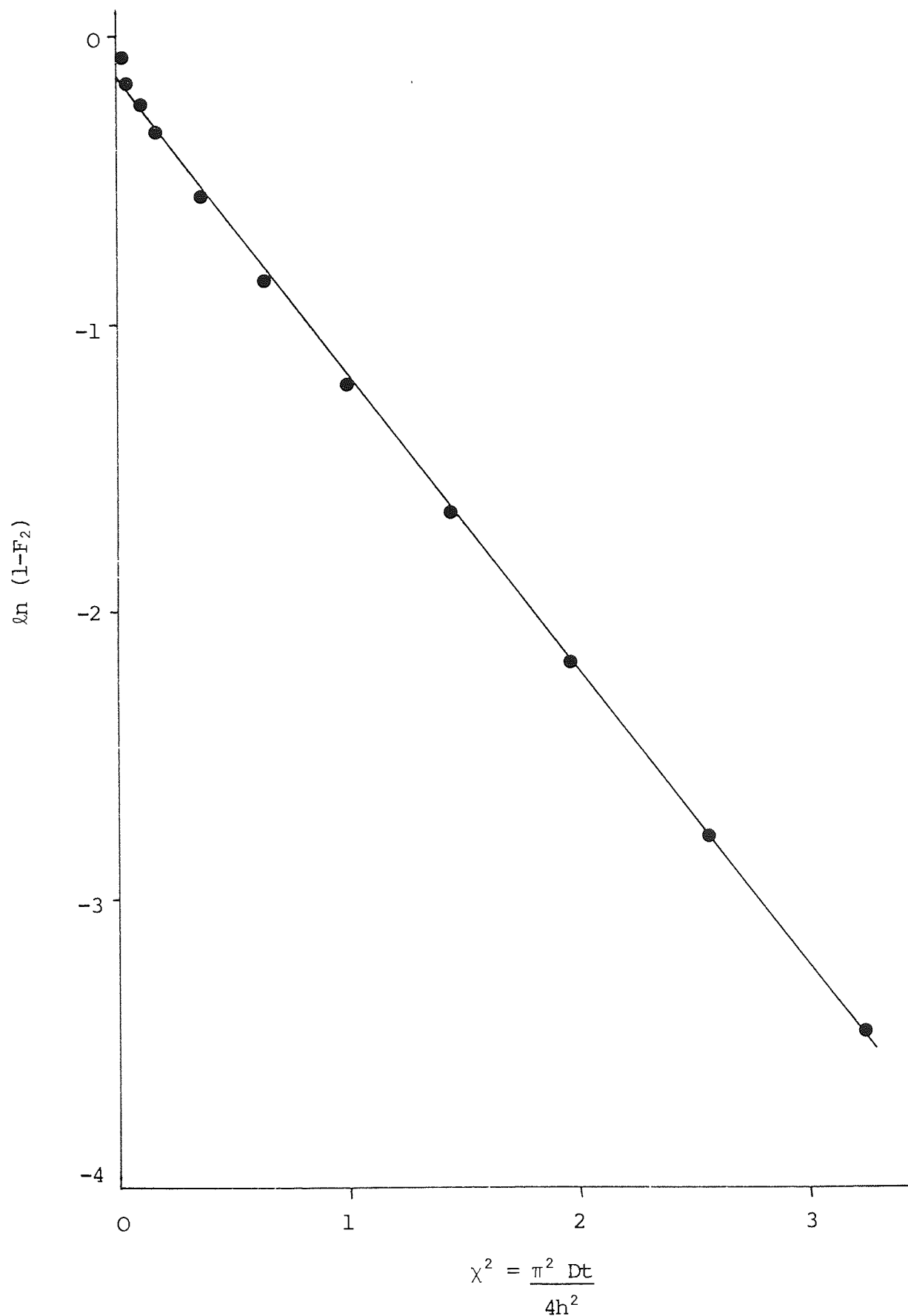


Table 4.3. Diffusional Data used for the First Order Plot of Figure 4.4.

χ^2	F_2	$\ln(1-F_2)$
0.01	0.07184	-0.075
0.04	0.14364	-0.155
0.09	0.21550	-0.243
0.16	0.28734	-0.339
0.36	0.43095	-0.564
0.64	0.57231	-0.849
1.00	0.70180	-1.210
1.44	0.80795	-1.650
1.96	0.88582	-2.170
2.56	0.93734	-2.770
3.24	0.96825	-3.450

Appendix I. Glossary of Terms not Directly Explained in the Text.

Term	Equation of first appearance	Meaning	Units
a_o, a_r, b_r	4.22.	Constant terms in Fourier Series	
C	4.1.	Concentration	ML^{-3}
C	4.4.	Initial Concentration in donor phase matrix.	ML^{-3}
dC/dx	4.1.	Concentration gradient	ML^{-4}
D	4.1.	Diffusion Coefficient	$L^2 T^{-1}$
E	4.36.	% error incurred from Eqn.4.4.	
E	4.37.	" " " " " 4.9.	
F	4.30.	Fraction released according to Eqn.4.4.	
F	4.31.	Fraction released according to Eqn.4.3.	
F	4.32.	Fraction released according to Eqn.4.9.	
F	4.1.	Flux: amount released per unit area per unit time.	$ML^{-2} T^{-1}$
h	4.3.	Thickness of donor phase matrix	L
ℓ	4.19.	Hypothetical thickness of donor phase matrix	L
n	4.3.	Summation Index	
Q	4.3.	Amount released per unit area at time, t.	ML^{-2}
Q_1	4.30.	Release rate according to Eqn. 4.4.	ML^{-2}
Q_2	4.31.	Release rate according to Eqn. 4.3.	ML^{-2}
Q_3	4.32.	Release rate according to Eqn. 4.9.	ML^{-2}

r	4.22.	Summation index for Fourier Series	
t	4.2.	Time	T
x	4.1.	Distance	L
z	4.8.	Arbitrary variable	
χ	4.33.	Dimensionless variable = $(\pi^2 Dt/4h^2)^{\frac{1}{2}}$	

M = Mass, L = Length and T = Time.

5. DIFFUSIONAL AND RHEOLOGICAL PROPERTIES OF ALGINATE GELS.

5.1 Introduction

This chapter is concerned with the relationship of dynamic rheological properties of Alginate cross-linked by means of Calcium, Ca^{2+} ions, with the diffusion of a drug, Ibuprofen, in the gel matrix.

As discussed in Section 1.2, Alginate forms rigid gels with with all divalent metal ions except magnesium. This characteristic has found wide application in the food industry (104, 105) as well as the pharmaceutical uses explained in Section 1. In Section 2, the problems of determining the molecular properties of a biological material were considered: this yielded detailed information about the particular Alginate used in this study. Section 3 was concerned with the wide variety of rheological properties available in Alginate systems when combined with other polyelectrolytes. The dynamic rheological data obtained by oscillatory shear testing provided fundamental parameters describing the flow properties.

In this Section, the diffusional aspects of Calcium Alginate gels are investigated. The results of the numerical analysis of diffusion equations in Section 4. are borne in mind for the interpretation of drug release data. By way of comparison with diffusional characteristics, the mechanical properties of the gels are examined using oscillatory shear tests.

Such rheological testing is particularly convenient for the brittle Calcium Alginate gels encountered: small amplitude oscillatory shear between parallel plates means that the net deformation of the sample is negligible and the material is effectively unchanged during testing. Continuous shear testing would not be feasible in this case because sample slippage and fracture would occur. Also, locating an intact Calcium Alginate gel in any continuous shear geometry would be manipulatively difficult.

The diffusion of solutes through viscous and gel-like media is of wide academic and industrial interest. In the pharmaceutical field, much interest has been centred on hydrogels and their use as controlled release drug delivery systems (213-215), and the study of diffusion is widespread in the formulation of ointments and creams (203, 208, 216, 217) and suppositories (218). Most systems of pharmaceutical interest involve the diffusion of a drug through a viscous and often non-Newtonian medium. Hence, we are faced with two problems. Firstly, as Tyrrell pointed out, (194), even with modern experimental methods, the determination of diffusion coefficients with reasonable precision is difficult, especially in viscous media. Although it is often assumed that diffusion coefficients are inversely proportional to the shear viscosity, this is the exception rather than the rule. It has been shown that the product of diffusion and viscosity coefficients, $D\eta$, increases with the viscosity of the

continuous phase (219, 220). Secondly, to get an insight into the diffusion-rheology relationships, rheological measurements should represent the physical equilibrium rest state of the material as exists for diffusion experiments. The second problem can be largely overcome with the use of established rheological techniques.

There have been very few studies, especially in the pharmaceutical literature that have attempted to link the diffusion of a solute through a gel or viscous phase with dynamic rheological data. A recent example of such a study is that of Sherriff and Enever (221). The diffusion of Methyl Salicylate was monitored as a function of the Storage Modulus $G'(\omega)$ of oil gels prepared by dispersing colloidal silica in n-dodecane and 1-dodecanol. For the 1-dodecanol system, the drug release rate was inversely proportional to G' . Even so, the authors considered only the elastic and not the viscous components of the dynamic rheological data. From a consideration of the Stokes-Einstein relationship that the product $D\eta/T$ should be constant for a given solute, one would expect that the viscous component would most likely dominate the effect on the diffusion coefficient. However, it has not been firmly established whether or not the elastic component makes a significant contribution, albeit smaller than the viscous component.

Previous studies have shown conflicting evidence as to the effect on the diffusion coefficient of low concentrations

of gelling agents or polymers in solution. Most of the published work has involved widely differing materials and this makes absolute comparisons difficult. The material most regularly studied is gelatin. Friedman and Kramer (222, 223) found that the diffusion of sucrose and urea increased by about 40% when the gelatin concentration was decreased from 4 to 12%. Nixon and co-workers (224) showed that diffusion of methylene blue dye was dependent on concentration in the range 10 to 15% gelatin in gelatin-glycerol-water gels. Taft and Malm (225) used the analogy of electrical conductivity with diffusion to show that diffusion of elemental cations was almost independent of gelatin concentration up to 13.2%, (specific conductivity decreased by only 4 to 8%). Marriott and Kellaway (218) found that the time taken for 75% release of proflavine from erodable gelatin-glycerol-water gels at 37°C increased from 9 to 30 min in the range 2 to 14% gelatin.

Other results have varied widely according to the system studied. Shaw and Schy (226) showed that D for $^3\text{H}_2\text{O}$ was reduced by 76% in Collagen 5% gel compared with the free diffusion coefficient in water. Chen-Chow and Frank (227) found that Pluronic F127 in concentrations of 20 to 30% reduced D for lidocaine from 1.75 to $1.05 \times 10^{-6} \text{ cm}^2 \text{ sec}^{-1}$. Rickard et al (228) found D for iodide ions to be unaffected by Xanthan gum concentrations of 0.01 to 1.3%. Gerasimova and Bromberg (229) showed that D for thiosulphate,

thioglycolic acid and mercaptosuccinic acid decreased in the presence of 5 to 20% gelatin, hydroxyethylcellulose, carboxymethylcellulose and polyvinylalcohol. Shul'man et al (230) found that D for ferricyanide ions decreased in aqueous carboxymethylcellulose solutions in the range 0 to 15% polymer.

Little attempt was made in any of these studies to quantitatively link diffusional with rheological properties. It appears that when diffusion is studied in depth, then rheological considerations are neglected. A study of diffusion by Farag et al (231) even claimed that solutions of polyacrylamide and polyethylene oxide up to 1% were Newtonian as 'confirmed' using a Brookfield viscometer.

In a comprehensive review of mass transport models, Flynn et al (232) suggested that the three dimensional network of a polymeric gel matrix can affect diffusion rate either by interaction and adsorption or by mechanical blocking of the diffusant. This is based on the generally accepted theory that diffusion takes place only in the fluid phase so that the microscopic viscosity and the number of polymer segments determine the diffusion rate. Hence, the bulk viscosity or gel rigidity can be affected by the degree of polymerisation or cross-linking of the polymer but the diffusion rate can remain unchanged because of a constant microscopic viscosity.

In this study, the aim is to develop a simple experimental

system whereby the diffusional and dynamic rheological properties of rigid gels can be examined. When applied to Alginate gel systems, data from the two experimental techniques can be compared.

5.2 Theory

This section deals with the theoretical aspects of the techniques used in subsequent sections. The theory of gelling has been discussed in Section 1; the theory appropriate to oscillatory rheometry was given in Section 2 and the calculation of diffusion coefficient from experimental data was discussed in Section 4.

5.2.1 Diffusion Coefficient

The simplest relationship between diffusion and viscosity is provided by the Nernst-Einstein Equation (233, 234):

$$D = \frac{RT}{f} \quad 5.1$$

where D = diffusion coefficient

R = universal gas constant

T = absolute temperature

f = frictional coefficient

In this relationship, diffusion is influenced by molecular energy, as reflected in R, temperature, and the resistance to molecular motion, as quantified by f. The value of f for a particle in a homogeneous fluid can be defined using the Sutherland Equation (235):

$$f = 6\pi\eta r \frac{2\eta + r\beta}{3\eta + r\beta} \quad 5.2$$

where r = solute radius

η = solvent viscosity

β = 'slip factor'

The 'slip factor', β , or more formally, the coefficient of sliding friction, is a measure of the tendency of solute molecules to adhere to solvent molecules. For a large diffusant, solvent molecules tend to be dragged along and therefore β is large. Hence, Equation 5.2 reduces to Stokes Law (236).

$$f_{\beta \rightarrow \infty} = 6\pi\eta r \quad 5.3$$

Substitution of Equation 5.3 into 5.1. gives the Stokes-Einstein Equation.

$$D = \frac{RT}{6\pi\eta N_{AV} r} \quad 5.4$$

where N_{AV} = Avogadro's number

This was derived for describing the diffusion of large, spherical molecules where the solvent appears to act as a continuum for the diffusant.

When β is small, there is little resistance to slip and Equation 5.2. becomes

$$f_{\beta \rightarrow 0} = 4\pi\eta r \quad 5.5$$

This equation is useful for the case of self-diffusion, i.e.,

when solvent and diffusant molecules are approximately the same size. Often, f becomes less than $4\pi\eta r$ if solvent molecules are larger than solute molecules.

Although the above relationships apply to spherical diffusants, frictional coefficients can be calculated for ellipsoids from molecular dimensions using equations derived independently by Perrin (237) and Herzog et al (238). Hence, the frictional ratio, F , is obtained ie, the ratio of the frictional resistance of an ellipsoid to that of a sphere of equal volume.

When the diffusant molecule is small, $\beta \rightarrow 0$ and substitution of Equation 5.5 into 5.1. gives:

$$D = \frac{RT}{4\pi\eta N_{AV}} \left(\frac{4\pi N_{AV}}{3v} \right)^{1/3} = \frac{kT}{4\pi\eta} \left(\frac{4\pi N_{AV}}{3v} \right)^{1/3} \quad 5.6$$

where v = molar volume

$$k = \frac{R}{N_{AV}} = \text{Boltzmann's constant.}$$

The molar volume, v , is usually approximated as the partial molar volume in $\text{cm}^3 \text{ mol}^{-1}$, which is a hydrodynamic property of the molecule. Values for the partial molar volume from elements and substituent groups are tabulated by Flynn et al (232). By substituting values for the constants for diffusion in water at 25°C ie, π , η , k and T , we obtain

$$D = \frac{4.92 \times 10^{-5}}{v^{1/3}} \text{ cm}^2 \text{ sec}^{-1} \quad 5.7$$

By a similar treatment of Equation 5.4. and assuming a spherical molecule so that $F = 1$, then the diffusion coefficient in water at 25°C is given by

$$D = \frac{3.28 \times 10^{-5}}{v^{1/3}} \quad \text{cm}^2 \text{ sec}^{-1} \quad 5.8$$

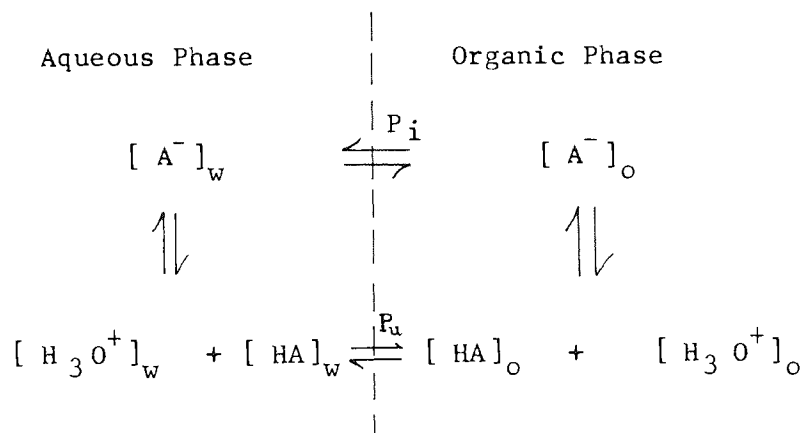
5.2.2 Partition Coefficient

The experimental system employed to obtain diffusion coefficients in Calcium Alginate gels utilised the transfer of Ibuprofen from an aqueous gel phase to n-octanol. In such a system, the partitioning behaviour of the solute is important in determining the rate-controlling mechanism for drug transfer.

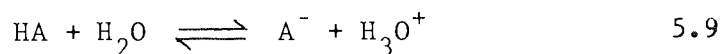
It is well known that the apparent partition coefficient of weakly ionised compounds such as Ibuprofen, varies with pH and ionic strength. However, with a knowledge of the absolute partition coefficient, P_u , of the unionised species between aqueous and organic phases, the apparent partition coefficient, P_{app} , at any particular pH can be calculated. Irwin and Li Wan Po (239) suggested that the partition coefficient of the ionised species, P_i , should also be considered when lower alcohols are used in the partitioning systems. These authors went on to derive a relationship for obtaining P_u and P_i from data of pH, P_{app} and dissociation constant, K_a . The derivation for a weak acid follows similar steps to the original derivation for a weak base (239).

If we consider the scheme given in Figure 5.1., we can obtain expressions for P_u , P_i and P_{app} .

Figure 5.1 Partitioning of a Weak Acid



Subscripts o and w represent the organic and water phases respectively. The dissociation of a weakly acidic compound can be represented by.



and

$$K_a = \frac{[A^-][H_3O^+]}{[HA]} \quad 5.10$$

then

$$P_u = \frac{[HA]_o}{[HA]_w} \quad \text{and} \quad P_i = \frac{[A^-]_o}{[A^-]_w} \quad 5.11, 5.12.$$

Therefore

$$P_{app} = \frac{[A^-]_o + [HA]_o}{[A^-]_w + [HA]_w} \quad 5.13$$

Substituting Equations 5.13. and 5.14. in the numerator of 5.15., we obtain:

$$P_{app} = \frac{P_i[A^-]_w + P_u[HA]_w}{[A^-]_w + [HA]_w} \quad 5.14$$

Substitution of $[A^-]_w$ from Equation 5.12., cancellation of the common factor $[HA]_w$ and rearrangement leads to:

$$P_{app} \left(1 + \frac{K_a}{[H_3O^+]} \right) = P_u + P_i \frac{K_a}{[H_3O^+]} \quad 5.15.$$

Hence, using data for P_{app} against $[H_3O^+]$, a plot of P_{app}

$\left(1 + \frac{K_a}{[H_3O^+]} \right)$ against $\frac{K_a}{[H_3O^+]}$ should yield a straight

line with slope P_i and intercept P_u . If P_i is small, then

P_{app} at any pH can be obtained by putting $P_i = 0$

$$P_{app} = P_u \frac{1}{1 + K_a/[H_3O^+]} \quad 5.16.$$

For diffusion of the drug through the Alginate gel matrix to be the rate controlling step in mass transfer, then P_{app} should be sufficiently high for sink conditions to be maintained.

5.3 Materials and Methods

5.3.1 Diffusion Experiments

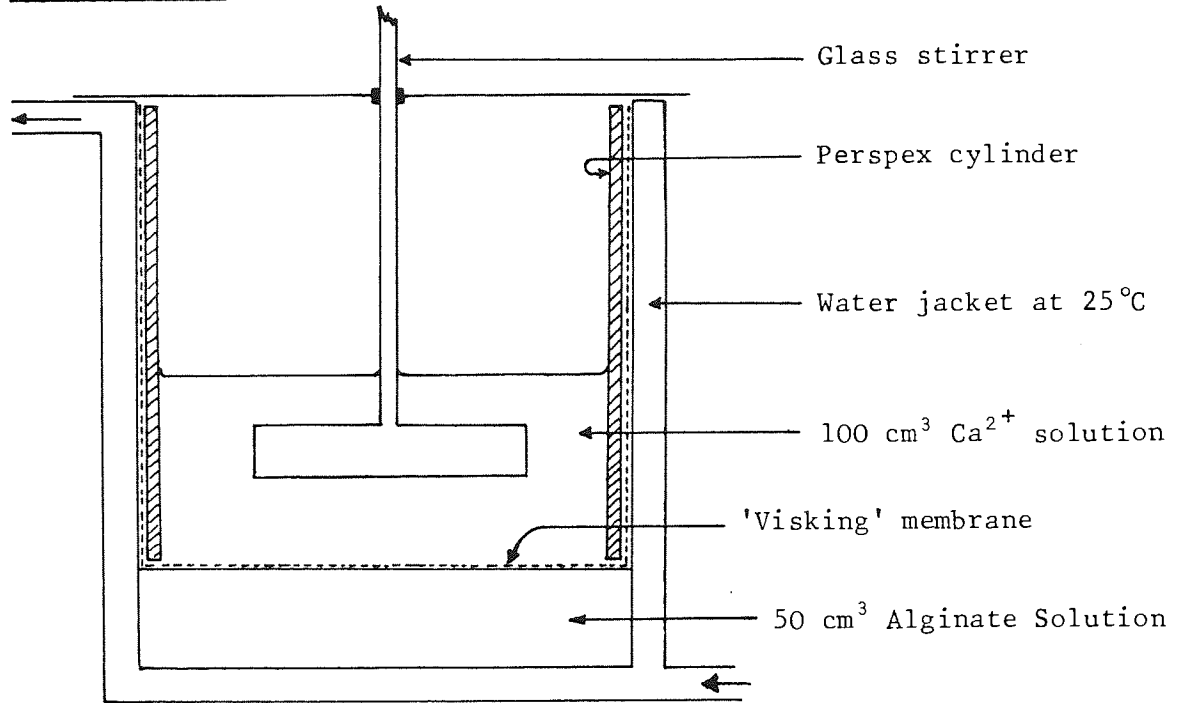
5.3.1.1 Apparatus and Protocol

The apparatus used to monitor the diffusion of Ibuprofen in various concentrations of Calcium Alginate gels is shown schematically in Figure 5.2.. The cell consisted of a jacketted glass beaker of internal diameter 6.6 cm. which allowed thermostatic control at 25° C¹. Initially, 50 cm³ of Borate Buffer B.P. pH 7.5 containing Sodium Alginate² and Ibuprofen 0.5 mg cm⁻³, was poured into the cell. Borate buffer was used as an alternative to the phosphate buffers usually employed at pH 7.5 because the presence of Calcium would cause precipitation. On top of this solution, a layer of dialysis membrane³ was placed by covering one end of a perspex cylinder such that a close fit was achieved with the vessel wall. Stretching the membrane over the end of the cylinder ensured that the surface of the resulting Alginate gel was flat. Any entrapped air, was removed by sliding a fine stainless steel, blunt ended needle between the membrane and the vessel wall, and withdrawing air through a syringe.

1. Churchill Thermocirculator
2. Protanal LFR5/60: same batch as used previously.
3. Visking 10 cm dry dia.tubing.

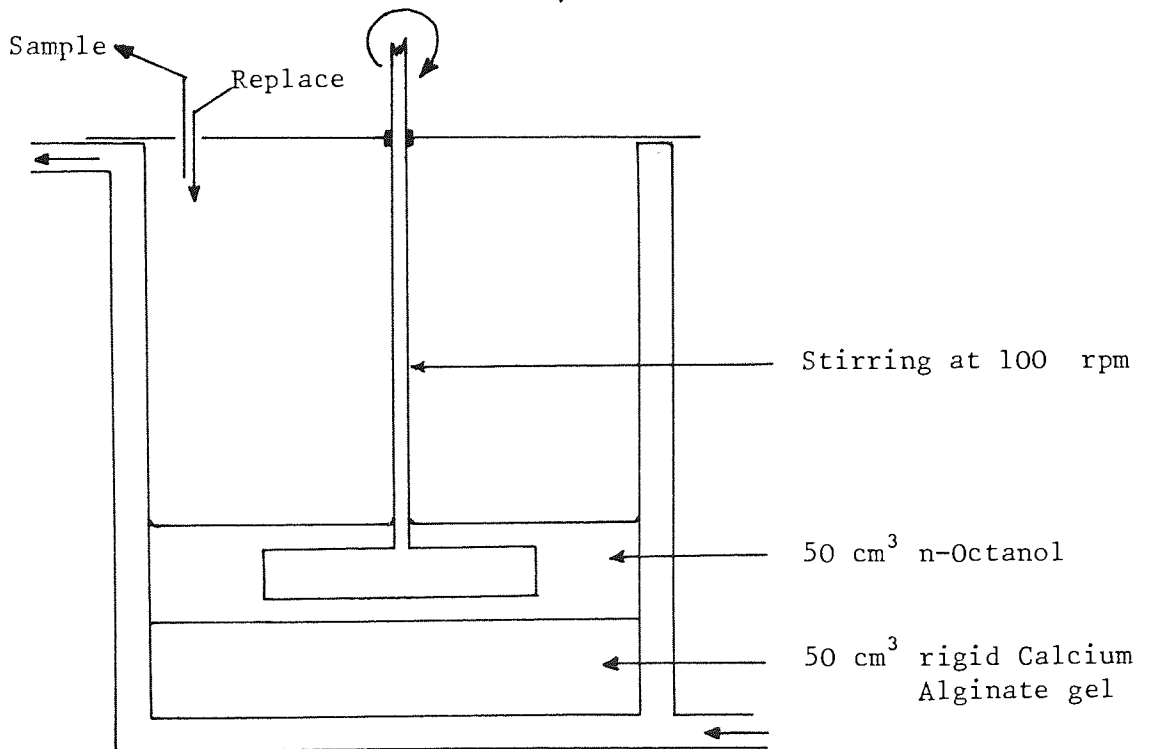
Figure 5.2 APPARATUS FOR THE DETERMINATION OF DIFFUSION COEFFICIENTS OF IBUPROFEN THROUGH ALGINATE GEL.

(a) Dialysis Step



↓
Dialysis 48 hr.

(b) Diffusion Step



Above the membrane and within the cylinder was added 100 cm^3 of Borate buffer containing Ibuprofen 0.5 mg cm^{-3} and a known concentration of calcium chloride¹. Dialysis with stirring of the upper phase was then carried out for 48 hr.

In order to obtain a flat, circular area of membrane in contact with the Alginate solution, it was necessary to force a fraction of the solution up between the vessel wall and the dialysis membrane. On withdrawal of the membrane after 48 hr., this excess Alginate, by then in gel form, was removed; it represented up to about 3% of gel by weight.

After dialysis, the dialysate, perspex cylinder and dialysis membrane were all removed from the cell and replaced by 50 cm^3 of n-octanol². The initial concentration of Ibuprofen in the gel phase was checked by assaying the dialysate and applying mass balance. A solution of Ibuprofen 0.5 mg cm^{-3} which was stirred in the presence of dialysis membrane for seven days at room temperature showed no decrease in the assayed Ibuprofen concentration, therefore there appeared to be no significant interaction. The thickness of each phase, gel and n-octanol was approximately 1.5 cm and the latter phase was stirred at 100 rpm.¹ with a glass paddle stirrer $3.8 \times 1.0 \text{ cm}$. 1 cm^3 samples of the n-octanol phase were removed from a consistent position at various time intervals and replaced by 1 cm^3 of clean n-octanol.

1. $\text{Ca Cl}_2 \cdot 6 \text{ H}_2 \text{ O}$, Laboratory Reagent, BDH
2. Analytical Reagent, Fisons.
3. Citenco variable speed motor.

5.3.1.2 Dialysis Method of Gel Formation

The method by which an Alginate gel is formed may be important in determining its characteristics. Sudden mixing of a calcium ion solution with an Alginate solution will lead to precipitation or at least heterogeneity of gel formation and syneresis (15, 105). This is due to a rapid, localised ie, autocoo-operative binding of Ca^{2+} in certain regions of the Alginate solution where calcium is most concentrated. Hence, the reaction must be slowed down so that there is a gradual supply of Ca^{2+} ions throughout the Alginate solution. This can be achieved by dialysis or chemical means. The latter method will be dealt with in Section 5.3.2.2..

The dialysis method has been extensively used by Smidsrød et al (15, 240) for measuring the rigidity of gels formed using various Alginates and divalent metal ions. They determined the conditions for a state of 'practical equilibrium' of the Alginate gels by measuring rigidity and decrease in gel volume as a function of dialysis time. They therefore determined the time necessary to ensure that dialysis was complete.

To determine the conditions necessary to achieve a 'practical equilibrium' for Calcium Alginate gels in the diffusion cell, the dialysis system may be compared with that of Smidsrød et al. These workers produced gels in a cylinder of height 1.5 cm and internal diameter 1.4 cm. The Alginate solution was contained in the cylinder by sealing at each end with a

dialysis membrane. Dialysis took place in 4 x 50 cm³ of 0.34 M calcium chloride solution. It was found that the gel rigidity increased rapidly but showed no change after 24 hr. dialysis; gel volume decreased rapidly during the first 24 hr., but showed little change in the next 12 days. Therefore, it was assumed that for practical purposes, a state of equilibrium was reached after 48 hr. dialysis.

The time taken to reach 'practical equilibrium' depends on the exposed membrane area, A, the maximum distance that Ca²⁺ ions are required to travel, h_{max}, and the number of Ca²⁺ ions present, N_{Ca}. This assumes that transfer of Ca²⁺ ions to and across the dialysis membrane are not rate-determining. Smidsrød et al used Alginate with an intrinsic viscosity, [η] of 1.24 x 10³ cm³ g⁻¹, in concentrations of up to 5.0 g dl⁻¹. From Section 2.4., Protanal LFR5/60 used in the present study was found to have [η] = 105 cm³ g⁻¹ and for dialysis, concentrations of 0.25 to 5.0 g dl⁻¹ were used.

A low value of h_{max} and [η], and high values of A and N_{Ca} are favourable for a short dialysis time. This can be quantified by using a proportionality constant R' such that

$$t_d = \frac{R' h_{\max} [\eta]}{A N_{\text{Ca}}} \quad 5.17$$

where t_d = dialysis time required to achieve 'practical equilibrium'.

N_{Ca} = molar concentration of Ca²⁺ multiplied by the volume of dialysate.

Assuming that Smidsrød et al (240) changed the 50 cm³ of dialysate four times during the experiment, only 50 cm³ was present at any one time. Substituting $h_{\max} = 0.75$ cm, $A = 2\pi(0.7)^2$ cm², $N_{\text{Ca}} = 0.34 \times 10^{-3} \times 50$ Mol, $t_d = 24$ hr., and $[\eta] = 1.24 \times 10^3$ cm³ g⁻¹, then $R' = 1.35 \times 10^{-3}$ g Mol hr cm⁻².

If corresponding values are substituted for the experimental system detailed in Section 5.3.1.1., then t_d can be determined. Two strengths of Ca²⁺ solution were used: 0.1 M for Alginate concentrations of less than 3.0 g dl⁻¹ and 0.4 M for 3.0 and 5.0 g dl⁻¹ of Sodium Alginate. Hence, $N_{\text{Ca}} = 0.01$ and 0.04 mol respectively. Other quantities are $h_{\max} = 1.5$ cm, $A = \pi(3.3)^2$ cm² and $[\eta] = 105$ cm³ g⁻¹. Therefore, $t_d = 0.6$ and 2.5 hr for $N_{\text{Ca}} = 0.01$ and 0.04 mol respectively. From these results, it was concluded that a dialysis time of 48 hr. was ample to ensure that a 'practical equilibrium' existed.

Because of a possible detrimental effect on the dialysis membrane, the Alginate solution and dialysate were not pre-saturated with n-octanol. This would cause a slight discrepancy between the apparent partition coefficient as calculated from the absolute coefficients, and the apparent partition coefficient found from the asymptote of the experimental drug release profile.

In addition to this, the osmotic effect dictates that water

will tend to pass into the dialysate Ca^{2+} solution from the Alginate phase if the chemical potential, or concentration, of the solvent molecules is greater in the latter than the former.

5.3.1.3 Effect of Stirrer Speed

For the mechanism of drug release from the Alginate gel to be diffusion and not partitioning of the Ibuprofen into the n-octanol phase, then mass transfer should be independent of the stirrer speed with 0.1 M Ca^{2+} being dialysed against a 1.0 g dl^{-1} solution of Sodium Alginate. Five experiments using a stirrer speed of 100 rpm were compared with corresponding experiments using 50 and 150 rpm stirrer speeds.

5.3.1.4 Concentration Gradient within the Gel

Since the Ibuprofen is in solution in the gel phase, then transfer into the n-octanol phase is rate-limited either by diffusion through the gel or partitioning between the aqueous and organic phases. To discern which is the dominating mechanism, duplicate experiments were carried out using the regimen given in Section 5.3.1.1. The initial Sodium Alginate concentrations used were 1.0 and 5.0 g dl^{-1} dialysed against 0.1 and 0.4 M Ca^{2+} respectively. After a time corresponding to about 50% of drug transfer, each gel was removed and sliced laterally, using a sharp blade, into five approximately equal 0.3 cm fractions. Particular care was necessary because of the brittle nature of the gel. Each slice was weighed, then

the Ibuprofen extracted with excess 0.5 M HCl and 5 cm³ of n-octanol. The n-octanol phase was then assayed, using the HPLC method detailed in Section 5.3.4.

5.3.2 Rheological Experiments

5.3.2.1 The Use of Oscillatory Rheometry.

In Section 2.2.3., the principles of each of the three major methods of rheological testing, namely continuous shear, creep and oscillatory testing, were considered. The continuous shear method does not lend itself to the measurement of elastic solids such as Alginate gels. This is not only because the data produced in the form of a shear stress - shear rate curve cannot be interpreted in terms of elasticity, but also because the gel is liable to fracture when subject to high shear rates.

The method of creep testing was used by Mitchell and Blanchard (105) with a parallel plate viscometer designed by Sharma and Sherman (241). The creep compliance - time response was fitted by a mechanical model with a Maxwell element in series with two or three Voigt elements.

Nevertheless, the use of low amplitude oscillatory shear testing is particularly suited to samples of a brittle nature since the net deformation during testing is negligible.

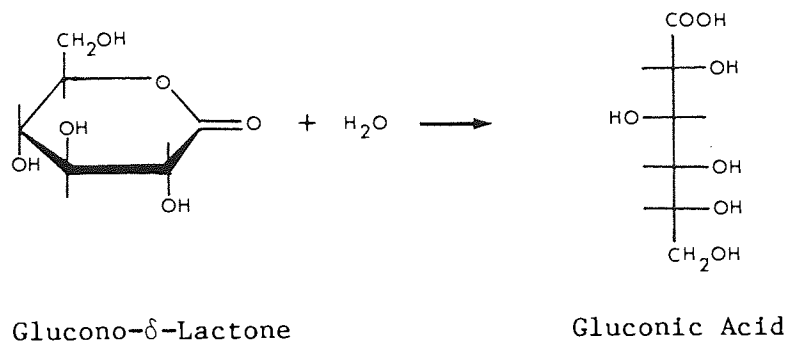
Apart from a brief investigation into the application of the theory of ideal rubber-like elasticity (242) to Alginate gel

systems (243) results from the oscillatory shear testing of Alginate gels have not been published. In the present study, parallel plate geometry was used to quantify the rigidity of Calcium Alginate gels containing 0.25 to 5.0 g dl⁻¹ of Alginate (calculated as the sodium salt) and 0.01 to 0.1 M Ca²⁺. The experimental regimen using the Weissenberg Rheogoniometer was the same as that detailed in Section 2.3.5.. The input amplitude of the lower platen was 2.8 x 10⁻³ rad.

5.3.2.2 Chemical Method of Gel Formation

In Section 5.3.1.2, it was pointed out that a gradual supply of Ca²⁺ is necessary in the Alginate solution if a homogeneous Calcium Alginate gel is to be formed. As an alternative to dialysis, Mitchell and Blanchard (104) first employed Glucono- δ -lactose, GDL, to form Alginate gels in a matter of minutes instead of days. In aqueous solution, GDL is gradually hydrolysed to gluconic acid, see Figure 5.3.. A freshly prepared 1.0 g dl⁻¹ solution has a pH of 3.6 which falls to 2.5 within 2 hr. (244).

Figure 5.3 The Hydrolysis of Glucono- δ -Lactone in Water



When preparing samples of Calcium Alginate for rheological testing, the dialysis method was inappropriate due to manipulative difficulties in preparing a gel of the appropriate dimensions. To overcome this problem, the GDL method was used as follows. A freshly prepared solution of GDL was added to a dispersion of Calcium Hydrogen Phosphate, CaHPO_4 , in Sodium Alginate solution, the volume ratio of the former to the latter being 1:3. Stirring with a magnetic follower ensured rapid mixing and gelling usually took place within 2 min.

Samples for rheogoniometry were prepared by pouring the mixture prior to gelling, into polyethylene petri dishes. After gelation, circular gels of exactly 7.5 cm diameter were cut using a bladed tin template. This ensured that each sample exactly fitted between the rheogoniometer parallel plates. The thickness of the gel sample was not critical in parallel plate geometry since this is taken into account in the calculation of G' , see Equation 2.25..

To determine their effect on gelation, the pH of the resulting gels was measured for various concentrations of ingredients GDL, and Alginate.

Since the GDL causes gel formation by lowering the pH to allow calcium salt dissolution, the resultant gel may be dependent on the presence of H^+ ions as well as the Na^+ replacement by Ca^{2+} ions. This would be likely to occur close to the

pKa of the Alginic acid. The method of Haug (245) was used to determine the overall pKa of Alginic acid from Protonal LFR5/60 Sodium Alginate. Mannuronic and guluronic acids have pKa's of 3.38 and 3.65 respectively (1), therefore one may expect the Alginic acid copolymer to possess an overall pKa somewhere between these two values. Haug used a modified form of the Henderson-Hasselbach Equation as follows:

$$\text{pH} = \text{pKa} + n \log \left[\frac{\alpha}{1 - \alpha} \right] \quad 5.18$$

where α = degree of neutralisation

$$n = \text{activity correction} = \left\{ \frac{f_{\text{H}_3\text{O}^+} f_{\text{A}^+}}{f_{\text{HA}}} \right\} \quad 5.19$$

Alginic acid was prepared by precipitation with excess 0.5 M HCl in a 12.0 g dl⁻¹ solution of Sodium Alginate and stirring for 8 hr. The precipitate was rinsed thoroughly with distilled water and dried at 50 ° C for 48 hr. A range of volumes of 0.1 M NaOH and 0.1 M NaCl (the latter to ensure constant ionic strength) were added to 20 cm³ aliquots containing exactly 0.1 g of Alginic acid thereby giving 0.0258 molar Alginate based on an equivalent weight of 194 g mol⁻¹. After addition of the alkali, the samples were placed in a shaking water bath at 25 ° C for 6 hr. and their pH values were determined.

5.3.3 Partition Coefficient of Ibuprofen

The derivation of Equation 5.15. by Irwin and Li Wan Po (206) for the determination of the partition coefficients

of ionised and unionised species was given in Section 5.2.2.. The experimental determination of P_{app} for Ibuprofen was carried out as follows. Eight solutions of Ibuprofen 0.5 mg cm^{-3} in Kolthoff's buffer (246) were used in the pH range 8.02 to 9.19, with the ionic strength adjusted to 1.5 using KCl. Distilled water that had been pre-saturated at 25°C with n-octanol was used to make these solutions and duplicates were prepared of each sample. 20 cm^3 of aqueous phase was added to 5 cm^3 of n-octanol that had been pre-saturated with water. To avoid emulsification, the specimen tubes were inverted gently several times and placed in a slowly shaking water bath at 25°C for 13 days.

At the end of this time, the concentration of Ibuprofen in the aqueous and organic phases was measured using the HPLC method described in Section 5.3.4., from which P_{app} could be calculated.

5.3.4 HPLC Assay of Ibuprofen

The method used to assay Ibuprofen in n-octanol was based on the work of Dusci and Hackett (247) who used a reversed-phase High Performance Liquid Chromatographic, HPLC, system. Acetonitrile, CH_3CN with water mobile phases were used to separate seven anti-inflammatory drugs in serum. Ibuprofen eluted at 5.4 min when 35% CH_3CN in 0.7% aqueous ammonium chloride solution adjusted to pH 7.8 was used as the mobile phase. The flow rate was $1.0 \text{ cm}^3 \text{ min}^{-1}$ using a $30 \text{ cm} \times 0.39 \text{ cm}$ I.D. Column packed with $\mu\text{Bondapak C}_{18}$.

In another mobile phase system, 60% CH₃CN, 45 mM KH₂PO₄ adjusted to pH 3.0 was used with a flow rate of 0.8 cm³ min⁻¹. Ibuprofen was eluted at 8.6 min.

Ali et al (248) used a similar column to that of Dusci and Hackett, and found that a mobile phase of 55% CH₃CN in 0.1M acetic acid pumped at 1.0 cm³ min⁻¹ gave a retention time for Ibuprofen assayed in plasma, of 8.5 min.

In the present study, using a 25 cm x 0.4 cm. I.D. column containing 10 μm C₁₈ bonded Partisil ODS-2¹, a suitable mobile phase was found to be 72% CH₃CN² in distilled water adjusted to pH 3.0 with phosphoric acid. The mobile phase flow rate was 1.0 cm³ min⁻¹.³ The octanolic drug solution was diluted 1:1 with methanol⁴ containing 20 μg cm⁻³ of benzoic acid⁵ as internal standard. The sample was injected into the column via a 20 μl injector loop⁶ and the eluted compounds were detected by UV at 225 nm⁷. Calibration lines of six samples in the appropriate concentration range were performed on each occasion of use.

1. Whatman, Maidstone, UK.
2. Acetonitrile, HPLC grade, Fisons
3. Altec 100A Pump, Anachem, Luton, U.K.
4. Methanol, HPLC grade, Fisons
5. Analytical Reagent grade, BDH, Poole, UK.
6. Rheodyne, Berkeley, California, USA.
7. Pye Unicam LC3 Detector, Cambridge, UK.

Figure 5.4. shows a typical trace of the resultant chromatogram. The retention times were 1.3, 3.6 and 5.1 min for benzoic acid, Ibuprofen and n-octanol respectively. Analytical reagent grade of n-octanol was employed since the use of a spectroscopic grade did not significantly reduce the size of the broad peak due to n-octanol which eluted after Ibuprofen.

The methanol: water mobile phases used by Pitre and Grandi (249) and Thomas et al (250) produced very broad peaks using the above equipment despite variation in the methanol: water ratios.

The use of the above system with 72% CH_3CN at pH 3.0 for the mobile phase provided a significant reduction in retention times compared to previous methods.

Figure 5.4

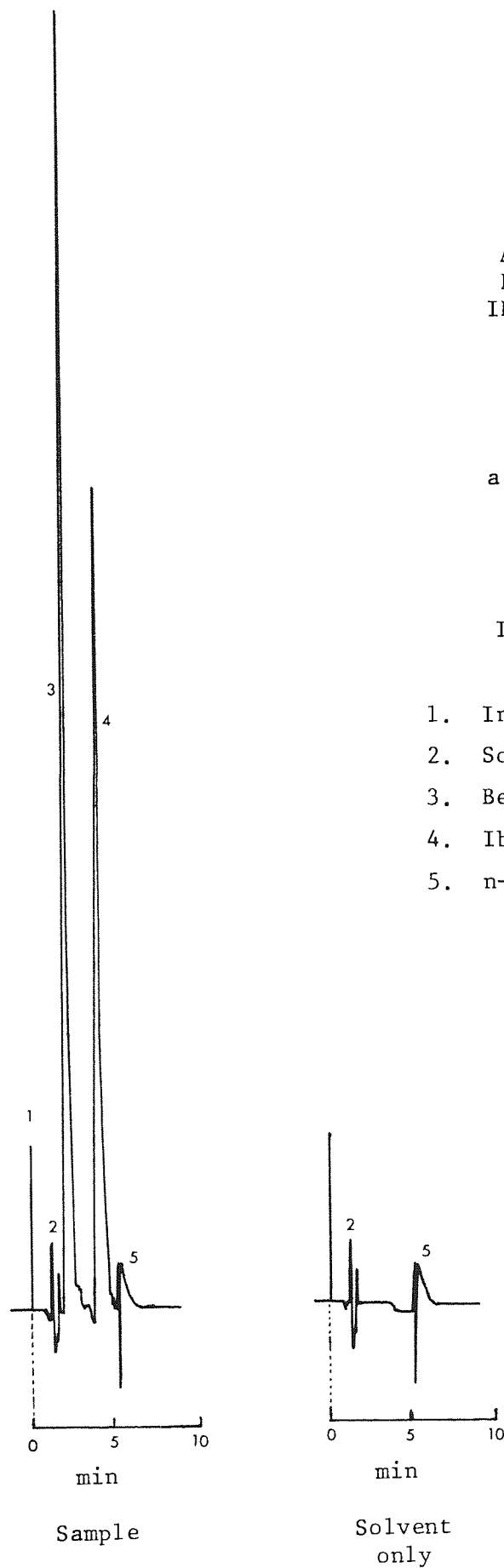
A TYPICAL HPLC TRACE
FOR IBUPROFEN ASSAY
IN N-OCTANOL: METHANOL,
1:1.

a.u.f.s. = 0.16

$\lambda = 225 \text{ nm}$

Injection volume $20 \mu\text{l}$

1. Injection
2. Solvent front
3. Benzoic acid $30 \mu\text{g cm}^{-3}$
4. Ibuprofen $50 \mu\text{g cm}^{-3}$
5. n-Octanol



5.4 Results

5.4.1 Partition Coefficient of Ibuprofen

Using the method given in Section 5.3.3., values of P_{app} for Ibuprofen as a function of pH were obtained. This data was transformed according to Equation 5.17.. The results are listed in Table 5.1.. The value of the pKa of Ibuprofen at 25 ° C used was 4.45 (251) which is in good agreement with a value of 4.5 quoted elsewhere (252). The plot of $P_{app} (1 + K_a / [H_3 O^+])$ as ordinate against $(K_a / [H_3 O^+])$ shows good linearity, see Figure 5.5.. The least mean square linear correlation coefficient was 0.996; the slope, $P_i = 0.476$ and the intercept, $P_u = 9.07 \times 10^3$. From Equation 5.17., P_{app} at pH 7.5, the pH of the buffered Calcium Alginate gel in diffusion experiments, was calculated to be 8.55. However, after the dialysis step, the pH of a 5.0 g dl⁻¹ Alginate gel (calculated as the sodium salt), was found to be as high as 7.85, which corresponds to $P_{app} = 4.1$. The high pH was probably due to the presence of Alginate, although measurement of the pH of a rigid gel is prone to inaccuracies because of poor mixing and poor contact with the electrode. The deviation from pH 7.5 was less significant for lower Alginate concentrations.

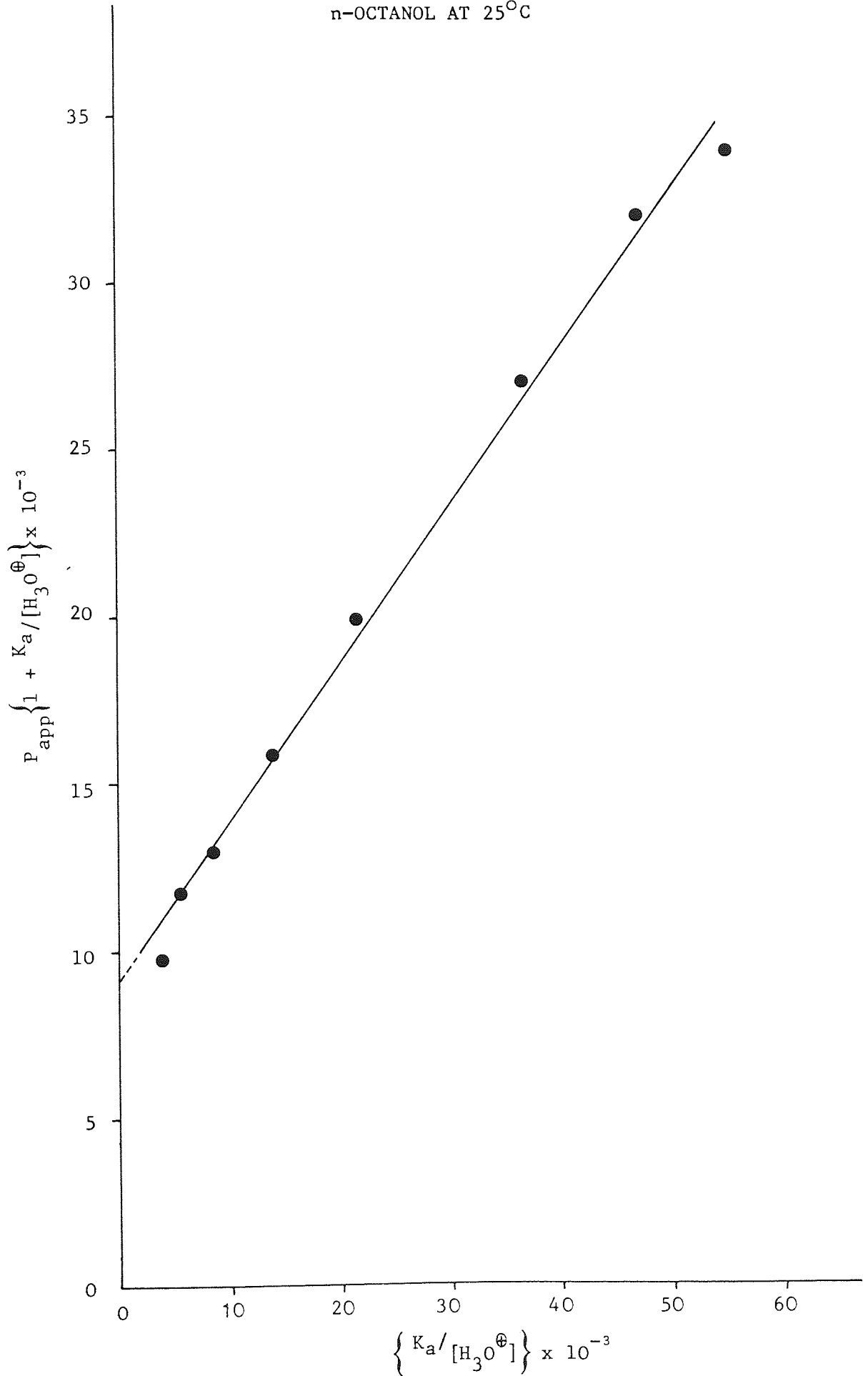
When diffusion experiments using a 5.0 g dl⁻¹ Alginate gel were carried out to completion, ie, the concentration of Ibuprofen in n-octanol became asymptotic with time, then values of $P_{app} \approx 4.0$ were found, see also Section 5.4.2.3.. This result was consistent with a gel pH of approximately 7.9.

Table 5.1. Results for the Determination of the Ionised and Unionised Partition Coefficients of Ibuprofen.

pH	Mean Concentrations ($\mu\text{g cm}^{-3}$)		Assay as % of theoretical concentration	P_{app}	$\frac{K_a}{[\text{H}_3\text{O}^+]} \times 10^{-3}$	$P_{\text{app}} \left\{ 1 + \frac{K_a}{[\text{H}_3\text{O}^+]} \right\} \times 10$
	Aqueous Phase	n-Octanol Phase				
8.02	290.5	706.0	96	2.602	3.715	9.671
8.18	382.8	734.5	103	2.207	5.370	11.85
8.38	362.3	553.2	100	1.527	8.511	12.99
8.59	412.9	475.2	106	1.151	13.80	15.89
8.78	399.6	373.5	99	0.935	21.38	19.99
9.01	440.9	328.8	105	0.746	36.31	27.08
9.12	441.0	302.5	103	0.686	46.77	32.08
9.19	443.2	273.0	102	0.616	54.95	33.85

Figure 5.5.

DETERMINATION OF THE IONISED AND UNIONISED
PARTITION COEFFICIENTS OF IBUPROFEN IN WATER/
n-OCTANOL AT 25°C



5.4.2 Diffusion Experiments

5.4.2.1 Effect of Stirrer Speed

Using the protocol outlined in Sections 5.3.1.1 and 5.3.1.3, five experiments were carried out with a stirrer speed of 100 rpm. To compare the rate of drug release at different stirrer speeds by a consistent method, data for less than 50% released was applied to the square root approximation, Equation 4.4., by plotting the amount transferred per unit area at time t , ie Q , against $t^{\frac{1}{2}}$. From the slope, K , values of the diffusion coefficient were obtained using the equation:

$$D = \frac{\pi}{4} \left(\frac{K}{C_0} \right)^2 \quad 5.20.$$

At 100 rpm, $D = 5.11 \pm 0.54 \times 10^{-6} \text{ cm}^2 \text{ sec}^{-1}$ (mean \pm 95% confidence limits) whereas at 50 rpm, $D = 3.13 \times 10^{-6} \text{ cm}^2 \text{ sec}^{-1}$. Hence, D at 50 rpm is significantly less than D at 100 rpm ($P > 0.999$).

Using a stirrer speed of 150 rpm, $D = 5.01 \times 10^{-6} \text{ cm}^2 \text{ sec}^{-1}$ was obtained; this was not significantly different from D for 100 rpm stirrer speed. These results suggest that mass transfer was partition-controlled at 50 rpm but not at 100 or 150 rpm stirrer speeds. Subsequently, the 100 rpm speed was used in all experiments.

5.4.2.2 Concentration Gradient Within the Gel.

Using the protocol detailed in Sections 5.3.1.1 and 5.3.1.4, it was possible to obtain values for the concentration of Ibuprofen in the gel as a function of the distance from the interface with the n-octanol. The results are listed in Tables 5.2. (a) and (b). The figures show that a significant concentration gradient existed in the gel which suggests that diffusion was the rate-controlling mechanism of drug release.

Unfortunately, due to the brittle nature of the gel, it was not possible to obtain a sufficient number of values of concentration as a function of distance in the gel, to apply the relationship for unsteady state diffusion, ie, Equation 4.28.. However, bearing in mind the findings of the numerical analysis of Section 4, it is possible to apply correctly the square-root-time approximation, Equation 4.4., to describe drug release data for less than 50% release.

Table 5.2. The Concentration of Ibuprofen in the Gel Phase as a function of the Distance from the Interface.

(a) Gel Containing 1.0 g dl⁻¹ Alginate

Mean Distance from Interface (cm)	Weight of Gel Sample (g)		Extracted Concentration ($\mu\text{g cm}^{-3}$)		Concentration of Ibuprofen in Gel Fraction ($\mu\text{g cm}^{-3}$)		
	1	2	1	2	1	2	Mean
0.15	5.052	2.007	58.2	63.5	57.6	63.3	60.4
0.45	5.210	1.748	102.8	114.9	98.7	131.5	115.1
0.75	4.448	1.745	122.5	165.4	137.7	189.6	163.6
1.05	3.391	1.945	110.3	212.5	162.6	218.5	190.6
1.35	3.975	2.300	122.3	252.8	153.9	219.8	186.8

(b) Gel Containing 5.0 g dl⁻¹ Alginate

Mean Distance from Interface (cm)	Weight of Gel Sample (g)		Extracted Concentration ($\mu\text{g cm}^{-3}$)		Concentration of Ibuprofen in Gel Fraction ($\mu\text{g cm}^{-3}$)		
	1	2	1	2	1	2	Mean
0.15	6.011	2.212	83.3	51.4	69.3	46.5	57.9
0.45	6.199	1.882	84.1	80.3	67.9	85.8	76.5
0.75	6.774	1.956	155.6	151.0	134.8	154.4	144.6
1.05	6.196	3.025	221.5	263.1	178.7	173.9	176.3
1.35	6.538	2.575	264.5	258.6	202.3	200.8	201.6

5.4.2.3 Drug Release Profiles

A range of concentrations of Sodium Alginate from 0.25 to 5.0 g dl⁻¹ was used to obtain Calcium Alginate gels by dialysis. The concentration of Ibuprofen released from the gel into the n-octanol phase was monitored with time. After correction for solute loss due to sampling, values for the amount released were divided by the interfacial area, A, to obtain Q, the amount released per unit area. The collective results for those diffusion experiments are given in Tables 5.3. to 5.7. for 0.25, 0.50, 1.0, 3.0 and 5.0 g dl⁻¹ Alginate gels respectively.

Since the initial concentration of Ibuprofen in the gel, ie, C₀, is squared in Equation 5.22. its determination needs to be accurate to obtain realistic values of D. After dialysis, the volume and Ibuprofen concentration of the dialysate was determined and by mass balance, the concentration in the gel was calculated. The mean value of C₀ for all 20 experiments quoted was 492.1 μg cm⁻³ with a standard error of 3.6% and 95% confidence limits of ± 8.2 μg cm⁻³. Hence, the initial concentration in the Alginate gel was not significantly different from the value of 500 μg cm⁻³ expected.

A specimen drug release profile is given in Figure 5.6. where the concentration of Ibuprofen in n-octanol is followed to equilibrium. The Alginate concentration 50 g dl⁻¹. The curve appears to become asymptotic after

Table 5.3 Experimental Data for the Diffusion of Ibuprofen
in 0.25 g dl⁻¹ Alginate Gels.

Time (Min)	Amount Released per Unit Area ($\mu\text{g cm}^{-2}$)			
	1	2	3	4
10	-	-	39.41	40.41
15	41.87	38.50	-	-
20	-	-	55.14	62.76
30	61.80	53.97	66.37	70.96
45	75.76	74.94	78.41	74.45
60	86.10	83.86	89.76	93.12
90	104.7	102.9	108.2	108.1
120	120.2	117.0	121.9	124.1
150	121.1	112.7	130.8	130.1
180	141.1	136.7	143.8	139.7
210	-	-	150.5	147.6
270	-	-	166.8	170.5
300	183.4	179.2	-	-
360	194.7	199.2	191.4	191.1
420	207.8	206.4	202.7	200.8
450	218.8	221.7	216.9	215.1
540	227.4	225.0	230.5	222.4
600	235.7	233.4	238.7	234.8
Interfacial Area, A (cm^2)	33.9	33.9	33.9	33.9
C_0 ($\mu\text{g cm}^{-3}$) *	505.7	505.7	487.5	491.4

* C_0 = Concentration of Ibuprofen in the gel phase at time zero.

Table 5.4 Experimental Data for Diffusion of Ibuprofen in
0.50 g dl⁻¹ Alginate Gels.

Time (Min)	Amount Released per Unit Area ($\mu\text{g cm}^{-2}$)	
	1	2
15	39.62	38.51
30	56.90	52.68
45	69.32	66.68
60	82.14	77.27
90	96.77	94.90
120	113.7	109.6
210	145.9	159.3
250	155.3	162.5
310	170.7	172.6
360	182.7	184.8
420	194.4	195.3
480	199.1	-
540	213.2	210.8
600	214.5	221.6
Interfacial Area, A (cm ⁻²)	33.9	33.9
C ₀ ($\mu\text{g cm}^{-3}$) *	464.7	472.1

* C₀ = Concentration of Ibuprofen in the gel phase at time zero.

Table 5.5 Experimental Data for Diffusion of Ibuprofen in 1.0 g dl⁻¹ Alginate Gels.

Time (min)	Amount Released per Unit Area ($\mu\text{g cm}^{-2}$)					
	1	2	3	4	5	6 †
15	40.23	38.88	41.43	47.46	47.72	37.69
30	56.49	50.73	57.60	64.39	66.23	54.33
45	66.40	61.87	68.71	82.94	70.67	61.78
60	77.37	69.65	78.16	91.26	84.62	76.17
90	95.67	81.67	93.57	103.3	102.0	91.58
120	110.5	104.8	106.8	-	115.1	106.6
150	120.9	-	118.3	123.2	126.4	-
180	136.6	124.6	128.9	143.9	138.5	133.9
240	159.7	136.9	157.8	161.8	158.0	164.6
300	175.9	160.3	177.5	180.5	181.2	177.4
360	201.1	172.1	188.9	-	199.5	189.4
420	216.2	183.9	199.4	192.0	217.4	191.2
480	224.0	191.5	-	202.8	235.6	210.1
540	-	204.6	222.6	222.6	-	216.0
600	-	215.1	231.5	243.8	255.8	224.3
Interfacial Area, A (cm^{-2})	34.2	34.2	34.2	34.2	34.2	34.2
C_0 ($\mu\text{g cm}^{-3}$)*	507.0	461.2	481.3	465.5	501.4	478.9

† Experiment conducted using 150 rpm stirrer speed, see Section 5.4.2.1..

* C_0 = Concentration of Ibuprofen in the gel phase at time zero.

Table 5.6. Experimental Data for Diffusion of Ibuprofen in 3.0 g dl⁻¹ Alginate Gels.

Time (Min)	Amount Released per Unit Area ($\mu\text{g cm}^{-2}$)			
	1	2	3	4
16	42.67	38.54	28.53	35.30
30	50.65	56.66	43.53	48.17
45	58.49	69.42	60.54	61.89
60	70.34	80.26	63.72	71.97
90	86.53	89.27	77.21	85.91
120	97.68	101.7	91.55	103.5
150	114.1	114.9	99.39	112.1
180	122.8	127.8	-	-
215	-	-	121.0	134.5
245	142.6	152.9	-	-
300	161.2	164.7	-	-
335	-	-	154.0	179.0
360	170.4	179.4	161.7	186.4
420	192.3	196.1	173.5	199.1
480	194.9	202.7	190.9	207.3
540	202.2	210.0	200.7	211.2
600	218.0	-	210.1	220.3
Interfacial Area, A (cm ⁻²)	33.9	33.9	34.7	34.3
C ₀ ($\mu\text{g cm}^{-3}$)*	502.2	503.1	495.9	485.1

* C₀ = Concentration of Ibuprofen in the gel phase at time zero.

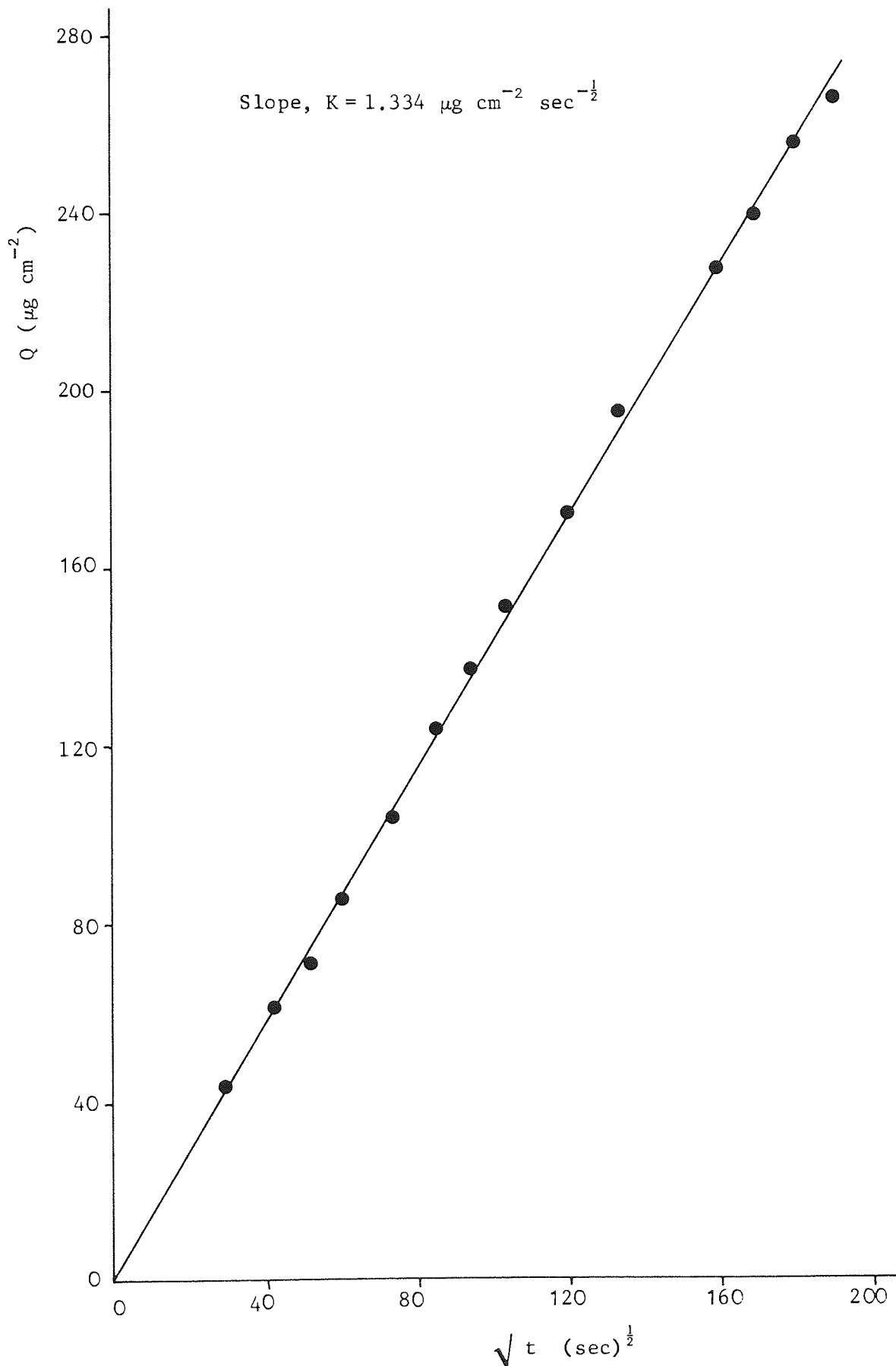
Table 5.7. Experimental Data for Diffusion of Ibuprofen in
5.0 g dl⁻¹ Alginate Gels.

Time (min)	Amount Released per Unit Area ($\mu\text{g cm}^{-3}$)			
	1	2	3	4
10	-	-	29.66	23.24
15	45.15	43.04	-	-
20	-	-	46.25	35.79
30	60.91	61.70	56.88	44.67
45	74.63	71.30	69.56	57.63
60	83.11	85.83	86.42	68.79
90	102.4	103.8	100.2	85.84
120	122.3	124.5	115.1	98.79
150	129.6	137.7	127.3	109.5
180	141.0	151.9	138.5	122.4
210	-	-	151.1	132.7
240	165.3	172.9	-	-
270	-	-	164.1	153.2
300	180.9	195.8	-	-
360	-	-	186.0	182.3
420	214.7	228.1	202.5	201.2
480	233.4	239.8	215.0	210.4
540	245.9	255.7	229.5	224.4
600	252.3	266.8	237.3	226.4
Interfacial Area, A(cm^{-2})	34.3	34.7	34.3	34.7
C_0^* ($\mu\text{g cm}^{-3}$)	491.2	498.1	518.4	524.2

* C_0 = Concentration of Ibuprofen in the gel phase at time zero.

Figure 5.7

THE AMOUNT RELEASED PER UNIT AREA, Q
PLOTTED AGAINST $(\text{TIME})^{1/2}$ FOR DIFFUSION
IN A 5.0 g dl^{-1} ALGINATE GEL.



approximately 80 hr. at a concentration of approximately
400 $\mu\text{g cm}^{-3}$. 50% drug release took place within 14 hr.

A sample plot of Q against $t^{\frac{1}{2}}$ is given in Figure 5.7. for
Ibuprofen diffusion from a 5.0 g dl^{-1} Alginate gel, which shows
good linearity. The collective data for all such plots with least
mean square linear regression analyses, is given in Table 5.8..
The diffusion coefficients obtained are summarized with 95%
confidence limits, in Table 5.9.. It is clear from these results
that the increasing concentration of Alginate did not significantly
reduce the diffusion coefficient of Ibuprofen. This suggests that
the microscopic viscosity in the gel was unaffected by increasing
Alginate content and that the increasing number of polymer chains
and cross-links was insufficient to cause mechanical blocking of
the diffusant. This will be discussed further in Section 5.5..

Figure 5.6. Drug Release Profile for the Diffusion of Ibuprofen from a 5.0 g dl⁻¹ Alginate Gel to a n-Octanol Sink.

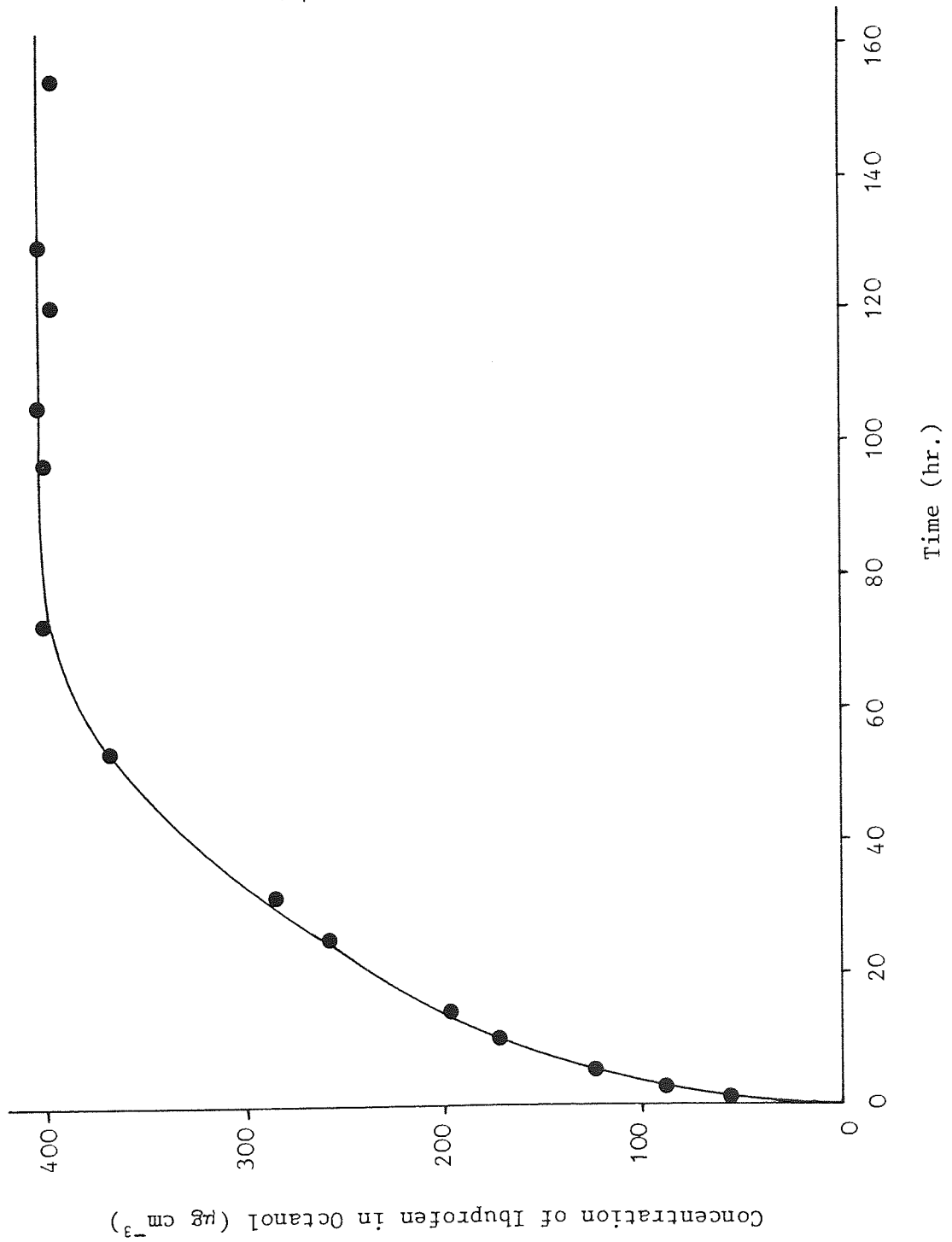


Table 5.8 Results of Linear Least Mean Square Regression
 Analysis of Data for the Amount of Ibuprofen
 Released per Unit Area, Q, against $(\text{Time})^{1/2}$.

Alginate Concentration (g dl ⁻¹)	Correlation Coefficient	Slope, K ($\mu\text{g cm}^{-2}$ $\text{sec}^{-1/2}$)	Intercept ($\mu\text{g cm}^{-2}$)	Diffusion Coefficient, D ($\text{cm}^2 \text{sec}^{-1}$) x 10 ⁶
0.25	0.9977	1.218	12.14	4.556
	0.9968	1.241	7.84	4.731
	0.9980	1.218	12.47	4.660
	0.9982	1.129	23.05	4.002
0.5	0.9961	1.119	13.51	4.556
	0.9916	1.175	8.73	4.849
1.0	0.9989	1.356	-3.31	5.618
	0.9986	1.122	4.39	4.650
	0.9982	1.222	5.21	5.063
	0.9951	1.143	19.12	4.736
	0.9986	1.326	4.40	5.493
	0.9946	1.210	4.61	5.013
3.0	0.9981	1.138	3.70	4.032
	0.9981	1.166	6.40	4.220
	0.9970	1.221	-1.56	4.759
	0.9991	1.132	-4.69	4.277
5.0	0.9986	1.243	6.24	5.026
	0.9990	1.274	-7.46	5.135
	0.9995	1.334	3.92	5.201
	0.9996	1.419	1.29	5.798

Table 5.9 Summary of Results for the Diffusion of Ibuprofen
in Calcium Alginate Gels.

Alginate Concentration (g dl ⁻¹).	Mean Diffusion Coefficient (cm ² sec ⁻¹) x 10 ⁶	95% Confidence Limits	Number of Experiments
0.25	4.487	<u>+</u> 0.412	4
0.5	4.703	-	2
1.0	5.096	<u>+</u> 0.411	6
3.0	4.322	<u>+</u> 0.492	4
5.0	5.280	<u>+</u> 0.520	4

5.4.3 Rheological Experiments

5.4.3.1 Effect of Glucono- δ -Lactone and Alginate Concentrations on Calcium Alginate Gels.

The chemical method of gel formation using Glucono- δ -Lactone, GDL, was examined according to the method given in Section 5.3.2.2.. The results for the effects of GDL and Alginate concentration on Calcium Alginate gels are given in Tables 5.10. and 5.11. respectively. It appeared that a concentration of 2.0 g dl^{-1} GDL was the maximum that would bring about gelation, therefore the pH needed to fall below 4.7 before gelation took place. If gelation occurred after the arbitrary 2 min., then the resulting gel was usually incompletely formed.

In the presence of low concentrations of Ca^{2+} ions, the resulting gels were weak, ie, the available sites for cross-linking were not saturated. The data is summarized in Figure 5.8. where it appears that Ca^{2+} Alginate has a relatively small effect on pH compared to GDL.

The dissociation constant for Alginic acid prepared from Sodium Alginate was determined according to the method give in Section 5.3.2.2.. The results for the pH at a function of the degree of neutralisation, α , are given in Table 5.12.. The value of $\alpha = 1.0$ was calculated by considering one carboxylic acid moiety per monomeric unit with an equivalent weight of 194 g mol^{-1} . According to the modified Henderson-Hasselbach Equation, see Equation 5.20., pH was plotted against $\log(\alpha/1-\alpha)$. The slope ie, $n = 0.86$ was then used to obtain a plot of pH against

Table 5.10 The Effect of Glucono- δ -Lactone Concentration on pH and Gelation of Calcium Alginate Gels.
 Ca^{2+} = 50 mM ; Alginate = 3.0 g dl⁻¹ .

Concentration of Glucono- δ -Lactose (g dl ⁻¹)	pH	Gelation < 2 min
0.4	7.10	-
0.8	6.40	-
1.2	5.55	-
1.6	4.70	-
2.0	4.25	+
2.4	3.83	+
2.8	3.68	+
3.2	3.50	+
3.6	3.38	+
4.0	3.27	+

Table 5.11 The Effect of Alginate Concentration on pH and Gelation of Calcium Alginate Gels.
 Ca^{2+} = 50 mM ; Glucono- δ -Lactone = 2.0 g dl⁻¹ .

Concentration of Alginate (g dl ⁻¹)	pH	Gelation < 2 min
0.59	3.13	+
1.01	3.30	+
2.10	3.50	+
3.05	3.74	+
4.22	3.94	+
4.96	4.07	+
6.06	4.23	+

Figure 5.8. The Effect of the Concentrations of Glucono- δ -Lactone, ●, and Alginate, ○, on the pH of Calcium Alginate Gels.

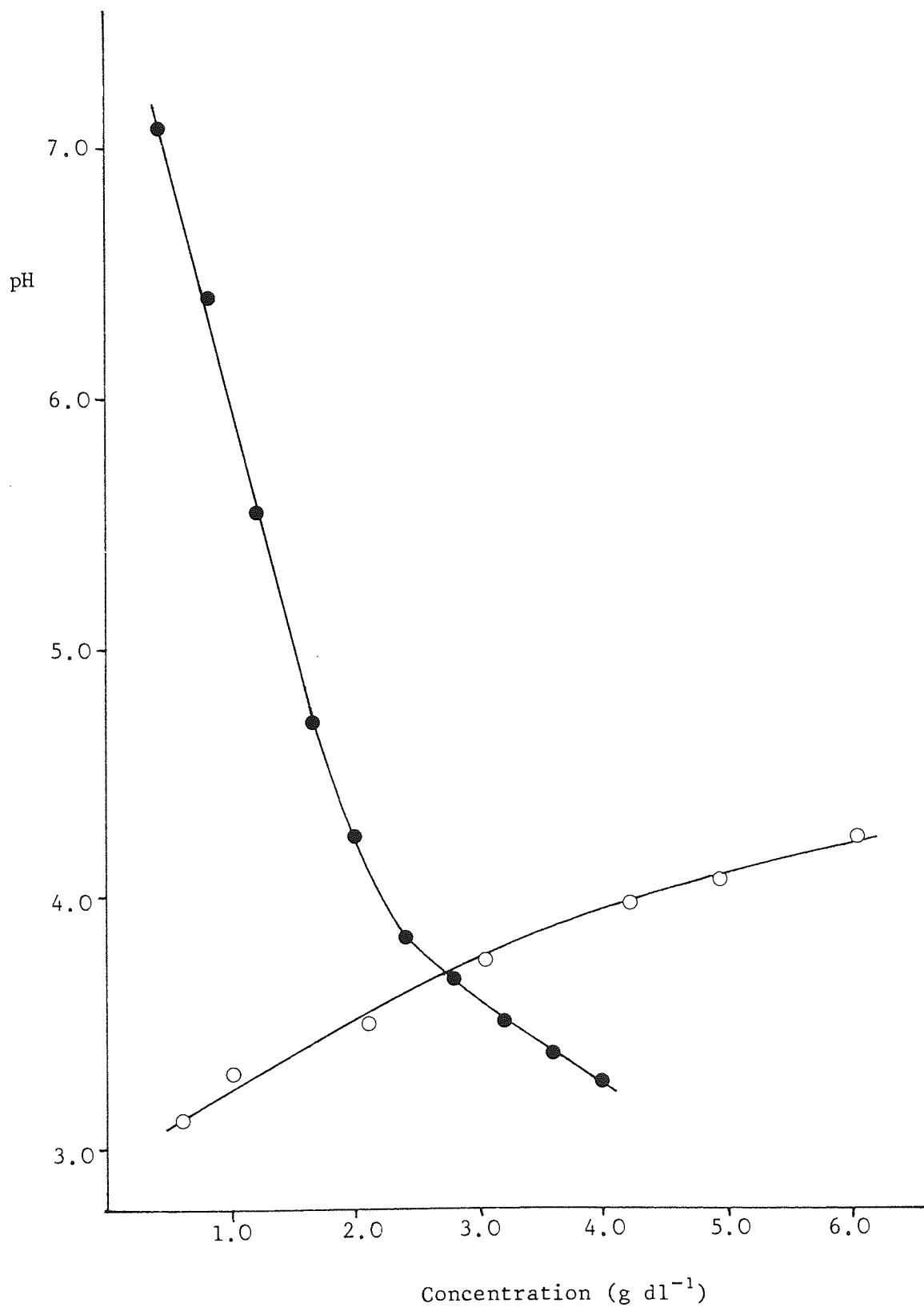


Table 5.12. Results for the Potentiometric Titration of Alginic Acid according to the method of Section 5.3.2.2..

Volume of * 0.1 Na OH added (cm ³)	Volume of * 0.1 NaCl added (cm ³)	pH	Degree of Neutralisation α	$\log \left(\frac{n\alpha}{1-n\alpha} \right)$
2.0	8.0	3.28	0.385	-0.306
3.0	7.0	3.61	0.577	0.007
4.0	6.0	3.83	0.769	0.290
4.2	5.8	4.05	0.808	0.358
4.4	5.6	4.09	0.846	0.428
4.6	5.4	4.18	0.885	0.503
4.8	5.2	4.35	0.923	0.586
5.0	5.0	4.71	0.962	0.679
5.2	4.8	6.53	1.000	0.788

* These volumes were added to individual 20 cm² aliquots containing Alginic Acid 0.100 g.

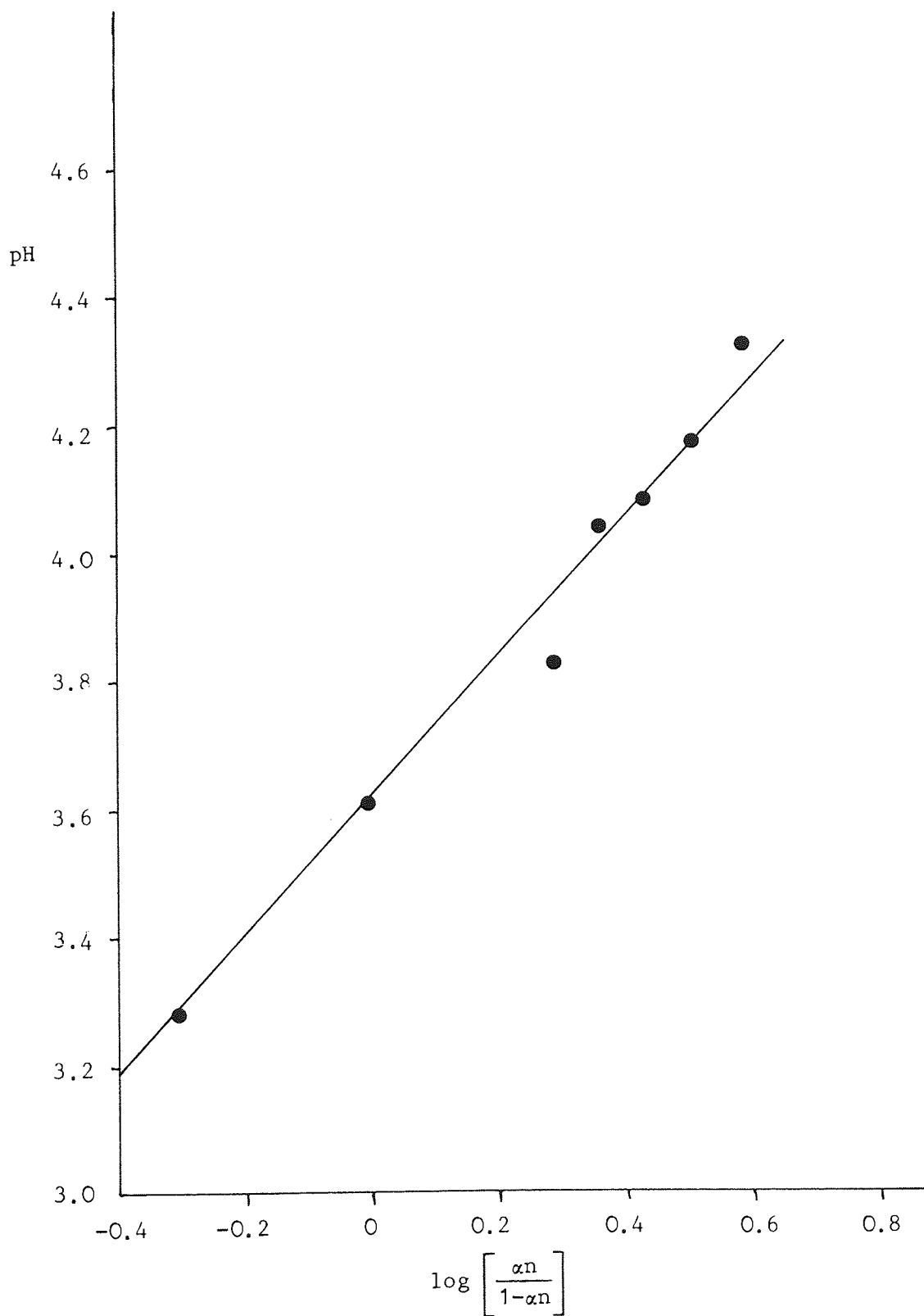
$(n_{\alpha} / 1 - n_{\alpha})$ as given in Figure 5.9.. Bearing in mind that much of the titration was carried out with Alginic acid present in suspension, the plot shows reasonable linearity. The value of pKa was obtained from the ordinate when $\log (n_{\alpha} / 1 - n_{\alpha}) = 0$, ie, pKa = 3.61.

By contrast, using the method advocated by Albert and Serjeant (253) by considering Alginic acid as a monoprotic acid with a molecular weight of 194 g mol^{-1} , a value of pKa = 3.33 ± 0.16 was obtained. This is in fair agreement with the value of 3.61 from the previous method. The wide standard deviation, however, probably results from using a two phase titration system.

From these results, it can be concluded that for gelation to occur by the GDL method, and to be independent of the presence of Alginic acid, the pH of the gel should be in the range 3.61 to 4.70. To achieve this, the concentration of GDL used subsequently was 2.0 g dl^{-1} and the relatively small effect of Alginate on pH enabled various concentrations to be used.

Figure 5.9.

DETERMINATION OF THE DISSOCIATION
CONSTANT FOR ALGINIC ACID USING THE
MODIFIED HENDERSON - HASSELBACH EQUATION



5.4.3.2 Effect of Calcium Ion Concentration on the Storage Modulus and Dynamic Viscosity.

The concentration range of 10 to 100 mmol Ca^{2+} was used for 30 g dl^{-1} Alginate gels measured using the oscillatory shear method given in Sections 2.3.4.2. and 5.3.2.2.. The distinct characteristic that arose from the results was that all of the gels, except the lowest Ca^{2+} concentration, showed purely elastic properties, ie, the phase angles were negligibly small. The dynamic viscosity curve, $\eta'(\omega)$, for 10mM Ca^{2+} is given in Figure 5.10. Here, the viscosity component changed dramatically whilst the storage modulus, G' , remained virtually unchanged.

The plateau in the $G'(\omega)$ curve within the frequency range used was a consistent feature for all Calcium Alginate gels measured in this way. The collective results for $G'(\omega)$ are given in Table 5.13., and a specimen $G'(\omega)$ curve for 70 mMol Ca^{2+} is given in Figure 5.11. By calculating the mean value of G' from the plateau, representative values for the gel rigidity were obtained. These results are listed in Table 5.14. and illustrated in Figure 5.12.. It is clear that when the Ca^{2+} concentration was greater than 40 mMol, there was no significant increase in gel rigidity. This may be attributed to saturation of the available sites for Ca^{2+} cross-linking.

Figure 5.10. The Effect of the Frequency of Oscillation on the Storage Modulus G' , \circ , and the Dynamic Viscosity η' , \bullet , of a Calcium Alginate Gel.

Alginate Concentration = 3.0 g dl^{-1}

Ca^{2+} Concentration = 10.0 mMol .

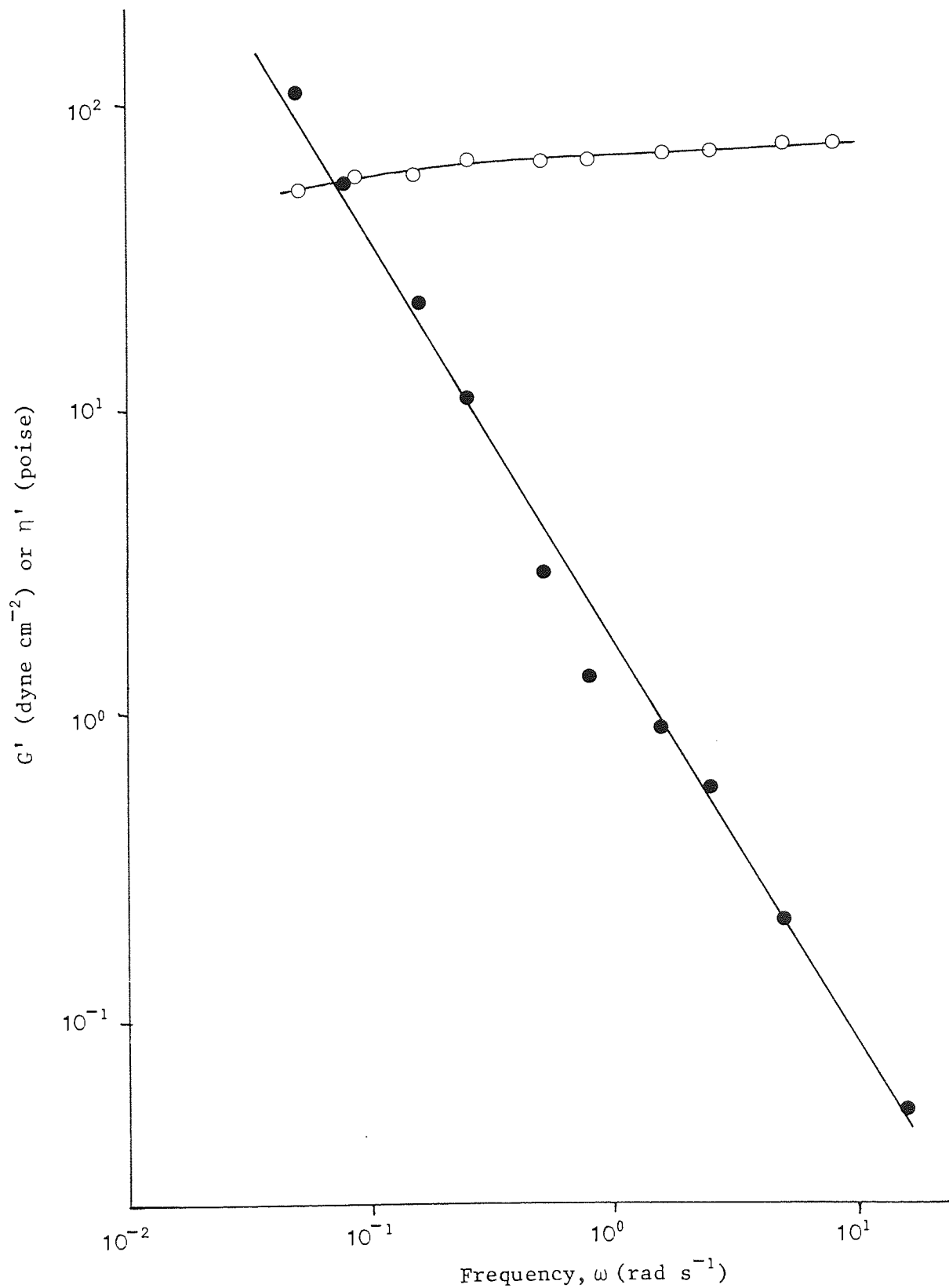


Table 5.13. Storage Modulus, $G(\omega)$, of 3.0 g dl⁻¹ Alginate Gels as a function of the Calcium Ion Concentration.

Frequency (ω) (rad s ⁻¹)	Storage Modulus, G' , (Dyne cm ⁻²)									
	Calcium Ion Concentration (mMol.)									
	10	20	30	40	70	80	90	100		
0.0497	54.04	2208	6270	7950	7423	5154	8402	5650		
0.0792	56.69	3177	6152	8190	7063	6187	7586	8907		
0.157	60.44	3065	5899	8982	7450	7120	6986	8953		
0.249	67.64	3637	6094	8982	8771	7625	9231	8536		
0.497	65.41	3664	6036	7711	7447	7306	8511	6903		
0.792	68.21	3491	5965	7706	7462	7302	8070	8266		
1.57	71.48	3443	7661	8375	7495	8560	9131	7592		
2.49	72.17	3460	7131	6954	7711	8184	8282	7872		
4.97	77.63	3472	6660	6214	7340	8120	7838	7478		
7.92	76.62	3515	6843	6595	5444	8720	7576	6929		
15.7	98.95	2820	5181	4512	3850	5460	5381	4787		

Figure 5.11. The Effect of the Frequency of Oscillation on the Storage Modulus, G' , of a Calcium Alginate Gel showing the Effect of the Natural Frequency, ω_0 .

Alginate Concentration = 3.0 g dl^{-1}

Calcium Ion Concentration = 70 mMol

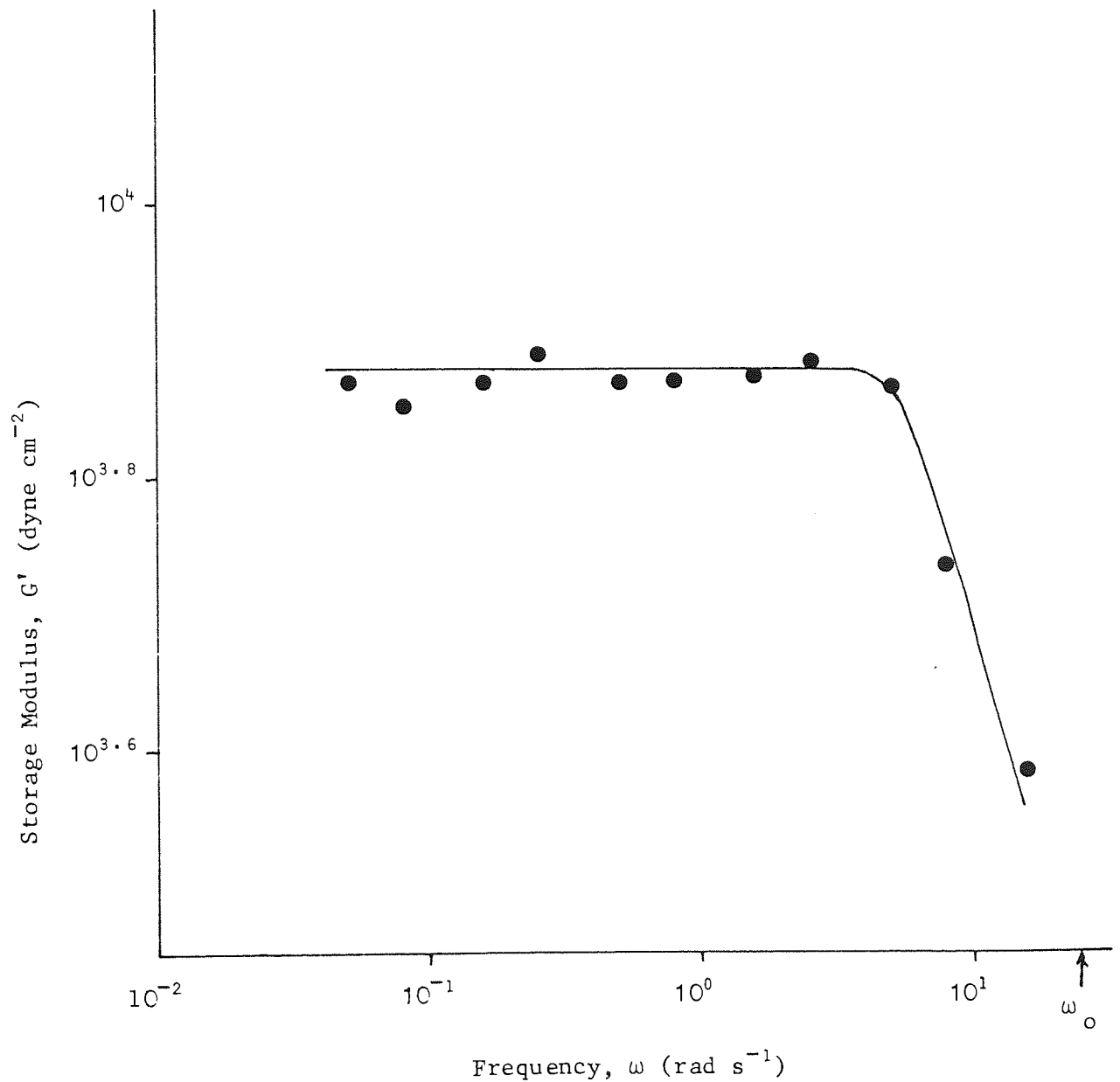
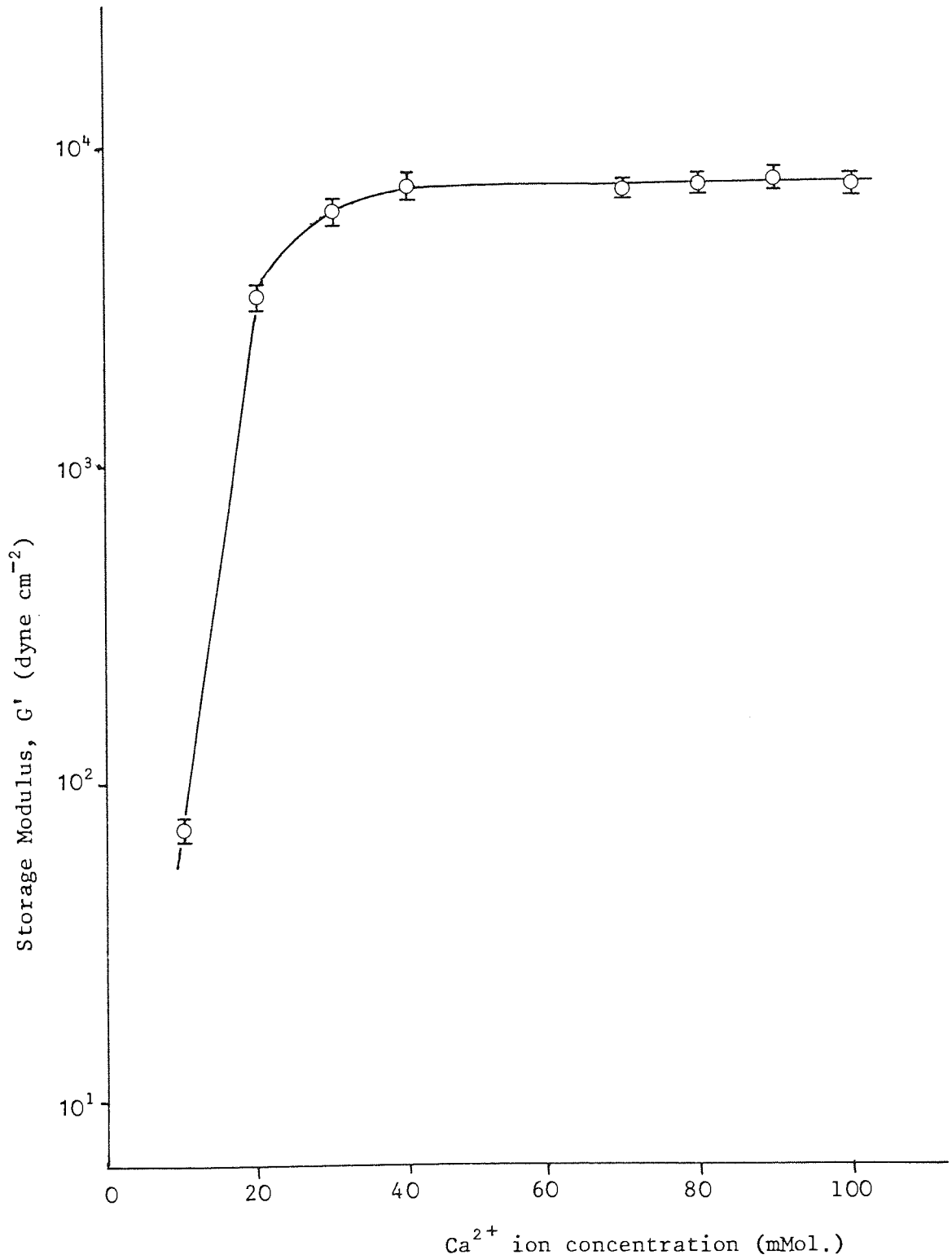


Table 5.14. Summary of the Results for Gel Rigidity, G' , as a function of Calcium Ion Concentration.

Ca ²⁺ Concentration (mMol)	Mean G' from plateau of G'(ω) (dyne cm ⁻²)	95% Confidence limits	Number of Readings
10	71.31	4.22	7
20	3436	151	9
30	6430	432	10
40	7766	786	8
70	7574	370	9
80	7867	511	8
90	8160	505	10
100	7937	600	9

Figure 5.12

THE EFFECT OF CALCIUM ION CONCENTRATION
ON THE STORAGE MODULUS, $G'(\omega)$, OF 3.0 g dl^{-1}
ALGINATE GELS



5.4.3.3 Effect of Alginate Concentration on the Storage Modulus.

The effect of Alginate concentration in the range 1.0 to 6.1 g dl⁻¹ on gel rigidity as quantified by the storage modulus, $G'(\omega)$, was determined using the oscillatory shear method. The collective results for $G'(\omega)$ are given in Table 5.15.. The mean value of G' was obtained from the plateau of the $G'(\omega)$ curve as carried out in Section 5.4.3.2.. The resulting representative values are listed in Table 5.16. and illustrated graphically in Figure 5.13..

Within experimental error, the phase angles in oscillatory shear were zero for all gels and therefore they were purely elastic. The increase in G' with Alginate concentration was less marked than the increase in G' with Ca²⁺ concentration. This can be seen by comparison of Figures 5.10. and 5.11., remembering that the ordinate of the former bears a logarithmic scale. Data for concentrations of Alginate less than 1.0 g dl⁻¹ was not available because the brittle nature of such gels prohibited their transfer, intact, to the parallel plate geometry of the rheogoniometer.

Usually, up to six Alginate gels had to be prepared by the Glucono- δ -lactone method in order to obtain one sample suitable for rheometry. There were two reasons for this. Firstly, some gels set rapidly after pouring giving a non-horizontal or non-flat upper surface. Secondly, air occasionally became trapped in the gel as small bubbles: for low viscosity Alginate Solutions prior to

Table 5.15. The Effect of Alginate Concentration on the Storage Modulus, $G'(\omega)$, of Calcium Alginate Gels containing 50 mMol. Ca^{2+} .

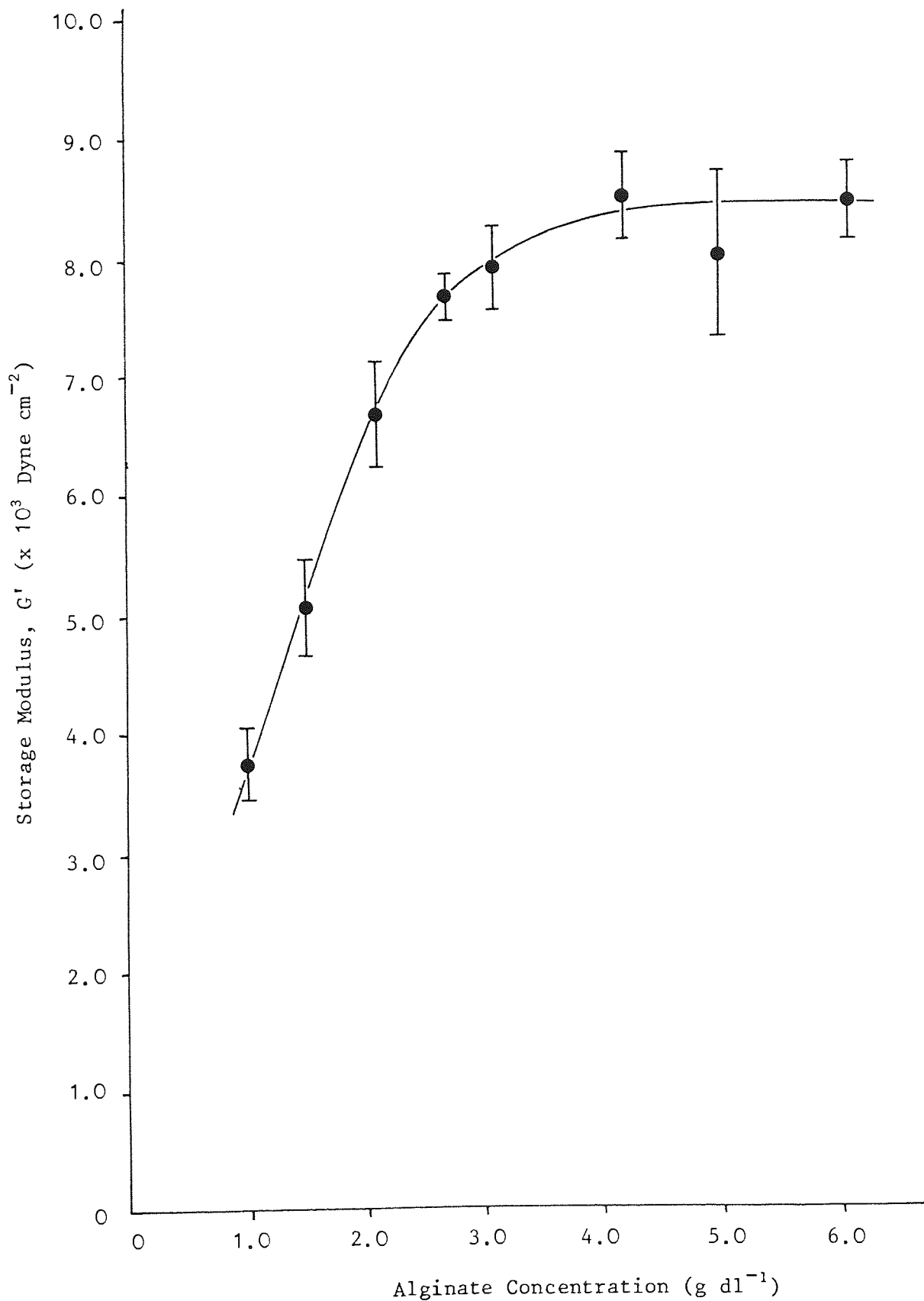
Frequency ω (rad s ⁻¹)	Storage Modulus, G' (Dyne cm ⁻²)									
	Alginate Concentration (g dl ⁻¹)									
	1.0	1.5	2.1	2.7	3.1	4.2	5.0	6.1		
0.0497	3900	3084	4353	5282	7706	6576	6942	7496		
0.0792	3927	4345	5061	7895	6982	8284	6980	7791		
0.157	4060	4742	5653	7656	7232	8695	8012	8623		
0.249	4174	5471	5818	7842	8605	8546	7047	8502		
0.497	4130	5543	7303	7412	7973	9280	7415	8462		
1.792	3774	5158	7298	7753	8276	9348	7376	8150		
1.57	3510	4794	7130	7517	8296	8355	8394	9217		
2.49	3070	4708	7049	8012	8529	8463	7914	8934		
4.97	3146	4211	6812	7940	8238	8010	9870	8700		
7.92	4061	4394	6510	4980	8116	8106	8398	8156		
15.7	2786	1535	3662	5171	6980	5708	5522	5776		

Table 5.16. Summary of Results for the Effect of Alginate Concentration on the Storage Modulus, G' , for Gels containing 50 mMol Ca^{2+} .

Alginate Concentration (g dl ⁻¹)	Mean G' from plateau of $G'(\omega)$ (dyne cm ⁻²)	95% Confidence limits	Number of Readings
1.0	3735	291	10
1.5	5069	359	6
2.1	6697	542	8
2.7	7697	210	8
3.1	7941	350	10
4.2	8565	364	9
5.0	8053	735	8
6.1	8504	334	9

Figure 5.13.

THE EFFECT OF ALGINATE CONCENTRATION ON THE STORAGE MODULUS OF GELS CONTAINING 50 mM Ca^{2+} .



mixing with GDL, vigorous stirring was necessary to prevent sedimentation of the calcium salt. At higher viscosities, any air which became trapped was not liberated before gelation occurred.

5.5 Discussion

In Section 4.4., the results of numerical analysis showed that the plotting of diffusion data in a first order fashion gave good agreement. From this, it was concluded that without sound evidence of the mechanism of rate control, drug release profiles can be misinterpreted.

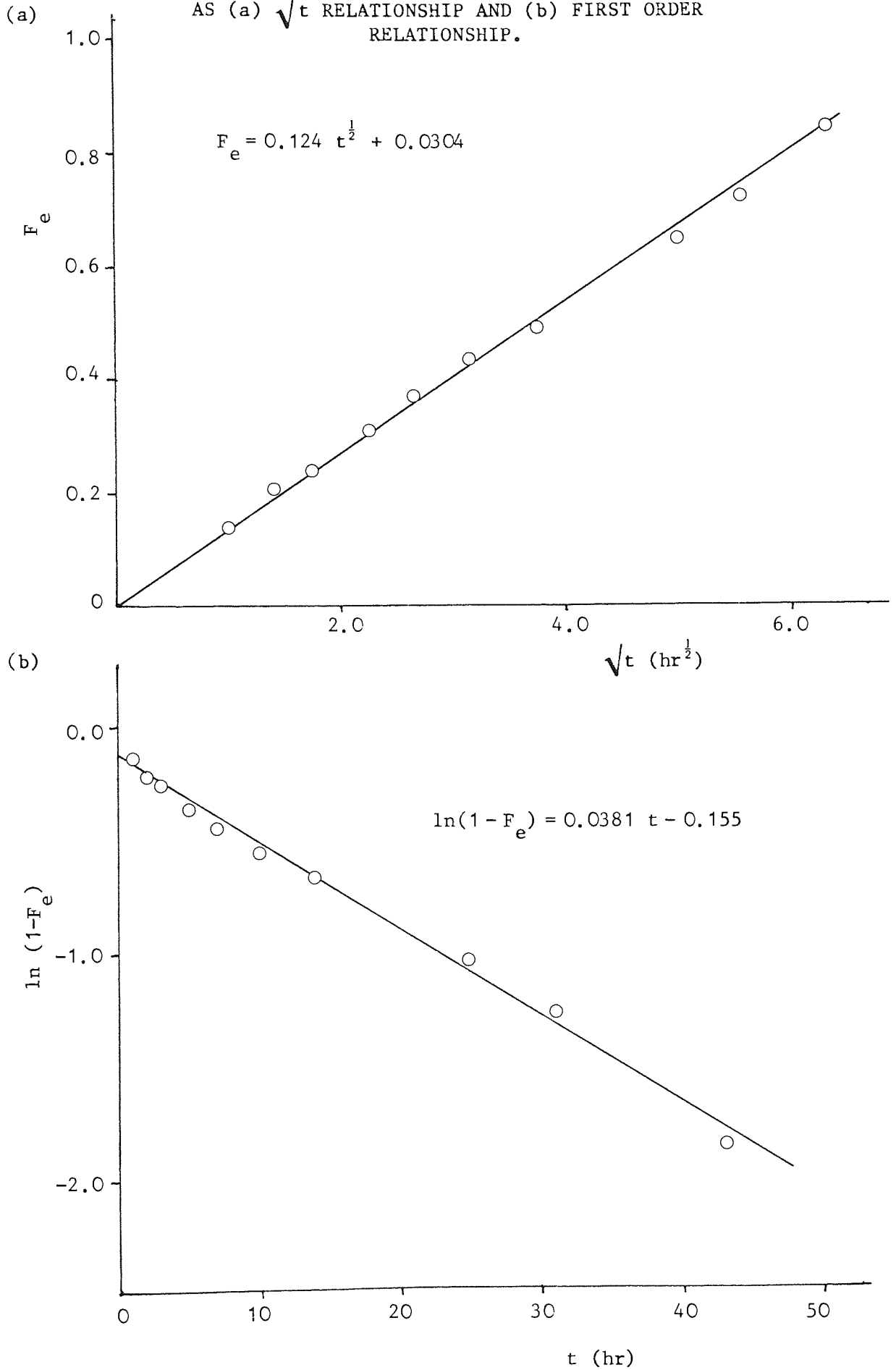
Consideration of experimental data provides an illustration of this. Table 5.17. lists the results of an experiment for the release of Ibuprofen from a Calcium Alginate gel in terms of the fraction released, F_e , against time. The experimental system is fully explained in Section 5.3.1.. From evidence given in earlier sections, the process was found to be diffusion controlled, and described by the planar diffusion equation described in Section 4.2.. By comparing the results of plotting F_e in a first order fashion with F_e against \sqrt{t} , then Figures 5.14(a) and (b) are obtained. The linear least mean square correlation coefficients are 0.9967 for the first order plot and 0.9996 for the \sqrt{t} plot. Clearly, if a process known to be diffusion controlled gives such a high correlation in a first order plot then with more complex systems such as suspensions, creams and ointments, it is likely to be difficult to distinguish between a diffusion

Table 5.17. Sample Set of Experimental Data for the Diffusion of Ibuprofen through a Calcium Alginate 5% Gel : the experimental method is give in Section 5.3.1.1. F_e is the Fraction Released at Time, t .

$t(\text{hr})$	$\sqrt{t} (\text{hr}^{\frac{1}{2}})$	F_e	$\ln(1-F_e)$
1	1.000	0.143	-0.154
2	1.414	0.210	-0.236
3	1.782	0.242	-0.277
5	2.236	0.311	-0.373
7	2.646	0.369	-0.460
10	3.162	0.434	-0.569
14	3.742	0.492	-0.677
25	5.000	0.647	-1.041
31	5.568	0.722	-1.280
43	6.557	0.845	-1.864

Figure 5.14

EXPERIMENTAL DATA FOR DRUG RELEASE BY DIFFUSION : THE FRACTION RELEASED, F_e , PLOTTED AS (a) \sqrt{t} RELATIONSHIP AND (b) FIRST ORDER RELATIONSHIP.



process and first order kinetics.

In Section 5.2.1., the calculation of the free diffusion coefficients of simple compounds was discussed. By calculating the free diffusion coefficient, D_f , of Ibuprofen in water at 25 ° C using Equations 5.7. and 5.8. derived from the Nernst-Einstein Equation 5.1., the values obtained can be compared with values of D ^{from} _A the diffusion experiments in Section 5.4.2..

For the calculation, the molecular volume should be determined; this is approximated by the partial molal volume for which tabulated values are available (232, 254). The application to Ibuprofen in aqueous solution at a pH significantly above its pKa, is shown in Figure 5.15.. Substituting the resulting value of $v = 183.4 \text{ cm}^3 \text{ mol}^{-1}$ into Equations 5.7 and 5.8. for small and large molecules, we obtain $D_1 = 8.71 \times 10^{-6}$ and $D_2 = 5.81 \times 10^{-6} \text{ cm}^2 \text{ sec}^{-1}$ respectively. In the case of the latter value, the molecule is assumed to be spherical and the frictional ratio, $F = 1$; corrections for non-sphericity usually account for less than a 10% change in F unless the molecule is highly elongated. By tabulating values of D_f for six homologous series of small molecules, Flynn (232) showed that species containing four or more carbon atoms gave experimental diffusivities within 25% of values calculated from Equation 5.8.. Albery et al (255) determined the values of D_f for the molecular weight carboxylic acids using a Stokes cell with a pH-Stat

Figure 5.15. Partial Molal Volume of Ibuprofen from Substituent Values.

Substituent	Partial Molal Volume ($\text{cm}^3 \text{mol}^{-1}$)		Summation
-CH ₃	19.3	x 3	57.9
-H	3.1	x 2	6.2
-COO ⁻	11.5		11.5
-C-	9.9	x 2	19.3
-C ₆ H ₄ -	71.8		71.8
-CH ₂ -	16.2		16.2
			183.4
			$\text{cm}^3 \text{mol}^{-1}$

Molecular Weight = 206.3 g mol⁻¹

modification. They found that the theoretical D_f over-estimated the actual values by about $0.6 \times 10^{-6} \text{ cm}^2 \text{ sec}^{-1}$ for oxalic and succinic acids. Therefore, the estimate of D_f for Ibuprofen, ie, either D_1 , or D_2 , may be greater than the true value.

In the experiments for diffusion of Ibuprofen through Alginate gels, it appeared that the values of D obtained were independent of the concentration of Alginate. If this was the case, then an overall value of D can be obtained from Table 5.8., ie, $\bar{D} = 4.82 \times 10^{-6} \text{ cm}^2 \text{ sec}^{-1}$ with 95% confidence limits of $\pm 0.228 \times 10^{-6} \text{ cm}^2 \text{ sec}^{-1}$ ($N = 20$). This value is lower than D_2 calculated from a theoretical approach. However, when an estimate of error of 25% for D_2 is taken into account, the lower limit is $D_2 = 4.36 \times 10^{-6} \text{ cm}^2 \text{ sec}^{-1}$; D_2 becomes insignificantly different from \bar{D} .

From this information, then according to the accuracy of the method for determining the theoretical D_f , then the diffusion coefficients of Ibuprofen in Calcium Alginate gels may not be significantly lower than the true value of D_f . To further investigate this aspect, there are several relationships available which equate D_f with values of D in gel matrices.

Lauffer (256) studied the theory of diffusion in gels and developed the equation:

$$D_g = D_f \frac{(1 - \frac{5}{3} \phi)}{(1 - \phi)} \quad 5.21$$

where D_g = Diffusion coefficient in the gel.

ϕ = Volume fraction from which solvent is effectively excluded.

5/3 = Coefficient of obstruction for gels consisting of random rods.

Substituting $D = 5.81 \times 10^{-6} \text{ cm}^2 \text{ sec}^{-1}$ and $\phi = 0.05$ for a 5.0 g dl⁻¹ Alginate gel, a value of $5.61 \times 10^{-6} \text{ cm}^2 \text{ sec}^{-1}$ is obtained. Before including estimates of errors, this is significantly higher than \bar{D} .

Another relationship was developed by Friedman and Kramer (223) to explain the diffusion of urea, sucrose and glycerol in gelatin gels:

$$D_f = D_g(1 + 2.4r_s/r_p)(1 + \alpha)(1 + \pi) \quad 5.22$$

where α = viscosity correction factor obtained by comparing D_f with D_g extrapolated to zero gelatin concentration.

$$\text{ie, } \alpha = \frac{D_f - D_{\text{extrap.}}}{D_f} \quad 5.23$$

π = mechanical blocking constant due to Dumanski (257)

$$\text{ie, } \pi = (g/d)^{2/3} \quad 5.24$$

g = gelatin concentration

d = density of gel

$(1 + 2.4r_s / r_p)$ = Ladenberg's correction to Stokes' Law for the fall of spherical bodies in capillary tubes (258,259).

r_s = radius of solute diffusant molecule

r_p = radius of pores in the gel matrix.

Therefore, from a knowledge of r_s , α , π , D_g and D_f , the pore radius r_p can be calculated. If it is assumed that D_f

and D_g are 5.81×10^{-6} and $4.82 \times 10^{-6} \text{ cm}^2 \text{ sec}^{-1}$

respectively and putting $\alpha = 0$ by assuming the microscopic viscosity remains unchanged, $g = 0.05$, $d = 1.0 \text{ g cm}^{-3}$, $r_s = (3 \times 183.4 / 4\pi N_{AV})^{1/3}$, ie, $r_s = 4.17 \times 10^{-8} \text{ cm}$. Therefore we obtain $r_p = 1.63 \times 10^{-6} \text{ cm}$ which compares with a mean of $0.53 \times 10^{-6} \text{ cm}$ determined by Friedman and Kramer (223) for a 5.0 g dl^{-1} gelatin gel, with the inclusion of a viscosity correction. Using Equation 5.22., Nixon and coworkers (224) found it necessary to include an "aggregation factor", X , to explain their data for diffusion of methylene blue in gelatin-glycerol-water gels such that

$$D_f = D_g^{(1+X)} (1 + 2.4 r_s / r_p) (1 + \alpha) (1 + \pi) \quad 5.25$$

where X approached unity when the dye molecules were not aggregated.

When the concentration of gelling agent is sufficiently high as to impede diffusion, the effect can be described in terms of a reduction in the pore radius in the matrix such that free diffusion no longer occurs. Therefore, the diffusivity in small pores, D_p , will be less than D_f . The two quantities have been equated by Renkin (260) in terms of the equivalent solute radius and the cylindrical pore radius, r_s and r_p respectively:

$$\frac{D_p}{D_f} = \left\{ 1 - \frac{r_s}{r_p} \right\}^2 \left[1 - 2.104 \left\{ \frac{r_s}{r_p} \right\} + 2.09 \left\{ \frac{r_s}{r_p} \right\}^3 - 0.95 \left\{ \frac{r_s}{r_p} \right\}^5 \right] \quad 5.26$$

such that r_s / r_p approaches zero when D_p / D_f approaches

unity, and r_s approaches r_p when D_p approaches zero. The equation was developed to describe the diffusion of various molecules in cellulose membranes.

A useful approximation to Equation 5.26. exists when $r_s/r_p < 0.2$

(261) which was obtained empirically:

$$\frac{D_p}{D_f} = 1 - \left(\frac{r_s}{r_p} \right)^4 \quad 5.27$$

Using the information obtained from Equation 5.22. that

$r_p = 1.63 \times 10^{-6}$ cm, then $r_s/r_p = 0.0256$ and from Equation 5.27., $D_p/D_f = 0.902$. Therefore, substituting $D_f = 5.81 \times 10^{-6}$ cm² sec⁻¹, we obtain $D_p = 5.24 \times 10^{-6}$ cm² sec⁻¹, which is in closer agreement with D_g for Ibuprofen in Alginate than the value of 5.61×10^{-6} from Equation 5.23. due to Lauffer (256).

From this calculation, it can be seen that because of the estimates of error of D_f and its possible over-estimation for carboxylic acids (255), then it is difficult to discern whether the diffusion coefficient of Ibuprofen in various Calcium Alginate gels is significantly different from D_f . In addition, the nature of the dialysis gel formation method meant that a range of Calcium ion concentrations could not be used: unsaturated Ca^{2+} binding was found to give rise to a Ca^{2+} concentration gradient in the gel.

However, with increasing Alginate concentration, the diffusion coefficient of Ibuprofen appeared to remain

unchanged despite an increase in the gel rigidity as measured by the Storage Modulus, G' . Therefore, the reduction in pore radius which inevitably resulted from increasing the Alginate concentration was insufficient to retard the diffusion of a molecule of the size of Ibuprofen. It is possible that a further increase in Alginate concentration or the use of a larger diffusant may produce a more marked effect.

6. CONCLUSION

In this thesis, several different experimental techniques have been used to quantitatively describe the functions of Alginate in pharmaceutical systems.

Studies on the molecular properties of Alginate using viscometry and light scattering were carried out in order to obtain estimates of molecular weight, radius of gyration, second virial coefficient and statistical segment length. Centrifugation at 100,000 x g was necessary to clarify Alginate solutions for light scattering. The results showed good agreement with similar parameters obtained in previous studies. Continuous and oscillatory shear rheometry were used to describe the flow properties of Alginate solutions in terms of the non-Newtonian behaviour and the viscous and elastic components. The onset of non-Newtonian behaviour with increasing Alginate concentration was coincidental with the appearance of a significant elastic component.

By blending Alginate with other polyelectrolyte suspending agents namely Xanthan gum and 'Carbopol', it was found that a very wide range of rheological 'profiles' existed. From the use of such a wide range of properties, the formulation of pharmaceutical disperse systems is rationalised because of reduced dependence upon the rheological characteristics of the limited number of commercially available suspending agents. The use of oscillatory shear testing can describe a non-Newtonian suspending agent solution in terms of the viscous and elastic components. It has been shown here that this technique is particularly suited to the description of the rheological 'profiles' of suspending agent blends.

Many of the problems of dispersion rheology in pharmaceuticals are common to other industries. For example, the prevention of sedimentation during storage is important in liquid abrasive cleaners, paints and printing inks as well as drug suspensions (139). Because of the variable properties of the drugs which must be suspended, it would not be possible to derive a single desirable rheological 'profile' for all drug suspensions. Nevertheless, it appears that relatively little research has been carried out in pharmaceutical institutions into the rheological parameters important in suspension formulation.

In addition, other industries such as the food and paper industries have found that by using microprocessor based controllers, fewer batches of product are wasted from failure to comply with rheological standards. It is likely that closer attention to rheological properties in pharmaceuticals will yield a higher quality product at a lower final cost.

It has been known for many years that the diffusion of a solute is affected by the viscosity of the medium. However, an inverse proportionality relationship is frequently inadequate to describe the diffusion and for non-Newtonian media such as gels, quantifying the viscosity becomes a problem in itself. In the literature, studies on the diffusion of solutes in viscous and non-Newtonian media have only rarely used a non-empirical rheological approach. Consequently, little work has emerged concerning the effect of viscoelasticity on diffusion.

In this study, diffusional and oscillatory shear rheological techniques have been used for Calcium Alginate systems. Numerical analysis showed that calculations from drug release profiles alone

do not demonstrate the presence of a diffusion mechanism, therefore further evidence for diffusion is essential. The diffusion mechanism was fully characterised for Ibuprofen as solute in Calcium Alginate gels. The elastic moduli from oscillatory testing, varied by changes in Alginate and Calcium ion concentrations, was found to have little or no significant effect on the diffusion coefficient. This was attributed to the fact that the pore size within the gel matrix remained significantly greater than the diameter of the diffusant molecule. There is much scope for future work in this field to discern more precisely, the relationship between diffusion and viscoelasticity.



Aston University

Content has been removed for copyright reasons



Aston University

Content has been removed for copyright reasons

Pages

Have been removed.



Aston University

Content has been removed for copyright reasons

APPENDIX II GLOSSARY OF TRADITIONAL AND SI UNITS

Throughout the text of this thesis a consistent system of units has been used for molecular, rheological and diffusional parameters such that the numbers produced were not cumbersome. However, the units were not necessarily in accordance with the SI convention. The Table below provides a list of the 'traditional' units used and their conversion to the SI system.

<u>Measurement</u>	<u>Traditional Units</u>	<u>SI Equivalent</u>
Viscosity	Poise	10^{-1}Nsm^{-2} (or Pas)
Force	Dyne	10^{-1}N
Shear Stress	Dyne cm^{-2}	10^{-1}Nm^{-2} (or Pa)
Volume	dl	10^{-4}m^3
Volume	cm^3	10^{-6}m^3
Weights	g	10^{-3}kg .

1. McDowell, R.H., "Properties of Alginates", Alginate Industries Ltd., London (1977).
2. Remington's Pharmaceutical Sciences', Ed. A.Osol, 16th Ed. (1980), Mack Pub. Co., Easton, Pennsylvania, Chap. 67.
3. Martin, A.N., Swarbrick, J. and Cammarata, A., "Physical Pharmacy" 2nd Ed. (1970), Lea & Febiger, Chap. 19.
4. Martindale, "The Extra Pharmacopoeia", Ed. A.Wade, Pharmaceutical Press, London, 27th Ed. (1977) p.683.
5. Haug, A. "Composition and Properties of Alginates", Report No.30, Norwegian Institute of Seaweed Research, Trondheim, Norway (1964).
6. Stanford, E.C.C., J. Soc. Chem. Ind. 4 518 (1885).
7. Hoagland, D.R. & Lieb, L.L., "The complex carbohydrates and forms of Sulphur in marine algae of the Pacific coast," J. Biol.Chem. 23 287-297 (1915).
8. Atsuki, K. & Tomoda, Y., J.Soc.Chem. Japan, 29 509-513 (1926).
9. Schmidt, E. & Vocke, F., "Zur Kenntniss der Polyglykuronsauren" Chem.Ber. 59 1585 - 1588 (1926)
10. Nelson, W.L. & Cretcher, L.H., "Alginic Acid from Macrocystis Pyrifera", J. Am.Chem.Soc. 51 1914 - 1922 (1929)
11. Bird, G.M. & Haas, P., "Nature of the cell wall constituents of Laminaria Spp.", Biochem. J. 25 403 - 411 (1931).
12. Hirst, E.L., Jones, J.K.N. & Jones, W.O., "Structure of Alginic Acid", J.Chem.Soc. 1880 - 1885 (1939).
13. Fischer, F.G. & Dörfel, H., "The Polyuronic Acids of Brown Algae", Z.Physiol. Chem. 302 186 - 203 (1955).
14. Hirst, E.L., Percival, E. & Wold, J.K., "Structural Studies of Alginic Acid", Chem.Ind. 257 - 262 (1963) & J. Chem.Soc. 1493 - 1499 (1964).
15. Smidsrød, O., "Physical Properties of Alginate in the Gel State", Report No.34, Norwegian Institute of Seaweed Research, Trondheim, Norway, (1970).
16. Buchner, P., Cooper, R.E. & Wassermann, A., "Influence of Counterion Fixation on Molecular Weight and Shape of a Polelectrolyte", J.Chem.Soc. 3974 - 3983 (1961).

17. Katachalsky, A., Cooper, R.E., Upadhyay, J. & Wassermann, A., "Counterion Fixation in Alginates". J.Chem.Soc. 5198 - 5204 (1961).
18. Mongar, J.L. & Wassermann, A., "Adsorption of electrolyte by Alginate gels without and with cation exchange" J.Chem.Soc. 492 - 497 (1952).
19. Haug, A., "Ion exchange properties of Alginate fractions" Acta Chem.Scand. 13 1250 - 1251 (1959).
20. Smidsrød, O., "Molecular basis for some physical properties of Alginates in the gel state", Farad. Disc.Chem.Soc. 57 263 - 274 (1974).
21. Atkins, E.D.T., Mackie, W., Parker, K.D. & Smolko, E.E. "Crystalline structures of Poly- α -mannuronic and Poly-L-guluronic acids", J. Polymer.Sci.(B) 9 311 - 316 (1971).
22. Rees, D.A., "Polysaccharide Gels - A molecular view", Chem.Ind. 630 - 636 (1972).
23. Kohn, R. "Ion-binding on Polyuronates, Alginate & Pectin", Pure Appl.Chem. 42 (3) 371 - 397 (1975).
24. Rees, D.A., "Shapely Polysaccharides", Biochem. J. 126 257 - 273 (1972).
25. Smidsrød, O., Haug, A. & Whittington, S.G., "The molecular basis for some physical properties of Polyuronides", Acta Chem. Scand. 26 2563 - 2566 (1972).
26. Anthonsen, T., Larsen, B. & Smidsrod, O., "NMR studies of the interation of metal ions with Poly (1,4 - hexuronates), Acta Chem. Scand. 26 2988 - 2990 (1972).
27. Data Sheet Compendioum ABPI., Datapharm Pub.Ltd. (1981/2) 'Gaviscon' p.942.
28. Merck Index, 8th Ed. Pub. Merck & Co. (1968).
29. 'Gaviscon' Information Manual Pub. Reckitt & Colman Pharmaceuticals Ltd., Hull, UK.
30. Beeley, M. & Warner, J., "Medical treatment of symptomatic hiatus hernia with low density compounds", Curr.Med.Res. Opinion 1 (2) 63 - 72 (1972).
31. Barnardo, D.E., Lancaster-Smith, M., Strickland, I.D. & Wright, J.T., "A double blind controlled trial of 'Gaviscon' in patients with symptomatic gastro-oesophageal reflux", Curr. Med.Res. Opinion 3 388 - 391 (1975).

32. Scobie, B.A., "Endoscopically controlled trial of Alginate and antacid in reflux oesophagitis, Med. J.Aust. 1 (17) 627 - 628 (1976).
33. Selleri, R., Orzalesi, G., Mari, F. & Bertol, E., "Influence of the type of Alginic Acid on the activity of remedies used for gastric disorders", Boll. Chim. Farm. 119 41 - 51 (1980).
34. Rendall, M., "Hiatus hernia and oesophageal reflux"" Proc. Roy. Soc.Med. 65 33 - 35 (1972).
35. Stancin, C. & Bennett, J.R., "Alginate/antacid in the reduction of gastro-oesophageal reflux", Lancet 1 109 - 111 (26 Jan.1974).
36. Goodall, J.S., Orwin, J.M. & Invie, M.J., "Combined pH and X-ray study of a liquid Alginate/antacid formulation using a novel X-ray contrast medium", Acta Therapeutica 3 141 - 153 (1977).
37. Beckloff, G.L., Chapman, J.H. & Shiverdecker, P., "Objective evaluation of an antacid with unusual properties - radiographic studies" J.Clin. Pharmacol. 12 11 - 21 (1972).
38. Flynn, G.L., Yalkowsky, S.H. & Roseman, T.J., "Mass transport phenomena and models: theoretical concepts" J.Pharm.Sci. 63 479 - 510 (1974).
39. Wilke, C.R. & Chang, P., "Correlation of diffusion coefficients in dilute solutions" Am.Inst.Chem.Eng.J. 1 (2) 264 - 270 (1955).
40. Buscall, R., Goodwin, J.W., Ottewill, R.H. & Tadros, Th.F., "The settling of particles through Newtonian and non-Newtonian media". J.Coll.Interface Sci. 85 78 - 86 (1982).
41. Strenge, K. & Sonntag, H., "Beziehungen zwischen interpartikularer Wechselwirkung and rheologischem Verhalten Konzentrierter disperser systeme", Coll.Polym.Sci. 252 133 - 137 (1974).
42. Ferry, J.D., "Viscoelastic Properties of Polymers" J. Wiley, 3rd Ed. (1980) Chap.1.
43. *ibid*, Chap.2.
44. *ibid*, Chap.3.
45. *ibid*, Chap.9.

46. Haug, A., "Composition and Properties of Alginate", Report No.30, Norwegian Inst.Seaweed Res. Trondheim, Norway (1964) p.32.
47. *ibid*, p.25 ff.
48. Haug, A., Larsen, B & Smidsrød, O., "Uronic acid sequence in Alginate from different sources", Carbohyd. Res. 32 217 - 225 (1974).
49. Smidsrød, O., Glover, R.M. & Whittington, S.G., "The relative extension of Alginates having different chemical composition", Carbohyd.Res. 27 107 - 118 (1973).
50. Whittington, S.G., "Conformational energy calculations on Alginic acid" Biopolymers 10 1481 - 9 (1971).
51. Flory, P.J. "Principles of Polymer Chemistry", Cornell Univ. Press, Ithaca (1953) p.637.
52. Smidsrød, O., "Solution properties of Alginate", Carbohyd.Res. 13 359 - 372 (1970).
53. Smidsrød, O., "A light scattering study of Alginate", Acta Chem. Scand. 22 797 - 810 (1968).
54. Dingsøyr, E. & Smidsrød, O., "Light scattering properties of Sodium and Magnesium Alginate", Br. Polym. J. 9 (1) 56 - 61 (1977).
55. Brucker, R.F., Wormington III, C.M. and Nakada, H.I., "Comparison of some physicochemical properties of Alginic acids of differing composition", J.Macromol.Sci. - Chem. A5 (7) 1169 - 1175 (1971).
56. Mackie, W., Noy, R. and Sellen, D.B., "Solution properties of Sodium Alginate", Biopolymers 19 1839 - 1860 (1980).
57. Graessley, W.W., "The entanglement concept in polymer rheology". Adv. Polym.Sci. 16 1 - 179 (1974).
58. Schurz, J., "Rheological structure investigation with concentrated polymer solutions", Proc.5th Int. Congress on Rheology, Ed. S. Onogi, 4 215 - 230 (1970).
59. Dreval, V.Y., "Rheology of concentrated polymer solutions" Fluid Mechanics - Sov. Res. 8 (2) 63 - 87 (1979).
60. Bird, R.B., Hassager, O., Armstrong, R.C. and Curtiss, C.F. "Dynamics of Polymeric Liquids, Volume 2: Kinetic Theory", J. Wiley, New York (1977).

61. Staudinger, H. and Wodzn, T., "On the binding of high polymers Ber. 63 721 - 724 (1930).
62. Elias, H.-G., "Macromolecules: I. Structure & Properties", J. Wiley, New York (1977) p.364.
63. *ibid.* p.358.
64. *ibid.* p.345.
65. Kuhn, W., "On the atomic size and atomic shape from viscosity and streaming birefringence". Z.physik. Chemie Al61 1 - 32 (1932).
66. Huggins, M.L. "Viscosity of dilute solutions of long chain molecules". J.Phys.Chem. 43 439 - 456 (1939).
67. Kramers, H.A., "Behaviour of macromolecules in inhomogeneous flow", J.Chem.Phys. 14 415 - 424 (1946).
68. Flory, P.J., "Principles of Polymer Chemistry", Cornell Univ. Press, Ithaca (1953) p.611.
69. Takahashi, A. and Nagasawa, M. "Excluded volume of polyelectrolyte in salt solutions", J.Amer.Chem.Soc. 86 543 - 8 (1964).
70. Schneider, N.S. and Doty, P. "Macro-ions, IV : The ionic strength dependence of the molecular properties of Sodium Carboxymethylcellulose", J.Phys.Chem. 58 762 - 9 (1954).
71. Smidsrød, O. and Haug, A., "Estimation of the relative stiffness of the molecular chain in polyelectrolytes from measurements of viscosity at different ionic strengths". Biopolymers 10 1213 - 1227 (1971).
72. Tanford, C. "Physical Chemistry of Macromolecules" J.Wiley, New York & London (1961) p.407.
73. *ibid* p.275.
74. *ibid* p.501.
75. Flory, P.J. "The configuration of real polymer chains" J.Chem.Phys. 17 303 - 310 (1949)
76. Flory, P.J. and Fox Jr., T.G., "Molecular conformation and thermodynamic parameters from intrinsic viscosity", J.Polym. Soc. 5 745 - 7 (1950).
77. Krigbaum, W.R. and Carpenter, D.K. "The configuration of polymer molecules: Polystyrene in Cyclohexane", J.Phys.Chem. 59 1166 - 1172 (1955).

78. Kirkwood, J.G. and Riseman, J., "The intrinsic viscosities and diffusion constants of flexible macromolecules in solution" J.Chem.Phys. 16 565 - 573 (1948).
79. Bloomfield, V. and Zimm, B.H. "Viscosity, sedimentation et cetera of ring- and straight-chain polymers". J.Chem.Phys. 44 315 - 323 (1966).
80. Huglin, M.B. (Ed), "Light Scattering in Polymer Solutions", Acad.Press, London (1972).
81. Flory, P.J. "Principles of Polymer Chemistry", Cornell Univ. Press, Ithaca (1953) p.283.
82. J.W.Strutt (Lord Rayleigh) Phil.mag. [4] 41 107, 447 (1871).
83. Mie, G., "Beitrage zur optik triber medien, speziell kolloidaler metallosungen", Ann.Physik 25 377 - 445 (1908).
84. Einstein, A. "Theorie der opaleszenz von homogenen flussigkeiten and flussigkeitsgemischen in der nahe des kritischen zustaudes", Ann. Physik. 33 1275 - 1304 (1910).
85. Debye, P., "Light scattering in solutions" J.Appl.Phys. 15 338 - 342 (1944).
86. Debye, P., "Molecular weight determination by light scattering", J.Phys.Chem. 51 18 - 32 (1947).
87. Chiang, R., "Intrinsic viscosity - molecular weight relationship for fractions of linear Polyethylene", J.Phys.Chem. 69 1645 - 1653 (1965).
88. Kuhn, W., Kuhn, H. and Buchner, P., "Hydrodynamic behaviour of macromolecules in Solution". Ergebn. exakt. Naturwiss 25 1 - 108 (1951).
89. Astbury, W.T. "Structure of Alginic acid" Nature 155 667 - 8 (1945).
90. Scott-Blair, G.W. "Elementary Rheology" Acad.Press, London (1969).
91. Barry, B.W., "Rheology of pharmaceutical and cosmetic semisolids", Adv.Pharm.Soc. 4 1 - 72 (1974).
92. Davis, S.S., Shotten, E. and Warburton, B. "Some limitations of continuous shear methods for the study of pharmaceutical semisolids", J.Pharm.Pharmac. 20 (Suppl.) 157S - 167S (1968).
93. Davis, S.S., "Viscoelastic properties of pharmaceutical semisolids, I.Ointment Bases", J.Pharm.Sci. 58 412 - 417 (1969).

94. Metzner, A.B., "Recent developments in the engineering aspects of rheology". *Rheol. Acta* 1 205 - 212 (1958).
95. Bingham, E., "Fluidity and Plasticity" McGraw Hill, New York (1922).
96. Casson, N., "A flow equation for pigment-oil suspensions of the printing ink type" in 'Rheology of Disperse Systems' Ed. C.C.Mill, Pergamon Press (1959) p.84 - 104.
97. Shangraw, R., Grim, W. and Mattocks, A.M., "An equation for non-Newtonian flow", *Trans.Soc.Rheol.* 5 247 - 260 (1961).
98. Yakatan, G.J. & Arango, O.E., "Analog computer simulation of rheological systems, I. Pseudoplastic flow.", *J.Pharm. Sci.* 57 155 - 158 (1968).
99. Cross, M.M., "Rheology of non-Newtonian fluids: A new flow equation for pseudoplastic systems". *J. Colloid Sci.* 20 417 - 437 (1965).
100. Cheng, D.C-H., "Macroscopic flow properties of suspensions", Seminar in Suspension Rheology, Warren Springs Laboratory, Stevenage (1981).
101. Barry, B.W. and Meyer, M.C., "The rheological properties of Carbopol gels, I: Continuous shear and creep properties", *Int.J.Pharm.* 2 1 - 25 (1979).
102. Warburton, B. and Barry, B.W., "Concentric cylinder creep investigation of pharmaceutical semisolids", *J.Pharm. Pharmacol.* 20 255 - 268 (1968).
103. Davis, S.S. and Khanderia, M.S., "Rheological characterisation of Plastibases and the effect of formulation variables on the consistency of these vehicles". *Int.J.Pharm.Technol.Prod. Manuf.* 1 (3) 15 - 21 (1980).
104. Mitchell, J.R. and Blanchard, J.M.V., "Viscoelastic behaviour of Alginates", *Rheol. Acta* 13 180 - 4 (1974).
105. Mitchell, J.R. and Blanchard, J.M.V., "Rheological properties of Alginate gels", *J.Texture Studies* 7 219 - 234 (1976).
106. Walters, K. and Kemp, R.A., "On the use of a rheogoniometer: III, oscillatory shear between parallel plates", *Rheol. Acta* 7 1 - 8 (1968).
107. Walters, K. "Basic Concepts and Formulae for the Rheogoniometer", Pub. Sangamo Controls Ltd., Bognor Regis, UK. (1968).

108. Warburton, B. and Davis, S.S., "The oscillatory testing of pharmaceutical semi-solids using a transfer function analyser", *Rheol. Acta* 8 205 - 214 (1969).
109. Cox, W.P. and Merz, E.H. "Correlation of dynamic and steady flow viscosities", *J.Polymer Sci* 28 (118) 619 - 623 (1958).
110. Kitano, T., Nishimura, T., Kataoka, T. and Sakai, T., "Correlation of dynamic and steady flow viscosities of filled polymer systems"., *Rheol. Acta* 19 671 - 3 (1980).
111. Kulicke, W.-M. and Porter, R.S., "Relation between steady shear flow and dynamic rheology", *Rheol. Acta* 19 601 - 5 (1980).
112. Williams, R.W. "Determination of viscometric data from the Brookfield RVT Viscometer", *Rheol. Acta* 18 345 - 359 (1979).
113. 'Handbook of Chemistry and Physics' Eds. Weast, R.C. and Astle, M.J., Chemical Rubber Publishing Company, Florida, U.S.A. 59th Ed. (1978 - 9) F-11.
114. *ibid* F-51.
115. Scott, J.E. Tigwell, M.J. Phelps, C.F. and Nieduseynski, I.A., "On the mechanism of scission of Alginate chains by periodate" *Carbohyd. Res.* 47 105 - 117 (1976).
116. Dubois, M., Gilles, K.A., Hamilton, J.K., Rebers, P.A. & Smith, F., "Colorimetric method for determination of sugars and related substances", *Anal. Chem.* 28 350 - 356 (1956).
117. Walters, K. "Rheometry" Chapman and Hall, London, (1975) p.151.
118. Jones, T.E.R. and Walters, K., "An interpretation of discontinuities occurring in dynamic testing near the natural frequency", *Rheol. Acta* 10 365 - 7 (1971).
119. Barry, B.W. and Meyer, M.C. "The rheological properties of Carbopol gels: II, Oscillatory Properties", *Int. J. Pharm.* 2 27 - 40 (1979).
120. Shaw, D.J. "Introduction to Colloid and Surface Chemistry", Butterworths, London, 2nd Ed. (1970) p.190.
121. Zimm, B.H., "The scattering of light and the radial distribution function of high polymer solutions", *J.Chem. Phys.* 16 1093-1099 (1948).
122. Huglin, M.B. (Ed) "Light Scattering from Polymer Solutions", Acad. Press, London, (1972) p98.

123. Cohen, G. & Eisenberg, H., "Light scattering of water, Deuterium Oxide and other pure liquids", J.Chem.Phys. 43 3881-3887 (1965).
124. Holt, C., Mackie, W & Sellen, D.B., "Configuration of Cellulose Trinitrate in solution", Polymer 17 1027-1034 (1976).
125. Kirkwood, J.G. & Riseman, J., "Errata: The intrinsic viscosities and diffusion constants of flexible macromolecules in solution", J.Chem.Phys. 22 1626-1627 (1954).
126. Kabre, S.P., DeKay, G. & Banker, G.S., "Rheology and suspension activity of pseudoplastic polymers," J.Pharm.Sci. 52 492-495 (1964).
127. Pavics, L., "Comparison of rheological properties of mucilages", Acta Pharm.Hung. 40 52-59 (1970).
128. Rees, D.A., "Structure, conformation and mechanism in the formation of polysaccharide gels and networks", Adv.Carbohyd. Chem. Biochem. 24 267-332 (1969).
129. Rees, D.A., "Polysaccharide Shapes", Outline Series in Biology, Chapman & Hall, London (1977).
130. Morris, E.R., Rees, D.A., Thom, D. & Walsh, E.J., "Conformation and intermolecular interactions of carbohydrate chains", J. Supramol. Struct. 6 259-274 (1977).
131. Morris, E.R., "Polysaccharide structure and conformation in solutions and gels" in 'Polysaccharides in Food', Proc. Easter School, Agric. Sci., Nottingham. Eds, Blanshard, J.M.V. & Mitchell, J.R. (1977) p.15 - 32.
132. Franks, F., "Solvent interactions and the solution behaviour of carbohydrates", *ibid* p.33-50.
133. Mitchell, J.R., "Rheology of polysaccharide solutions and gels", *ibid*, p.51-72.
134. Debye, P., "Intrinsic viscosity of polymer solutions", J.Chem.Phys. 14 636-639 (1946).
135. Bueche, F., "Influence of the rate of shear on the apparent viscosity", J.Chem.Phys. 22 1570-1576 (1954)
136. Rouse Jr., P.E., "A theory of linear viscoelastic properties of dilute solutions of coiling polymers", J.Chem.Phys. 21 1272-1280 (1953).
137. Zimm, B.H., "Dynamics of polymer molecules in dilute solution, viscoelasticity, flow birefringence and dielectric loss", J.Chem.Phys. 24 269-278 (1956).

138. Ferry, J.D., "Viscoelastic Properties of Polymers", J.Wiley. New York, 3rd Ed. (1980) p.192.
139. Barnes, H., "Dispersion Rheology : A survey of Industrial Problems", Pub. Unilever PLC. Port Sunlight, Wirral, UK (1980).
- 140 Jarzebski, G.J., "On the effective viscosity of pseudoplastic suspensions", Rheol. Acta 20 280-287 (1981).
141. Ferrini, F., Ercolani, D., de Cindio, B., Nicodemo, L., Nicolais, L. and Ranaudo, S., "Shear viscosity of settling suspensions", Rheol. Acta 18 289-296 (1979).
142. Onogi, S. & Matsumoto, T., "Rheological properties of polymer solutions and melts containing suspended particles", Polym. Eng. Rev. 1 (1) 45-87 (1981).
143. Berney, B.M. & Deasy, P.B., "Evaluation of Carbopol 934 as a suspending agent for Sulphadimidine suspensions", Int.J.Pharm. 3 73-80 (1979).
144. Ward, J.B., Kinney, J.F. & Saad, H.Y., "Application of rheological studies to product formulation, stability and processing problems", J.Soc.Cosmet.Chem. 25 437-454 (1974).
145. Pexz, M & Bartos, J. "Colorimetric and Fluorimetric Analysis of Organic Compounds and Drugs", in 'Clinical and Biochemical Analysis' Vol.I, pub. Dekker (1977), Chap.14.
146. Fischer, W.H., Bauer, W.H. & Wiberley, S.E., "Yield stresses and flow properties of Carboxypolymethylene-Water Systems", Trans.Soc.Rheol. 5 221-235 (1961).
147. Brodnyan, J.G. & Kellay, E.L., "The rheology of polyelectrolytes: I. Flow-curves of concentrated Poly (acrylic acid) solutions", Trans.Soc.Rheol 5 205-220 (1961).
148. Taylor, N.W. & Bagley, E.B. "Rheology of dispersions of swollen gel particles", J.Polym.Sci. (P.P.E.) 13 1133-1144 (1975).
149. Whitcomb, P.J. & Macosko, C.W., "Rheology of Xanthan Gum", J.Rheol. 22 493-505 (1978).
150. Elliot, J.H., "Rheology of Xanthan gum solutions", ACS Symp. Ser. 45 'Extracellular Microbial Polysaccharides' 144-159 (1977).
151. Whistler, R.L. (Ed) "Industrial Gums" 2nd Ed. Acad.Press. London & New York (1973).
152. Holzwarth, G.M. "Is Xanthan a worm-like chain or a rigid rod?", ACS Symp. Ser. 'Solution Properties of Polysaccharides' 150 15-23 (1981).

153. Walkling, W.D. and Shangraw, R.F., "Rheology of microcrystalline Cellulose/Carboxymethylcellulose gels", *J.Pharm.Sci.* 57 1927-33 (1968).
154. Ory, A.M. and Steiger-Trippi, K. "Über die rheologischen Eigenschaften einiger Schleinstoffe and deren Mischungen", *Pharm. Acta Helv.* 39 702-712 (1964).
155. Martin, A.N., Swarbrick, J. and Cammarata, A. "Physical Pharmacy" 2nd Ed. (1969), Lea and Febiger, Philadelphia.
156. Tanford, C., "Physical Chemistry of Macromolecules", *J. Wiley*, New York & London (1961).
157. Dea, I.C.M., McKinnon, A.A., and Rees, D.A. "Tertiary and quaternary structure in aqueous polysaccharide systems which model cell wall cohesion" *J.Mol.Biol.* 68 153-172 (1972)
158. Dea, I.C.M. "Specificity of interactions between polysaccharide helices and -1,4-linked polysaccharides" *ACS Symp.Ser.* 'Solution Properties of Polysaccharides', 150 439-454 (1981).
159. Jansson, P.E., Kenne, L. and Lendberg, B. "Structure of the extracellular polysaccharide from Xanthomonas campestris" *Carbohyd.Res.* 45 275-282 (1975).
160. Chen, C.S.H. and Sheppard, E.W. "Conformation and shear stability of Xanthan gum in solution", *Pdym.Eng.Sci.* 20 512-6 (1980).
161. Gelman, R.A. and Barth, H.G. "Atypical viscosity behaviour of dilute solutions of Xanthan gum", *J.Appl.Polym.Sci.* 26 2099-2101 (1981).
162. Brown, H.P. "Carboxylic polymers insoluble in water and organic solvents" *U.S.Pat.* 2,798,053; July (1957).
163. Goodrich, B.F. "Carbopol Water Soluble Resins", *B.F. Goodrich Chemical Ltd.*, (1980).
164. Testa, B. "Contribution a l'etude galenique d'hydrogels medicamentaux de Carbopol"; These, Universite de Lausanne (1970), from 'Repertoire des Theses Europeenes".
165. Bloemers, H.P.J. and Van der Horst, A., "Inhibition of RNA-dependent DNA polymerase of Oncorna viruses by Carbopol 934", *FEBS Letters* 52 141-4 (1975).
166. Kumar, B.V., "Inhibition of reverse transcriptase and rDNA polymerase by Carbopol GD4", *Microbios. Lett.* 2 219-223 (1976).

167. Testa, B. & Etter, J.C., "Apport de la rheologie a l'etude des interactions entre les macromolecules de Carbopol", Pharm.Acta Helv. 48 378-388 (1973).
168. Goodwin, J.W. & Khidher, A.M. "The effect of addition of a water soluble polymer on the elasticity of polymer latex gels", Coll. Interface Sci.Proc.Int.Conf.50M. 4 529-547 (1976).
169. Cheng, D.C-H., "Sedimentation of suspensions and storage stability" Chem. Ind. 407-444 (1980).
170. Ferry, J.D., "Viscoelastic Properties of Polymers", J.Wiley, New York, 3rd Ed. (1900) p.257.
171. *ibid.* p.219.
172. Bueche, F., "Physical Properties of Polymers" Interscience, New York (1962).
173. Ree, T. & Eyring, H., "Theory of non-Newtonian flow", J.Appl. Phys. 26 793-800 (1955).
174. Doi, M. & Edwards, S.F., "Dynamics of concentrated polymer systems: I. Brownian motion in the equilibrium state", J.Chem. Soc., Farad.Trans. 74 1789-1801 (1978).
175. Doi, M. & Edwards, S.F., "Dynamics of concentrated polymer systems: II. Molecular motion under flow", J.Chem.Soc., Farad. Trans. 74 1802-1817 (1978).
176. Doi, M. & Edwards, S.F., "Dynamics of concentrated polymer systems: III. The constitutive equation.", J.Chem.Soc., Farad. Trans. 74 1818-1832 (1978).
177. Doi, M. & Edwards, S.F., "Dynamics of concentrated polymer systems: IV. Rheological properties", J.Chem.Soc., Farad. Trans. 75 38 - 54 (1979).
178. Williamson, R.V., "The flow of pseudoplastic materials", Ind. Eng.Chem. 21 1108-1111 (1929).
179. Metzler, C.M. Elfing, G.L. & McEwen, A.J., "A user's manual for NONLIN and associated programs", Upjohn Co., Michigan (1974).
180. Neibergall, P.J., Schaare, R.L. & Sugita, E.T., "Non-linear regression applied to non-Newtonian flow", J.Pharm.Sci 60 1393-1402 (1971).
181. Davis, S.S., "Viscoelastic properties of pharmaceutical semisolids: III. Non-destructive oscillatory testing", J.Pharm. Sci 60 1351-1356 (1971).

182. Cheng, P.Y. & Schachman, H.K., "Studies on the validity of the Einstein Viscosity Law and Stoke's Law of sedimentation", *J.Polym. Sci.* 16 19-30 (1955).
183. Maude, A.D. & Whitmore, R.L., "A generalised theory of sedimentation", *Br.J.Appl.Phys.* 9 477-481 (1958).
184. Batchelor, G.K., "Sedimentation in a dilute dispersion of spheres", *J.Fluid Mech.* 52 245-268 (1972).
185. Reed, C.C. & Anderson, J.L., "Analysis of sedimentation velocity in terms of binary particle interactions", *Coll. Interface Sci., Proc. Int. Conf.* 50th 4 501-512 (1976).
186. MacDonald, I.F., "Rate dependent viscoelastic models", *Rheol. Acta* 14 906-918 (1975).
187. Thurston, G.B., "Shear rate dependence of the viscoelasticity of polymer solutions", *J.Non-Newt. Fluid Mech.* 9 57-68 (1981).
188. Chien, Y.W., Lambert, H.J. and Lin, T.K. "Solution-solubility dependency of controlled release of drug from polymer matrix: mathematical analysis" *J. Pharm.Sci.* 64 1643-7 (1975).
189. Zentner, G.M., Cardinal, J.R. and Kim, S.W. "Progesterin permeation through polymer membranes" *J.Pharm.Sci.* 67 1347-1351 (1978).
190. Paul, D.R. and Harris, F.W. (Eds): *ACS Syrup. Ser.* 33 "Controlled Release Polymeric Formulations" *Pub.Amer.Chem.Soc.*, New York (1976).
191. Roseman, T.J. and Higuchi, W.I. "Release of medroxyprogesterone acetate from a silicone polymer", *J.Pharm.Sci.* 59 353-357 (1970).
192. Barzegar-Jalali, M. and Richards, J.H. "Effect of suspending agents on the release of Aspirin from aqueous suspensions in vitro". *Int.J.Pharm.* 2 195-201 (1979).
193. Barzegar-Jalali, M. and Richards, J.H. "The effects of various suspending agents on the bioavailabilities of Aspirin and Salicylic acid in the rabbit" *Int.J.Pharm.* 3 133-141 (1979).
194. Tyrrell, H.J.V., "Diffusion and Viscosity in the Liquid Phase". *Science Progress* 67 (266) 271-293 (1981).
195. Fick, A. *Am Physik* 170 59 (1855).
196. Fourier, J.B. (1822) "Theorie Analytique de la Chaleur" English translation by A.Freeman, Dover Publ., New York (1955).

197. Crank, J. "Mathematics of Diffusion" Oxford Clarendon Press, 2nd Ed. (1975).
198. Barrer, R.M., "Diffusion In and Through Solids", Cambridge Univ.Press, England (1941).
199. Carslaw, H.S. and Jaeger, J.C. "Conduction of Heat in Solids" Oxford Clarendon Press, 2nd Ed. (1959).
200. Crank, J. "Mathematics of Diffusion" Oxford Clarendon Press, 2nd Ed. (1975), Chap.11 p.254.
201. Higuchi, W.I. "Analysis of data on the medicament release from ointments" J.Pharm.Sci. 51 802-4 (1961).
202. Higuchi, W.I. "Diffusional models useful in biopharmaceutics" J.Pharm.Sci. 56 315-324 (1967).
203. Ostrenga, J., Haleblian, J., Poulsen, B., Ferrel, B., Mueller, N. and Shastri, S. "Vehicle design for a new topical steroid, Fluocinonide" J. Invest.Dermatol. 56 392-9 (1971).
204. Hadgraft, J. "Calculations of drug release rate from controlled release devices: the slab" Int.J.Pharm. 2 177-194 (1979).
205. Carslaw, H.S. and Jaeger, J.C. "Conduction of Heat in Solids" Oxford Clarendon Press, 2nd Ed (1975), Appendix 2.
206. Abramovitz, M. and Stegun, I.A. (Eds). "Handbook of Mathematical Functions" Dover Publ., New York (1965).
207. Guy, R.H. and Hadgraft, J. "Calculations of drug release rates from cylinders" Int.J.Pharm. 8 159-165 (1981).
208. Chowhan, Z.T. and Pritchard, R. "Release of corticoids from oleaginous ointment bases containing drugs in suspension". J.Pharm.Sci. 64 754-9 (1975).
209. Wood, J.M., Attwood, D. & Collett, J.H., "The influence of gel formulation on the diffusion of salicylic acid in polyHEMA hydrogels", J.Pharm.Pharmac. 34 1-4 (1982).
210. Stephenson, G. "Mathematical Methods for Science Students" 2nd Ed. (1973) p.469.
211. *ibid*, p.254.
212. *ibid*, p.255.
213. Cardinal, J.R. Kim, S.R. & Song, S.Z., in "Controlled Release of Bioactive Materials" Ed. R.Baker, Acad. Press (1980) p.123-133.

214. Song, S.Z., Cardinal, J.R., Kim, S.R. & Kim, S.W., "Progesterone permeation through polymer devices V: progesterone release from monolithic hydrogel devices", *J.Pharm.Sci.* 70 216-219 (1981).
215. Attwood, D., Johansen, L., Tolley, J.A. & Rassing, J., "A new ultrasonic method for the measurement of the diffusion coefficient of drugs within hydrogel matrices", *Int.J.Pharm.* 9 285-294 (1981).
216. Higuchi, T. "Physical chemical analysis of percutaneous absorption process from creams and ointments" *J.Soc.Cosmet. Chem.* 11 85-97 (1960).
217. Bottari, F., Carelli, V., Dicolo, G., Saettone, M.F. & Serafini, M.F., "A new method for determining the diffusion coefficient of drugs in semi-solid vehicles from release rate data", *Int.J.Pharm.* 2 63-79 (1979).
218. Marriott, C.M. & Kellaway, I.W., "Release of anti-bacterial agents from glycerol-gelatin gels", *Drug Dev.Ind.Pharm.* 4 195-222 (1978).
219. Amu, T.C., "Diffusion in Paraffin Hydrocarbons", *J.Chem.Soc. (Faraday I)* 75 1226-1231 (1980).
220. Amu, T.C., "Diffusion in n-Alkyl Benzenes", *J.Chem.Soc. (Faraday I)* 76 1433-1441 (1980).
221. Sherriff, M. & Enever, R.P., "Rheological and drug release properties of oil gels containing Silicon Dioxide," *J.Pharm.Sci.* 68 842-845 (1979).
222. Friedman, L., "Diffusion of non-electrolytes in Gelatin gels", *J.Am.Chem.Soc.* 52 1305-1311 (1930).
223. Friedman, L. & Kramer, E.O., "The structure of gelatin gels from studies on diffusion", *J.Am.Chem.Soc.* 52 1295-1304 (1930).
224. Nixon, J.R., Georgakopoulos, P.P. & Carless, J.E., "Diffusion from Gelatin-glycerol-water gels", *J.Pharm.Pharmacol.* 19 246-252 (1967).
225. Taft, R. & Malm, L.E., "The electrical conductance of sols and gels and its bearing on the problem of gel structure, I. Gelatin.", *J.Phys.Chem.* 43 499-512 (1939).
226. Shaw, M. & Schy A., "Diffusion coefficient measurement by the 'stop-flow' method in a 5% collagen gel", *Biophysical J.* 34 375-379 (1981).
227. Chen-Chow, P-C., & Frank, S.G., "In vitro release of lidocaine from Pluronic-F127 gels", *Int.J.Pharm.* 8 (2) 89-99 (1981).

228. Richard, K.A., Hubbard, D.W. & El-Khadem, S.H., "Shear rate effects on mass transfer and diffusion in polysaccharide solutions", Am.Inst.Chem.Eng., Symp.Ser. 74 (182) 114-119 (1974).
229. Gerasimova, T.N. & Bromberg, A.V., "Diffusion of solvents for Ag halides in gel-like media", Zühr.Nauchn.i.Prikl. Fotogr. i Kinematogr. 11 210-216 (1966) ; 11 425-428 (1966).
230. Shul'man. Z.P., Pokryvailo, N.A., Kordonskii, V.I. & Nersterov, A.K., "Mass transfer peculiarities of a disk rotating in a non-Newtonian fluid", Int.J.Heat Mass Transfer 16 1339-1346 (1973).
231. Farag, A.A., Sedahmed, G.H., Farag, H.A. & Negawi, A.F., "Diffusion of some dyes in aqueous polymer solutions", Br.Polym.J. 9 (6) 54-57 (1976).
232. Flynn, G.L., Yalkowsky, S.H. & Roseman, T.J., "Mass transport phenomena and models: theoretical concepts", J.Pharm.Sci. 63 479-510 (1974).
233. Nernst, W., "Zur Kinetik der in Lösung befindlichen Körper", Z.Physik Chem. 2 613-637 (1888).
234. Einstein, A., "Über die von der molekularkinetischen", Ann.Physik 17 (4) 549-560 (1905).
235. Sutherland, W., "A dynamical theory of diffusion for non-electrolytes and the molecular mass of Albumin", Phil.Mag. 9 781-785 (1905).
236. Stokes, G.G., Proc.Camb.Phil.Soc. 9 5 (1896).
237. Perrin, F., "Brownian movement of an ellipsoid", J.Phys.Radium, 5 497-511 (1934).
238. Herzog, R.O., Illig, R. & Rudar, H., "Über die Diffusion in molekulardispersen Lösungen", Z.Phys.Chem.Leipzig. A167 329-342 (1934).
239. Irwin, W.I. & Li Wan Po, A., "The dependence of Amitriptyline partition coefficients on lipid phase", Int.J.Pharm. 4 47-56 (1979).
240. Smidsrød, O., Haug, A. & Lian, B., "Properties of poly (1,4-hexuronates) in the gel state, I.Evaluation of a method for determination of gel stiffness", Acta Chem.Scand. 26 71-78 (1972).

241. Sharma, F. & Sherman, P., "An automated parallel plate viscoelastometer for studying the rheological properties of solid food materials", SCI Monograph 27 'Rheology & Texture of Foodstuffs', p.77, Soc.Chem.Ind. (1968).
242. Segeren A.J.M., Boskamp, J.V. & Van Den Tempel, M., "Rheological and swelling properties of Alginate gels", Farad. Disc.Chem.Soc. 57 255-262 (1974)
243. Treloar, L.R.G., "The Physics of Rubber Elasticity", Oxford Clarendon Press, 3rd Ed. (1975).
244. Merck Index, Pub.Merck & Co.Inc., 9th Ed. (1976) p.575, Compd. 4288.
245. Haug, A., "Dissociation of Alginic Acid", Acta Chem.Scand. 15 950-952 (1961).
246. Documenta Geigy Scientific Tables, Ed. K.Diem & C.Lentner, Geigy Pharmaceuticals, Macclesfield, 7th Ed. (1970).
247. Dusci, L.J. & Hackett, L.P., "Determination of some anti-inflammatory drugs in serum by HPLC", J.Chrom. 172 516-519 (1979).
248. Ali, A., Kazmi, S. & Plakogiannis, F.M., "High pressure liquid chromatographic determination of Ibuprofen in plasma", J.Pharm.Sci. 70 944-945 (1981).
249. Pitre, D. & Grandi, M., "Rapid determination of Ibuprofen in plasma by HPLC", J.Chrom. 278-281 (1978).
250. Thomas, W.O.A., Jeffries, T.M. & Parfitt, R.T., "Determination of four non-steroidal anti-inflammatory agents by HPLC", J.Pharm. Pharmacol. 31S 91P (1979).
251. Stevens, J., Boots Co. Ltd., Beeston, Nottingham; Private communication.
252. Sallman, A., "The chemistry of Diclofenac Sodium", Supp. to Rheumatology & Rehabilitation No.2 (1979): Proc.Syrup. Tangier, March 1978.
253. Albert, A. & Serjeant, E.P., "The Determination of Ionization Constants", Chapman & Hall, 2nd Ed (1971), Chap.2.
254. Traube, J., "Uber den Raum der Atome", Sammlung chem. chem-tech. Vortrage 4 255-333 (1899).
255. Albery, W.J. Greenwood, A.R. & Kibble, R.F., "Diffusion coefficients of carboxylic acids", Trans.Farad.Soc. 63 360-366 (1967).

256. Lauffer, M.A., "Theory of diffusion in gels", Biophysical J. 1 (3) 205-213 (1961).
257. Dumanski, A., "Diffusion in a colloidal medium", Z.Chem.Ind. Kolloide 3 210-212 (1908).
258. Ladenberg, R., "Über den Einflu von Wänden auf die Bewegung einer Kugel in einer reibenden Flüssigkeit", Ann.Physik. 23 (4) 447-458 (1907).
259. Bird, R.B., Stewart, W.E. & Lightfoot, E.N., "Transport Phenomena", London, Wiley, (1960) p.206.
260. Renkin, E.M., "Filtration, Diffusion and molecular sieving through porous cellulose membranes", J.Gen. Physiol. 38 225-243 (1954).
261. Beck, R.E. and Schultz, J.S., "Hinderance of solute diffusion within membranes as measured with microporous membranes of known pore geometry", Biochem. et Biophys. Acta 255 273-303 (1972).